Final Report 2000-09

Research

Release Methodology of Prestressing Strands

Technical Report Documentation Page

1. Report No.	2.	3. Recipient's Accession No.
MN/RC - 2000-09		

4. Title and Subtitle	5. Report Date
RELEASE METHODOLOGY OF PRESRESSING STRANDS	May 1998
	6.

7. Author(s)	8. Performing Organization Report No.
Jeffrey J. Kannel Catherine E. French Henry K. Stolarski	

9. Performing Organization Name and Address	10. Project/Task/Work Unit No.
University of Minnesota Department of Civil Engineering 500 Pillsbury Dr., S.E. Minneapolis, MN 55455-0220	11. Contract (C) or Grant (G) No. c)72629 wo) 162

12. Sponsoring Organization Name and Address	13. Type of Report and Period Covered
Minnesota Department of Transportation 395 John Ireland Boulevard Mail Stop 330 St. Paul, Minnesota 55155	Final Report
	14. Sponsoring Agency Code

15. Supplementary Notes

16. Abstract (Limit: 200 words)

This report presents the results of numerical and experimental investigations to determine the causes of prestressed concrete girder end cracks. The cracks, which develop during the flame-cutting release process, result from the restraining effect of unreleased strands as the girder shortens from the partially transferred prestress and from shear stresses generated by the cutting order of the strands. Researchers examined several methods to elimate the cracks such as making changes to the strand cutting pattern, debonding some of the strands in the end regions, and increasing the slope of the top surface of the bottom flange. Implementation of the first two of these methods in the field proved successful.

17. Document Analysis/Descriptors		18. Availability Statement
prestresseed bridge girders	strand cutting order	No restrictions Document available from: National Technical Information Services, Springfield, Virginia 22161
end cracking	flame-cutting release	

19. Security Class (this report)	20. Security Class (this page)	21. No. of Pages	22. Price
Unclassified	Unclassified	257	

RELEASE METHODOLOGY OF PRESTRESSING STRANDS

Final Report

Prepared by:

Jeffrey J. Kannel
Catherine E. French
Henryk K. Stolarski

Department of Civil Engineering
University of Minnesota
CivE, Civil Engineering Bldg.
500 Pillsbury Drive, S.E.
Minneapolis, MN 55455

May 1998

Published by:

Minnesota Department of Transportation
Office of Research and Strategic Services
Mail Stop 330
395 John Ireland Boulevard
St. Paul, MN 55155

ACKNOWLEDGMENTS

This research was sponsored by the Minnesota Department of Transportation. Computer resources were provided by a grant from the Minnesota Supercomputer Institute. The authors also express appreciation to the personnel of Elk River Concrete, a division of Cretex Companies, for their cooperation and assistance throughout the project. The views expressed herein are those of the authors and do not necessarily reflect the views of the sponsors.

TABLE OF CONTENTS

LIST OF TABLES

LIST OF FIGURES

EXECUTIVE SUMMARY

Cracks have been observed to develop in the end regions of prestressed bridge girders when using the flame-cutting technique to release the strands. The presence of these cracks provides a path for the ingress of chlorides which can promote strand corrosion in the end regions. In addition, the presence of the cracks upon full release indicates that there may be a reduction in the assumed bond between the strands and the concrete in the end regions. A numerical and experimental investigation was conducted to determine the source of the end cracks and a method to alleviate the cracks.

The research encompassed the study of 45, 54, and 72 in. deep girders. Variations in the strand cutting pattern were studied numerically with three sets of 54 in. deep bridge girders which were later monitored in the field during construction. The girders were chosen for the study based on the relatively short length of free strand available in the precasting bed during construction which exacerbates the end cracking problem.

The numerical simulation was conducted using a finite element code with elements that enabled characterization of the three-dimensional stress distribution in the end regions of the girders. The experimental study, which accompanied the numerical simulations, comprised surface strain measurements of prestressed bridge girders during the flame-cutting release process. In addition, field surveys were conducted at a local precasting plant to determine the extent of the end cracking problem.

The source of the cracks was attributed to the restraining effect of unreleased strands as the girder shortens from the partially transferred prestress during the flame-cutting process and from shear stresses generated by the cutting order of the prestressing strands.

Several methods were examined to eliminate the cracks including changes to the strand cutting pattern, debonding some of the strands in the end regions, and increasing the slope of the top surface of the bottom flange. The first two of these methods were implemented in the field and found to be successful.

CHAPTER 1
INTRODUCTION

1.1 Background

Cracks have been observed to form in the bottom flanges at the ends of prestressed bridge girders when using the flame-cutting technique to release girders from precasting beds. A literature search led to an earlier study by Mirza and Tawfik [4] which suggested the cracks form due to the restraining effect of unreleased strands as the girders shorten from the partially transferred load. According to their study, the shorter the free length of cables in the bed, the greater the restraint from the unreleased strands. This determination was based on a one-dimensional model of the casting bed which only accounted for stresses along the longitudinal axis of the girders. Because some cracks were observed at an angle to the girder axis, a model incorporating all stress components was needed. Therefore, a three-dimensional finite element model was developed for this study.

1.2 Objectives

The goal of this research was to investigate the causes of the cracking analytically and through field observation. The analysis was done with the finite element program ABAQUS [1] using a model that incorporated a three-dimensional state of stress in the zone of cracking. Field observations were supplemented with a survey of precast producers to determine the extent of the problem and the effectiveness of procedures used to mitigate the cracking. The expected solutions to the problem were to change the strand cutting pattern, provide supplementary reinforcement, and/or debond some of the strands for a short length. The final objective was to develop design recommendations to minimize or eliminate the cracks.

1.3 Preliminary Field Observations

The first step of the investigation was an examination of cracks in six 72 in. deep girders sitting in the yard at Elk River Concrete Products. The girder cross section, including the strand cutting pattern, is shown in Figure 1.1. The cracks were largely obscured by a surface grout, but

a very rough sketch of what was visible was made for every bottom corner. About 3/4 of the corners exhibited cracking, all within two feet of the end of the girder. Besides the expected vertical cracks, there were an equal number of cracks at approximately a 45 degree angle to the girder axis on the top surface of the bottom flange. These existed either independently or as extensions of vertical cracks on the face of the flange. Several locations also exhibited multiple short horizontal cracks in the corner between the flange and the web. An example of each type of crack is shown in Figure 1.2.

The sketches were examined to see if any patterns to the cracking could be discerned. For example, the analytical model used by Mirza and Tawfik (see section 2.1) suggests a *potential* for higher tensile stresses and more cracking in locations adjacent to shorter lengths of free strand. For the bed layout used, shown in Figure 1.3, girder ends 1S and 2N should exhibit the most cracks and those from the north end of the bed, 1N, should have the fewest cracks. However, there were cracks at most of the corners observed, including those from the north end of the bed. No patterns could be discerned in this limited database.

The second part of the observational analysis was watching *when* cracks formed during the detensioning process. Figure 1.4 shows the cracks in four corners observed during release. Notation is provided to indicate which strand pair was cut just prior to when each crack was first observed. Of the eight primary cracks, three were initiated before release stage #6 (see Figure 1.1), during the release of the draped strands. The rest were observed to form during release of the straight strands, between release stages #9 and #12. The vertical cracks were among the earlier cracks to form, while the angled cracks were the last to form. Most cracks reached a maximum width and then partially closed by the end of detensioning. The maximum observed crack width was 13 mils, with final widths ranging from hairline to 10 mils. The vertical cracks, and the vertical portions of combined vertical-angled cracks, typically closed more than the angled ones. The reason for this is discussed in Section 4.1.

1.4 Preliminary Field Data

On November 16, 1994, four displacement transducers were used to monitor strains during the detensioning process for the 72 in. deep girders. The transducers were attached to the

north end of the north girder in the bed (end 1N). The placement of the gages and the position of the single crack that formed at this end are shown in Figure 1.5. Unfortunately, due to the near freezing temperatures and the short time available to attach the gages to the girder between formwork removal and strand release, the epoxy used to bond the gages did not hold well. The bond of gages #2 and #3 was visibly poor. The other gages indicated reasonable trends, but because the quality of the gage bond was suspect and the data limited, it was decided to discard the results. There was not enough time to gather additional data before the end of the 1994 casting season. A different experimental method, described in Section 7.1, was utilized the following season.

1.5 Organization of Remainder of Report

The remainder of the report describes the analytical and experimental approaches used to determine the cause of the end cracks and to investigate potential solutions. Chapter 2 discusses the analytical model developed by Mirza and Tawfik to predict strand strains and concrete stresses during the detensioning process. Chapter 3 describes the three-dimensional finite element model developed for this research, including the method that was used to incorporate the transfer length of the prestressing strands. It also gives the stress and strain notation used throughout this report. In Chapter 4, a model of 72 in. deep girders is used to explain the causes of the cracks. The dynamic effects from flame cutting the strands are examined, along with the effects of bed layout and friction between the casting bed and the girders. The effects of the approximate transfer length method used in the model are also examined.

Three different methods of controlling the cracks were examined with the model and are described in Chapter 5. These methods include changing the strand cutting pattern, debonding a short length of selected strands, and altering the shape of the bottom flange. Chapter 6 discusses the implementation of the first two of these methods in the field at Elk River Concrete Products. New cutting patterns were tested on 45 in., 54 in., and 72 in. deep girders. Debonding was also used with some of the 54 in. girders. Chapter 7 discusses instrumentation that was used on the 54 in. girders to measure girder surface strains and strand strain. This data is compared to visual observations and the strains predicted by the finite element model.

Chapter 8 details the results of the survey forms. These forms were only given to the Elk River plant, where they were used to document end cracking for a period from August through October of 1995. A summary and recommendations to limit the end cracking are presented in Chapter 9.

Several appendices are also included. Appendix A describes how modifications to the model affect the results. Appendix B presents a study regarding the role of end blocks on the formation of horizontal cracks in the web of the girder. Appendix C contains the input file for the one-half girder model of the 54 in. girders, and Appendix D contains the Pascal code for a program to carry out the analysis method proposed by Mirza and Tawfik.

CHAPTER 2
EARLIER WORK BY MIRZA AND TAWFIK

2.1 Research and Conclusions of Mirza and Tawfik

Twenty years ago, Mirza and Tawfik [4] studied the problem of vertical cracking and proposed a theory to explain their observations. Based on this theory, they developed a one-dimensional analytical model to predict strains in the free strand and concrete stresses during release.

The theory stated that as the first strands are cut they put most of the girder into compression, causing elastic shortening of the girder. This is resisted by the remaining uncut strands, which must lengthen to accommodate the shortening. The resulting tension in the uncut strands causes vertical cracks to form near the end of the girder, where the compression from the cut strands has not been fully transferred. Because a short free strand must strain more than a long free strand to accommodate the same amount of elastic shortening, the restraint force will be greater for the short strand. Therefore, the shorter the length of free strand in a bed (as a percentage of total bed length), the greater the restraint force will be and the greater the cracking.

The lengthening and shortening of the strands and girders in a bed should correspond to their respective stiffness. A simple elastic spring model was developed, diagrammed in Figure 2.1, in which each girder and each length of free strand in the casting bed was treated as an individual spring, connected at nodes. The principal assumptions of the model were that the concrete and steel behaved linear-elastically, there was no friction between the girders and casting bed, and dynamic effects were negligible. Equilibrium is solved for according to the formula $[K] * [D] = [F]$, where

$[K]$ = stiffness matrix, $K_i = E_i A_i / L_i$

$[D]$ = vector of nodal displacements

$[F]$ = vector of nodal forces.

An independent solution of this matrix equation must be calculated at each stage of the detensioning process. This is because the stiffness of the springs representing the free strands must be reduced as each strand is cut. The force applied to the girders at the nodes is equal to the

total prestress force in the strands which have been cut. At any stage of detensioning, the strain in the uncut strands is calculated from the nodal displacements. These strains are used to find the total restraint force, R, which is used to calculate a concrete stress according to the formula $\sigma = R/A + Re/S$, where

σ = stress in concrete at bottom fiber

R = total tensile force from unreleased strands

A = area of girder cross section

e = eccentricity of force R

S = section modulus of the transformed section.

This stress is considered to exist at the face of the girder where there is no benefit of compression from the strands already cut. An additional concrete stress due to rotation of the ends of the girders can also be computed. The end rotation can be calculated by conventional means. From this a strand strain is determined based on the strand eccentricity, and a concrete stress is calculated as done above. However, the contribution to the total stress is generally negligible.

Consider the case of a frictionless bed containing a single girder, offset from the centerline of the bed such that the left free span is twice as long as the right free span, as depicted in Figure 2.2. Now consider an arbitrary stage of release in which the same number of strands are cut at both ends, so that the prestress force applied to both ends is the same. For equilibrium, the restraint force must also be the same at both ends. If the next strand is cut simultaneously at both ends, the restraint forces increase at each end and must remain equal to maintain equilibrium. However, due to the unequal stiffness of the free spans, the magnitude of displacement will be twice as high at the left end compared to the right end, effectively shifting the centerline of the girder to the right.

Because simultaneous release at both ends cannot be realistically achieved in the field, the effect of one end being cut before the other must be considered. When only the left end is cut, the prestress force is unbalanced and the entire girder shifts to the right. This increases the restraint force at the left end and decreases it slightly at the right end. The reverse occurs when the right end is cut before the left end. Notice that the greatest restraint force occurs at the right end when that end is cut first. In general, the shorter the free span, the worse it is to have that

span cut first. Mirza and Tawfik suggested that, while simultaneous release is best, consideration should be given to purposely cutting the end spans (typically the longest) first to eliminate the chance of cutting the interior spans (typically shorter) early.

For experimental confirmation of their theory, Mirza and Tawfik compared their model to cable strains for 12 in. square prestressed piles, 6 in. by 14.75 in. experimental members, and a 45 in. deep I-girder with 28 strands. The data correlated well with the model, with most discrepancies attributed to friction with the bed and nonsimultaneous release of the strands. They also found that friction tends to reduce the effects of nonsimultaneous release.

To summarize, Mirza and Tawfik concluded that the restraint of uncut strands is capable of causing vertical cracking in the ends of the girders. Their analytical model was judged to be satisfactory based on comparisons to experimental data. This model predicts that for simultaneous release with a frictionless bed, each of the girder ends is subjected to the same stress. Hence, what matters is the total length of strand in the bed, not its distribution. The exception is when one free span is cut before another, resulting in higher stresses at the location that was cut prematurely. Since this effect is worse when a short free span is cut before longer spans, consideration should be given to purposely cutting strands in the longer free spans first.

2.2 Mirza and Tawfik Analysis Applied to 72 in. Girders

Based on Mirza and Tawfik's elastic spring model, a computer program was developed at the University of Minnesota to perform the matrix calculations for any girder size and bed layout. The effect of end rotation was not included in the calculations, but the analysis was modified to include nonlinear behavior of the strands. The program was used to study the 72 in. deep girders described in section 1.3. The strands were given a trilinear stress-strain behavior, shown in Figure 2.3. The results from the program are given in Table 2.1. The listed values are the tensile stresses calculated at the end face of the girder, where no compression is available from the cut strands. Because of the assumption of a frictionless bed, the numbers for simultaneous release are valid at every location in the bed. The other columns list the results of cutting the north, middle, and south free spans first. In these cases the listed stress is for the girder end(s) adjacent to that span.

Table 2.1 Concrete Stress (psi) at Bottom of Girder Face, Obtained from Mirza and Tawfik Analysis Applied to 72 in. Girders

Release Stage	Simultaneous Cut All Spans	North Span Cut First	Middle Span Cut First	South Span Cut First
1	36	61	106	99
2	73	101	149	141
3	113	142	195	186
4	154	186	243	233
5	196	231	292	282
6	240	278	344	333
7	269	308	376	364
8	296	335	405	393
9	320	360	432	420
10	339	380	454	441
11	356	398	473	460
12	369	412	477	474
13	377	421	451	448
14	382	411	426	423
15	378	386	402	399
16	349	357	374	371
17	320	329	348	344
18	293	301	321	318
19	265	274	296	292
20	233	242	266	261
21	201	211	236	231
22	170	180	208	202
23	140	150	181	174
24	104	113	147	139
25	69	77	96	96
26	34	41	47	47
27	0	0	0	0

The table shows that the tensile stress in the concrete initially increases as more strands are cut. While the restraint force per uncut strand continues to increase throughout the release process, the number of uncut strands steadily decreases. The strands also become inelastic approximately midway through the release process. Therefore the total restraint force and the tensile stress in the girders reach a peak when about half the strands are cut, and then decrease to zero when all the strands are cut. It is apparent that cutting the middle span first, the shortest span, results in the highest stress.

The release strength of test cylinders was typically around 7000 psi, so the uniaxial tensile strength of the concrete, based on $6\sqrt{f_c'}$, was around 500 psi. The stress values in the table suggest that a few cracks might be expected, but not the number that were observed, as described in Section 1.3. There are a couple of possible reasons for this. First, the analysis uses beam theory to calculate the concrete stress, but this theory is only valid at a distance from the end of the girder approximately equal to the depth of the girder. This method applies the restraint force to the entire girder cross section, but in reality the tensile stresses are concentrated around the strands in the first few feet of the girder. Second, many of the cracks observed in the 72 in. girders formed at an angle to the girder axis, which suggests they were caused by shear stress, not axial stress. It will be shown in Section 4.1, using a three-dimensional finite element model, that the angled cracks were caused by shear stresses set up by the release pattern used. The one-dimensional model used by Mirza and Tawfik could not capture these shear effects.

CHAPTER 3
FINITE ELEMENT MODEL

While the analytical model developed by Mirza and Tawfik may have predicted strand strains fairly well, the use of beam theory to calculate the concrete stress at the very end of the beam is inaccurate. The model is also one-dimensional, which fails to capture the complicated stress state in the end region of the girder. For these reasons, a three-dimensional finite element model was used in this study to model the flow of forces within the end regions of concrete I-girders during prestress transfer.

The complexity of the problem prompted several simplifications. Although the concrete behavior is likely to be inelastic, a simple elastic material model was used. Since the objective of the research was to prevent crack initiation, the simplicity of the linear elastic model was felt to be sufficient. Symmetry of the girder cross section and assumed symmetry of the casting bed were used to limit the demand on computer resources. A particular problem was modelling the mechanisms of bond by which force is transferred from the strands to the concrete. Initially, the compressive transfer length was crudely modelled and the tensile transfer length of uncut strands was ignored entirely, resulting in high levels of tensile stress which decayed rapidly with distance from the end of the girder. This model was later replaced by a system which included springs to model both compressive and tensile stress transfer.

It is understood that the resulting model was too simple to capture the highly complex nature of the stress field in the end region of a girder. However, the modelling assumptions were judged adequate to reveal general trends such as those related to changing the cutting order of the strands. The ultimate verification of those trends was done through field observation.

3.1 Description of Model

Figure 3.1 depicts the basic model used in this study, the details of which are described in this section. All models were run on a Cray X-MP supercomputer at the Minnesota Supercomputer Institute using the finite element program ABAQUS, version 5.4 [1]. In order to efficiently utilize the supercomputer resources, it was decided to use a mesh of 3-D continuum

elements for only the end few feet of the girder and to use beam elements for the remainder. Multipoint constraints (MPC's) were used to force the continuum elements to maintain a plane section at the junction between the two element types. Symmetry of the girder cross section was also used to cut the model in half through the cross-sectional width. The continuum element mesh used for the 72 in. deep girders was 42 in. long and is shown in Figure 3.2. The length of the mesh was determined by the width of the web, which started to narrow from 16 in. to 6 in. wide at 42 in. from the end of the girder. Extending the continuum elements through this transition region would have distorted the elements.

The casting bed was assumed to be laid out as in Figure 3.3 with the symmetry planes shown. This allowed modelling of just one-half of a girder, further reducing the problem size. Note that this arrangement does not divide the strand into equal lengths for each free span, but equal lengths per girder end. This places the longest free span between the girders, which in practice is generally the shortest free span. However, with a frictionless bed and simultaneous release, there is no loss of accuracy compared with the Mirza and Tawfik analysis which predicts equal restraint forces in each free span regardless of the distribution of the free strand within the casting bed (see Section 2.1). In reality, friction and nonsimultaneous release cause unequal stresses at different points in the bed. This will be shown in Section 4.3 when a model of the full bed is discussed. Because the primary objective was to examine *relative* changes when new cutting patterns and other alterations were made, which required a large number of independent computer runs, use of the one-half girder model was assumed to be adequate for the majority of the analyses.

The eight-node continuum elements used for the first few feet of the girder were first order, meaning linear interpolation of displacements. Second order elements were tried early in the model development, but this resulted in locally high peaks of stress because of the concentrated nature of the forces applied by the strands. For a similar reason, the magnitudes of the stresses were highly dependent on the refinement of the mesh. Details on this phenomenon can be found in Appendix A. The response of first order elements in bending can be too stiff due to shear locking. Therefore "incompatible" elements were used which have thirteen additional internal kinematic variables. These allowed improved response in bending, but compatibility of

deformation along interelement boundaries was not guaranteed.

All the girders studied had sole plates the full width of the bottom flange and 15 in. long. These were attached using two large hooks welded to the sole plate, as shown in Figure 3.4. In the model, the same element type was used for the sole plate as for the concrete. Attempts were made to use separate nodes for the concrete and steel and to define a surface interaction between them. However, the solver routine had difficulty matching the surfaces at the edge of the sole plate. In addition, transfer of shear across the interface was done through friction, so that the shear was dependent on the normal force. During the draped strand release, the end of the girder curls up so there is no normal force, and at the end of release, the girder cambers and rests on an edge so that the normal force is poorly distributed. Therefore, this method of modelling the sole plate had to be abandoned and the sole plate was essentially "welded" to the concrete by using the same nodes on the interface. A notch was left open in the concrete at the end of the sole plate to prevent too much axial tension from being transferred from the sole plate to the concrete. A stress concentration still developed here and is discussed in Appendix A.

The models for the 72 in. girders included all the rebar in the endblock using the rebar definition capabilities of ABAQUS. However, defining the rebar is a very tedious process and comparisons to a previous model without the rebar did not show a significant difference. This is reasonable since post-cracking behavior was not being studied. Therefore the rebar were omitted from future models.

Modelling of the strands was done with three-dimensional, two-node truss elements. Boundary conditions were applied to fix the nodes at the abutments and to prevent vertical motion of the draped strands at the horses (hold up points). The truss elements for the straight strands used the same nodes as the continuum elements, while the nodes for the draped strands were linked to the nearest four continuum nodes with a bilinear MPC. In the region modelled with beam elements, the truss nodes for all strands were linked to the beam nodes with rigid beam MPC's. A boundary condition was applied to vertically fix the beam nodes at the hold down locations until the appropriate time in the release process.

The casting bed was modelled as a single rigid surface using a rigid surface definition built into ABAQUS. Friction between the bed and the girder was included using a coefficient of

friction of 0.4 between the concrete and the bed and 0.25 between the sole plate and the bed. These values were taken from the PCI Design Handbook, Table 6.6.1, for dry conditions [5]. Because of the use of lubricants at Elk River Concrete Products, actual friction coefficients were probably lower. The full bed analyses in Section 4.3 indicate the main effect of friction is to restrict rigid body shifting of the girders within the casting bed. Because the one-half girder models do not allow any shifting of the girders, the choice of friction coefficients did not greatly affect those models.

Because the goal of this research was to find ways to keep the concrete from cracking, not to model post-cracking behavior, an elastic material model was used for the concrete. It was assumed that for any release method which prevented cracking, the concrete would remain within the elastic range. Based on a compressive strength at the time of release of roughly 7000 psi, a modulus of elasticity of 4750 ksi was calculated using $E_c = 57000*\sqrt{f_c'}$ [2, ACI 318-89 8.5.1]. Poisson's ratio was taken to be 0.15 and the concrete density as 150 pcf. The steel for the strands and the sole plate was assumed to have an elastic modulus of 29000 ksi, Poisson's ratio of 0.30, and a yielding behavior shown previously in Figure 2.3. The strands used were 0.5 in. diameter, 270 ksi low-relaxation strands. Strand relaxation was calculated using "Estimating Prestress Loss" by Zia et. al. [6]. Based on an initial pull of $0.75f_{pu}$ and two days time elapsing between tensioning and release, the stress at release was calculated to be 200 ksi for the straight strands.

Release of the strands by flame cutting was simulated using the ABAQUS command "Model Change, Remove" to literally remove the section of free strand. For the dynamic procedure, removal was immediate. For the static procedure, the solver routine ramped down the forces from the removed elements linearly over the analysis step until a new equilibrium was established. Because calculating a new equilibrium after each individual strand is cut would be computationally expensive and would generate enormous data files, strands were cut in groups of three to four strands such that it took seven to ten steps for full release.

3.2 Transfer Length Approximation

After a strand is cut, the stress in the strand increases from zero at the face until it reaches

the effective prestress at a distance from the end defined as the transfer length. The change in stress over this region is due to a combination of mechanical anchorage and shear stress between the strand and the surrounding concrete. This is accompanied by slipping of the strand relative to the concrete. Modelling this slip would require using separate nodes for the truss and continuum elements, connecting them with springs defined to simulate an assumed bond-slip relationship. This approach was eventually tried and is described in Appendix A. However, the rest of the models discussed in this report used a different method which is discussed below.

First note that the force transferred from a strand to the concrete over a given length of strand equals the strand area multiplied by the change in strand stress over that length. In reality, the area of the strand remains constant while the stress increases approximately linearly within the transfer zone. However, the same bond force could be calculated if the stress remained constant and the area of the strand changed linearly. In the model, the same nodes were used for the concrete and the strands. Therefore the strand elements experienced the same strain as the concrete, but the change in stress was much smaller because the strands were over six times stiffer. For this reason the strand stress in the transfer region remained at nearly the full prestress level after the free strand was cut. Therefore a change in the area of the strands was used to model an appropriate rate of stress transfer between the cut strands and the concrete.

Instead of defining a single set of truss elements for each strand, two sets of truss elements were used within the transfer zone. The two elements at any given location were given a combined area equal to the total area of the strand, 0.153 in^2. In the step of the analysis in which a given strand was cut, one of the two elements was removed from the model along with the free strand. The areas of the remaining elements increased linearly from zero at the end of the girder until the full area was reached at the end of the transfer length. In all cases the transfer length was assumed to be 30 in., which falls between 50 bar diameters [2, ACI 318-89 Section 11.4.4] and the analytical formula $f_{se}d_b/3$ [2, ACI 318-89 Commentary R12.9].

The stress in the uncut strands changes in the opposite direction. The strands are under high tension at the end face, with tension decreasing to the initial prestress level within the girder at some unknown distance from the end. Attempting to use the same general method as above to model this would require *adding* extra prestressed strand at the end of the girder. This would

stiffen the strand relative to the concrete, causing most of the tensile force to be taken by the strand. The amount of added strand would be steadily reduced with distance from the girder face, transferring the tension to the concrete. This method was not practical because the amount of added strand would depend on the level of tension in the free strand, which is not known ahead of time. Further, the length of the transfer zone and the rate of stress transfer were not known. Therefore no attempt was made to model the reverse transfer length with this method. As mentioned earlier, a different method in which springs were used to connect the truss and continuum elements was eventually tried and is discussed in Appendix A. This method was able to incorporate the reverse transfer length. It should be noted that the tension in the strands increases by at most 70 ksi from the prestress level (200 ksi) to their ultimate strength (270 ksi), compared with a 200 ksi change in stress over the compressive transfer length, so the reverse transfer length would be at most 10 in., and generally much less.

3.3 Stress and Strain notation used by ABAQUS

ABAQUS notation is used throughout this report and should be understood. The model axes are shown in Figures 3.1 and 3.2. The normal stresses parallel to the model axes are designated by S11 (along the longitudinal axis), S22 (along the vertical axis through the girder depth), and S33 (along the horizontal axis through the girder width). The shear stresses are designated by S12 (in vertical plane along the longitudinal axis), S13 (in horizontal plane), and S23 (in vertical plane across the girder width). The principal stresses are designated by SP1, SP2, and SP3, where SP1 < SP2 < SP3. Strains are indicated in the same way as stresses, replacing the 'S' with an 'E'. The output from ABAQUS is in ksi, with positive values representing tension and negative values compression. However, the text of this report uses psi for units of stress.

CHAPTER 4
APPLICATION OF MODEL TO 72 IN. GIRDERS

In this chapter, a one-half girder model of 72 in. deep girders is used to explain the separate causes of the vertical and angled cracks, and the cracks at the base of the web. The dynamic effects from flame cutting the strands are examined and judged to play a minor role in the development of the cracks. A model of the full casting bed is used to explore the effects of bed layout and friction between the casting bed and the girders. The effects of the transfer length method used in the model are also examined.

4.1 Results for One-Half Girder Model Using Static Procedure

A model was developed for the 72 in. girders first described in Section 1.3. The strands were cut in the order originally used at Elk River Concrete Products, shown in Figure 1.1. This order is shown again in the left half of Figure 4.1 and is designated 72A. The right half of the figure shows which strands were released in each step of the analysis. In the first step, gravity was defined and the strands were given an initial prestress. The draped strands were then cut in two steps. In each of the remaining steps an entire column of straight strands was cut at once. The boundary condition simulating the hold down point was removed in the fourth step along with the first column of straight strands. In previous runs the hold down was removed as a separate step, but the change from the preceding step was negligible.

The results from steps 2 and 3, in which the draped strands were released, indicated primarily axial tension due to the restraint of the uncut straight strands. The results following step 3 are shown in Figure 4.2 with contours of the axial stress S11 on cross sections of the bottom flange covering the first two feet of the girder. The contour legend gives the stress in ksi and includes values from the back side of the plotted element layers, so the full range of stress in the legend may not appear in the contours shown. The peak stress from each cross section is listed in Table 4.1, along with the peak stress from contours of the maximum principal stress SP3.

Table 4.1 Peak Stresses for Step 3 of Pattern 72A (psi)

in. from end	0	3	6	9	12	15	18	24
axial stress S11	352	273	221	178	185	314	354	258
max principal stress SP3	367	277	223	179	186	314	354	258

Table 4.1 confirms that the maximum principal stress was almost purely axial through step 3, during release of draped strands. Stresses SP2 and SP1 did not exceed 44 psi in magnitude except at the face of the girder, where the peak SP2 stress was 195 psi tension and the peak SP1 stress was 92 psi tension. The table and contours also demonstrate the results of not modelling the reverse tensile transfer length of the uncut strands. Nearly the entire tensile force was introduced right at the end face of the girder resulting in locally high axial stresses. Moving away from the end, the tensile force spread out and the axial stress decreased. At the end of the sole plate, 15 in. from the end of the girder, the axial stress increased again as the tensile force that was in the sole plate was transferred back into the concrete.

The vertical cracks were typically observed to form during release of the draped strands. This is consistent with the orientation of the principal stress given by the model at this stage. Since the stress was nearly uniaxial, the initiation of cracking should correspond to the uniaxial cracking stress, calculated to be about 500 psi ($6\sqrt{f_c'}$) based on a typical release strength of approximately 7000 psi. However, the stress in the model did not reach this level during the draped strand release. Possible reasons for this discrepancy include the dynamic effects from sudden release of the strands; nonsimultaneous release of the north, middle, and south free spans; local stress concentrations due to the rebar in the flange; and flaws in the concrete due to poor consolidation or shrinkage cracks. The first two possibilities are discussed in Sections 4.2 and 4.3, respectively.

The model also fails to accurately predict where the axial cracks should form. For instance, the model suggests vertical cracks should form at the end of the sole plate, but no vertical cracks were found right at this location, suggesting the stress concentration given by the model may not exist in reality. This fact is noted again in Section 6.2.1 regarding a severe case

of axial cracking in some 54 in. deep girders. Appendix A.3 discusses the stress concentration at the end of the sole plate in more detail.

Figure 4.3 shows contours of the principal stress (SP3), axial stress (S11), and shear stress in the horizontal plane (S13) at 6 in. from the end of the girder for the rest of the release process. For release steps 4 through 7, the peak principal stress was typically located just inside the column of strands that was just released. The contours show that the location of the peak principal stress generally coincided with the shear stress in the horizontal plane, S13, rather than the axial stress. This explains why the cracks that formed during these stages of release grew at approximately a 45 degree angle with the axis of the girder. The opposing directions of force being applied by the cut strands on the outside of the flange and the uncut strands on the interior were effectively "shearing off" the flange. The shear stress gradually decreases with distance from the end of the girder. For instance, in step 5 the peak shear stress was 622 psi at 6 in. and 421 psi at 18 in. from the end. The principal stress decreases faster due to rapidly increasing compression. The peak principal stress in step 5 was 716 psi at 6 in. and 278 psi at 18 in. from the end. The peak axial stress was 541 psi at 6 in. and -157 psi (compressive) at 18 in. from the end.

The cracks at the base of the web were caused by a stress concentration which developed at the junction of the flange and the web at the end of the release process. This concentration was the result of S12 and S13 shear stresses transferring compression from the flange into the web of the girder. The contours in Figure 4.3 show a peak principal stress of 903 psi. This stress was high considering the small amount of cracking observed there.

In Section 1.3 it was noted that the cracks tend to close by the end of the detensioning process, particularly the vertical cracks and the vertical portions of combined vertical-angled cracks. This fact confirms that the cracks do not completely eliminate the bond between the strands and the concrete, although the axial compression across the cracks is presumably less than that given by the model. The angled cracks on the top surface of the bottom flange did not close as much as the vertical cracks. The model suggests that the shear stress at full release is still relatively high (see Figure 4.3f).

Reexamining the study by Mirza and Tawfik [4], their work focussed primarily on 12 in.

square piles and small 6 in. by 14.75 in. rectangular members which would not encounter the shear effects present in the flanges of the I-girders investigated in the current study. In the I-girders included in the Mirza and Tawfik study, the bottom flanges had a much steeper slope which would not be as susceptible to angled cracking or cracking at the base of the web. They also purposely used beds with short lengths of free strand, increasing axial restraint, which would dominate their observed failures. Therefore Mirza and Tawfik most likely did not encounter the problems of angled shear cracking and cracking at the base of the web and hence they did not account for them in their work.

4.2 Results for One-Half Girder Model Using Dynamic Procedure

The static release procedure resulted in stresses high enough to account for the angled shear cracks, but the axial stress during the draped strand release was not high enough to explain the formation of the vertical cracks. One possible explanation is that dynamic effects from flame cutting the strands increases the axial restraint from the uncut strands. Therefore dynamic analyses were performed for the release of the first and the last draped strand.

Figure 4.4 shows the resulting axial stress at a point in the middle of the flange (at the position of strand pair #17 in pattern 72A) for each analysis. Even though there are many degrees of freedom in the model, the stress variations resembled those of a single degree of freedom oscillator with small damping. The amplitude of the waves was double the stress *change* from cutting the strands statically. When cutting the first draped strand, this meant the total stress was doubled. The relative effect was smaller for cutting the final draped strand, when a majority of the vertical cracks formed, since there was already a moderate level of tension in the flange.

While the dynamic effects seem to be significant, the actual stress increases would be smaller for two reasons. First, due to the symmetry of the model, the results presented in Figure 4.4 correspond to cutting a pair of strands, not just a single strand. Second, the strand is released instantaneously in the model. In practice, there is a series of rapid "pops" as each of the seven wires is severed. Therefore the overall dynamic effect should be minimal, and was ignored in the rest of the investigation. This conclusion was confirmed by instrumentation of a strand during

the release process using a strain gage attached to a peak strain indicator (see Section 7.4).

4.3 Results for Full Bed Model Using Static Procedure

A few full bed analyses were conducted to compare the results with the one-half girder models and to test some of the issues regarding nonsimultaneous release as first described in Chapter 2 on Mirza and Tawfik's work. The bed layout was as shown previously in Figure 1.3. The full bed models used a complete mesh of continuum elements at both ends of each girder. To test the effects of friction, one model was run with friction defined as specified in Section 3.1 and another was run without friction. For the first analyses, the strands were released simultaneously at all points. The resulting maximum SP3 and S11 stresses at 6 in. from the ends of the girders are given in Table 4.2. The table uses the notation given in Figure 1.3 to designate the girder ends. Stresses in ends 1S and 2N were nearly identical and are averaged in the table.

First consider the full bed model without friction. Based on Mirza and Tawfik's work, one should expect equal restraint forces at each girder end to maintain equilibrium. The FEM model confirms this is essentially true except for step 2, in which half the draped strands are released. In this step, the ends of the girder curled up due to the released draped strands. The associated rotation caused the remaining uncut draped strands to lengthen more than the straight strands, so that a larger proportion of the restraint force came from the draped strands. This effect was magnified where the length of free strand was short, causing girder ends 1S and 2N to have the lowest tensile stress in the bottom flange. Once all the draped strands were cut, the concrete stress in the frictionless model was affected little by the adjacent length of free strand. This is because the girders shifted in the bed so that the strain in the strands was the same in each free span. In particular, the north girder tended to shift toward the middle of the bed.

On the other hand, shifting of the girders was resisted in the full bed model with friction. The north girder did not shift as far south, decreasing the strain in the strands in the north free span and increasing the strain in the middle span. As a result, the axial stress in end 1N was much lower than that in the other ends. In general, friction tends to decrease the stress in locations adjacent to long free spans, and increases the stress in locations adjacent to short free spans. Minimizing friction would therefore help to balance the stresses when the girders are not spaced evenly in the bed.

Table 4.2 Peak Stresses in Full Bed and One-Half Girder Models (psi)

Step	Full Bed Model Without Friction			Full Bed Model With Friction			One-Half Girder Model Without Friction	One-Half Girder Model With Friction
	1N	1S / 2N	2S	1N	1S / 2N	2S		
maximum SP3 at 6 in. from end								
1	0	0	0	0	0	0	0	0
2	123	85	112	79	126	133	114	103
3	238	239	235	169	298	281	237	223
4	461	462	461	431	507	508	461	459
5	720	720	720	687	762	762	720	716
6	852	848	849	822	891	894	851	849
7	848	848	848	845	846	844	848	845
8	885	885	885	881	882	880	885	880
9	909	911	911	903	905	906	909	903
maximum S11 at 6 in. from end								
1	0	0	0	0	0	0	0	0
2	122	85	111	78	125	132	113	102
3	236	238	233	167	298	280	235	221
4	416	406	410	343	482	486	415	409
5	550	542	545	490	617	620	549	541
6	604	600	603	560	677	693	603	610
7	437	445	450	431	499	515	438	454
8	-30	-17	-13	49	70	89	-29	60
9	-460	-463	-465	-379	-378	-377	-460	-379

The stress in the one-half girder models compared favorably with that of the full bed models. The stress in the one-half and full bed models without friction matched very well. This validates using the average length of free strand per girder end, and not per free span, in the one-half girder model. Comparing the one-half girder models to each other, the model with friction did not allow the girder to shorten as much, slightly decreasing the axial restraint from the uncut strands. Because the end of the girder is curled up at the end of the draped strand release (step 3), the friction itself did not affect the results. At full release, the girder cambers upward and the friction acts at the very end of the girder, decreasing the axial compression at full release.

The effect of nonsimultaneous cutting of a strand was easily demonstrated with the full bed models. Table 4.3 lists the maximum SP3 stress (S11 was nearly identical) at 6 in. from the ends of the girders due to nonsimultaneous release of the last draped strand. Due to symmetry, this actually represented cutting a pair of strands. It is apparent that the stress increased dramatically at the girder end(s) adjacent to the free span that was cut early, and decreased at the other ends. The effect of friction was to restrict shifting of the girders in the bed and reduce the effects of nonsimultaneous release. In particular, the stress at end 1N remained comparatively low even when the north free span was cut before the others. Therefore, while simultaneous release is ideal, purposely cutting the north free span first may be preferable to avoid accidental release of the middle span first, as Mirza and Tawfik would have suggested.

4.4 Effects of the Approximate Transfer Length Method

The approximate transfer length method described in Section 3.2 was designed to cause the prestress to be transferred from the strands to the concrete at a linear rate. During intermediate stages of release, the state of stress in the concrete and the interplay between cut and uncut strands could affect the stress transfer between the strands and the concrete. Consequently, the effect of the stress transfer rate was investigated. The areas of the truss elements in the transfer region were changed according to $x^{3/4}$ or $x^{1/2}$ functions, as well as linearly (x^1), as shown in Figure 4.5. Except for a single trial discussed below, none of the models examined in this report used the $x^{1/2}$ function. All of the 72 in. girder models discussed in the preceding sections used the $x^{3/4}$ function, while the 45 in. and 54 in. girder models discussed later in this report used

the linear function.

Table 4.3 SP3 Stress (psi) at 6 in. From Girder Face Due to Nonsimultaneous Release of the Final Pair of Draped Strands

Release Stage	Full Bed Without Friction			Full Bed With Friction		
	1N	1S / 2N	2S	1N	1S / 2N	2S
pair 5 cut all spans	200	175	191	139	230	233
pair 6 cut north span only	316	70	81	208	163	213
pair 6 cut middle span only	158	391	150	131	372	201
pair 6 cut south span only	156	134	385	137	194	335
pair 6 cut all spans	238	239	235	169	298	281

Table 4.4 lists the peak SP3 stress at 6 in. from the girder face for a one-half girder model run with each of the assumed transfer functions, along with the stresses from a model which did not employ any transfer length approximation. The only difference between the models was the rate at which the compression from cut strands was transferred into the girder. Therefore the models did not differ from each other significantly until most of the strands were cut. The faster the compression was transferred into the girder, the greater the stress concentration at the base of the web. Not using any transfer length method resulted in the greatest stresses.

Whether the approximate transfer length method accurately modelled the stress transfer between the strands and concrete was not known, but whether the method behaved as expected needed to be checked. Each strand in the transfer zone was modelled with two elements, one of which was removed at the same time as the free strand was cut. The method was based on the assumption that the stress in the remaining truss element remains at the full prestress level. Multiplying this stress by the area of the remaining truss element gave the force in the element. The difference in force between two adjoining truss elements equals the force transferred to the

concrete. Figure 4.6 shows the "assumed" forces ($x^{3/4}$ distribution) and the "modelled" forces in a one-half girder model at full release. The forces in the model were a little lower than those assumed, particularly at the end of the transfer length. This is because the remaining truss elements do not remain at the full prestress level, but lose a little stress due to elastic shortening of the concrete and strands. This occurs in the real girders as well.

Table 4.4 Peak SP3 at 6 in. From Girder Face for Various Transfer Length Functions

Step		1	2	3	4	5	6	7	8	9
Method	x^1	0	103	223	460	708	840	781	807	822
	$x^{3/4}$	0	103	223	459	716	849	845	880	903
	$x^{1/2}$	0	103	224	451	709	844	926	982	1020
	None	0	103	224	461	772	1000	1200	1360	1460

CHAPTER 5
CRACK CONTROL METHODS

Three methods of controlling cracking were explored with the model: changing the strand cutting pattern; debonding a small number of strands; and altering the flange shape. Each method is discussed below. A fourth method, adding supplementary reinforcement, was considered at the outset of this study, but would have been difficult to adequately model. Adding rebar would be of limited benefit because rebar works best to limit crack width, not prevent crack formation. It would be difficult to implement due to tight packing of existing strand and rebar.

5.1 Changing Strand Cutting Pattern

The vertical cracks typically form during the draped strand release because all the unreleased straight strands are in tension at once, restraining the shortening of the girder. One method to counter this is to "precut" some of the straight strands before the draped ones. This introduces some compression into the bottom flange and reduces the number of uncut straight strands restraining the movement of the girder. The first foot of the girder would still be susceptible to cracking since it would receive only a small amount of compression from the precut strands. Precutting was not explored in depth until later in this study and was not tested with the 72 in. girder model. A single pair of strands was precut for the 45 in. deep girders described in Section 6.1. A model of 54 in. deep girders was used to test multiple precutting patterns, two of which were used successfully in the field. The model results and field trials are discussed in Sections 6.2.2 and 6.3.

Three new cutting patterns not involving precuts, shown in Figure 5.1, were tested with the one-half girder model in an attempt to reduce the shear stress causing the angled cracks. The original cutting pattern was shown in Figure 4.1. The peak principal, axial, and horizontal shear stresses at 6 in. from the end of the girder for each pattern are listed in Table 5.1. The stress in steps 2 and 3 was unchanged since the draped strands were still cut first. The table shows that the final stress was also the same, indicating the final condition for the model is independent of the cutting order.

Table 5.1 Effects of Altering Cutting Pattern (all stresses in psi)

Step	72A	72B	72C	72D	72A	72B	72C	72D
	max SP3 at 6 in. from end				min SP1 at 6 in. from end			
1	0	0	0	0	0	0	0	0
2	103	103	103	103	-23	-23	-23	-23
3	223	223	223	223	-51	-51	-51	-51
4	459	473	473	385	-443	-523	-523	-350
5	716	660	499	366	-787	-846	-626	-348
6	849	705	443	418	-1100	-1200	-751	-696
7	845	715	724	664	-1450	-1370	-1320	-1110
8	880	720	720	706	-1540	-1550	-1550	-1450
9	903	903	903	903	-1600	-1600	-1600	-1600
	max +S11 at 6 in. from end				min -S11 at 6 in. from end			
1	0	0	0	0	0	0	0	0
2	102	102	102	102	27	27	27	27
3	221	221	221	221	58	58	58	58
4	409	360	360	337	-346	-187	-187	-33
5	541	469	434	323	-618	-529	-315	-60
6	610	513	231	294	-750	-798	-353	-460
7	454	401	274	35	-1020	-1010	-945	-754
8	60	206	206	-119	-1070	-1160	-1160	-1130
9	-379	-379	-379	-379	-1260	-1260	-1260	-1260
	max +S13 at 6 in. from end				min -S13 at 6 in. from end			
1	0	0	0	0	0	0	0	0
2	8	8	8	8	-6	-6	-6	-6
3	17	17	17	17	-16	-16	-16	-16
4	414	105	105	111	-86	-444	-444	-307
5	622	103	115	183	-123	-669	-436	-276
6	740	126	132	236	-161	-740	-206	-125
7	725	152	149	267	-196	-706	-504	-375
8	543	167	167	194	-225	-536	-536	-400
9	165	165	165	165	-251	-251	-251	-251

Pattern 72B, in which the direction of cutting was reversed, showed a small decrease in SP3 along with a slight drop in axial tension. The shear stress remained high, simply changing direction. Patterns 72C and 72D, in which the straight strands were cut in alternating columns, provided a significant improvement in the middle stages of release. By cutting the straight strands in alternating columns, the opposing tensile and compressive forces were better distributed on the flange cross section. The result was a reduction in both axial and shear stress. Pattern 72D resulted in the greatest stress reduction, so the full stress contours of SP3, S11, and SP3 at 6 in. from the end for steps 4 through 8 are given in Figure 5.2. The contours show that there are still concentrations of stress along vertical lines. Therefore a better cutting pattern should be possible in which the strands are cut in a more "random" fashion, but pattern 72D was considered to be relatively easy to apply in the field. It was later proven to be effective in reducing the shear cracks when tested in the field, as described in Chapter 6.

5.2 Debonding Strands

Debonding a short length of selected strands can help to control both axial and shear stresses. Debonding reduces the axial tension by increasing the effective free length of the debonded strands, decreasing the level of strain needed to accommodate the elastic shortening of the girders. More importantly, the axial restraint from the debonded strands is moved away from the end face, improving the stress distribution within the end of the girder. By reducing the axial stress gradient (range of tensile and compressive stress), the shear stress is reduced as well. Debonding strands will also reduce the stress concentration at the base of the web at full release due to the reduction in compressive force transferred at the end of the girder.

Debonding was accomplished in the model by using a single truss element for the debonded strands from the abutment to where the debonding terminates, at 18 in. from the girder face, at which point the transfer length method was initiated. The transfer length of the debonded strands was reduced from 30 in. to 24 in. to keep the transfer zone within the mesh of continuum elements. The model exhibited some curious behavior as the result of debonding. Figure 5.3 shows the S11 contours at 0, 3, and 6 in. from the girder face after the last draped strand was

released for pattern 72E (see next paragraph). At 0 and 3 in. it was apparent which strands were debonded, but at 6 in. from the end the pattern was reversed. The figure also shows the axial stress on a section view 4 in. above the base of the girder. It shows how the axial stress converged at 6 in. from the end to create the stress reversal. The section view also shows another phenomenon at 18 in. from the end, where the debonding ends. The debonded strands pulled on the nodes at 18 in., causing local concentrations of compression at 15 in. and tension at 21 in., with fairly uniform stress right at 18 in. In later stages of release these axial stress effects were masked somewhat by the larger shear stresses.

Three different patterns, shown in Figure 5.4, were tested with the model. The cutting orders were kept similar to that of 72A for a more direct comparison to that pattern. However, it should be noted that the greatest benefit from debonding would be achieved if the debonded strands were cut last. Stress contours at 6 and 24 in. for patterns 72A, 72E, 72F, and 72G are shown in Figures 5.5, 5.6, 5.7, and 5.8, respectively. For brevity, the figures only include every other step of the analysis (steps 3, 5, 7, and 9 for patterns 72A, 72E, and 72G; steps 4, 6, 8, and 10 for pattern 72F). The maximum values of SP3 for each step of the analyses are summarized in Table 5.2. Ten steps were used for pattern 72F, but they are shifted in the table for easier comparison. Step 3 in the table (actually step 4 of pattern 72F) indicates the end of the draped strand release for each pattern.

In step 3, pattern 72E reduced the stress at 6 in. because there were fewer strands pulling at the end face of the girder. The axial restraint from the debonded strands was being applied where the debonding terminated, increasing the stress at 24 in. from the end. In this particular case, debonding worsened the stress distribution by increasing the stress where it was already high due to the stress concentration at the end of the sole plate. The stress increase here was not as high as expected, however, because the drop in stress in the debonded region reduced the tension in the sole plate, decreasing the stress concentration at the end of the sole plate. In practice, the debonding should be extended further past the sole plate, but for the model this would have required extending the region of continuum elements to include the transfer length of the debonded strands. The main point is that debonding reduces the stress at the end, at the cost of increased stress where the debonding is terminated.

Table 5.2 Effects of Debonding on SP3 (psi)

Step	72A	72E	72F	72G	72A	72E	72F	72G
	max SP3 at 6 in. from end				max SP3 at 24 in. from end			
1	0	0	146	0	0	0	66	0
2	103	88	208	103	124	139	92	138
3	223	188	258	224	258	278	130	282
4	459	425	420	436	141	145	99	327
5	716	614	616	612	152	215	210	332
6	849	713	738	772	210	242	238	334
7	845	798	827	722	218	256	247	318
8	880	836	836	717	162	217	217	266
9	903	858	858	802	109	180	180	219

To avoid shifting the vertical cracking further into the girder, debonding should be combined with precutting, as was done with pattern 72F. The compression from the precut strands dramatically reduced the axial stress at 24 in., minimizing the principal stress at the end of the draped strand release. While the table indicates the stress increased at 6 in., the full contours in Figure 5.7 show the peak stress was rather localized, with the overall stress level below that of pattern 72A.

In the middle stages of release, both patterns 72E and 72F continued to reduce the axial stress at 6 in. a modest amount. Since the shear stresses are caused by the opposition of the tensile and compressive forces on a given cross section, reducing the axial stress gradient (range of tensile and compressive stress) reduced the shear stress as well. Because patterns 72E and 72F only differed in the cutting order of the strands, they resulted in the same stress at full release. However, the debonding did change the stress relative to pattern 72A. With fewer bonded strands transferring compression to the girder in the first 18 in., the stress concentration at the base of the web was reduced a little.

It was previously stated that the debonded strands should generally be cut last. In opposition to this principal, pattern 72G depends on cutting the debonded strands early in the release process. Unlike the other patterns which used debonding to redistribute axial tension

from uncut strands, pattern 72G attempted to reduce the shear stress in the outer flange by redistributing the compression from cut strands. This pattern did not control the axial stress at the end of the draped strand release very well because the peak tensile stress was located away from the debonded strands, toward the interior of the flange. While pattern 72G did decrease the shear stress at 6 in. during the middle stages of release, the reduction was no greater than for patterns 72E and 72F. However, 72G reduced the stress concentration at the base of the web more than the other patterns.

The drawback of debonding is that bond is forcibly eliminated along the few debonded strands, which is contrary to the project goal of protecting the bond in the end regions. The benefit of this technique is that the debonding is a controlled process and the effect can be checked and accounted for in the design of the girders, whereas cracking has a less predictable effect on bond.

5.3 Altering Shape of Flange

Increasing the slope of the top surface of the flange does two things. First, it stiffens the flange against the shearing forces which cause the angled cracks. Second, it reduces the stress concentration in the corner between the flange and the web, more evenly distributing the stress across the base of the web. The model was altered to double and then triple the slope of the top of the flange in the endblock. Each run was made using 72A, the original cutting pattern. The peak SP3, S13, and S12 stresses at 6 in. from the end are given in Table 5.3.

The table indicates no change in stress in steps 2 and 3, when the stress is primarily axial. There was a modest improvement during the middle stages, although much less than that achieved with cutting pattern 72D. The model with the tripled slope showed a localized increase in S12 during steps 4, 5 and 6, but this was due to using an extra row of elements in this model. At full release there was a significant improvement with the new models. The results at full release are shown in Figures 5.9 through 5.11. The side view given in each figure shows the stress concentration is confined to within the first 18 in. Changing the slope of the flange would therefore only be necessary in this region.

The side view in the above figures also indicates a high stress concentration within the

web at the end face of the girder. This is responsible for horizontal web cracks and will be discussed in detail in Appendix B.

Table 5.3 Effects of Altering Slope of Flange on SP3

Step		2	3	4	5	6	7	8	9
Normal Slope	S	103	223	459	716	849	845	880	903
Doubled Slope		103	223	438	694	825	737	767	822
Tripled Slope		103	223	434	685	813	725	673	768
Normal Slope	S	8	17	414	622	790	815	748	676
Doubled Slope		9	18	385	598	687	699	560	514
Tripled Slope		9	18	380	589	678	688	511	398
Normal Slope	S	18	43	-262	-418	-718	-973	-1040	-1070
Doubled Slope		18	42	-279	-391	-540	-767	-851	-986
Tripled Slope		18	42	-333	-476	-590	-680	-740	-969

CHAPTER 6
IMPLEMENTATION OF CRACK CONTROL METHODS

This chapter describes the field implementation of the various crack control methods at Elk River Concrete Products. First a new cutting pattern based on pattern 72D was used to eliminate angled cracking in some 45 in. deep girders. Next experimentation was performed on three beds of 54 in. deep girders. The first bed was cut with the original cutting pattern used by the precast plant. The second bed was released with a new cutting pattern which included precuts and cutting of the straight strands in alternating columns. The strands in the third bed were cut in the same order as the second bed, but debonding was also employed on five pairs of strands. The instrumentation used on these three beds is described in the next chapter. Finally, extensive precutting was successfully used to prevent any vertical cracking in a bed of 72 in. girders which had only a small length of free strand.

6.1 Test New Cutting Pattern on 45 in. Girders

On August 15, 1995, a bed of 45 in. deep girders was observed during release at Elk River Concrete Products. The girders had the same flange dimensions as the 72 in. girders, but there were no end blocks. The casting bed was 368 ft. chuck to chuck and contained three 92 ft. girders, as shown in Figure 6.1. The strand pattern and cutting order, designated 45A, are given in Figure 6.2. The cutting order was the original order used at the precast plant.

The first cracks observed were vertical cracks through the bottom flange, initiated toward the end of the draped strand release. Angled cracks on the slope then formed early during the release of the bottom strands. By the end of detensioning the vertical cracks had closed and could no longer be traced, but the angled cracks remained open. These results confirmed that both axial restraint and shear were responsible for cracking in these girders. No cracks were observed at the base of the web. It was decided to try a new release order the following day, designated 45B and shown in Figure 6.3. The new release order was based on pattern 72D, but also included a single pair of precut strands.

Prior to implementing the new pattern in the field, both cutting patterns 45A and 45B

were investigated with one-half girder models using linear functions for the transfer length. Figures 6.4 and 6.5 show the stress contours for patterns 45A and 45B, respectively. Figures 'a' and 'b' show the axial stress in the first 2 ft. of the girder at full draped strand release (step 3 of 45A, step 4 of 45B), while the remaining figures (c - g) show the SP3, S11, and S13 contours at 6 in. from the end for the rest of the release process.

The peak axial stresses at full draped release are summarized in Table 6.1. The precut strand of pattern 45B successfully reduced the axial stress beyond 9 in. from the end. Because of the transfer length of the precut strand, the stress remained high at the end, and even increased due to the greater number of strands cut. Therefore any vertical cracks which formed at this stage should be restricted to about the first 9 in. of the girder. The peak stresses at 6 in. from the end for the entire release process are summarized in Table 6.2. The steps for pattern 45B are shifted in the table for easier comparison, so that step 2 of pattern 45B is listed under step 1 in the table. By cutting the bottom strands in alternating columns, pattern 45B causes a significant reduction in shear stress in the middle stages of release. Despite the narrow web, the stress at the base of the web at full release was much less than that seen in the 72 in. girders. This is because of the fewer number of strands transferring compression in the 45 in. girders. This is consistent with the observed lack of base of web cracks.

The trial of pattern 45B gave promising results. A couple of vertical cracks were still observed, one of which extended at an angle halfway up the slope. However, these cracks completely closed by the end of detensioning and there were no other angled cracks. Due to the improvement, cutting pattern 45B was employed as the basic cutting pattern for the remainder of the casting season at the Elk River plant. During that time they have reported a large decrease in observed end cracking, as was evident in the survey forms completed before and after the new pattern was put into use (see Chapter 8).

Table 6.1 Peak S11 for 45 in. Girders at Full Draped Strand Release (psi)

in. from end	0	3	6	9	12	15	18	24
45A, step 3	447	340	252	193	211	425	463	343
45B, step 4	547	432	287	180	178	357	349	226

Table 6.2 Peak Stresses at 6 in. From Girder Face for 45 in. Girders (psi)

Step		1	2	3	4	5	6	7	8
45A	max SP3	0	115	253	479	671	667	520	456
45B		161	240	341	429	345	354	389	456
45A	min SP1	0	-32	-150	-322	-477	-760	-840	-945
45B		-167	-130	-121	-291	-414	-508	-705	-945
45A	+S11	0	114	252	394	436	248	63	-216
45B		30	151	287	374	295	154	-23	-216
45A	-S11	0	-2	-17	-164	-401	-685	-790	-870
45B		-52	-14	-20	-72	-180	-380	-460	-870
45A	+S13	0	8	16	339	503	572	529	491
45B		158	168	177	97	97	238	287	491
45A	-S13	0	-29	-45	-60	-99	-135	-167	-193
45B		-132	-128	-112	-289	-184	-108	-202	-193

6.2 Experimentation with 54 in. Girders

In this phase of the study, three different release methods were compared through visual observation, Finite element method (FEM) modelling, and instrumentation. Three beds of 54 in. deep girders were instrumented at Elk River Concrete Products. Each bed was 368 ft. long and contained three 110 ft. girders, as shown in Figure 6.6. These were the longest of a number of 54 in. girders on the production schedule, with free strand making up only 10.2% of the bed length. By comparison, the 72 and 45 in. girders were cast with 12.2% and 12.7% free strand, respectively.

The girders were released from the three beds using three different methods, shown in Figure 6.7. The first bed was cut out with the original cutting pattern used at Elk River Concrete Products, designated 54A. The second bed was cut with a new pattern, 54B, which included precuts to control vertical cracking. For the third bed, pattern 54C was implemented which had the same cutting order as 54B, but also incorporated five pairs of debonded strands. Each bed was instrumented with detachable mechanical (DEMEC) gages to measure strains on the surface of the bottom flange. Electrical resistance strain gages were used on the strands in the third bed to ascertain the effectiveness of the debonding and to measure dynamic effects (using peak strain indicators). This instrumentation is discussed in Chapter 7.

The stress contours from a one-half girder model using a linear function for the transfer length for patterns 54A, 54B, and 54C are shown in Figures 6.8, 6.9, and 6.10, respectively. Figures 'a' and 'b' show the axial stress in the first 2 ft. of the girder at full draped strand release (step 3 of 54A, step 4 of 54B and 54C), while the remaining figures (c - g) show the SP3, S11, and S13 contours at 6 in. from the end for the rest of the release process. The peak axial stresses at full draped release are summarized in Table 6.3. The peak stresses at 6 in. from the end for the entire release process are summarized in Table 6.4. The steps for patterns 54B and 54C are shifted in the table for easier comparison, so that step 5 of each pattern is listed under step 4 in the table. The patterns are discussed in detail below, along with the visual observations made when the beds were released.

Table 6.3 Peak S11 for 54 in. Girders at Full Draped Strand Release (psi)

in. from end	0	3	6	9	12	15	18	24
54A, step 3	466	365	280	247	226	430	488	362
54B, step 4	816	668	427	236	185	335	268	78
54C, step 4	838	534	271	98	67	191	126	42

Table 6.4 Peak Stresses at 6 in. From Girder Face for 54 in. Girders (psi)

Step	54A	54B	54C	54A	54B	54C
	max SP3 at 6 in. from end			min SP1 at 6 in. from end		
4	535	543	397	-330	-322	-345
5	771	573	348	-490	-353	-380
6	746	404	379	-776	-956	-840
7	673	496	459	-993	-1060	-948
8	685	685	575	-1270	-1270	-1090
	max +S11 at 6 in. from end			min -S11 at 6 in. from end		
4	463	486	279	-126	-150	-201
5	559	408	184	-372	-238	-251
6	329	119	133	-660	-452	-440
7	105	24	75	-812	-830	-700
8	-202	-202	-74	-920	-920	-772
	max +S13 at 6 in. from end			min -S13 at 6 in. from end		
4	364	347	302	-56	-58	-66
5	538	331	285	-94	-80	-85
6	626	374	373	-132	-105	-110
7	678	585	543	-167	-165	-134
8	658	658	605	-199	-199	-157

6.2.1 Bed #1, Release Method 54A

The first bed of girders was cut using pattern 54A, shown in Figure 6.7, which was the original cutting pattern used at the precast plant. The stress contours shown in Figure 6.8 were similar to those for pattern 45A (figure 6.4), but the magnitudes of both axial and shear stresses were generally a little higher. This was because the shorter length of free strand increased the restraint from the uncut strands. The stress at the base of the web at full release was between that of the 45 and 72 in. girders.

When pattern 54A was used to cut out the first bed, the result was a severe problem of vertical and angled cracking, shown in Figure 6.11. The numbers in the figure indicate which pair of strands was cut just prior to when each crack was first observed, although some cracks may have formed earlier without being detected. Most of the vertical cracks formed at the end of the draped strand release and cutting of the hold-downs. The maximum principal stress in the model at full draped release was 488 psi at the end of the sole plate, which was nearly equal to the uniaxial cracking stress, calculated to be 490 psi ($6\sqrt{f_c'}$) based on the tested release strength of 6700 psi. The other principal stresses in the model were negligible. One of the observers reported that during the draped strand release the worker cutting the strands between ends 2S and 3N was getting ahead of the other cutters. This should have increased the stress in ends 2S and 3N (see Sections 2.2 and 4.3), which would help explain the vertical cracking at these ends.

Because cracking invalidates elastic theory, the FEM model should only be accurate to the point when the first crack forms. Ideally it would predict where the crack would form. At the end of the draped strand release, when most of the vertical cracks formed, the model indicated the first crack should form at the end of the sole plate, 15 in. from the end of the girder. However, there were no cracks at this location. This contradiction of the model is discussed in Appendix A.3. One reason the model cannot accurately predict the location of the cracks is because it lacks the ability to simulate the reverse tensile transfer length from the uncut strands. The cracks may also form at arbitrary locations due to preexisting flaws (e.g. poor consolidation or shrinkage cracks) or at local stress concentrations (e.g. transverse rebar locations). The design plans called for G403 rebar around the perimeter of the strand group at 2, 6, 10, and 21 in. from the end, and G507 rebar at 2, 4, 6, 8, 10, and 12 in. from the end. The vertical cracks typically

formed around 5, 12, and 20 in. from the end, so there was no direct correlation.

6.2.2 Bed #2, Release Method 54B

While the most effective method of eliminating the vertical cracking was expected to be debonding, it was desired to first try to control the cracks by altering the cutting pattern. Since these cracks formed during the draped strand release, it was decided to try "precutting" some straight strands before the draped ones. The theory behind precutting has already been discussed in Section 5.1. Multiple precutting schemes, shown in Figure 6.12, were modelled prior to release of the second bed of girders. Table 6.5 lists the maximum axial stress through the draped strand release for each pattern. Pattern precut6 was not tested with the model prior to releasing the second bed and will be discussed in Section 6.3. It is included in the figure and table for convenience and later comparison with the other patterns.

Comparing the various precutting patterns to pattern 54A, it is apparent that the axial stress at full draped strand release was greatly increased at the very end of the girder. However, starting at 12 in. from the end the stress is lower for the precut patterns, and is significantly lower at 24 in. from the end. This is because the compressive force provided by the precut strands increases with distance from the end of the girder due to the transfer length.

Comparing the various patterns to each other, first notice that the effects of precut1 and precut5 were smaller because they entailed precutting 3 pairs of strands, while the other patterns precut 4 pairs. Patterns precut1 and precut2 were attempts to distribute the precut strands across the girder cross section and thereby minimize the peak stress. Patterns precut4 and precut5 were attempts to compress the surface of the flange, providing confinement to the core and preventing any cracks that did form from reaching the surface of the girder. Precut3 was a compromise between these two approaches. With regard to axial stress, each pattern behaved according to the approach that was used and to the number of precut strands. For instance, the maximum axial stresses from patterns precut2 and precut4 were similar because the same number of strands were precut in each pattern. However, precut4 compressed the outside of the flange more, which also had the effect of increasing the shear stress. The peak positive and negative S13 stresses at 6 in. from the end at full draped strand release were +85/-133 for precut 2, and +215/-129 for precut 4.

Table 6.5 Axial Stress Comparison for Multiple Precutting Patterns (psi)

	54A	Precut1	Precut2	Precut3	Precut4	Precut5	Precut6
0 in. from end							
precut	-	294	401	390	370	288	506
1/2 draped	209	598	701	683	655	558	795
all draped	466	885	1010	963	954	816	1120
6 in. from end							
precut	-	78	107	113	115	105	139
1/2 draped	126	248	242	229	248	272	231
all draped	280	406	406	379	411	427	397
12 in. from end							
precut	-	15	16	34	20	37	21
1/2 draped	103	35	24	33	28	64	8
all draped	226	136	107	135	115	185	106
18 in. from end							
precut	-	-147	-213	-197	-187	-109	-274
1/2 draped	220	-93	-166	-160	-140	13	-225
all draped	488	164	78	134	56	268	-11
24 in. from end							
precut	-	-182	-261	-260	-235	-197	-334
1/2 draped	170	-156	-236	-230	-211	-105	-312
all draped	360	-15	-128	-67	-119	78	-231

At the time when these patterns were originally compared, prior to the release of the second bed of girders, comparisons were made based on the principal stress, SP3, the peaks of which tended to be highly localized in many cases. For this reason, and because of the influence of shear stresses, it was not easy to compare the patterns and no clear favorite emerged. The pattern chosen for trial was precut5. This selection was based on the philosophy of confining the core of the flange and preventing cracks from reaching the surface of the flange. The pattern was also deemed easy for the plant workers to follow. The full cutting pattern, 54B, was shown in Figure 6.7. The stress contours were given in Figure 6.9 and summarized in Tables 6.3 and 6.4.

Like patterns 72D and 45B, the straight strands were cut in alternating columns. However, the direction of cutting was reversed so that the columns were cut from the outside to the inside, rather than from the inside to the outside. This was a continuation of the attempt to confine the core of the flange. A comparison of two models run without precuts suggested the direction of cutting had very little effect on the peak stresses. Steps 5, 6, and 7 in Table 6.4 show that the axial stress was more evenly distributed on the flange cross section due to cutting the strands in alternating columns. The magnitudes of both the peak tensile and compressive stresses were reduced, decreasing the axial stress gradient and reducing the horizontal shear stress which causes the angled cracks.

The actual release of the second bed of three girders gave good results, with less cracking than what was observed for the first bed. There was one less observer that day, so only two of the six girder ends were observed closely during release. The cracking at these ends is shown in Figure 6.13a. Figure 6.13b summarizes the data from a survey form filled out by a plant worker watching the opposite side of the bed. The worker had adequate time to examine the whole bed while cutting was suspended so that the DEMEC gages could be read (see Chapter 7). As anticipated, the cracks that did form were very close to the end of the girder. However, precutting strands near the surface of the girder did not prevent the cracks from reaching the girder surface. Further from the end, compression from the precut strands seemed to have successfully stopped the cracks. The angled cracks noted on the survey form suggest it was a poor choice to cut from the outside toward the inside. Since very few angled cracks were noted during the second half of the casting season, when the cutting patterns were based on 45B, this

suggests that cutting from the inside to the outside is more effective at controlling the shear stress.

6.2.3 Bed #3, Release Method 54C

Because vertical cracking was not completely eliminated from the second bed of girders, debonding was used in combination with pattern 54B for the third set of girders. The debonding pattern is shown in Figure 6.7. Debonding was accomplished by placing a plastic sheath around the selected strands. Because of concern over possible corrosion that could be associated with sheathing strand, debonding was restricted to the interior strands. In addition, the sheathing did not begin until a few inches from the girder face, leaving a short "plug" of fully bonded concrete for added corrosion protection. Sheathing was only applied to the south end of the middle girder (2S) and the north end of the south girder (3N). At end 2N there was a 4 in. plug of concrete and 16 in. of sheathing, while end 3N had a 2 in. plug of concrete and a sheathed length of 18 in. It was anticipated that the strand would slip through the plug, making the effective debonded length 20 in. in each case.

The SP3 contours from the corresponding model were shown in Figure 6.10, and summarized in Tables 6.3 and 6.4. Table 6.3 shows the expected drop in axial stress due to the debonding from 3 to 15 in. from the girder face. The table indicates similar stresses at the girder face for patterns 54B and 54C. This is because the table only lists the peak stress on the cross section. The full stress contours in Figures 6.9a and 6.10a show that the area of concrete under high axial tension was greatly reduced. While an increase in stress should be expected where the debonding terminates (at 18 in. in the model), the table and contours show a continued reduction compared to pattern 54B. This was because the drop in stress in the debonded region reduced the force in the sole plate, decreasing the stress concentration at the end of the sole plate. Table 6.4 shows a large drop in axial tension at 6 in. from the end for most of the release process, as well as a small decrease in the shear stress. Unlike method 54B, in which only the cutting order was changed, method 54C changed the stresses at full release. Debonding decreased the compression in the bottom flange, which also reduced the concentration of shear stress at the base of the web.

The release of the final bed of girders gave good results, this time with very little

Table A.1 Peak S11 for 54 in. Girders at Full Draped Strand Release, Original and Spring Models (psi)

in. from end	0	3	6	9	12	15	18	24
original models								
54A, step 3	466	365	280	247	226	430	488	362
54B, step 4	816	668	427	236	185	335	268	78
54C, step 4	838	534	271	98	67	191	126	42
spring models								
54A, step 3	260	240	236	212	219	415	479	377
54B, step 4	280	336	316	220	172	298	244	72
54C, step 4	245	210	140	88	46	147	76	16

A.2 Mesh Effects

While the mesh of continuum elements was finer in the region of cracking than elsewhere, it was still relatively coarse. The smallest basic element was 2 x 2 x 3 in., which matched the 2 in. grid of the strands. Therefore a test of the 54 in. one-half girder model was made using refined 1 x 1 x 2 in. basic elements. The resulting contours of SP3 using pattern 54A are shown in Figure A.5. Contours for the original mesh were shown in Figure A.3. At the end of the girder, the peak stresses for the fine mesh were significantly greater than those obtained with the original mesh. The reason can be seen in the contours at the end face when all the draped strands have been cut. The stress was high around the nodes where the truss elements were attached, but the stress was low at the other nodes since no force was applied directly to them. The larger elements of the original mesh caused the restraint force to be applied to every node within the strand group, eliminating the stress peaks and valleys. From the other perspective, the smaller the elements get, the smaller the area over which the tensile force is

shown in Figure 6.12. The maximum axial stresses, included in Table 6.5, were significantly lower than the other patterns due to the increased number of precut strands and their broad distribution.

The actual strand pattern and cutting order for the 72 in. girders is shown in Figure 6.15 and is designated 72H. The girders were not instrumented due to the short lead time and the expectation of significant cracking. When the bed was released on October 21, 1995, there were *no* cracks observed in the flange, despite having three people watching closely. There were still two to three horizontal cracks in the web at each end, although they were a little shorter than normal. It is worth noting that release was delayed about 3 hours due to failure of the control cylinders to meet the required strength at first testing. It was also a cold day, so the girders were covered with two tarps instead of one, but no steam was used. As mentioned previously, the plant personnel testified that more cracks are generally observed when it is cold.

CHAPTER 7
INSTRUMENTATION OF 54 IN. GIRDERS

7.1 DEMEC Gage Setup

The 54 in. deep girders were instrumented to obtain additional information regarding the effect of the cutting patterns and debonding on the stress distribution measured on the girder surface during the various stages of release. It enabled comparison among analytical, experimental, and visual evaluations of the problem. DEMEC gages were used to measure girder surface strains. These consisted of threaded brass inserts cast into the girder and contact seats which were screwed into the inserts after removal of the steel forms. The gages were set with a 4 in. gage length and read using a Whittemore gage equipped with a digital readout, accurate to 0.0001 in.

Figure 7.1 shows the locations of the gages within the bed and the arrangement of the DEMEC points at each location. The original plan called for at least one set of gages adjacent to every free span, with additional gages at the most critical location in the bed. This location should be adjacent to the shortest free span, based on the full bed analysis of the 72 in. girders (see Section 4.3). The two free spans between the girders were of equal length, but a full bed model of the 45 in. girders suggested the stresses would be slightly larger adjacent to the southern span. The original plan had to be scaled back because taking so many DEMEC readings would have slowed down the release process to an intolerable extent. Only four of the six gage locations were used for bed #1 (pattern 54A). For beds #2 and #3 only three locations were instrumented, but the number of gages at each location was increased to cover the entire transfer length region. It typically takes approximately 15 minutes to release girders from a bed. Even with the scaled down instrumentation, this time expanded to approximately 3 hours.

Gage locations D and F each had a single line of gages to measure axial strains, along with two rosettes to measure principal strains. Gage locations B and C each had three lines of gages to measure axial strains. A principal strain calculation was made for each gage on the middle line (e.g. using gages B-1, B-2, and B-16). Additional data points were generated by averaging the axial strain readings on the middle line (e.g. using gages B-2, B-3, and the average

of gages B-16 and B-17). Notice this allows a single crack to affect three data points.

7.2 Difficulties with DEMEC Gages

To minimize the time delay during release of the first set of girders, each DEMEC gage was read only once at selected stages of release, with a few second readings taken of random gages. As cutting progressed, a steady rain developed and the temperature dropped making reading conditions deteriorate. Due to this and a growing recognition of the variability of the readings, rereads were taken with increasing frequency and all gages were read twice at the end. If the second reading varied more than 0.0008 in. from the first, more readings were generally taken until the difference was resolved. The average difference when exactly two readings were taken (excluding three or more readings) was 0.00026 in., or 64 microstrains. Base readings taken on an invar bar were only slightly more repeatable.

Prior to the second set of measurements it was recognized that there was some play in the Whittemore gage due to twisting of the rod holding the contact point. This was tightened and on the second day two measurements were taken for the vast majority of the readings. Third readings were taken whenever the first two were more than 0.0003 in. apart. The average difference when exactly two readings were taken was 0.00016 in., or 41 microstrains.

While taking the third set of measurements it soon became apparent the Whittemore gage had loosened again. Therefore the gage was purposely rocked back and forth to read both ends of the range allowed. The value recorded was a quick estimate of the midpoint. The average difference when exactly two readings were taken in this manner was reduced to 0.00012 in., or 30 microstrains.

7.3 DEMEC Gage Results

The data from the first bed (release pattern 54A) is shown in Figures 7.2a through 7.2d, with positive strains indicating tension. At first glance the data appears erratic, but this is the result of cracks which passed through the instrumented area. The annotation in the figures reflects the cracks that were recorded and shown in Figure 6.11. Only the data from the middle lines of B and C are shown since the cracking invalidates the calculations of principal strains,

which assume elastic behavior. The maximum single reading was 1970 microstrains across a vertical crack running through the upper line of gage B (gage B-21 in Figure 7.1). If all the strain occurred at the crack, this would indicate a crack opening of about 0.008 in. The maximum strain at the end of detensioning was 1410 microstrains on an angled reading (gage B-8 in Figure 7.1) which crossed the angled crack passing through gage B. The corresponding crack width would be about 0.006 in.

The data from beds #2 and #3 (release patterns 54B and 54C) were much smoother and are shown in Figures 7.3a through 7.3j, and Figures 7.4a through 7.4j, respectively. These include the principal strain data, although some of the data for bed #2 was also affected by cracking. The data from the upper and lower lines of B and C are not shown since they were taken at fewer stages of release and just confirmed the results taken along the middle lines.

The data confirmed a number of visual observations and results from the model. The data from beds #2 and #3 confirmed a small amount of compression on the surface of the girder due to the precut strands. The DEMEC gages also verified the visual observation that the vertical cracks formed at the end of the draped strand release. In addition, the data showed that the release of the hold downs had very little effect on the strains, a fact that was evident from the model as well. Finally, the data clearly showed that the cracks at least partially closed by the end of release, especially the vertical cracks, many of which were difficult, if not impossible, to locate after full release even when their location was marked.

The principal strain data for bed #2 (pattern 54B) was influenced by the vertical crack that formed at the very end of the girder. Due to this crack, the calculated angle to the minimum principal strain was around 90 degrees from the girder axis, meaning the maximum principal strain was parallel to the girder axis (across the crack). Away from the crack, the angle was close to 0 degrees, indicating primarily axial compression. Likewise, the principal strain angles for bed #3 (pattern 54C) were between 0 and 30 degrees. The slight upward angle presumably indicates the flow of force up into the web.

A primary objective of the instrumentation was to compare the results to the FEM model. One important comparison was the strain at full release. For bed #1 (pattern 54A), the comparison was difficult due to the cracking and because the DEMEC gages did not cover the

entire transfer length. Despite the cracking, the data showed generally increasing compression with distance from the end. For bed #2 (pattern 54B), the final curves of the measured data indicated a transfer length of about 20 to 24 in., which was shorter than the 30 in. transfer length used in the model. At the end of the transfer length, the data gave compressive stresses ranging from 800 to 1000 microstrains for gage line C. For comparison, the model predicted a strain around 720 microstrains, and hand calculations gave a strain of about 800 microstrains. For bed #3 (pattern 54C), the end of the transfer length was less clear because the debonded strands extended the transfer zone. For gage line C, the data gave a maximum compression of 900 microstrains, while the model peaked at only 690 microstrains.

These results indicate the compressive strain in the model at full release was a little low. The reason may lie in how the concrete was modelled. First, the model used a linear-elastic material model for the concrete. Use of a nonlinear material model would increase the concrete strain at the end of the transfer length. Second, the elastic modulus used in the model, 4750 ksi, may have been too high. This value was calculated using ACI 318-89 (Revised 1992) 8.5.1, $E_c = 57000*\sqrt{f_c'}$, based on a compressive strength at the time of release of roughly 7000 psi. The actual measured release strengths for beds #1, 2, and 3 were a little lower at approximately 6700, 6550, and 6950 ksi, respectively. A smaller modulus of elasticity would also be calculated with the formula ACI 363 suggests for high strength concrete, $E_c = 40{,}000*\sqrt{f_c'} + 1{,}000{,}000$ psi. Decreasing the elastic modulus of the concrete would also increase the elastic shortening of the girder, increasing the axial restraint from the uncut strands.

7.4 Strand Gages for Bed #3, Pattern 54C

In addition to the DEMEC gages, ten electrical resistance strain gages were attached to the strands in the third bed of girders. The gages were positioned as shown in Figure 7.5. Gages #3, 6, and 8 were placed on free strands to measure the restraint force before the strands were cut. The effectiveness of the debonding was checked with gages #5, 7, 9, and 10. If the debonding was fully effective the strands should behave as free strand, so the strain in these strands should match the strain in gages #6 and 8. Gages #1, 2, and 4 were on bonded sections of strand to check the rate of stress transfer from the strands to the concrete. Gages #2 and #4 were attached

to peak strain indicators to investigate the extent of dynamic effects caused by the sudden release of the strands.

Gages #1, 7, and 9 failed either during set up or early in the detensioning process. Gages #4 and 5 continued to function, but the strain levels did not change much over the entire release process and did not give sensible results. The original plan called for gages #1, 2, and 3 to be placed on strand pair #10, but they were mistakenly placed on strand pair #1, causing gage #3 to be lost upon cutting the first strand. The remaining four strain gages gave reasonable results, shown in Figure 7.6. Both strain and stress axes are shown, assuming E_s = 29000 ksi and that the strands remain elastic. The series labelled "Model 6" gives the data from the one-half girder model for the strand on which gage #6 was placed.

Gages #6 and #8 were on the free strand between the girders and went into increasing tension as cutting progressed due to the elastic shortening of the girder. Because the strands started at 200 ksi tension, they should only be able to gain around 45 ksi tension, or about 1500 microstrains, before becoming inelastic. Therefore the strand with gage #6 appeared to have strained well into the inelastic range and the stress axis of the graph is no longer accurate for this gage. Both gages #6 and #8 were lost when the strands they were on were cut. The series Model 6 indicates a good correlation between the model and the measured strain during the early stages of release. The model did not predict the high inelastic strains, suggesting the 245 ksi yield level in the model may have been set a little high. Gage #10 was on the same strand as gage #8, but was in the debonded region. Its behavior closely paralleled gage #8 until it was cut, at which time it lost all of its pretension. This indicates the sheathing on this strand was successful in preventing any bond with the concrete and that the 4 in. concrete plug did not restrict the movement of the strand.

Gage #2 was on a fully bonded strand, 12 in. from the end of the girder. The strand was the first to be cut and it lost a quarter of its prestress immediately. During the rest of the release process it slowly lost more prestress as the concrete underwent elastic shortening. At the end it had lost half its prestress, consistent with being near the midpoint of the transfer length. Gage #2 was also attached to a peak strain indicator which recorded the maximum and minimum readings from the strain gage. After each strand was released these values were cleared from memory and

a "static" reading was taken before the next strand was released. The results are given in Figure 7.7. Notice that prior to cutting the hold downs, when the vertical cracks generally formed (although none this time), the maximum reading at a given release was approximately equal to the static reading from the previous release. There was no indication of any dynamic fluctuations. This agrees with the dynamic analysis presented in Section 4.2, which suggested the dynamic effects from sudden release of the strands were relatively minor. Near the end of release there were some apparent dynamic fluctuations. At this point the girder was fully cambered and the dynamic effects may have been due to friction on the sole plate as the girder shortened and shifted in the bed.

CHAPTER 8
SURVEY FORMS

A survey form was developed to be distributed to precast producers to determine the extent of the cracking problem and the effectiveness of any procedures used to mitigate the cracking. The survey was a two page inspection form, the first page of which was used for recording cracks as they were observed to form during the detensioning process, along with relevant information such as the layout of the casting bed. The second page was used for recording cracks visible after release for those ends not able to be directly observed during release. Sample forms are filled out and shown in Figure 8.1. A cover letter was attached requesting general comments about the formation of the cracks and any methods used to mitigate them.

These forms were only distributed to Elk River Concrete Products, where plant personnel filled out and returned 50 forms. Of these, only 13 were filled out prior to the general adoption of cutting pattern 45B, and 6 of these were of 81 in. segmented girders with post-tensioning ducts and very light prestressing which did not have a problem with the cracking in question.

There were seven forms filled out for the 45 in. girders discussed in Section 6.1. Three of these were filled out for beds released with cutting pattern 45A, and four with pattern 45B. The cracks shown on these forms are summarized in Figure 8.2. Figures a - c show the angled cracking which occurred on the three beds released with pattern 45A. This researcher observed some vertical cracks for the bed released on 8-15-95, but they were not recorded on the survey forms by the plant personnel because they closed completely and could not be traced at the end of release. Figure d shows a single combined vertical-angled crack which formed on the first bed released with pattern 45B. The survey forms for the other three beds released with pattern 45B did not show any cracks.

There were two beds of 63 in. deep girders which were released with the original cutting pattern used at the precast plant. These girders experienced angled cracking similar to the 45 in. girders, but no vertical cracks were recorded. The survey forms are summarized in Figure 8.3. A third bed of 63 in. girders was released with a cutting pattern based on 45B. No cracks were

recorded on the survey form for that bed.

There were 12 forms filled out for 81 in. deep, 140 ft. long girders, all released with a cutting pattern based on 45B. Except for being 9 in. deeper, these girders were almost identical to the 72 in. girders observed at the start of the project. In these forms, there was only a single vertical crack recorded in the flange. This crack and the one in the 45 in. girder were the only cracks in the bottom flange out of all the forms filled out after the cutting pattern change was made.

There were two other types of cracks recorded on the forms. The most common was a horizontal crack in the middle of the web that started at the end face and extended up to 2 ft. into the girder. This was only a significant problem for girders at least 63 in. deep, with the 81 in. girders having 3 or 4 of these cracks at every end. A typical example is shown in Figure 8.4. The exception was a bed of 81 in. girders that was left on the bed over the weekend before being cut out. In this case only one crack per end was observed. It should be noted that all these larger girders had end blocks. These cracks were not part of the scope of the project and were not studied in depth. However, a brief discussion has been included in Appendix B.

The other type of crack observed was one that ran along the corner between the web and the bottom flange. Similar cracks were seen on the 72 in. deep, 139 ft. long girders observed in the fall of 1994. However, these cracks were only recorded on the survey forms for two groups of girders, which happened to be the shortest length girders among all the survey forms. There were three survey forms of 40 in. deep, 61 ft. long girders. Two showed base of web cracks at every end, while the third did not show any cracking. There were two survey forms of 63 in. deep, 41 ft. long girders, with cracks at 5 of 16 ends. Because both groups of girders had light prestressing, the expected stress levels in an FEM model would be relatively low.

To test the effect of girder length, the one-half girder model of the 45 in. girders was modified, shortening the girder to 2/3 its original length. The peak SP3 at 6 in. from the end at full release was unchanged, indicating girder length has no effect on the stress concentration at the base of the web. However, Figure 8.5 shows that the peak stress within the web, which is associated with the horizontal cracks in the web, increased from 727 psi to 919 psi. This was likely due to the increased slope of the draped strands. Since the survey forms did not indicate

any cracking within the web, it is possible that the location of the peak stress shifted downward to the corner between the flange and the web. Such a shift may be due to preexisting shrinkage cracks. Another possibility is that the smaller mass of the girders increases the dynamic effects of releasing the final strands.

CHAPTER 9
CONCLUSIONS AND RECOMMENDATIONS

9.1 Summary

Observations of girders at Elk River Concrete Products revealed three primary types of cracks that formed in the bottom flange of prestressed I-girders during release by flame cutting strands. The first was a vertical crack through the flange, and the second was an angled crack on the top surface of the flange. The third type of crack, less common than the other two, was a small horizontal crack in the corner between the web and the bottom flange.

The vertical cracks typically formed during release of the draped strands, which were the first strands cut in the original cutting pattern used by the precast plant. These cracks were caused by the opposing effects of strands that were cut and those that were not. The cut strands cause the girders to elastically shorten and camber. The uncut strands resist this movement and introduce a tensile restraint force into the ends of the girders. The shorter the length of free strand in a bed (as a percentage of total bed length), the greater the restraint force will be and the greater the cracking. Bed friction restricts shifting of girders along the casting bed, causing stress imbalances within the bed. The stress is highest in girder ends adjacent to the shortest lengths of free strand in a bed, and smallest in girder ends adjacent to the longest free strands. This occurs even when the strands in each free span are cut simultaneously. However, greater stress imbalances occur when the strands are not cut simultaneously. Cutting the shortest free spans first results in the greatest stresses. Therefore, even spacing of the girders in the bed (as shown in Figure 3.3) would be advantageous, though perhaps impractical. Alternatively, purposely cutting the longest free spans before the others may be prudent to prevent accidental release of the shortest free spans first.

FEM analyses using static equilibrium did not indicate high enough stresses to cause vertical cracks in all cases where such cracks were observed. A dynamic analysis of a one-half girder model suggested that dynamic effects are present, but play a minor role in the development of the cracks (see Section 4.2). Reinforced concrete is a non-homogeneous material, and cracks may initiate from shrinkage, poor consolidation, or local stress

concentrations/discontinuities at rebar or ends of sole plates.

The angled cracks were caused by shear stresses generated from the original cutting pattern used at Elk River Concrete Products. Cutting the straight strands from the outside face toward the interior of the flange was placing the outside face in compression, while the interior of the flange was under tension from the uncut strands. This resulted in large shear stresses which were effectively "shearing off" the flange.

The cause of the cracks at the base of the web was not perfectly clear. The FEM models indicated that the cracks were caused by a shear stress concentration due to the transfer of compression from the flange into the web. The survey forms suggested that other factors may be involved (see Chapter 8).

Besides changing the bed layout and the overall cutting order of the bed, three different crack control methods were analyzed with the FEM model. These were to alter the individual strand cutting order, to debond a short length of selected strands, and to change the shape of the bottom flange.

Altering the strand cutting pattern was first tested with the 72 in. girder model. Pattern 72D, in which the straight strands were cut in alternating columns from the inside to the outside, proved quite effective in reducing the shear stresses causing the angled cracks. When this basic pattern was applied to a bed of 45 in. girders at the Elk River plant on Aug. 16, 1995, there was just one combined vertical-angled crack observed. The new pattern was immediately adopted for general use at the plant, resulting in a significant drop in angled cracking since that time.

The other change that can be made to the cutting order is to "precut" some of the bottom strands before the draped strands, which are usually cut first. This introduces some compression into the bottom flange and prevents the situation where all the straight strands are in tension at once. Due to the transfer length over which compression is added from the precut strands, limited cracking may still occur in the first foot of the girder. The first bed of 54 in. girders suffered severe vertical cracking in the first 30 in. of the girders. When precutting was applied to the second bed, there was a significant reduction in vertical cracking, and those that did form were in the first foot of the girder, as expected. When more extensive precutting was applied to a bed of 72 in. girders with a short length of free strand, which increases the restraint from the

uncut strands, there was no cracking observed in the bottom flange.

Debonding can be used to reduce the vertical and angled cracking, as well as the cracking at the base of the web. Debonding works by increasing the effective free length of the debonded strands and by redistributing forces within the end of the girder. The restraint force in the debonded strands is anchored further into the girder, reducing the stress in the debonded region, and increasing the stress where the debonding ends. Because precutting has the opposite effect, temporarily increasing the stress in the first few inches of the girder and greatly decreasing the stress further from the end face, combining debonding with precutting is an effective strategy. The debonding should probably extend at least 6 in. past the end of the sole plate, where a stress concentration may already exist, unless enough precutting is used to keep this region in compression. One of the primary reasons to prevent cracking is to avoid a loss of bond between the concrete and the strands. Although cracking can be reduced by debonding some strands, by definition it guarantees some loss of bond. The principal advantage of debonding is that it can be controlled and planned for in the design.

The final crack control method was to alter the shape of the bottom flange. Increasing the slope of the top of the bottom flange can reduce the stress concentration at the base of web. For the one-half girder model of the 72 in. girders, tripling the slope decreased the SP3 stress at 6 in. from the end of the girder by about 15%. Because other factors may be involved in the formation of the cracks at the base of the web, it is not clear whether increasing the slope of the flange would be effective in preventing the cracks. This method was never employed because it would have required modifying the girder forms.

9.2 Recommendations

1. Maintain a generous length of free strand to limit restraint from uncut strands. The total length of free strand should be at least 10 to 15 percent of the bed length.
2. While simultaneous release at all points in the bed is ideal, consideration should be given to purposely cutting the longest free strands first, to preclude the possibility of cutting the shortest free strands before the other free strands.
3. To limit angled shear cracking on the top surface of the bottom flange, the straight strands

in the bottom flange should be cut in alternating columns from the interior of the flange toward the exterior face. The outermost column of strands should not be the last column released.

4. To limit vertical cracking, some straight strands should be precut prior to cutting all the draped strands. At least one pair of straight strands should be precut for every three pairs of draped strands. The lower the percentage of free strand in the bed, the more strands should be precut. The pattern of precuts depends on the overall strand pattern and the number of precut strands, but should emulate patterns precut1, precut2, and precut6 (see Figure 6.12).

5. Because of the transfer length of the precut strands, the first foot of the girder is still susceptible to cracking. This shortcoming can be overcome by debonding a short length of some of the strands in the bottom flange. The debonding should extend at least 6 in. past the end of the sole plate, where a stress concentration may already exist, unless sufficient precutting is used to keep this region in compression. Although cracking can be reduced by debonding, by definition it guarantees some loss of bond. The principal advantage of debonding is that it can be controlled and planned for in the design of the girders.

6. Consideration should be given to increasing the slope of the top surface of the bottom flange. FEM results suggest this can reduce the stress concentration in the corner between the web and bottom flange. Since the stress concentration was only significant within 18 in. of the girder face, altering the flange would only be necessary in this region. Further study is needed to determine the precise cause of the cracks at the base of the web, and whether changing the shape of the flange can prevent them.

REFERENCES

1. *ABAQUS Users Manual, Version 5.4*, Hibbitt, Karlsson & Sorensen, Inc., 1994.

2. ACI Committee 318, *Building Code Requirements for Reinforced Concrete (ACI 318-89, Revised 1992)*. Detroit: American Concrete Institute, 1992.

3. Gergely, P., and Sozen, M.A., "Design of Anchorage Zone Reinforcement in Prestressed Concrete Beams," *Journal of the Prestressed Concrete Institute*, 12, 1967, pp. 63-75.

4. Mirza, J.F., and Tawfik, M.E., "End Cracking in Prestressed Members during Detensioning," *PCI Journal*, Vol. 23, No. 2, March-April 1978, pp. 66-78.

5. *PCI Design Handbook, fourth edition*, Precast/Prestressed Concrete Institute, Chicago, 1992.

6. Zia, Paul, H. Kent Preston, Norman L. Scott, and Edwin B. Workman, "Estimating Prestress Losses," *Concrete International*, 1, June 1979, pp. 32-38.

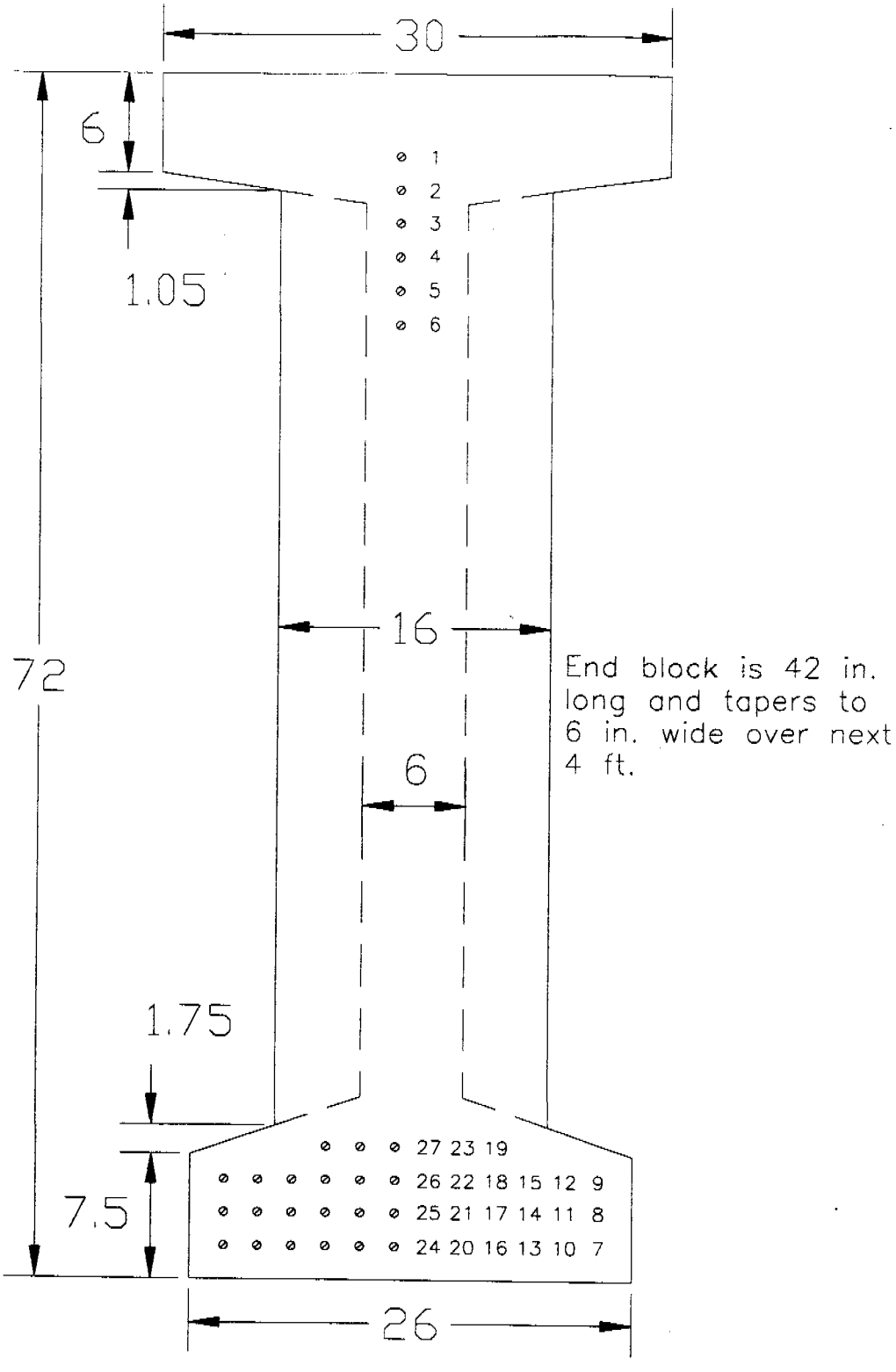

Figure 1.1 72 in. Girder Cross Section

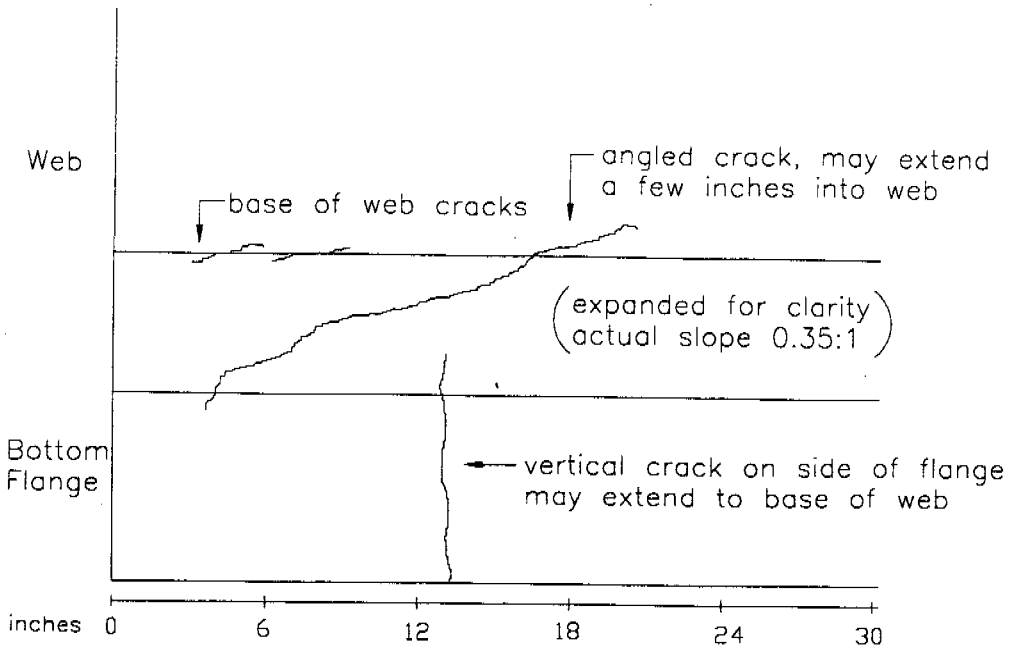

Figure 1.2 Types of Observed Cracks

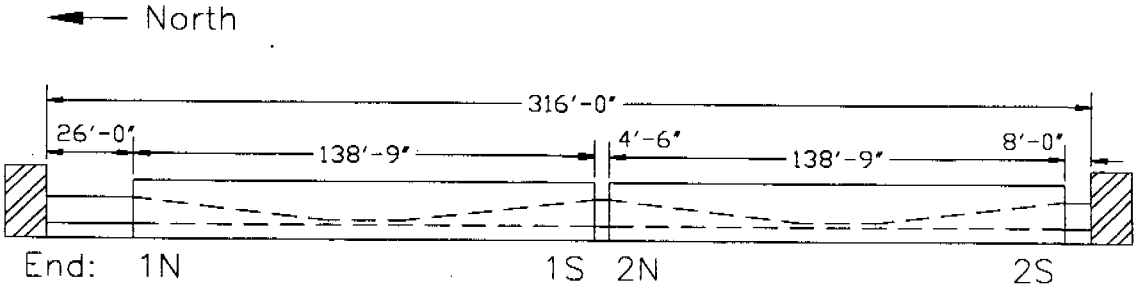

Figure 1.3 Bed Layout for 72 in. Girders

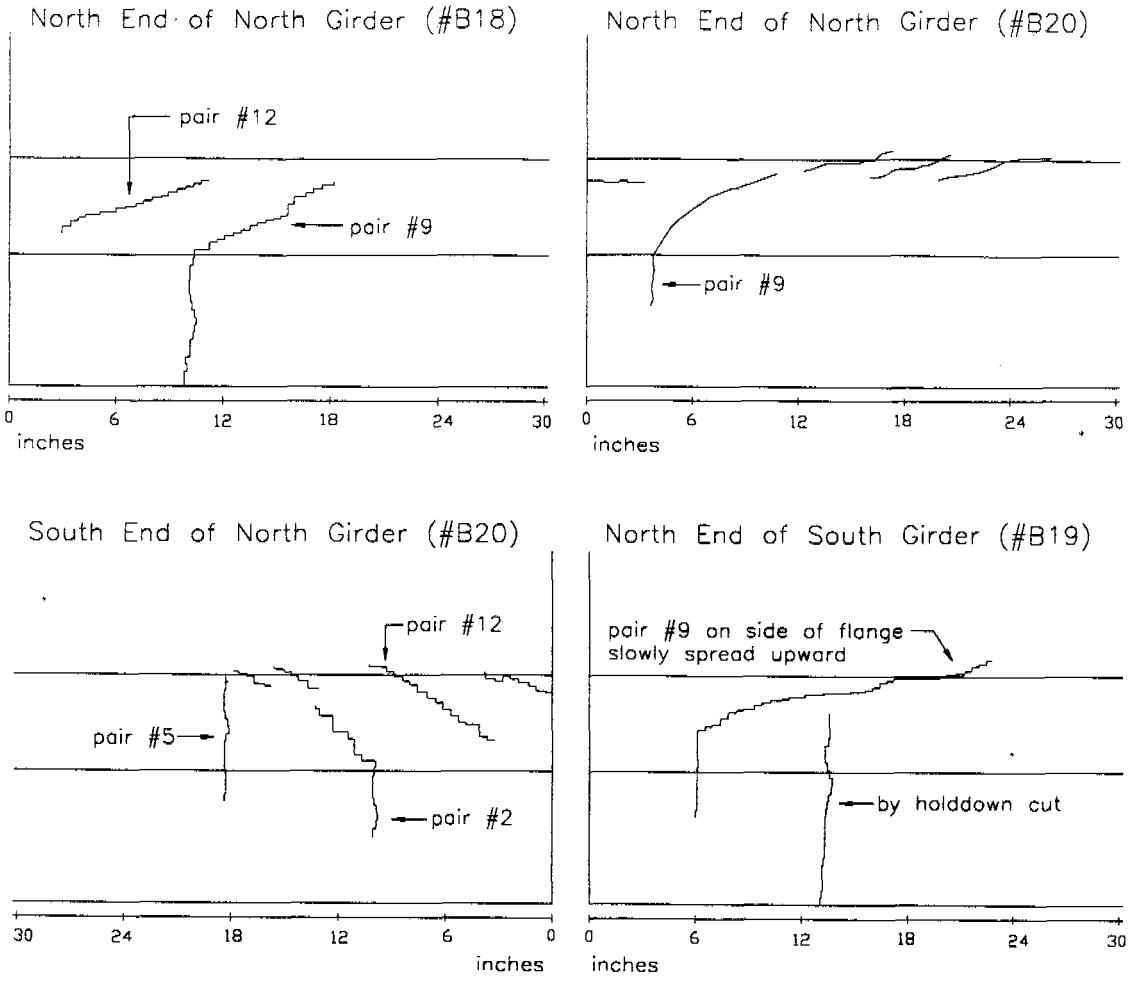

Notation refers to strand pair cut (pattern 72A) just before crack was first observed

Figure 1.4 Crack Observations During Release, 11-94

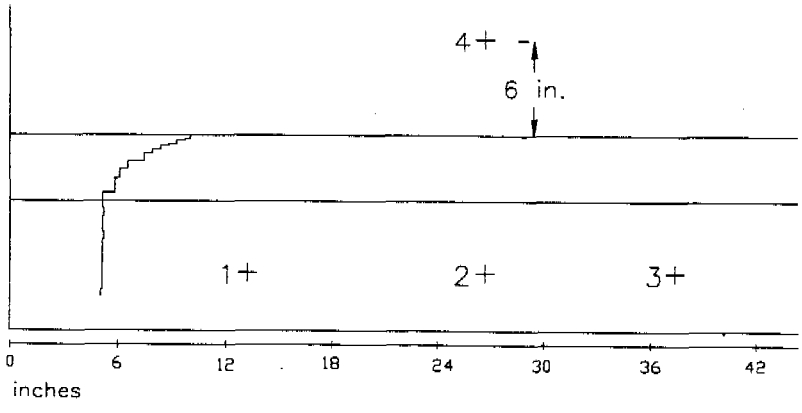

Figure 1.5 Displacement Transducers and Crack Location

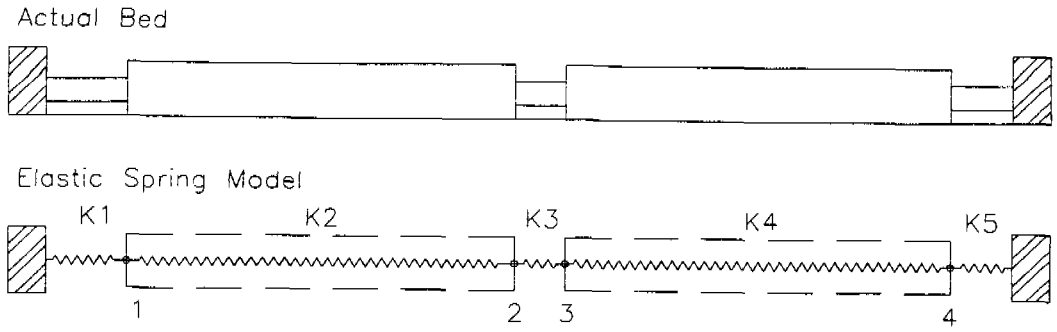

Figure 2.1 Analytical Model of Mirza and Tawfik

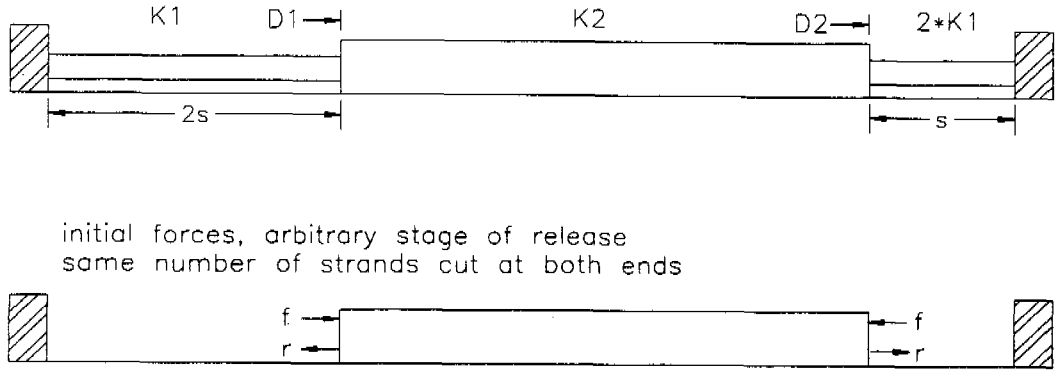

P = *prestress force per strand*

define $f = P \times$ *number of strands cut*

$$A = \frac{2K_1P}{2K_1+3K_2}\ ,\ B = \frac{P}{2K_1^2+3K_1K_2}$$

strands cut	prestress left end	prestress right end	restraint left end	restraint right end	change in D1	change in D2
initial	f	f	r	r	0	0
left end only	$f+P$	f	$r+A\left(1+\frac{K_2}{2K_1}\right)$	$r-A\left(\frac{K_2}{K_1}\right)$	$B(2K_1+K_2)$	BK_2
right end only	f	$f+P$	$r-A\left(\frac{K_2}{2K_1}\right)$	$r+A\left(1+\frac{K_2}{K_1}\right)$	$-BK_2$	$-B(K_1+K_2)$
both ends	$f+P$	$f+P$	$r+A$	$r+A$	$2BK_1$	$-BK_1$

Figure 2.2 Frictionless Bed with 1 Girder

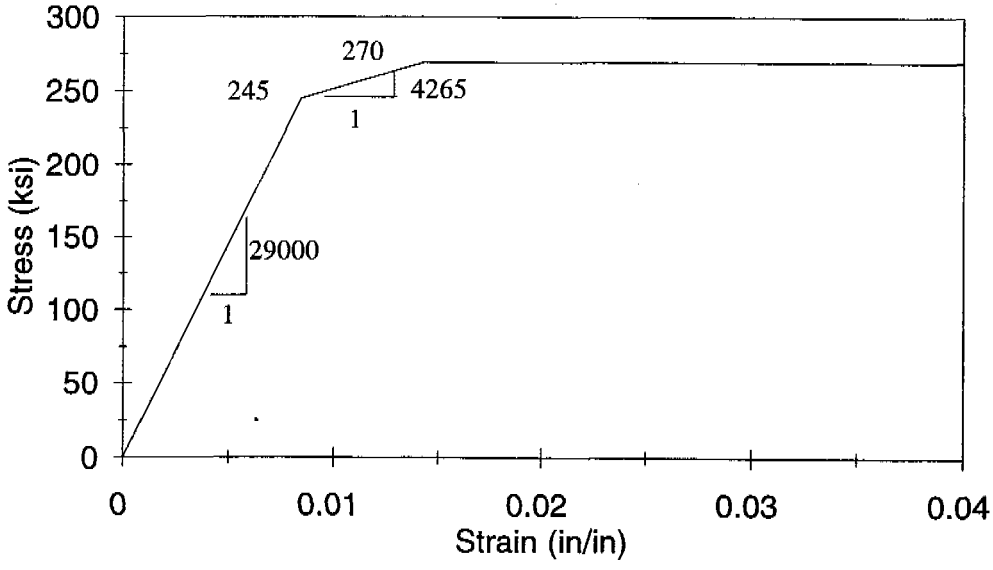

Figure 2.3 Defined Steel Behavior

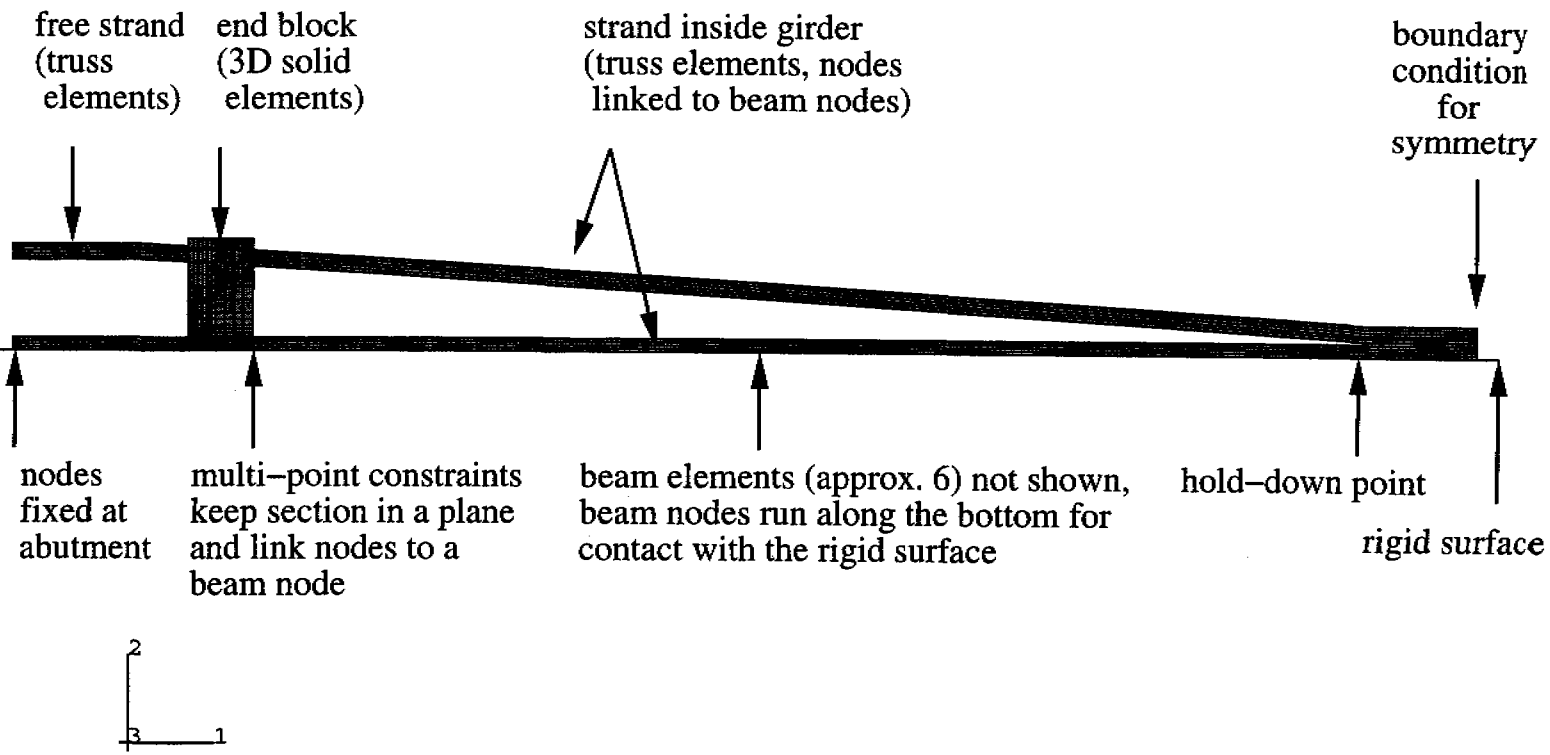

Figure 3.1 Typical One–Half Girder Model

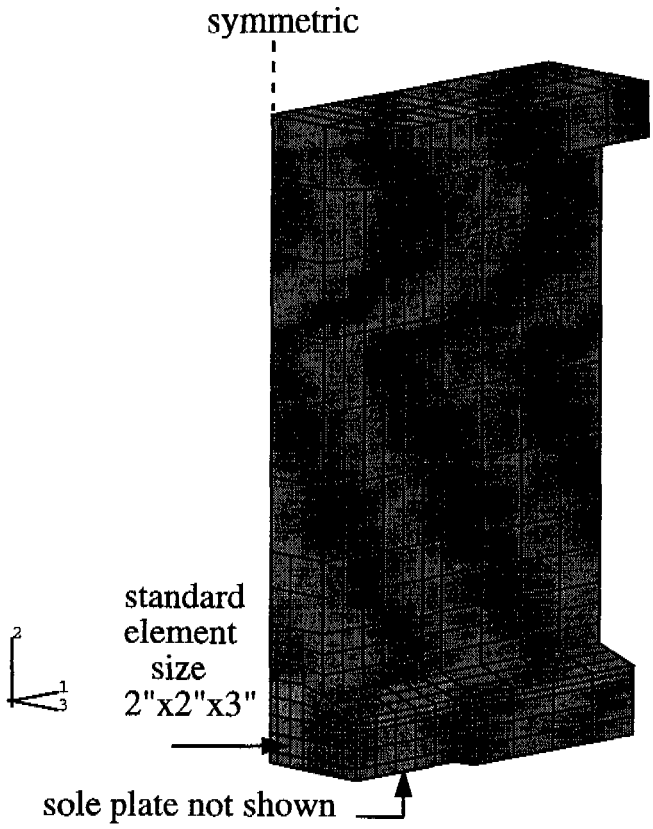

Figure 3.2 Continuum Element Mesh for 72 in. Girders

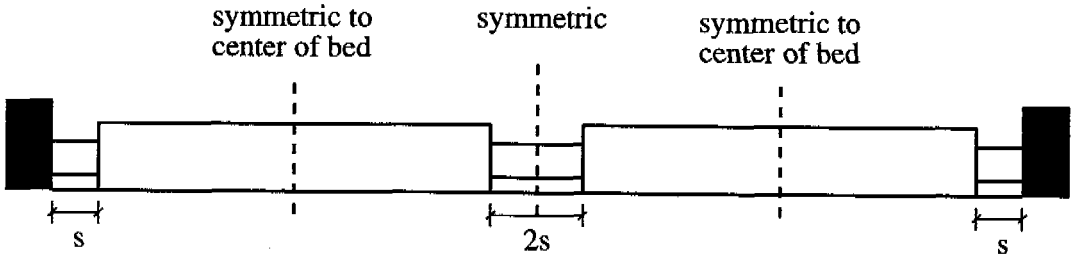

Figure 3.3 Assumed Symmetric Bed Layout

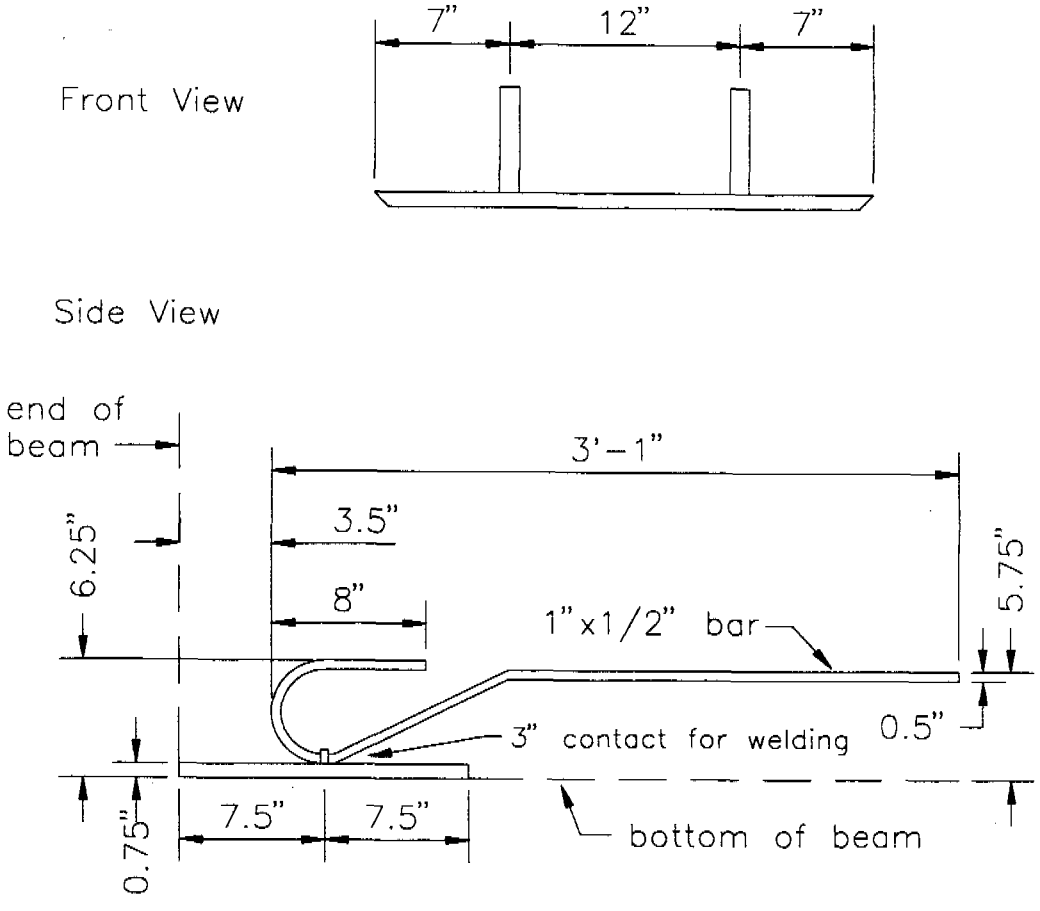

Figure 3.4 Sole Plate

Draped Strands = Pairs 1–6, Steps 2–3
Hold down cut after Pair 6, in Step 4

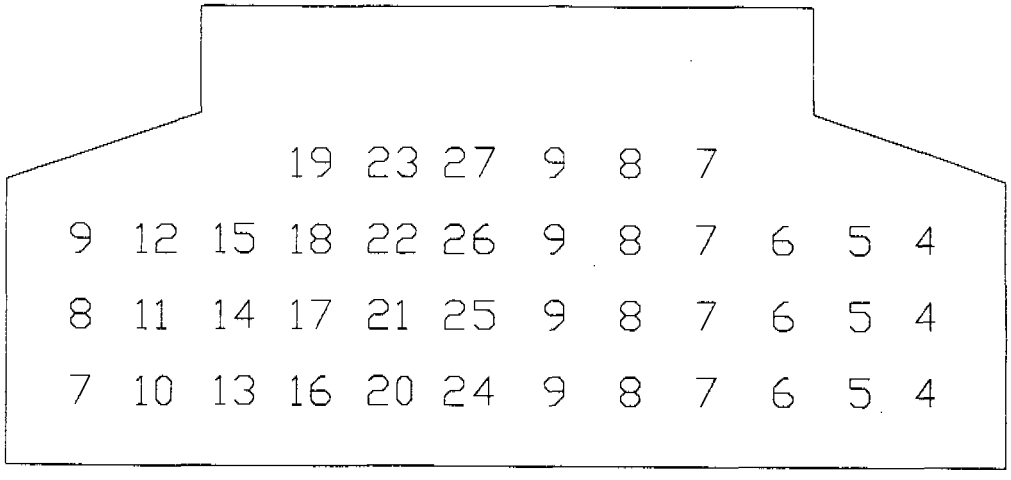

Left half shows actual cutting sequence. Right half indicates the analysis step in which each strand was cut.

Figure 4.1 Cutting Pattern 72A

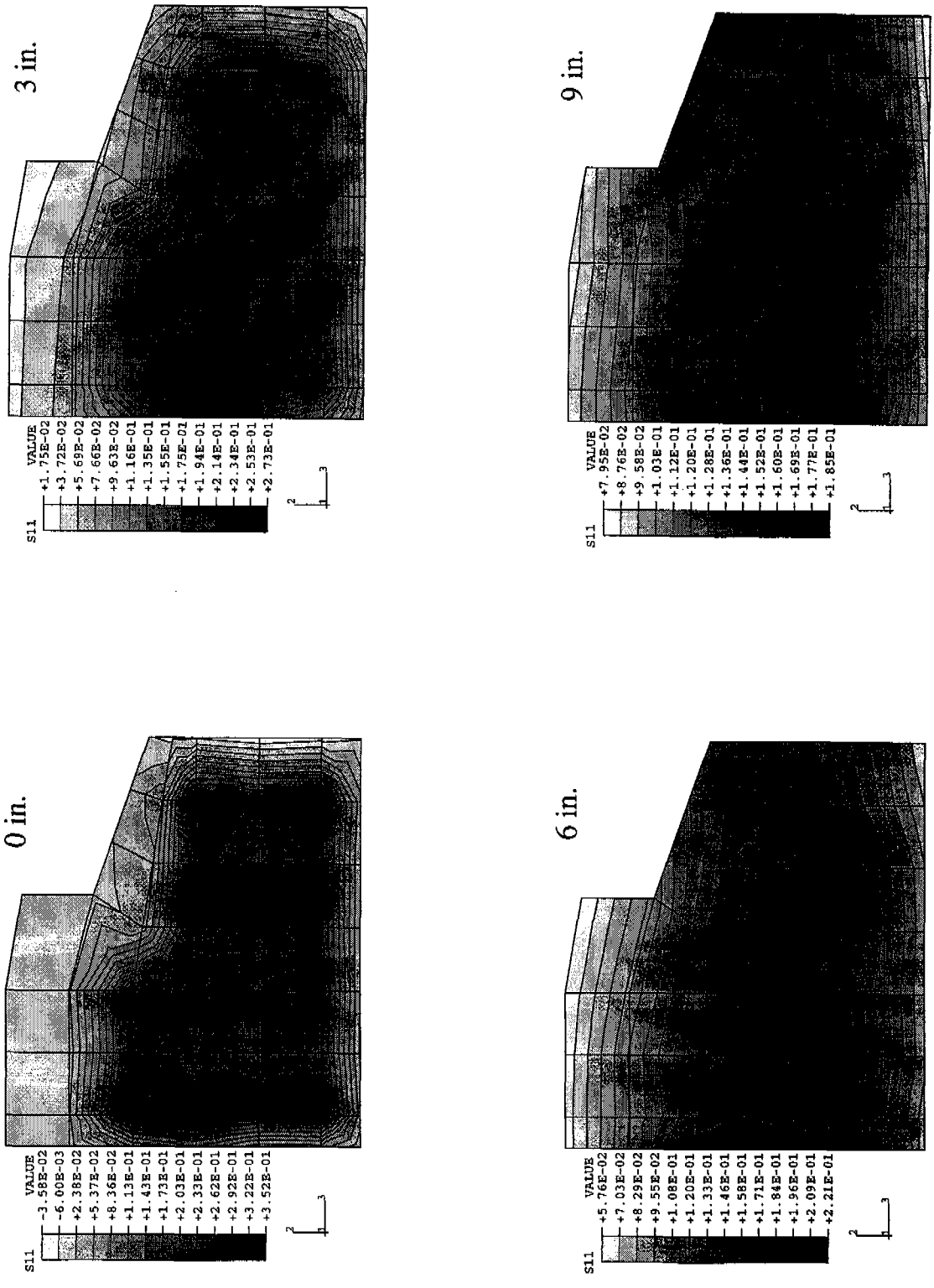

Figure 4.2a S11 Contours for Pattern 72A, Step 3

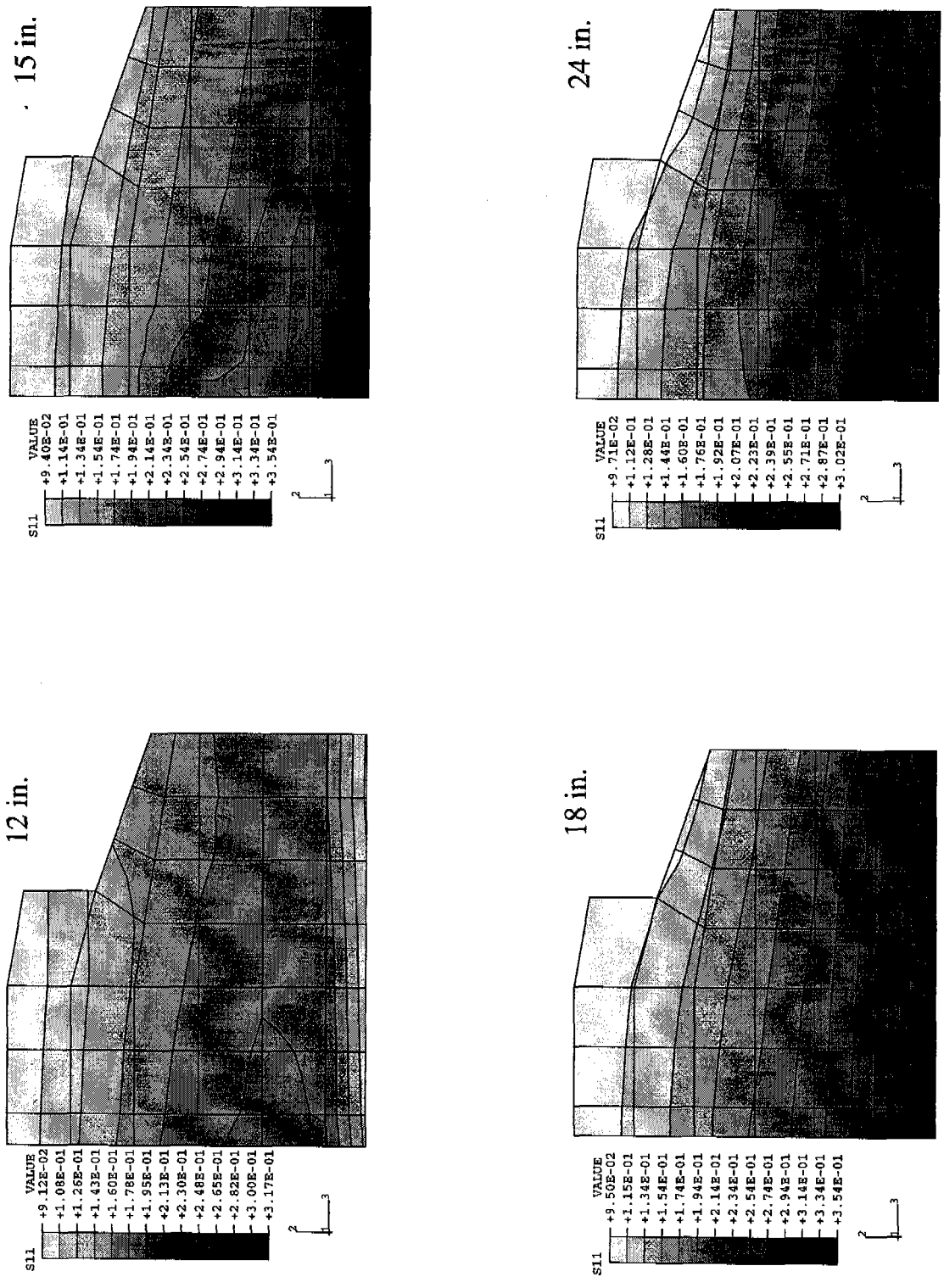

Figure 4.2b S11 Contours for Pattern 72A, Step 3

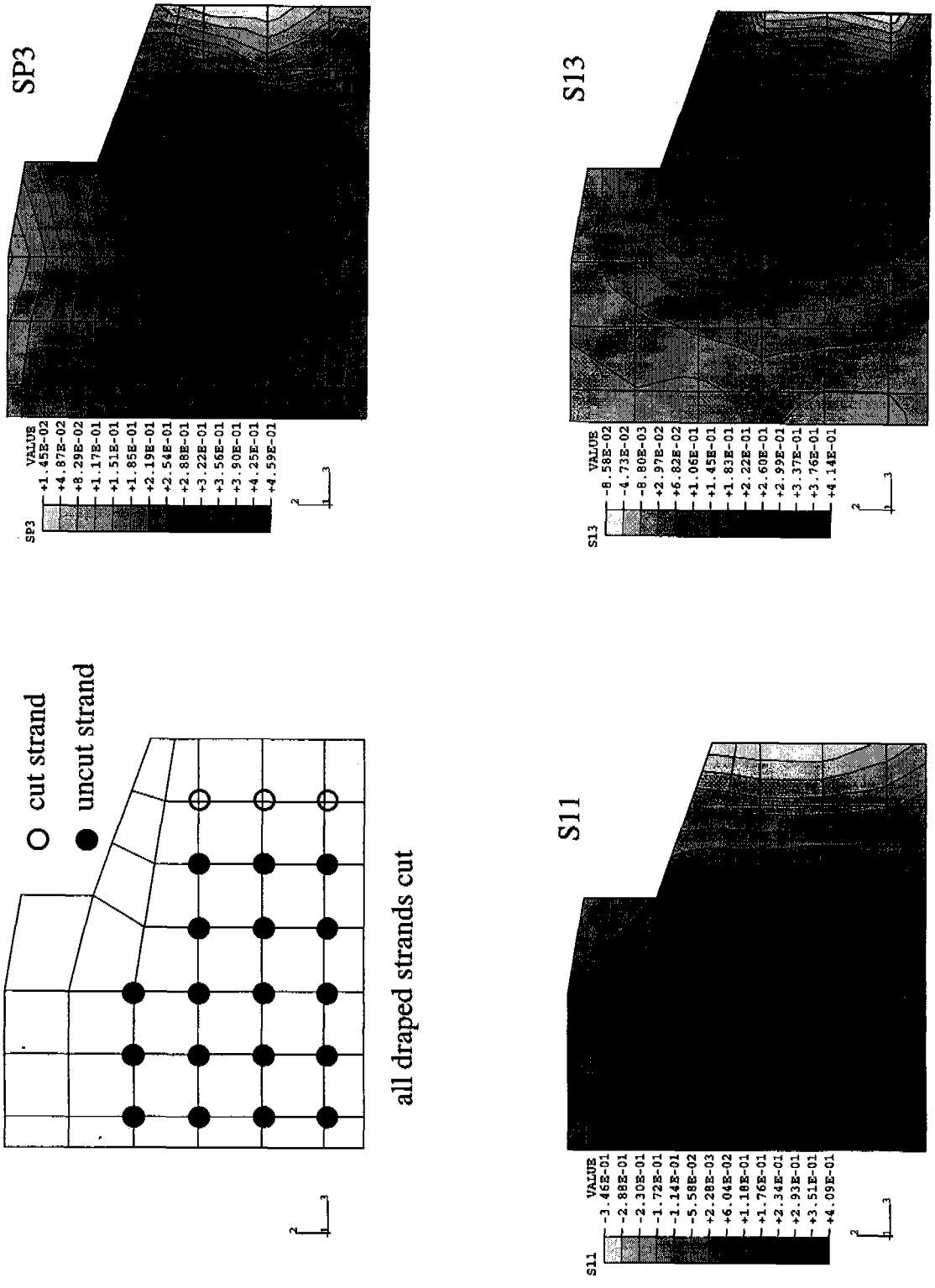

Figure 4.3a Stress Contours for Pattern 72A, Step 4, at 6 in. From End

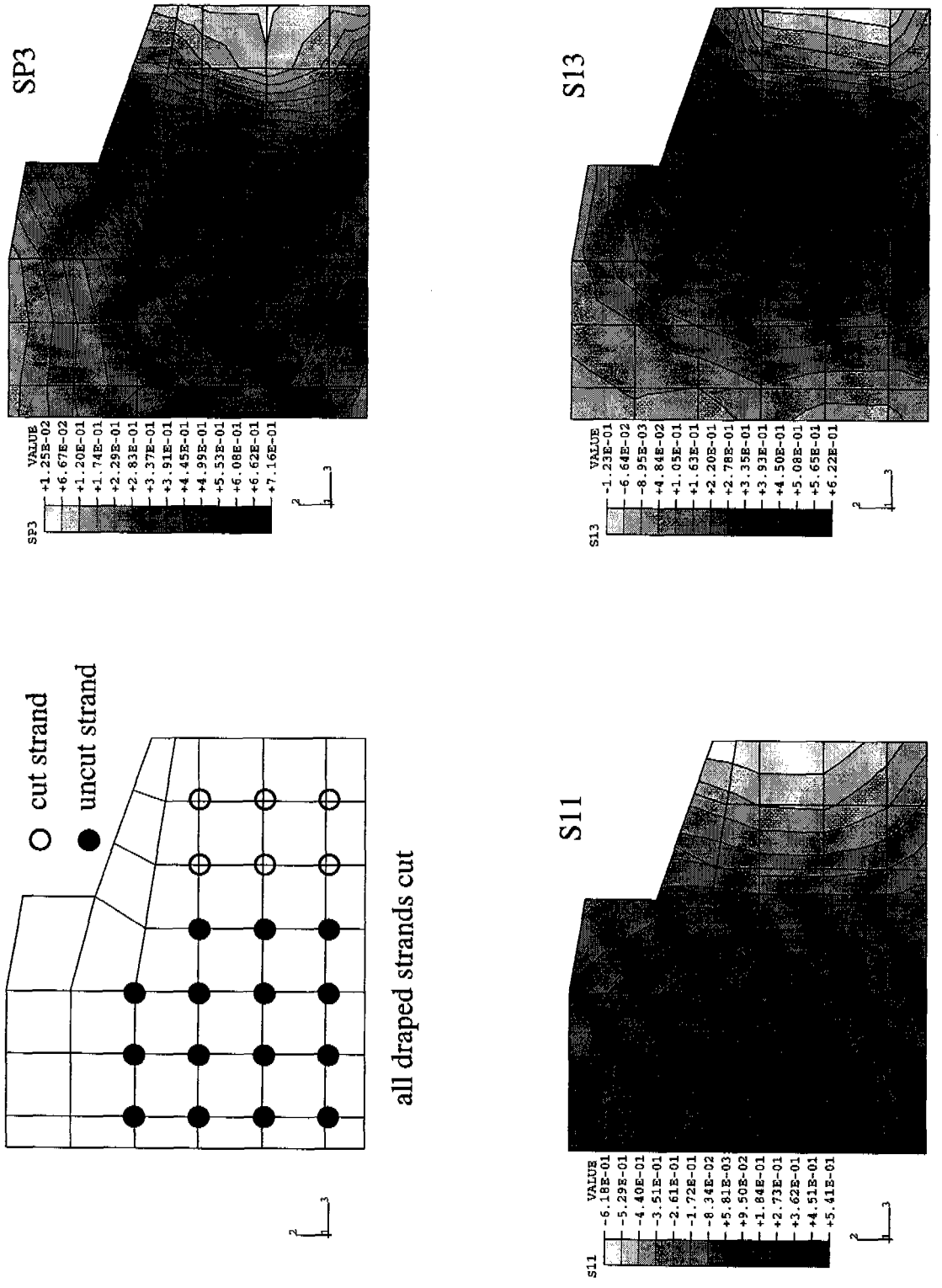

Figure 4.3b Stress Contours for Pattern 72A, Step 5, at 6 in. From End

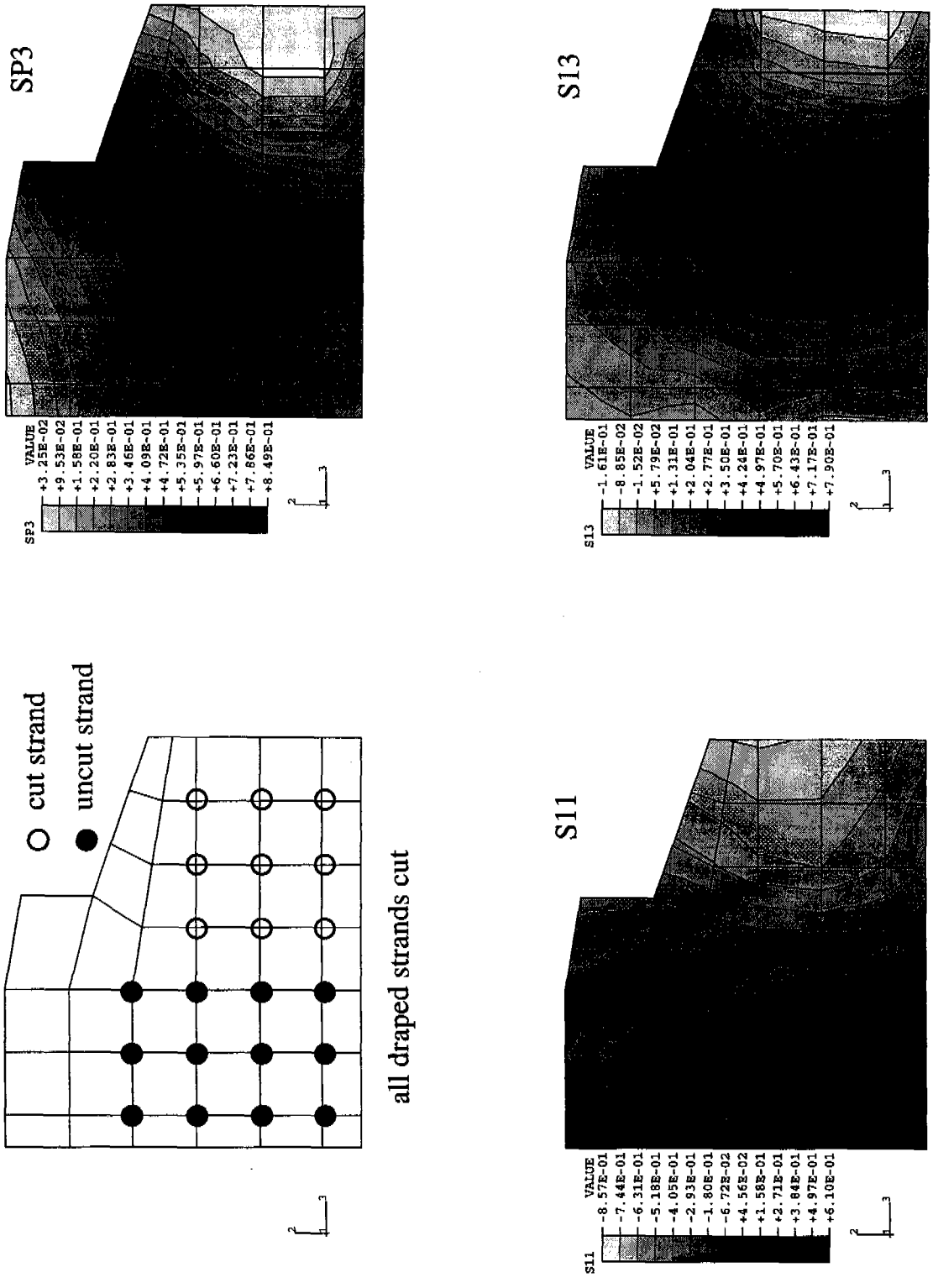

Figure 4.3c Stress Contours for Pattern 72A, Step 6, at 6 in. From End

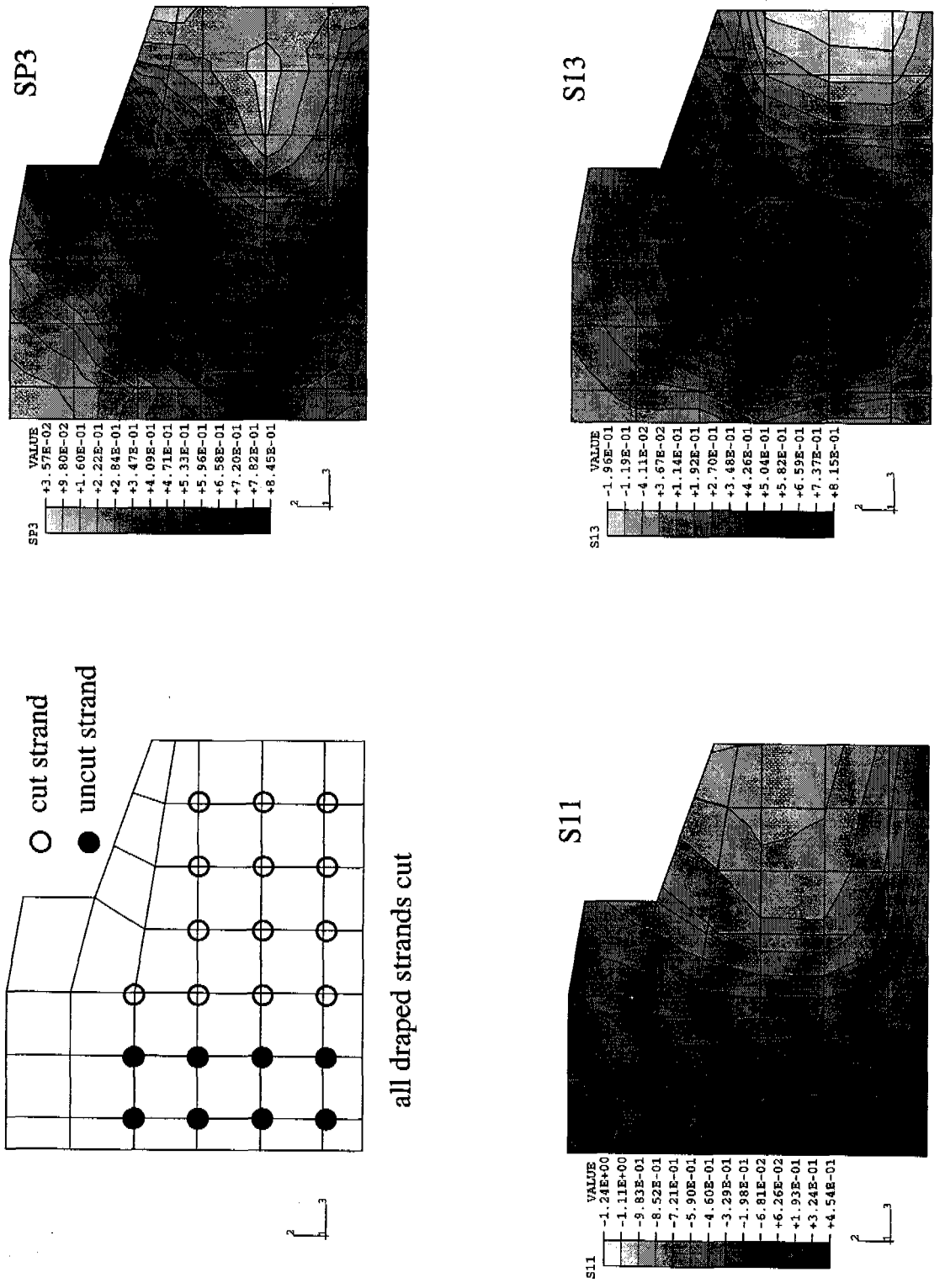

Figure 4.3d Stress Contours for Pattern 72A, Step 7, at 6 in. From End

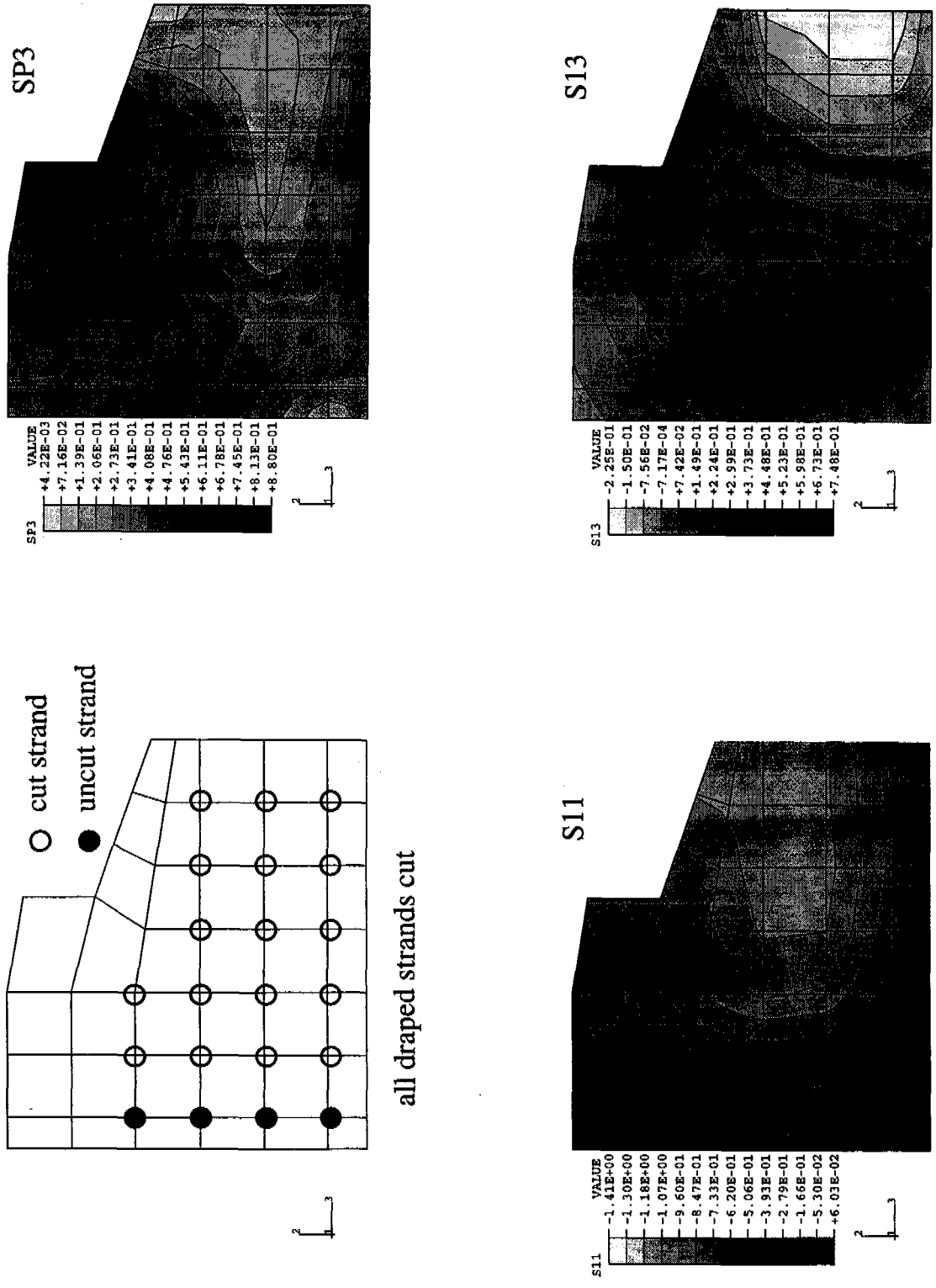

Figure 4.3e Stress Contours for Pattern 72A, Step 8, at 6 in. From End

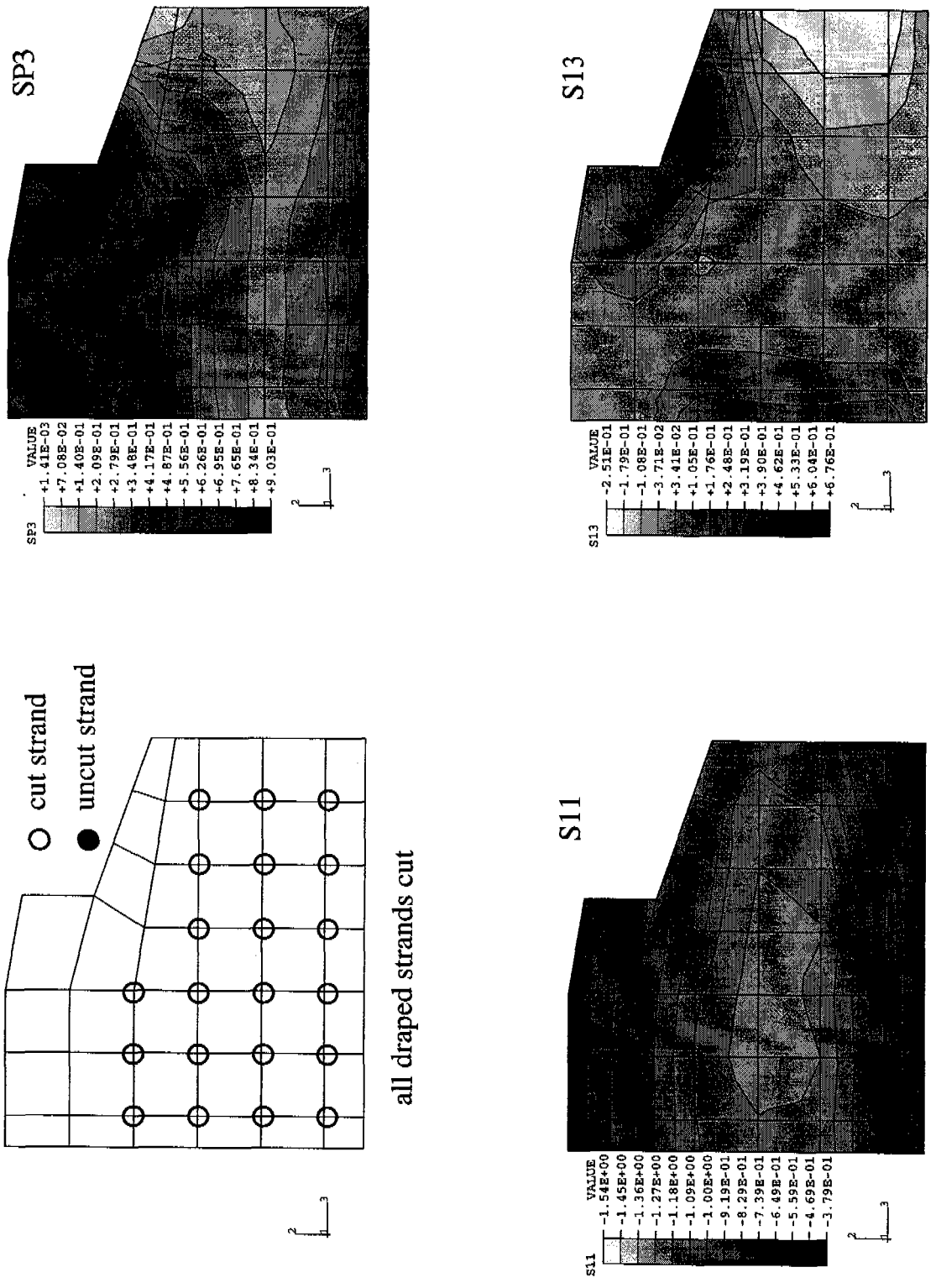

Figure 4.3f Stress Contours for Pattern 72A, Step 9, at 6 in. From End

Release of Pair 1, Pattern 72A (first draped strand)
Axial Stress in Concrete at Position of Strand Pair 17

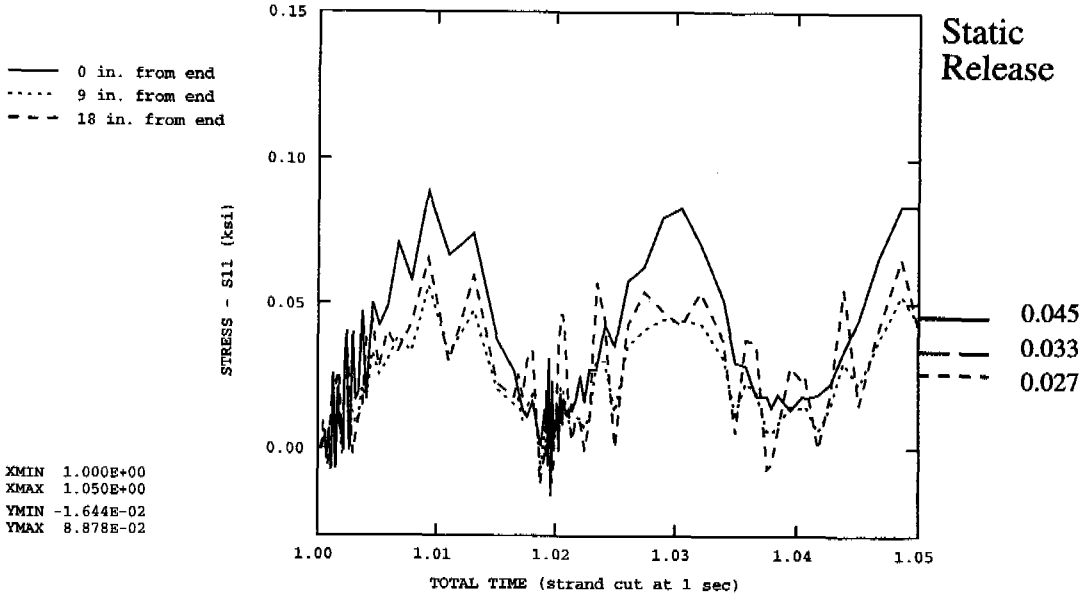

Release of Pair 6, Pattern 72A (last draped strand)
Axial Stress in Concrete at Position of Strand Pair 17

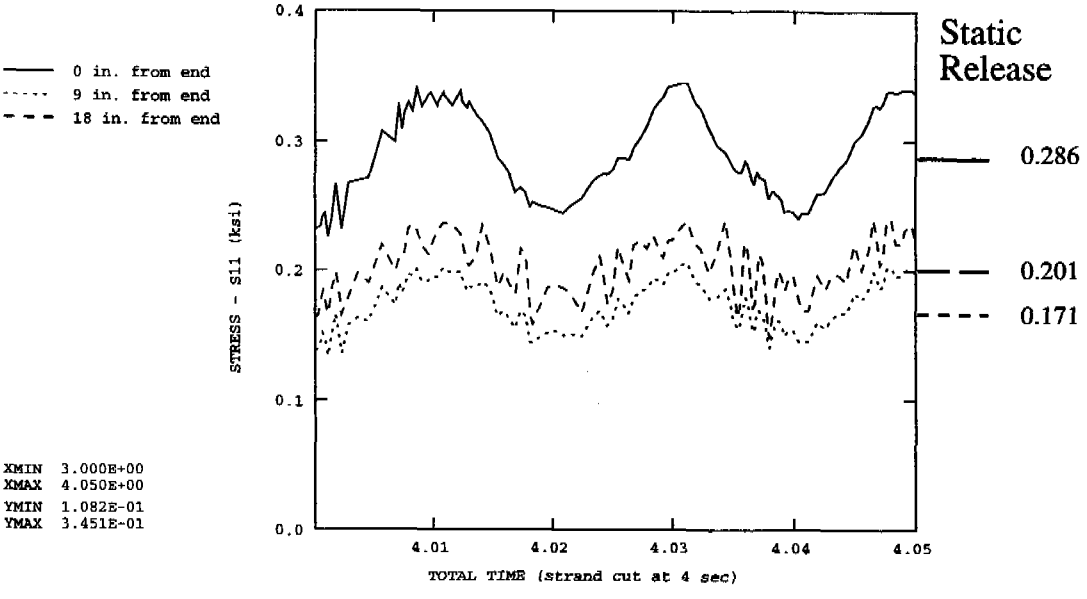

Figure 4.4 72 in. Girder Dynamic Results

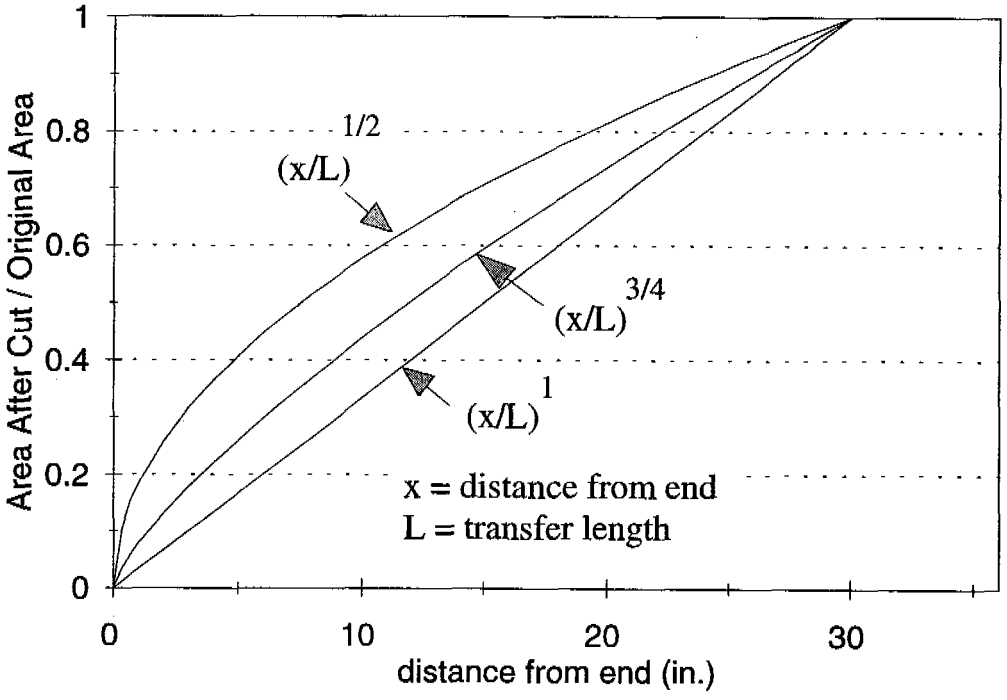

Figure 4.5 Transfer Length Area Functions

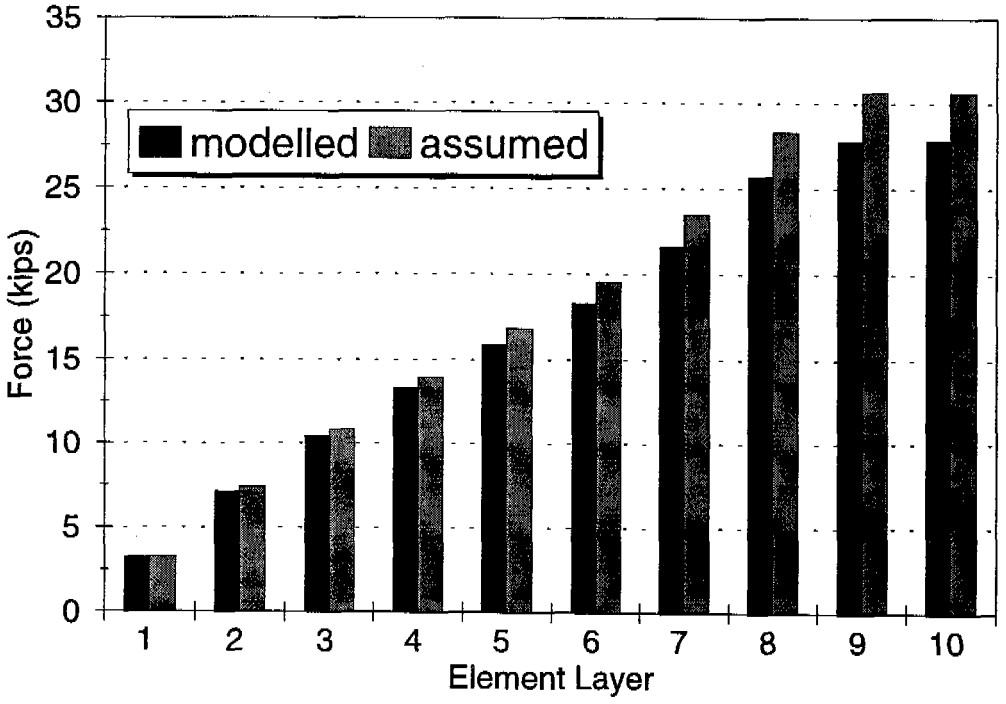

Figure 4.6 Forces in Strands at Full Release

All Patterns:

Draped Strands = Pairs 1–6, Steps 2–3

Hold down cut after Pair 6, in Step 4

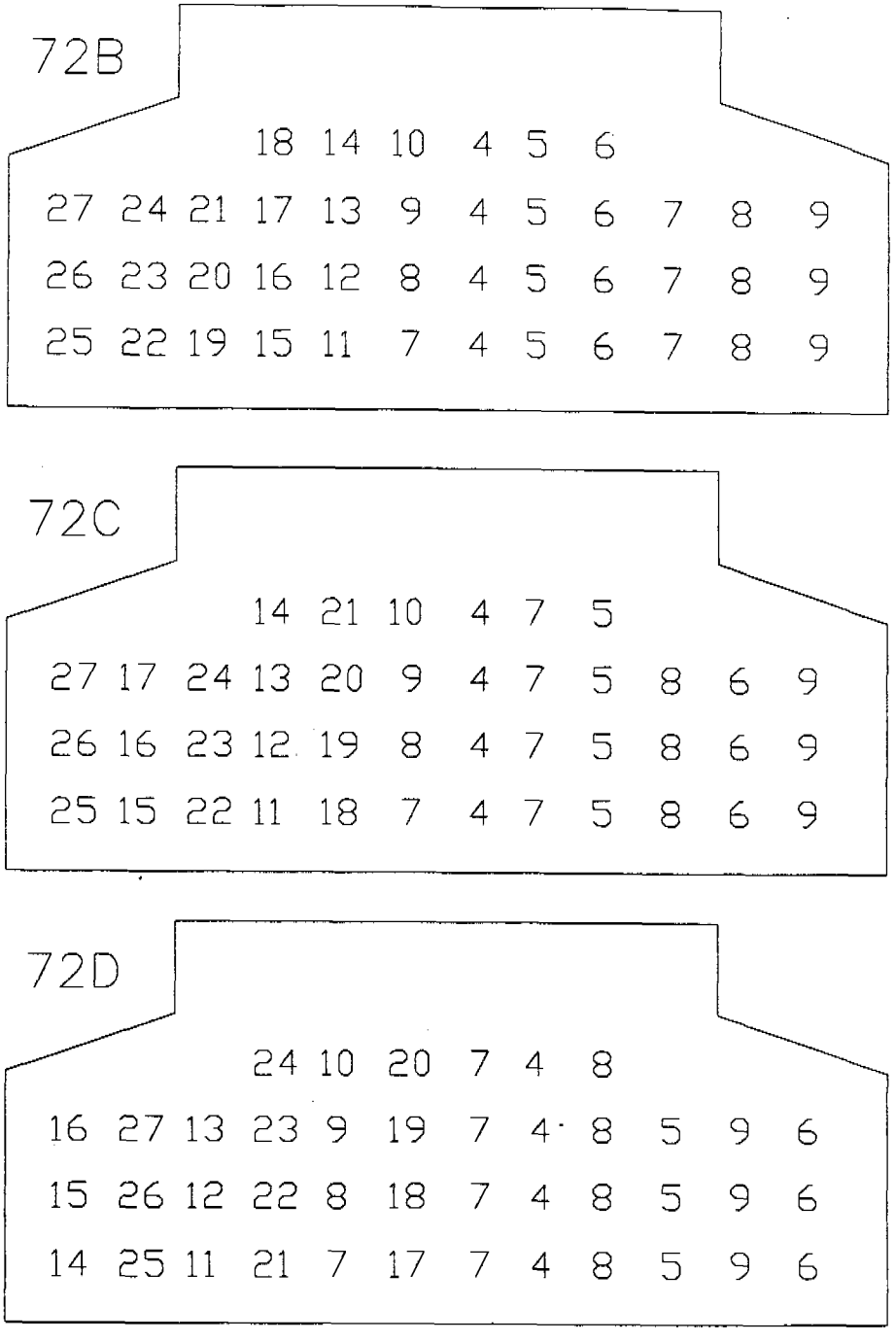

Figure 5.1 Cutting Patterns 72B, 72C, and 72D

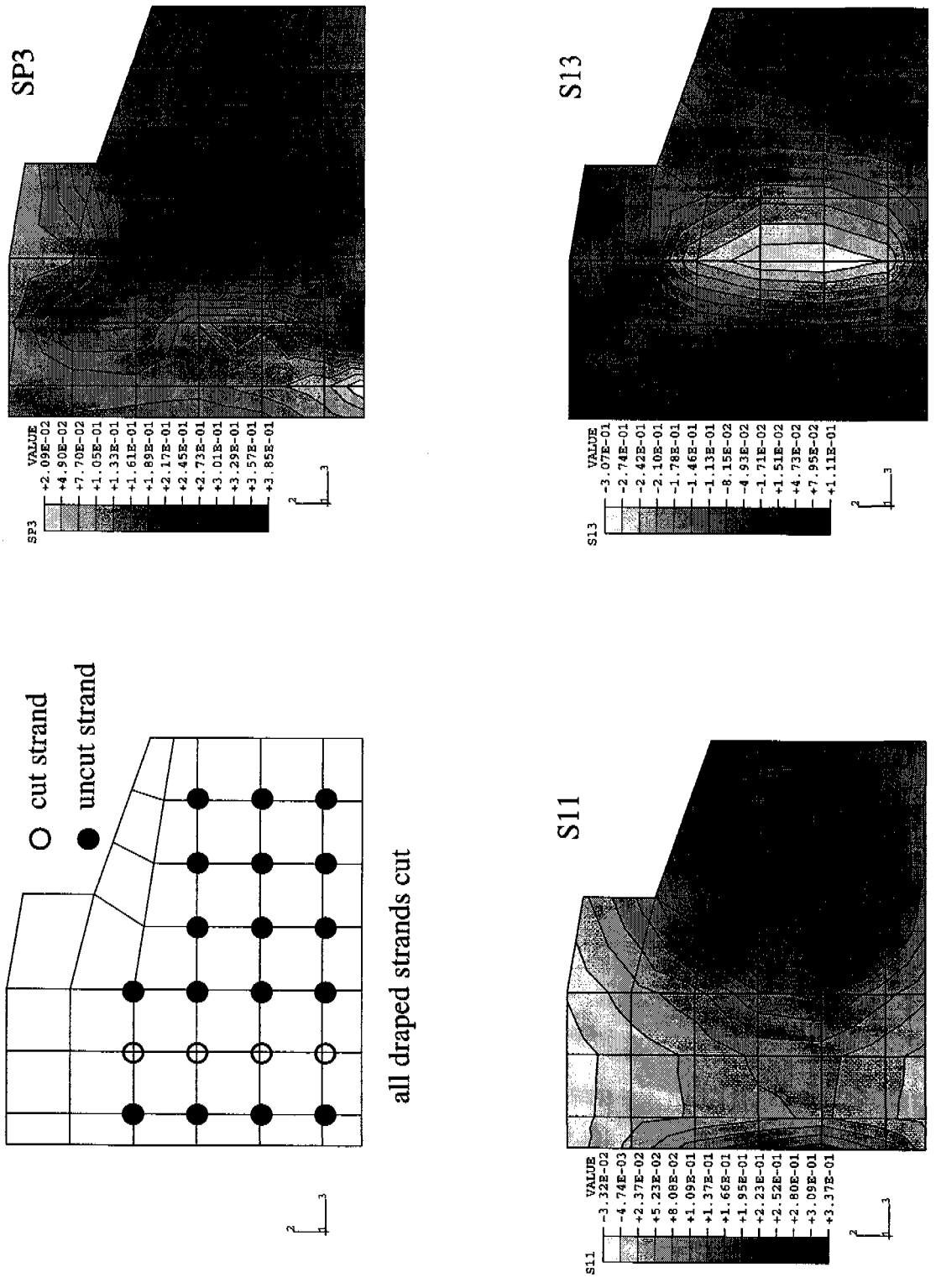

Figure 5.2a Stress Contours for Pattern 72D, Step 4, at 6 in. From End

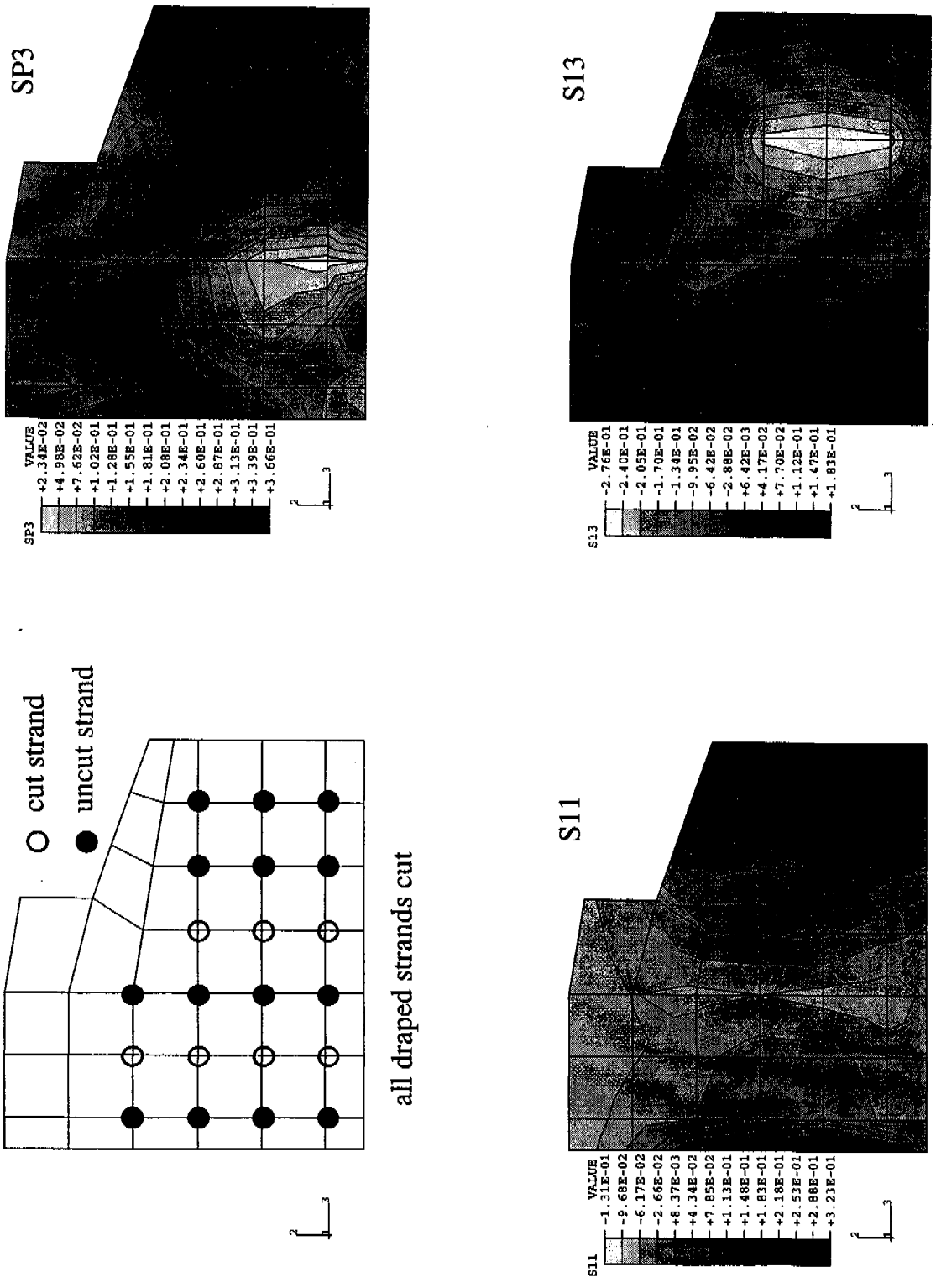

Figure 5.2b Stress Contours for Pattern 72D, Step 5, at 6 in. From End

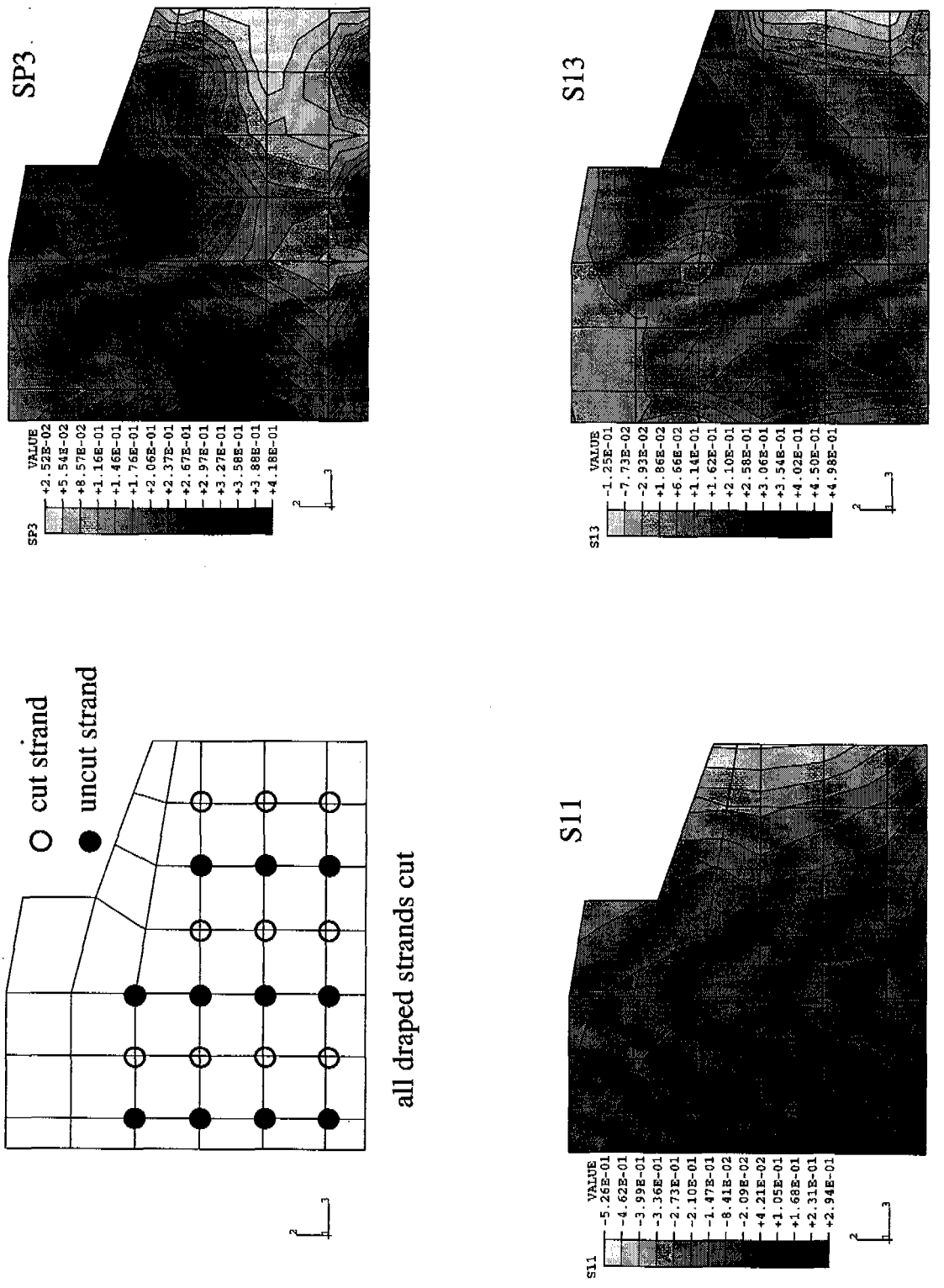

Figure 5.2c Stress Contours for Pattern 72D, Step 6, at 6 in. From End

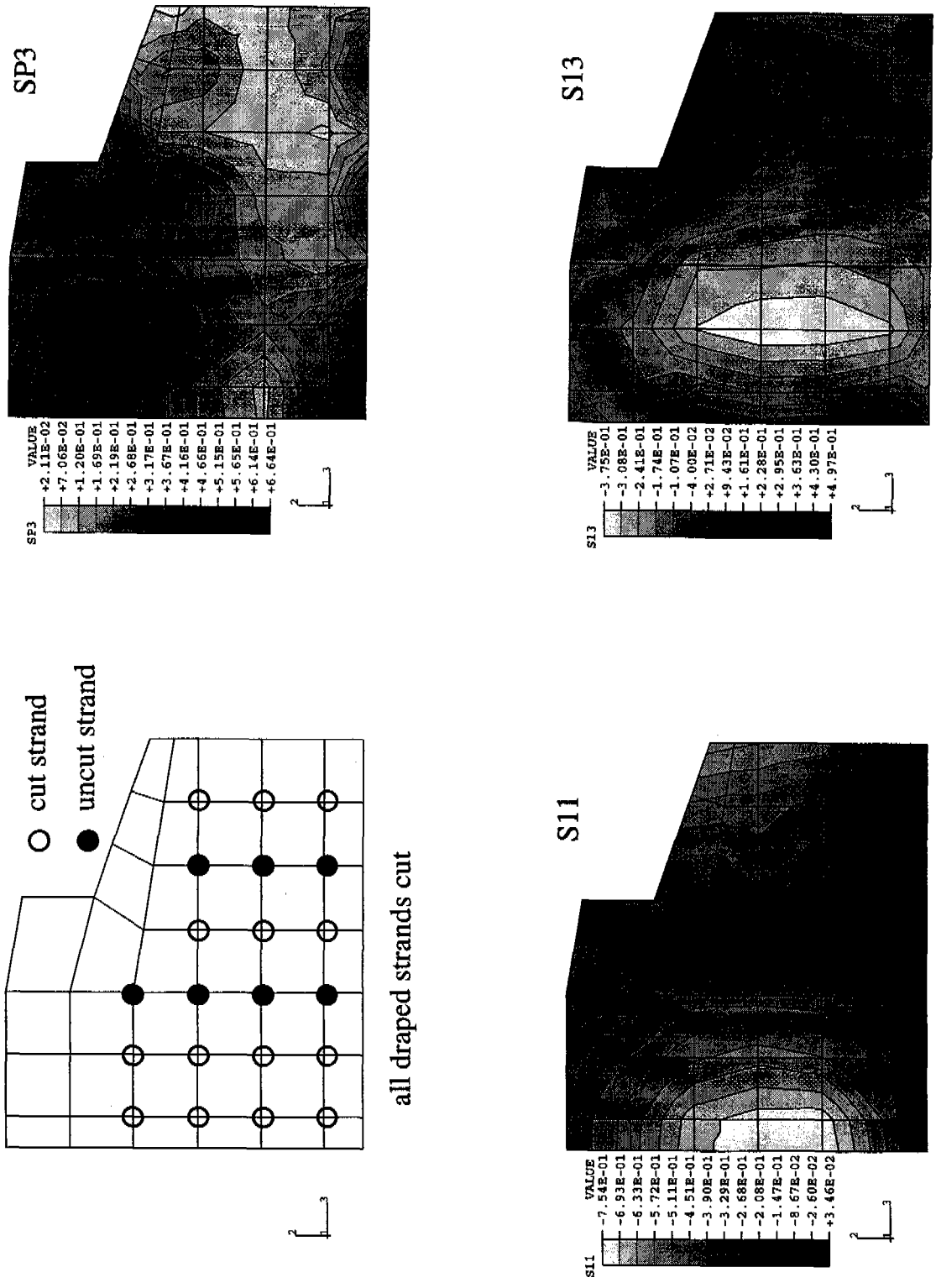

Figure 5.2d Stress Contours for Pattern 72D, Step 7, at 6 in. From End

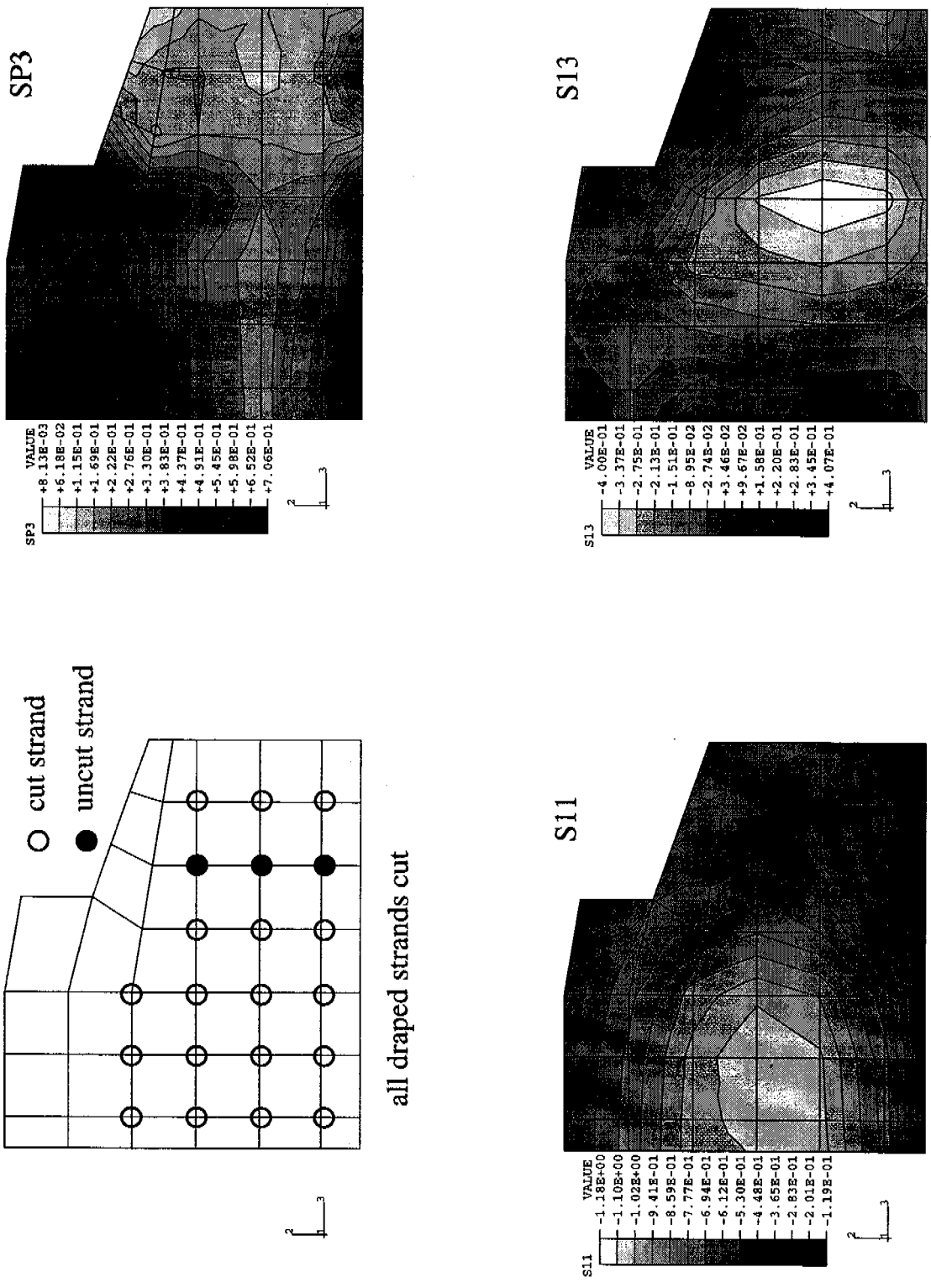

Figure 5.2e Stress Contours for Pattern 72D, Step 8, at 6 in. From End

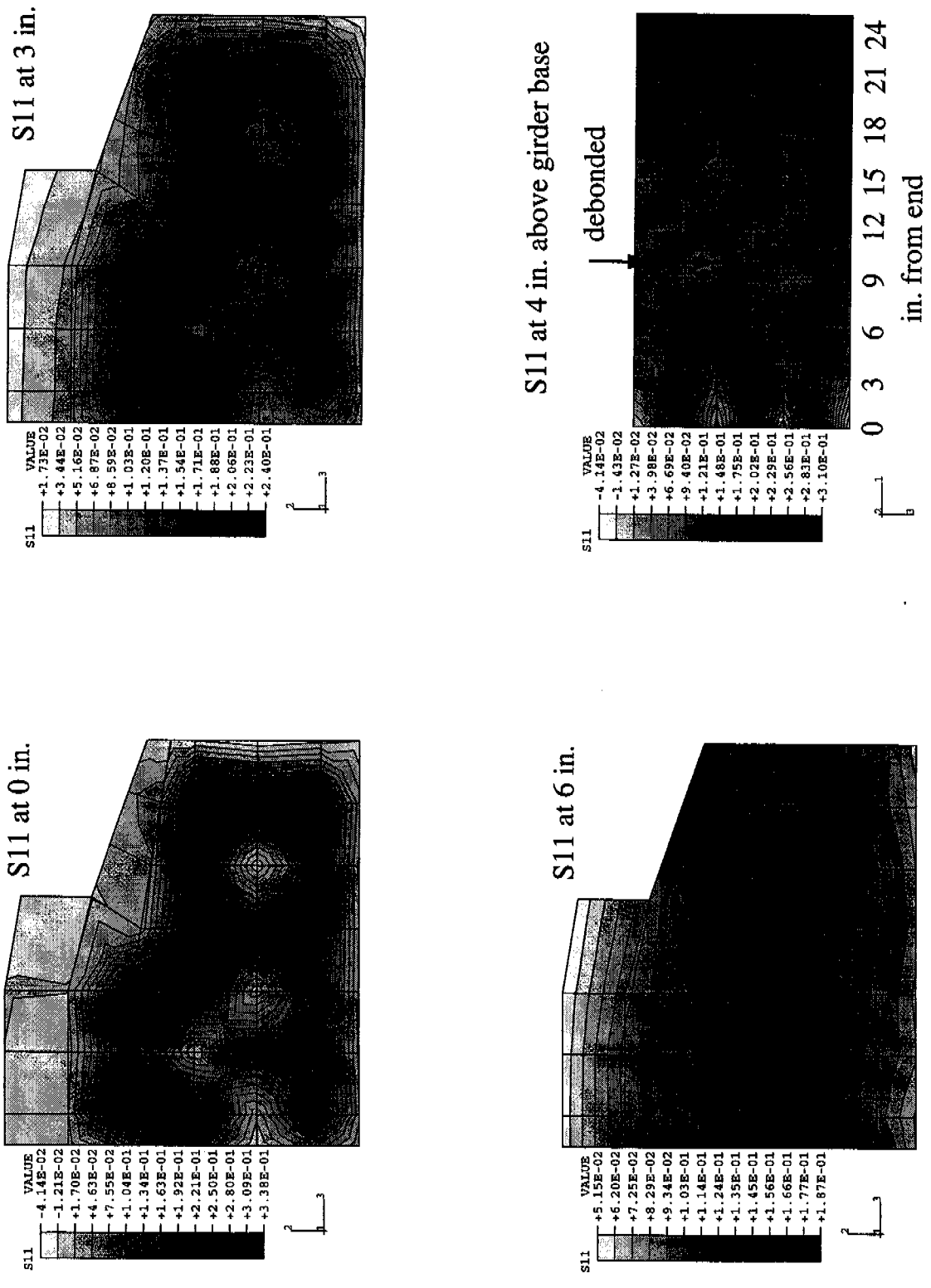

Figure 5.3 Effect of Debonding on S11 Contours, Pattern 72E, Step 3

Draped Strands = Pairs 1–6, Steps 2–3
Hold down cut after Pair 6, in Step 4

72E

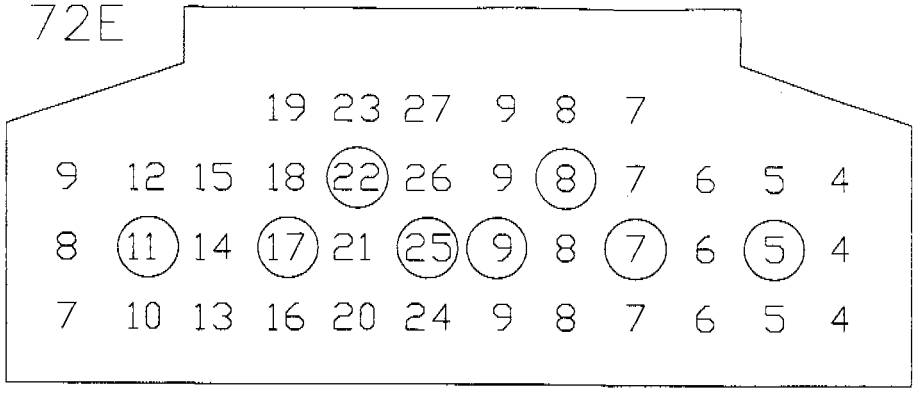

Draped Strands = Pairs 1–6, Steps 2–3
Hold down cut after Pair 6, in Step 4

72F

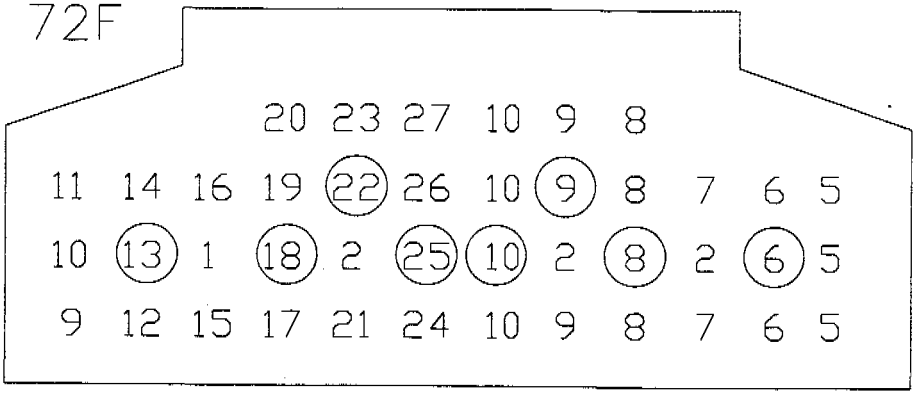

Draped Strands = Pairs 1–6, Steps 2–3
Hold down cut after Pair 6, in Step 4

72G

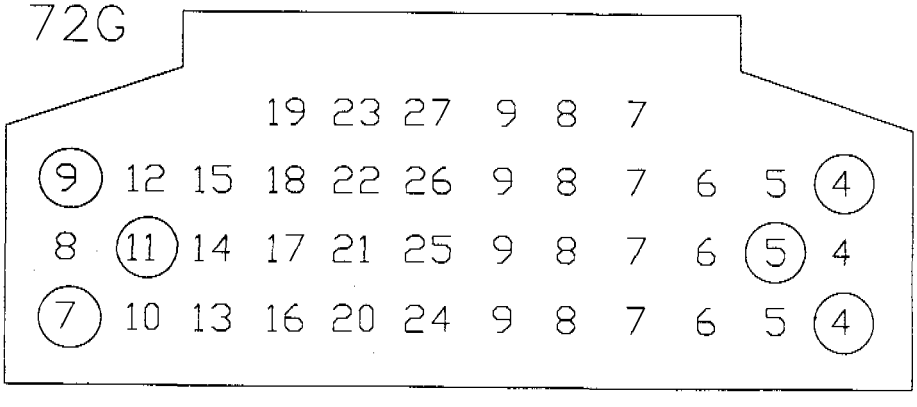

Figure 5.4 Cutting Patterns 72E, 72F, and 72G

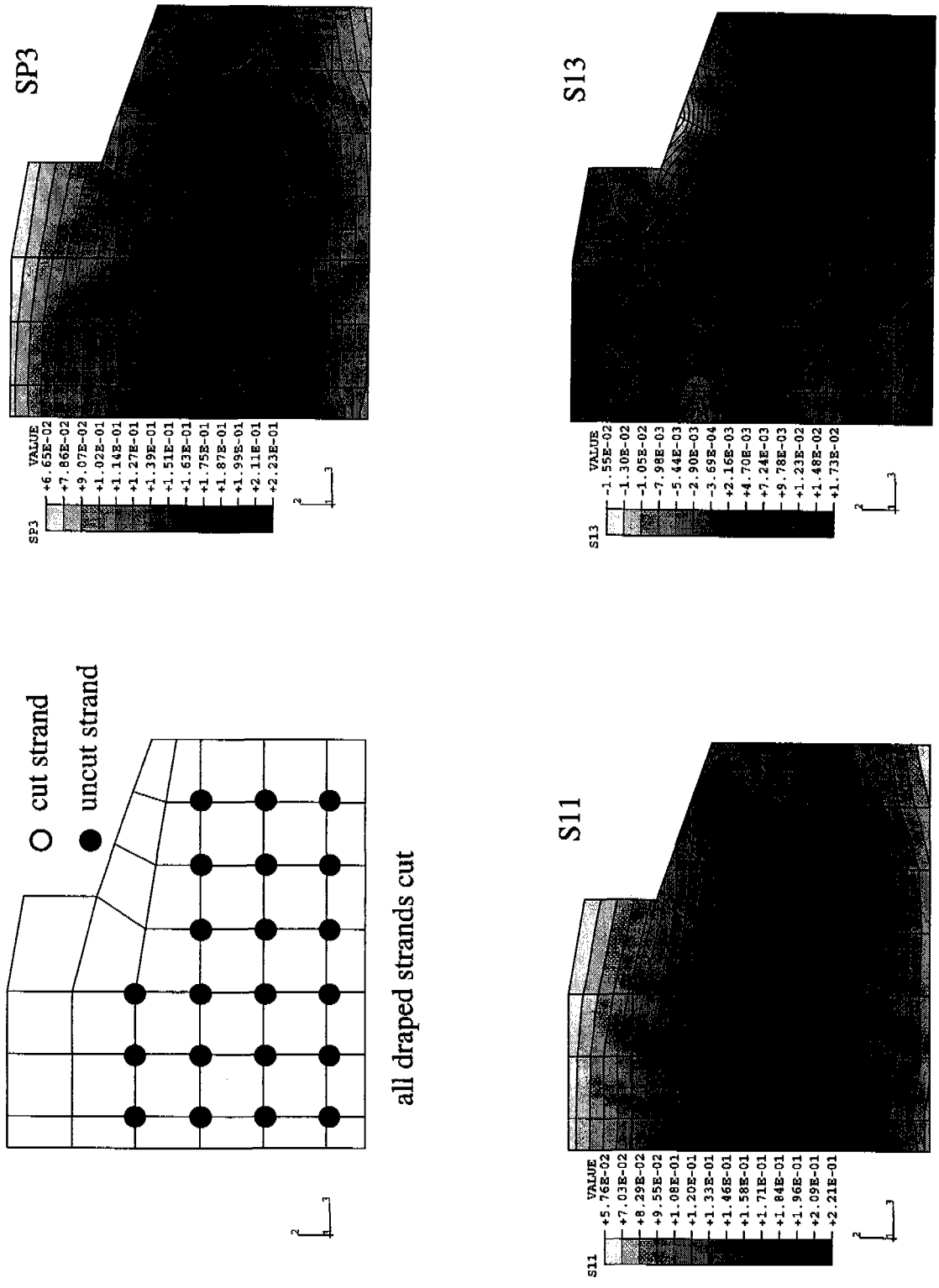

Figure 5.5a Stress Contours for Pattern 72A, Step 3, at 6 in. From End

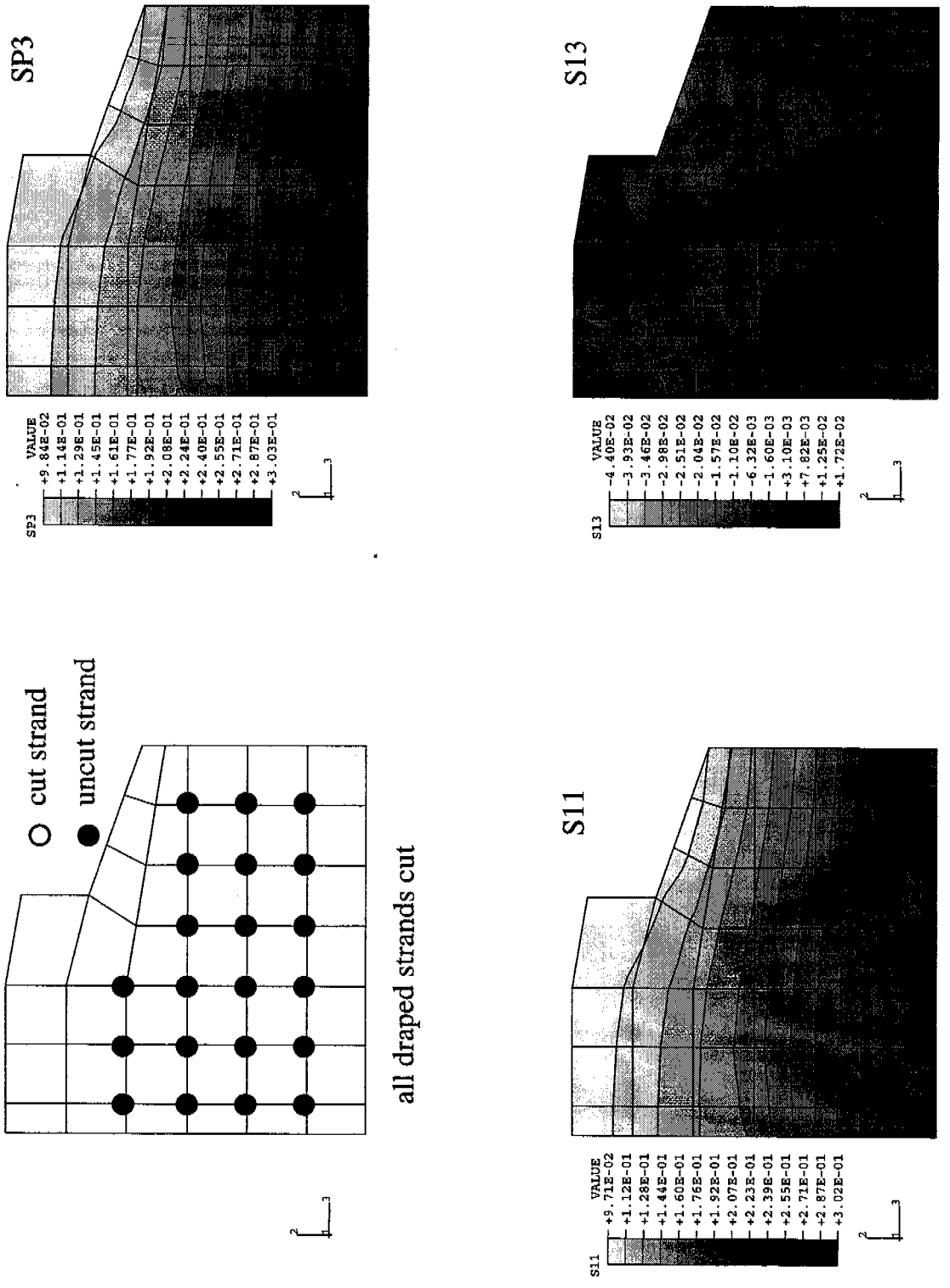

Figure 5.5b Stress Contours for Pattern 72A, Step 3, at 24 in. From End

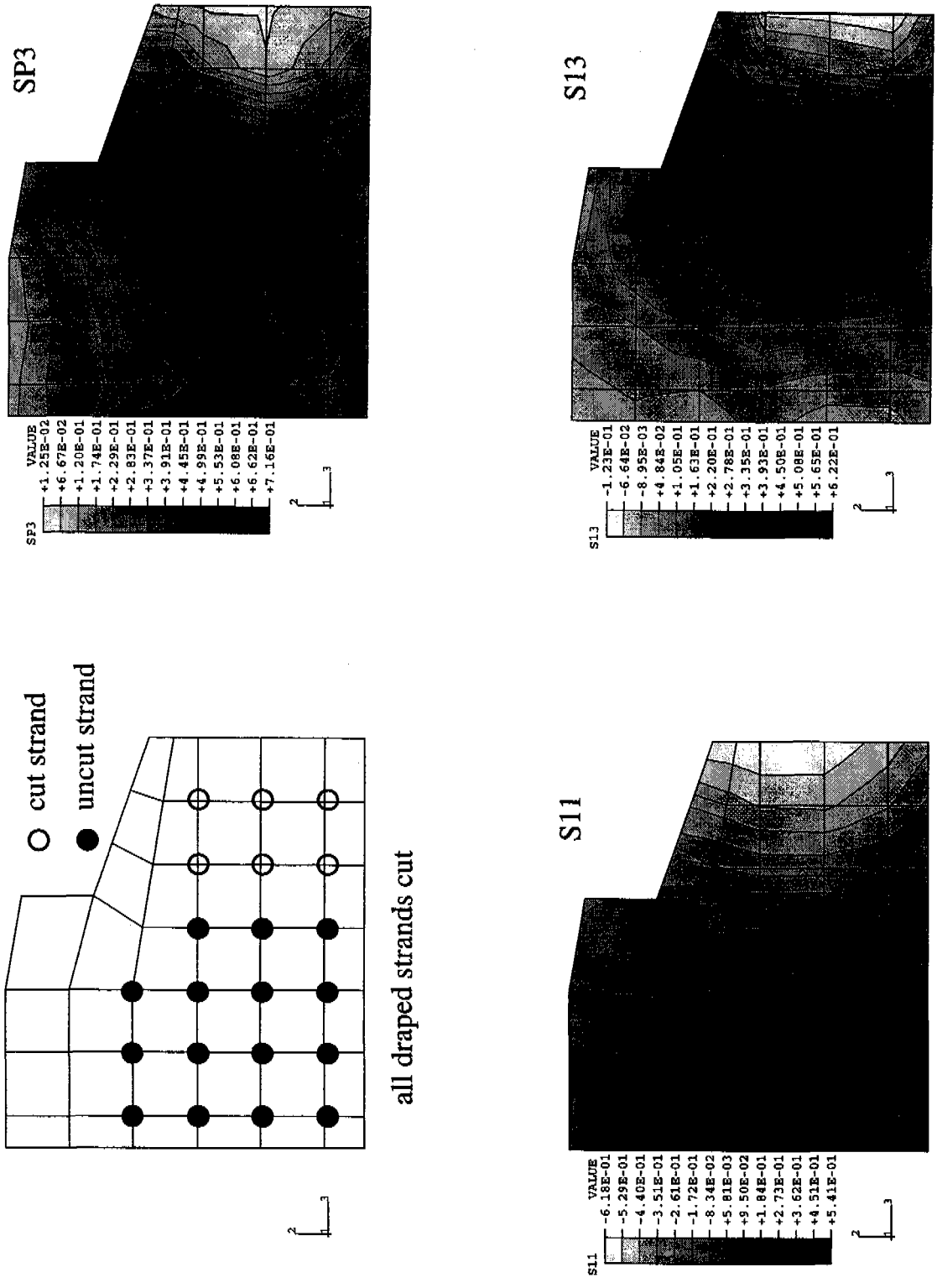

Figure 5.5c Stress Contours for Pattern 72A, Step 5, at 6 in. From End

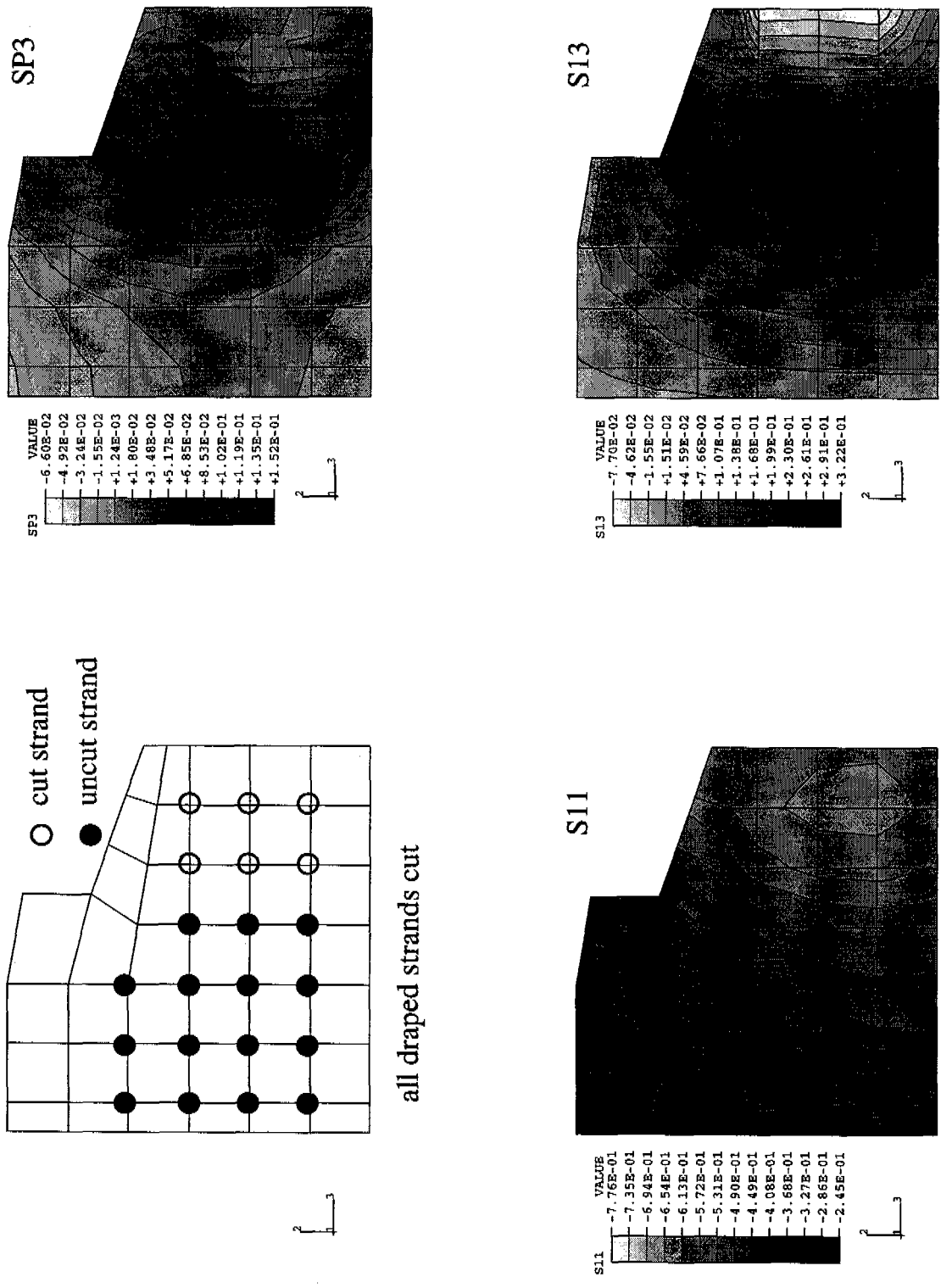

Figure 5.5d Stress Contours for Pattern 72A, Step 5, at 24 in. From End

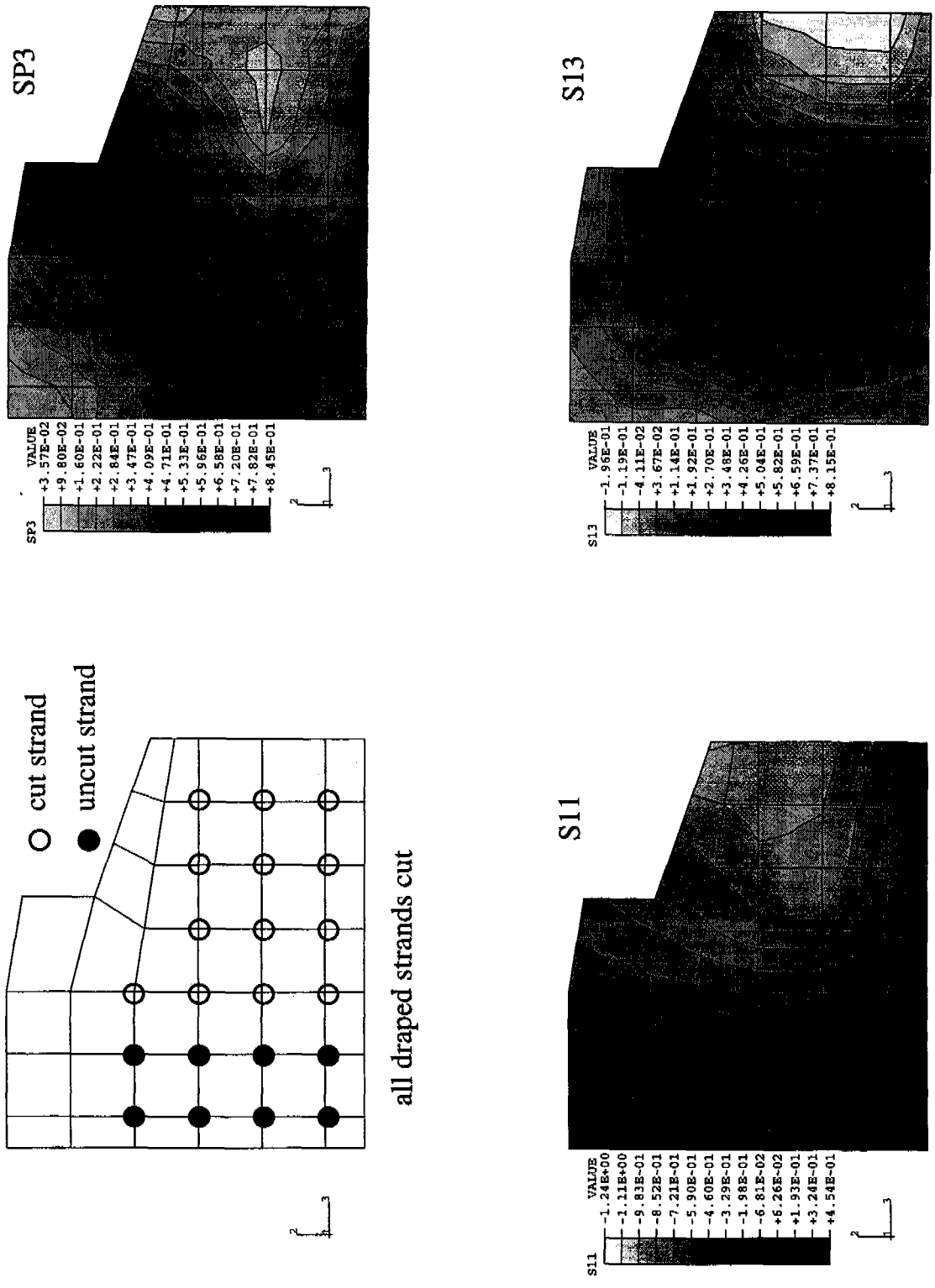

Figure 5.5e Stress Contours for Pattern 72A, Step 7, at 6 in. From End

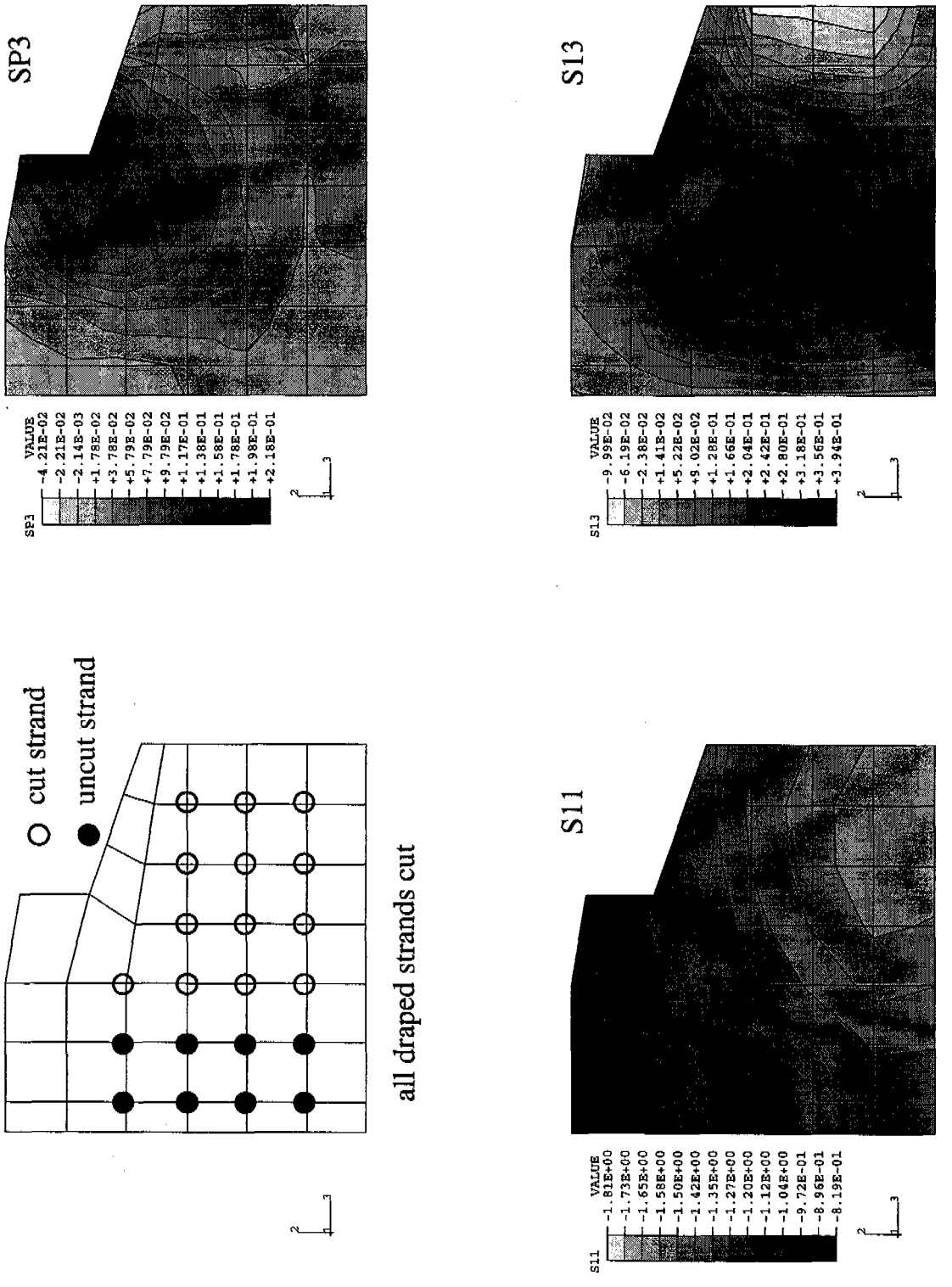

Figure 5.5f Stress Contours for Pattern 72A, Step 7, at 24 in. From End

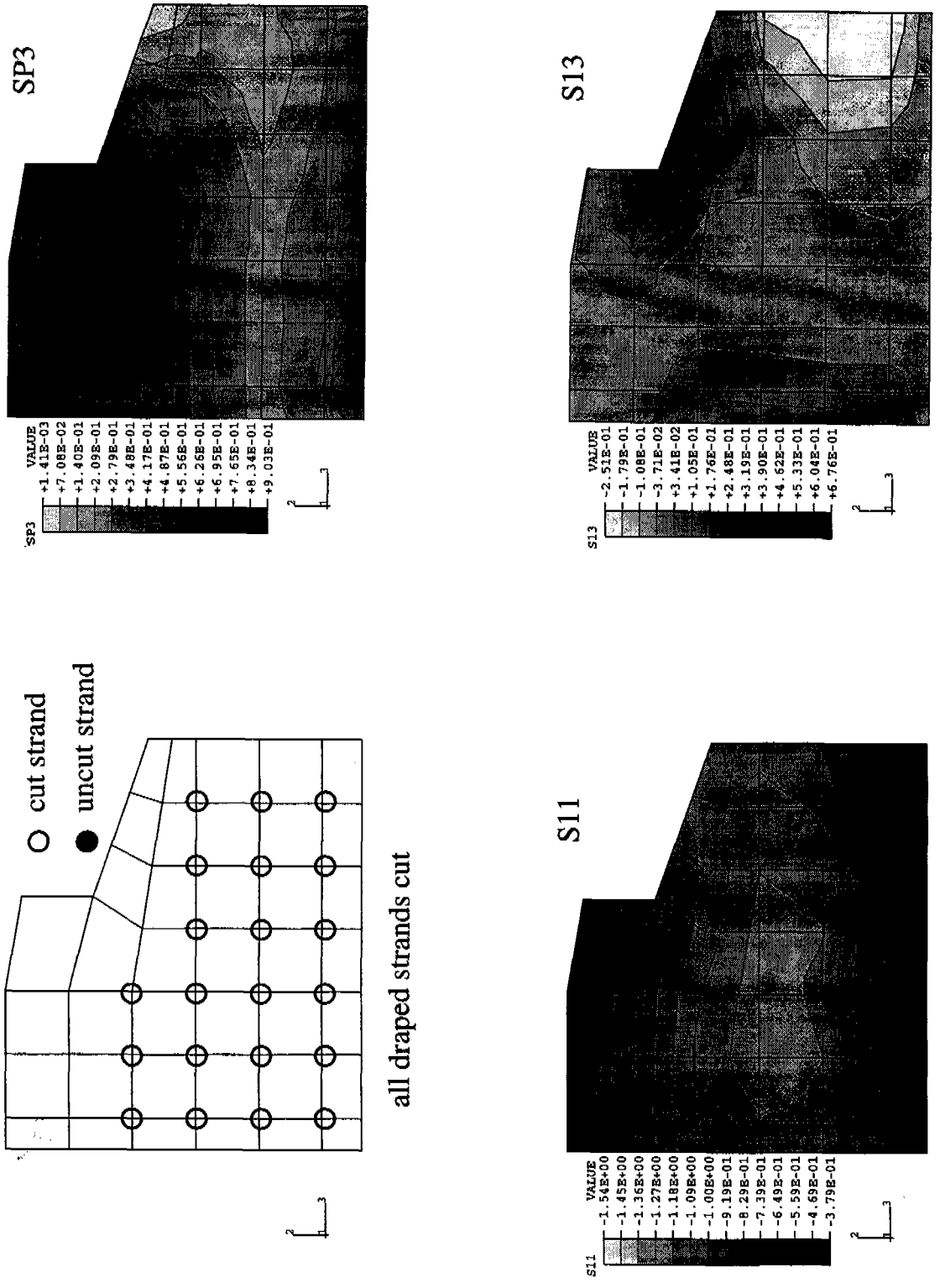

Figure 5.5g Stress Contours for Pattern 72A, Step 9, at 6 in. From End

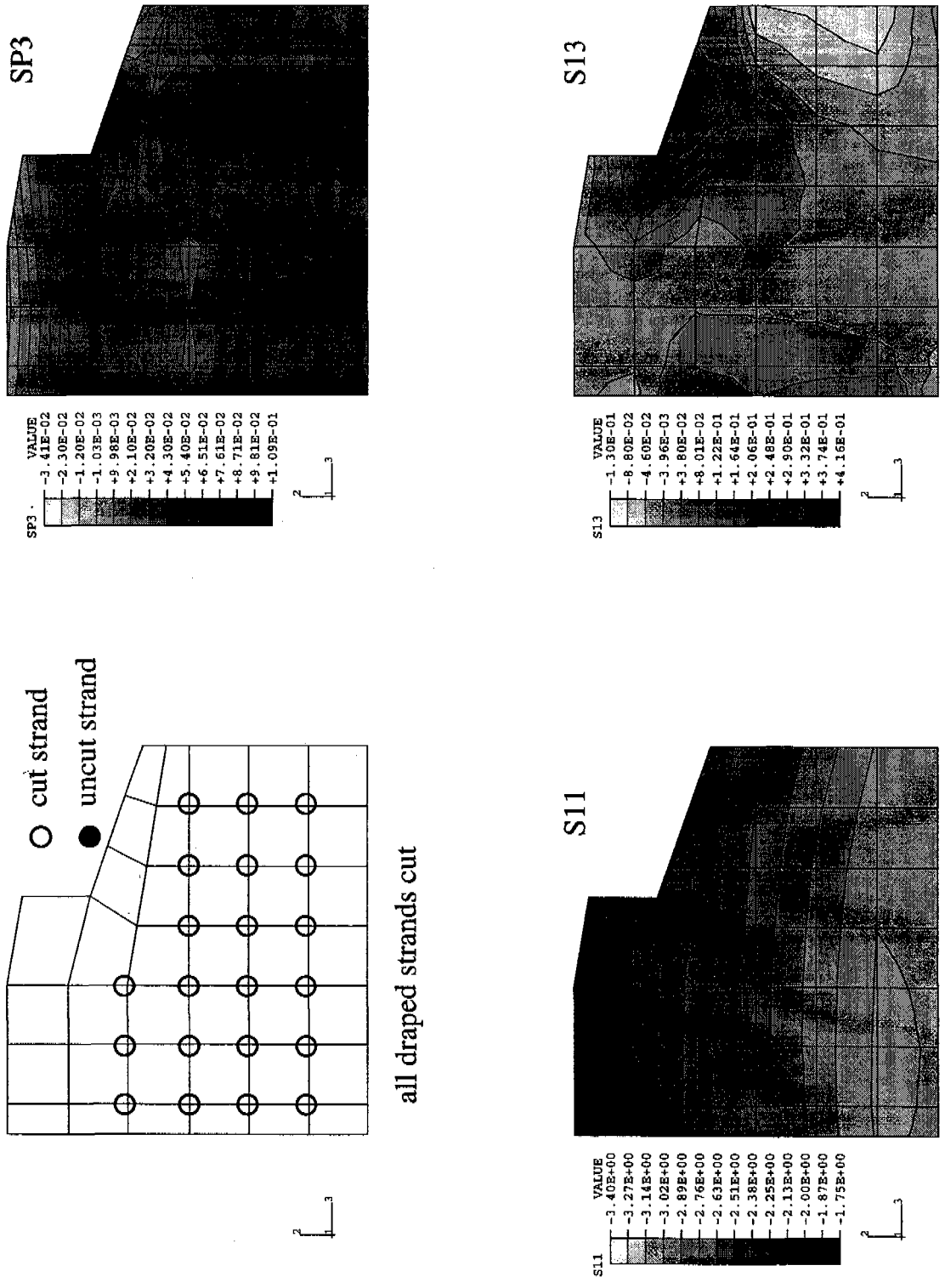

Figure 5.5h Stress Contours for Pattern 72A, Step 9, at 24 in. From End

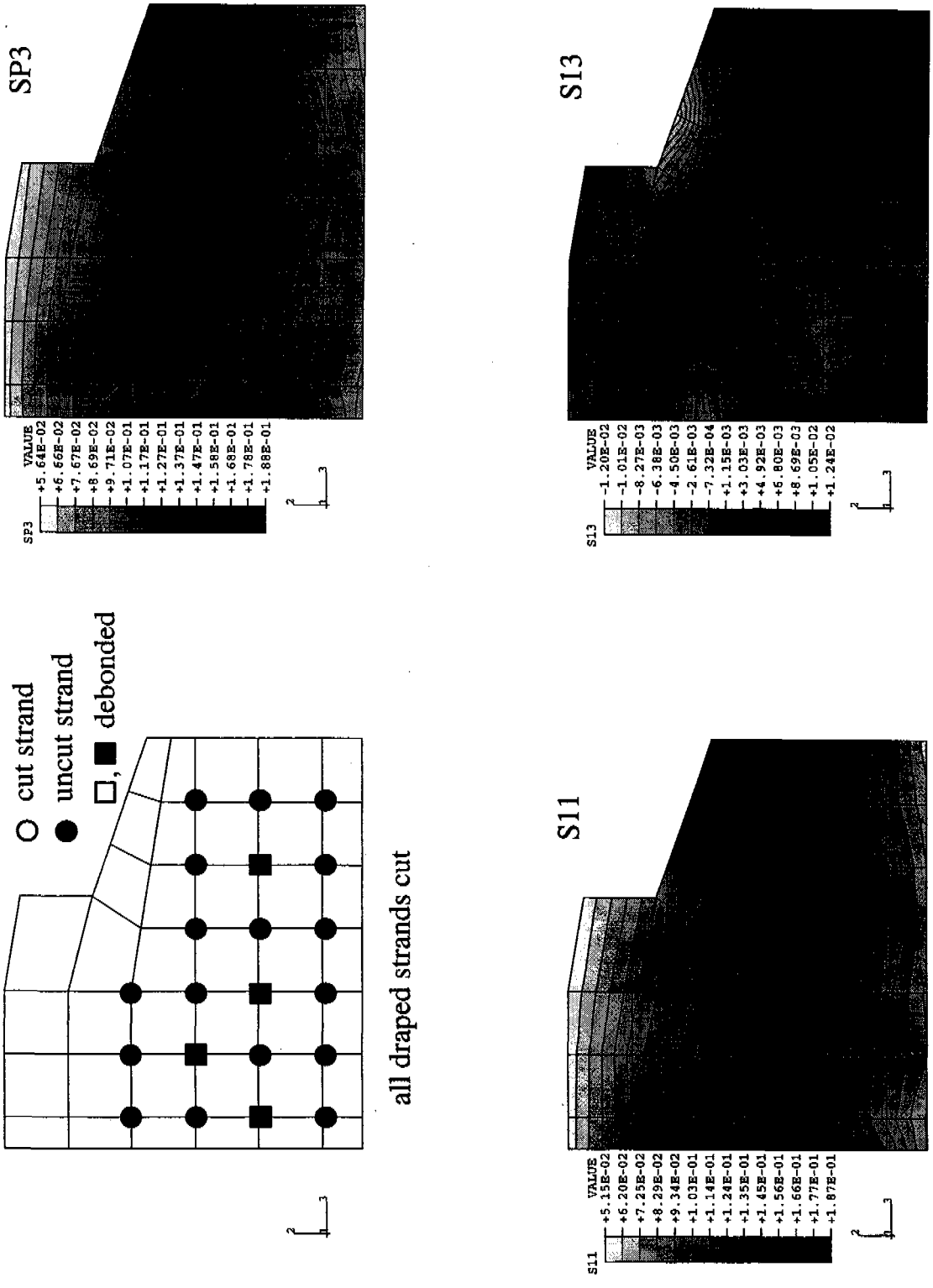

Figure 5.6a Stress Contours for Pattern 72E, Step 3, at 6 in. From End

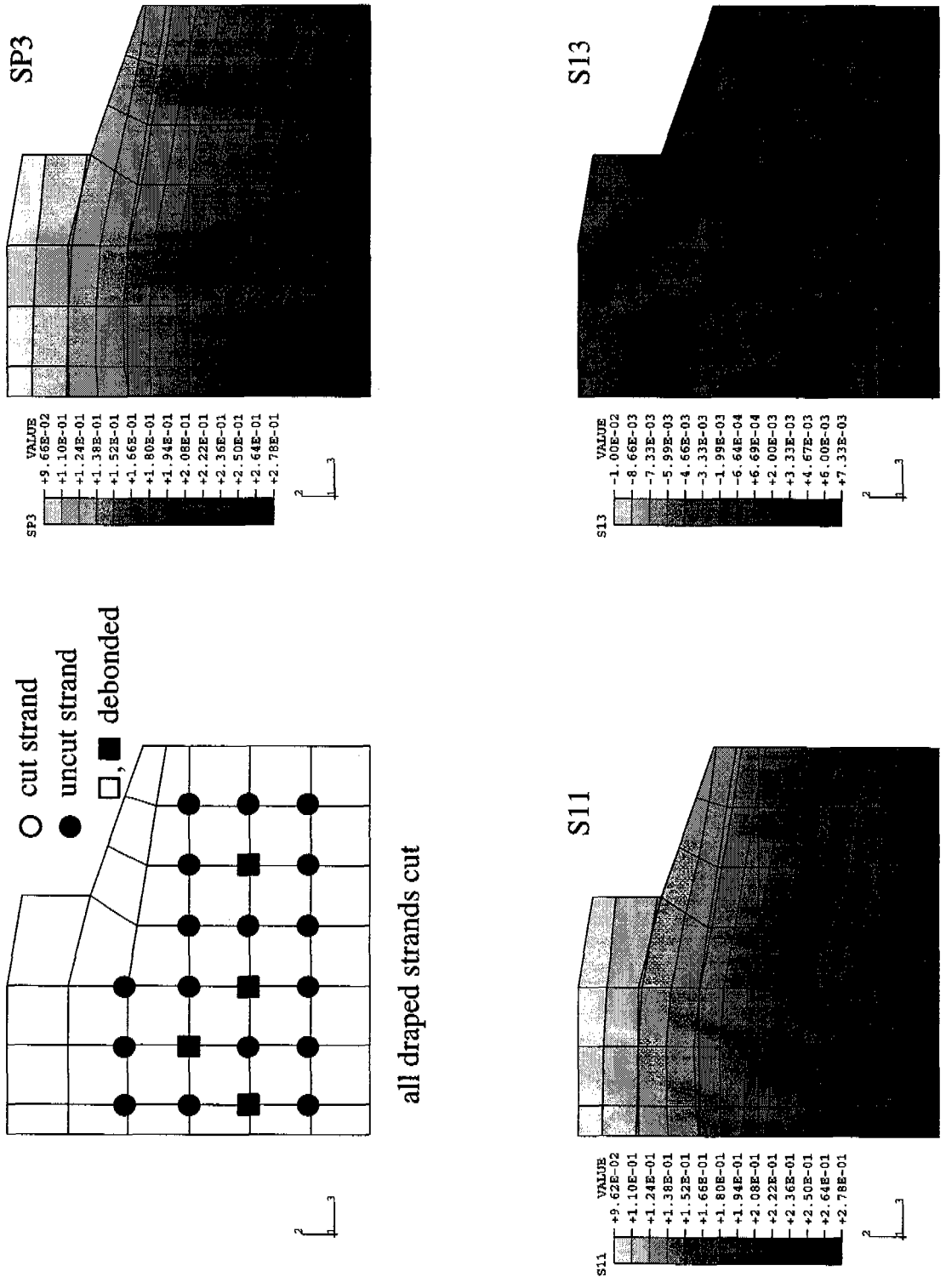

Figure 5.6b Stress Contours for Pattern 72E, Step 3, at 24 in. From End

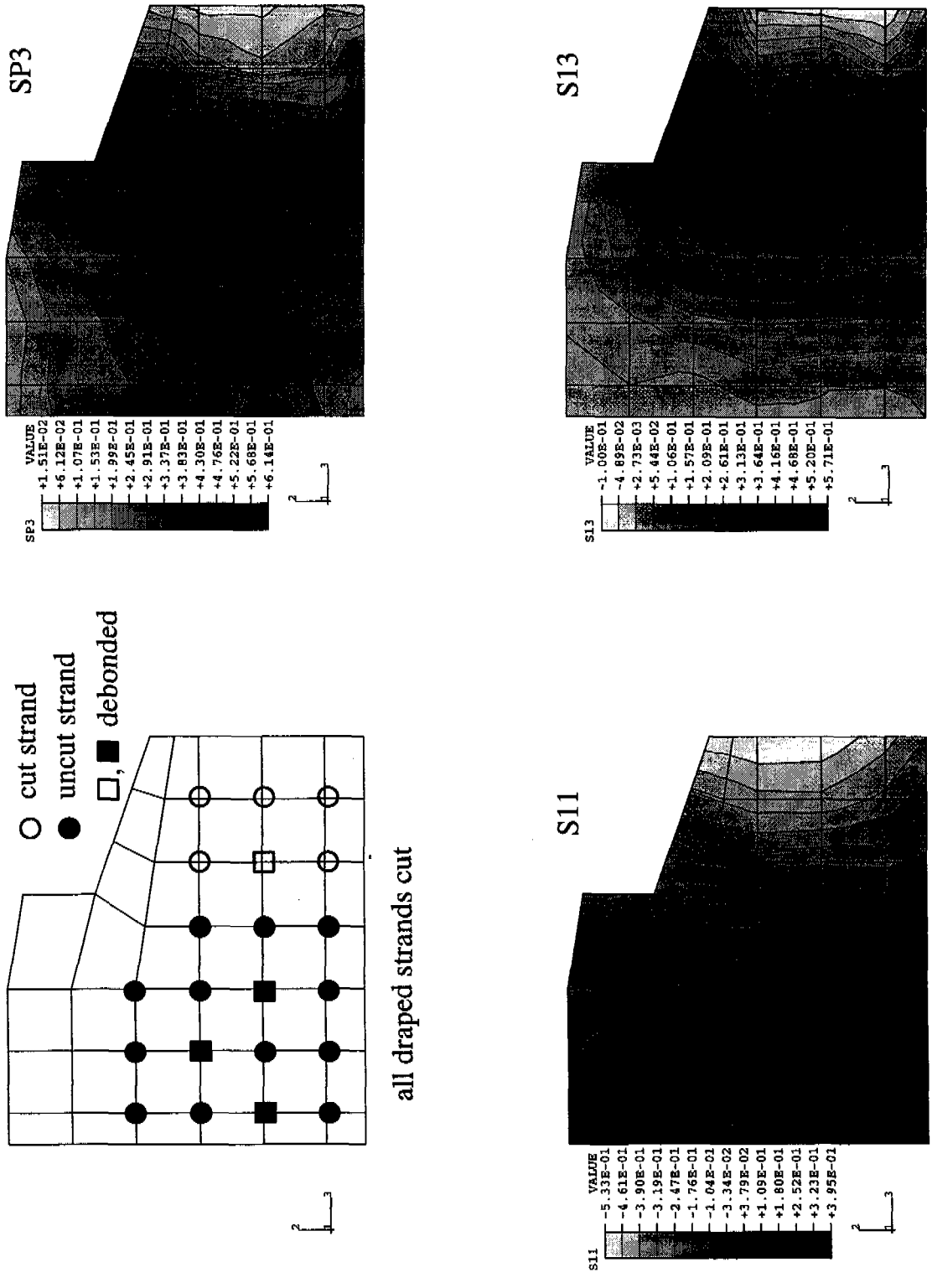

Figure 5.6c Stress Contours for Pattern 72E, Step 5, at 6 in. From End

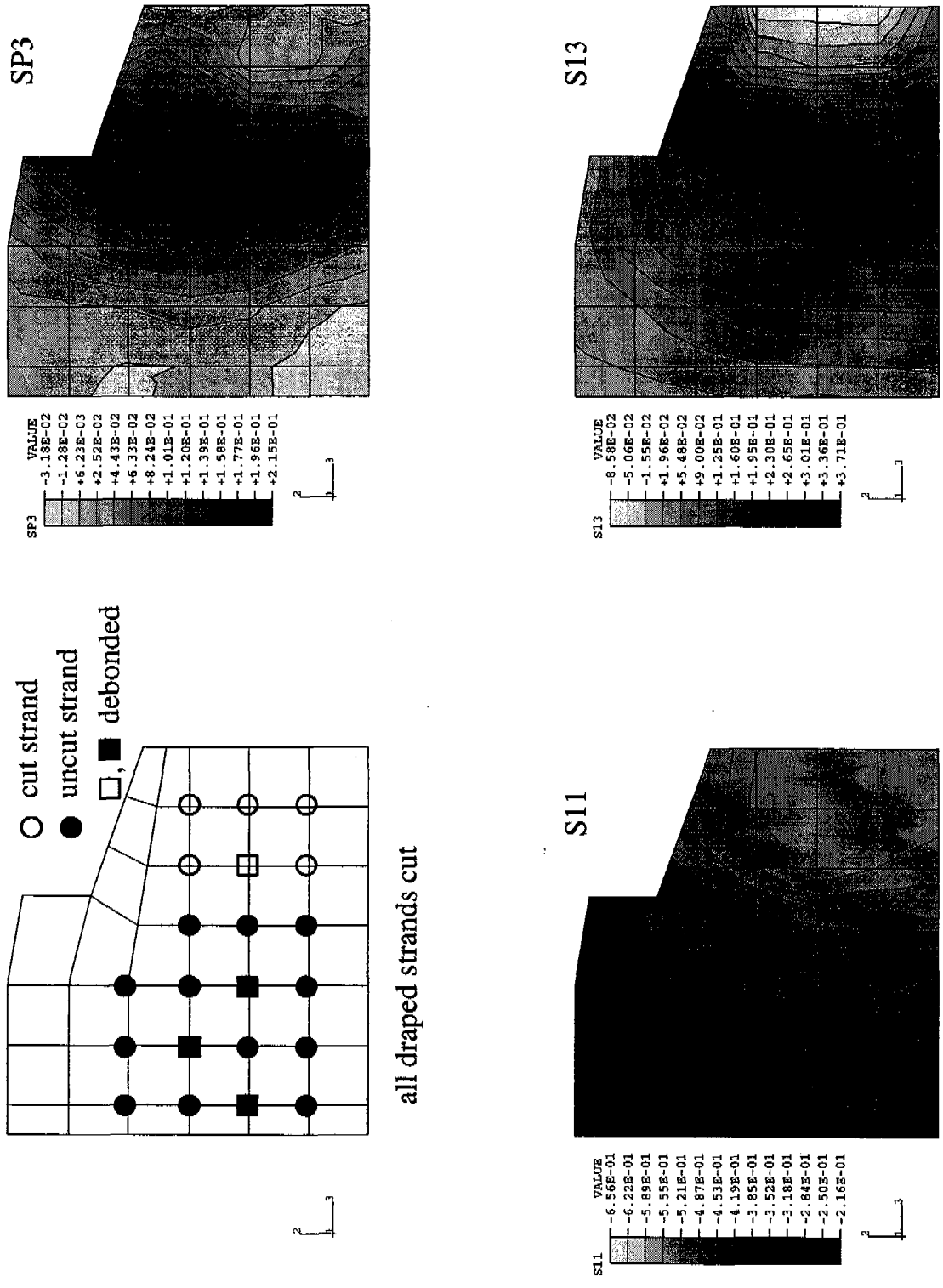

Figure 5.6d Stress Contours for Pattern 72E, Step 5, at 24 in. From End

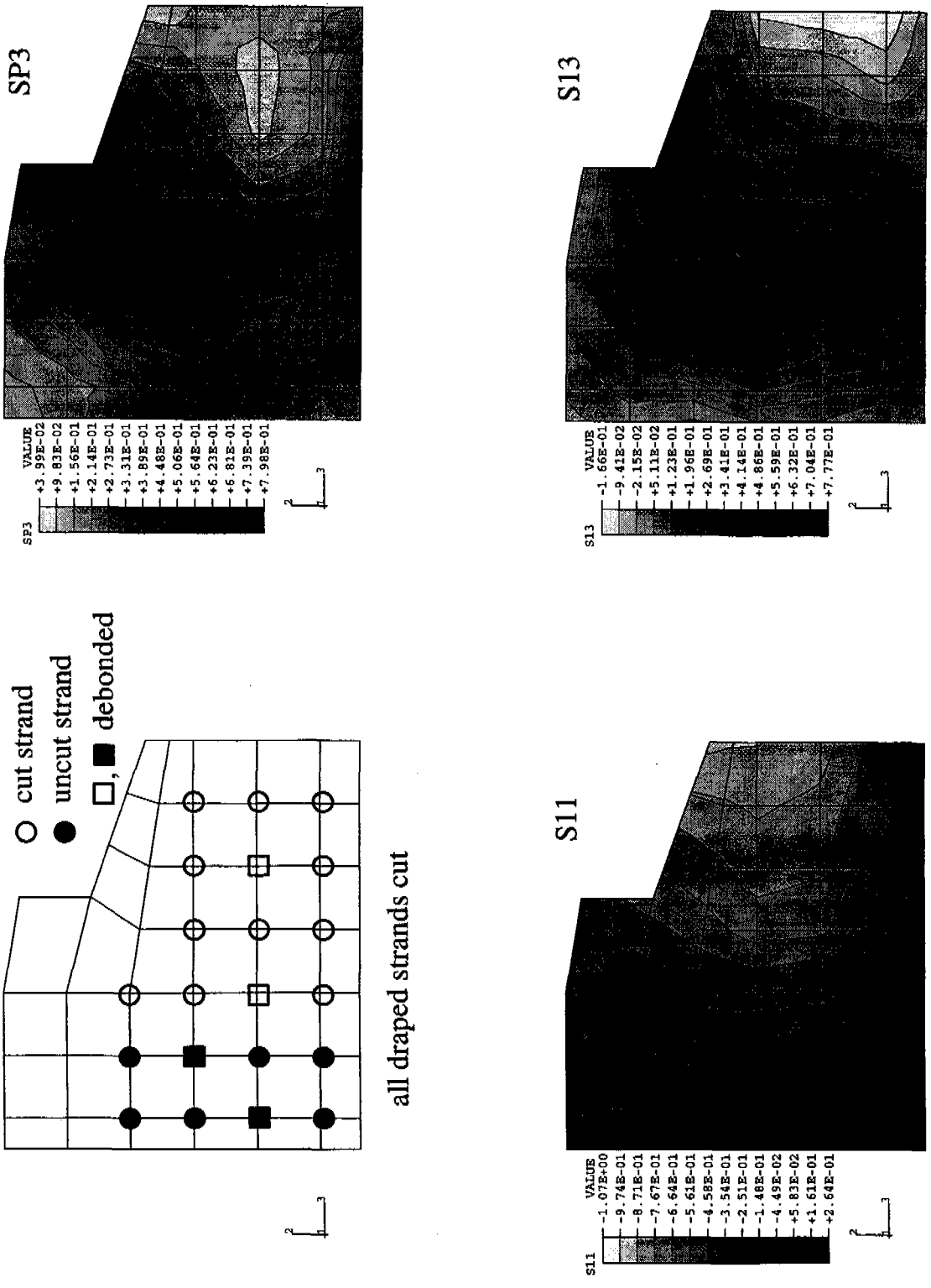

Figure 5.6e Stress Contours for Pattern 72E, Step 7, at 6 in. From End

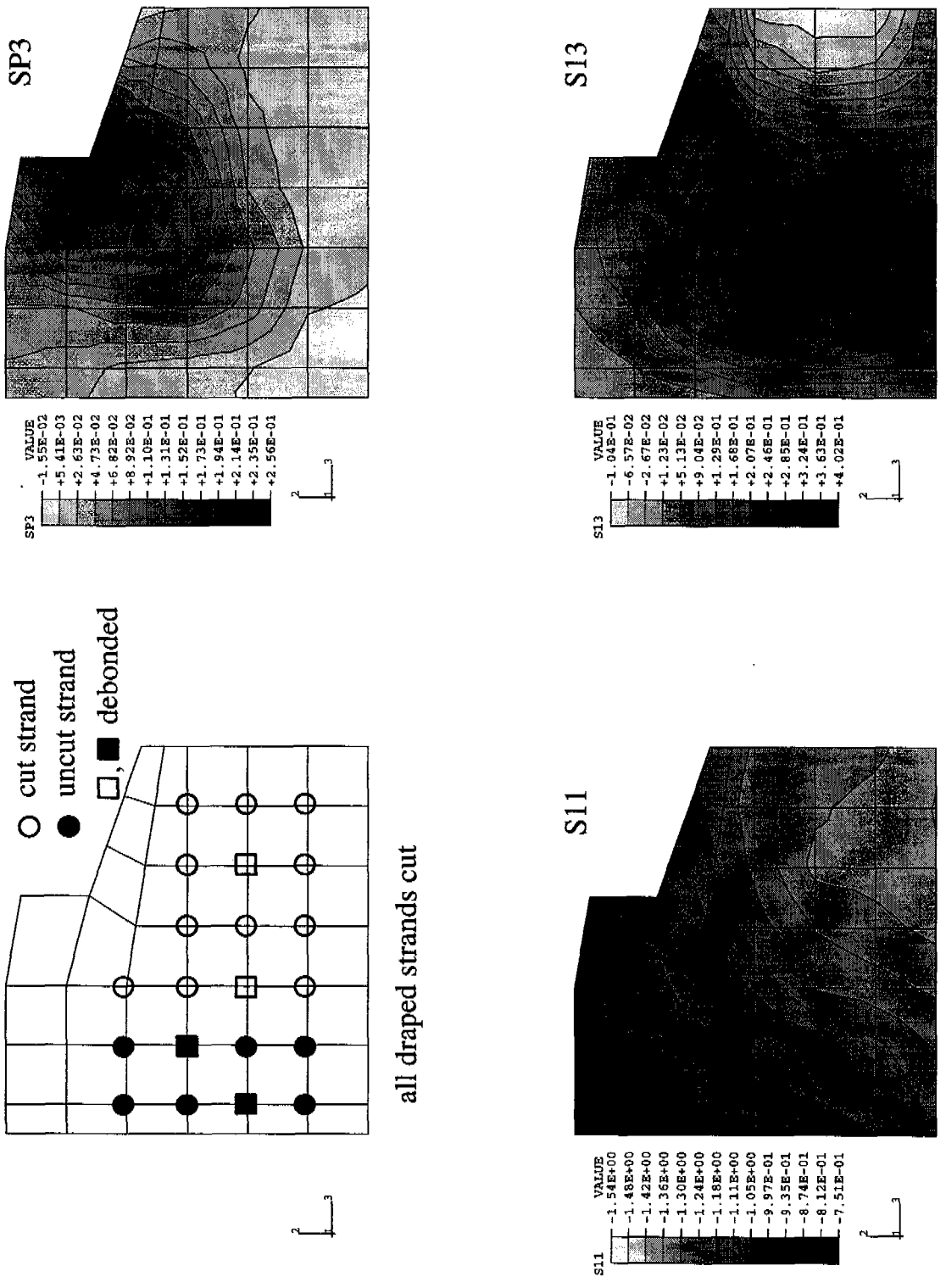

Figure 5.6f Stress Contours for Pattern 72E, Step 7, at 24 in. From End

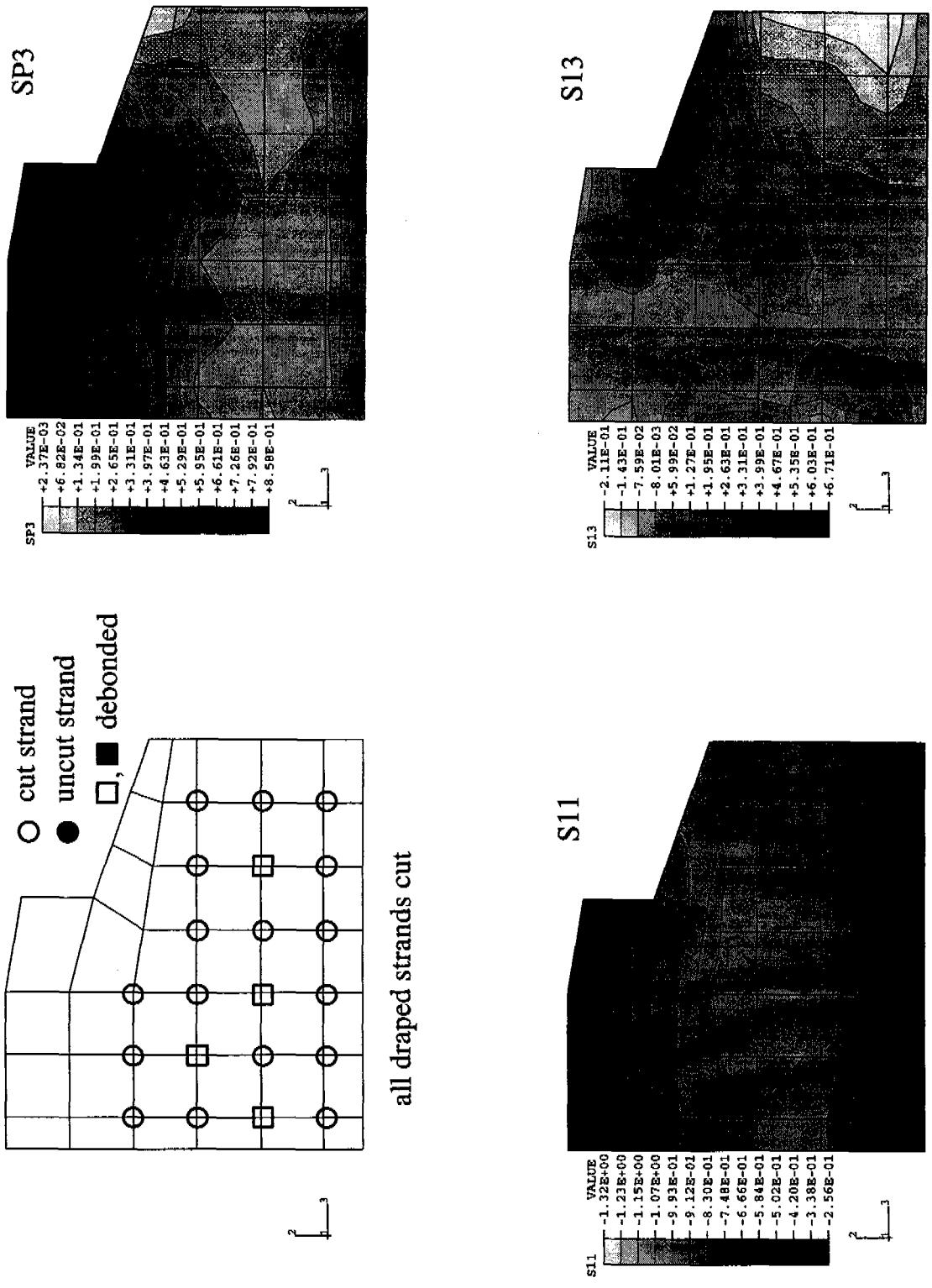

Figure 5.6g Stress Contours for Pattern 72E, Step 9, at 6 in. From End

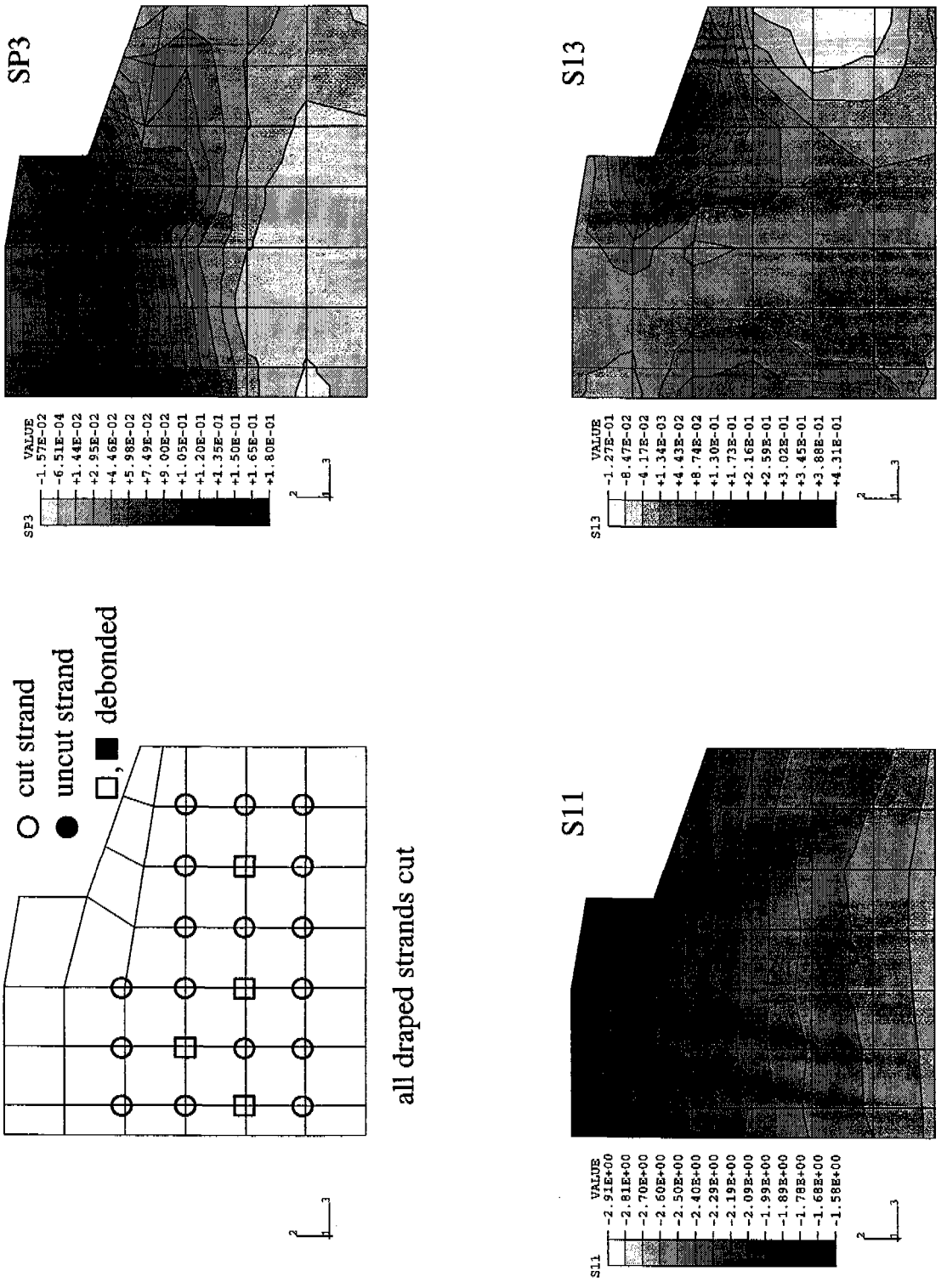

Figure 5.6h Stress Contours for Pattern 72E, Step 9, at 24 in. From End

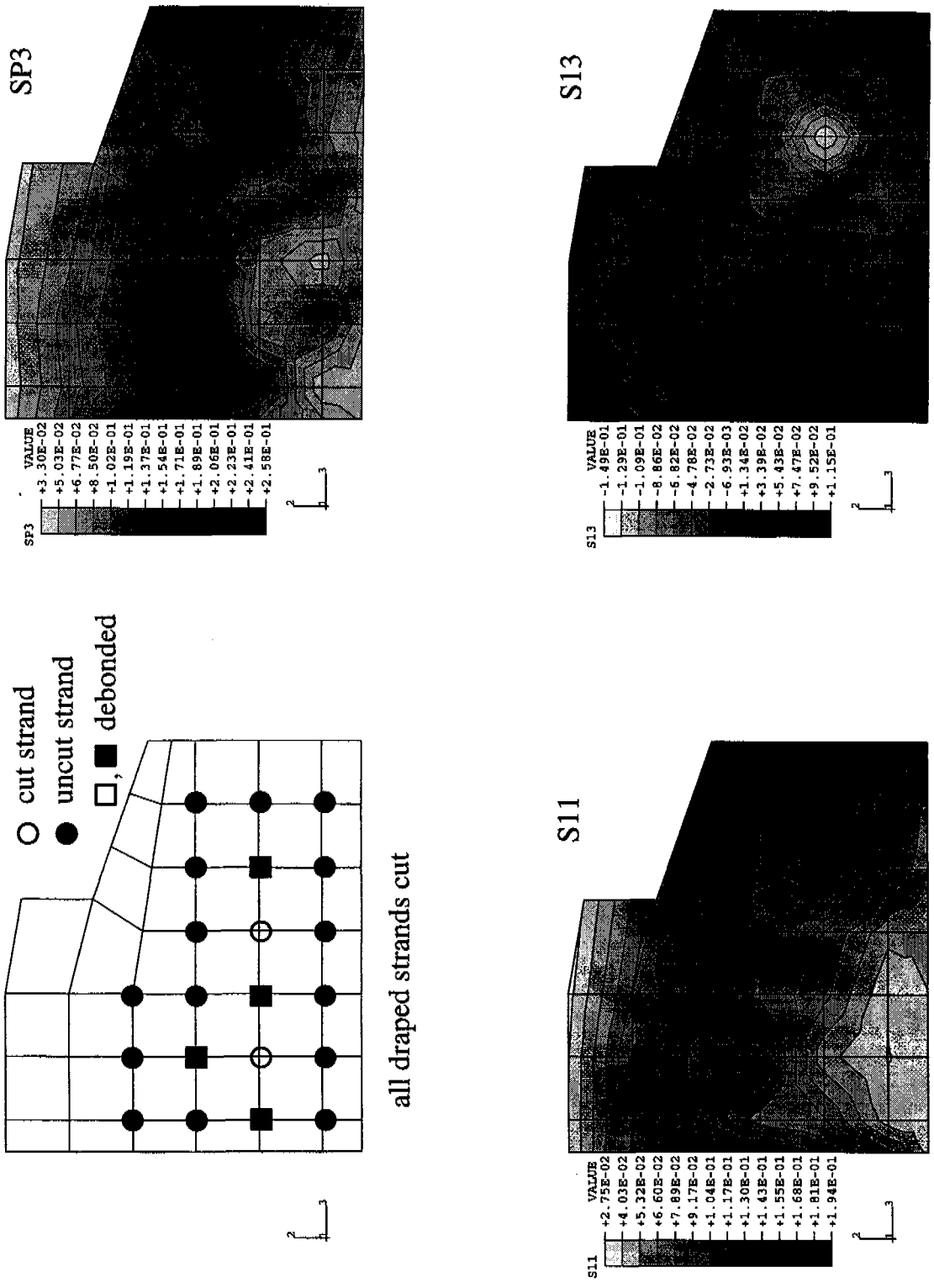

Figure 5.7a Stress Contours for Pattern 72F, Step 4, at 6 in. From End

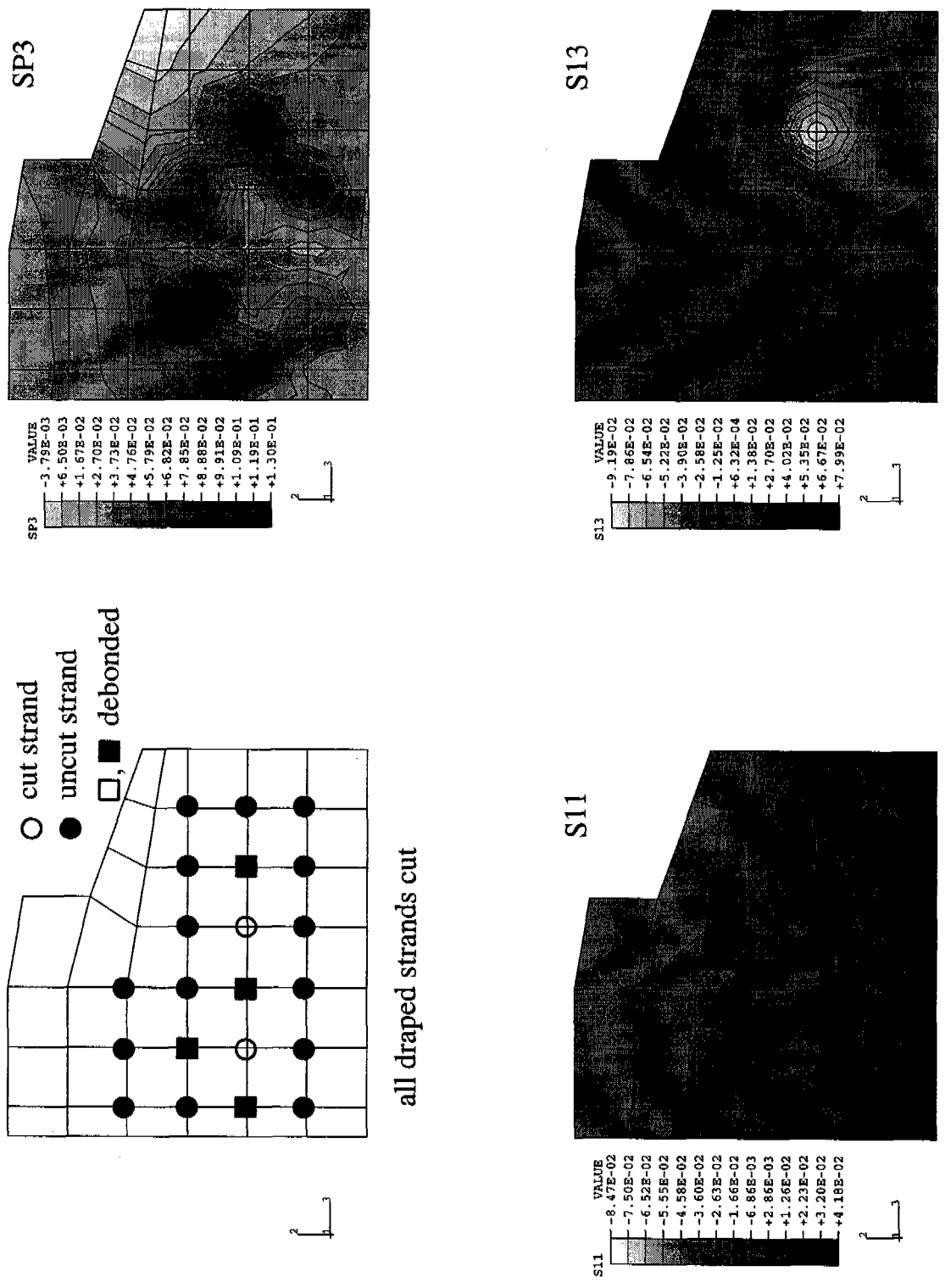

Figure 5.7b Stress Contours for Pattern 72F, Step 4, at 24 in. From End

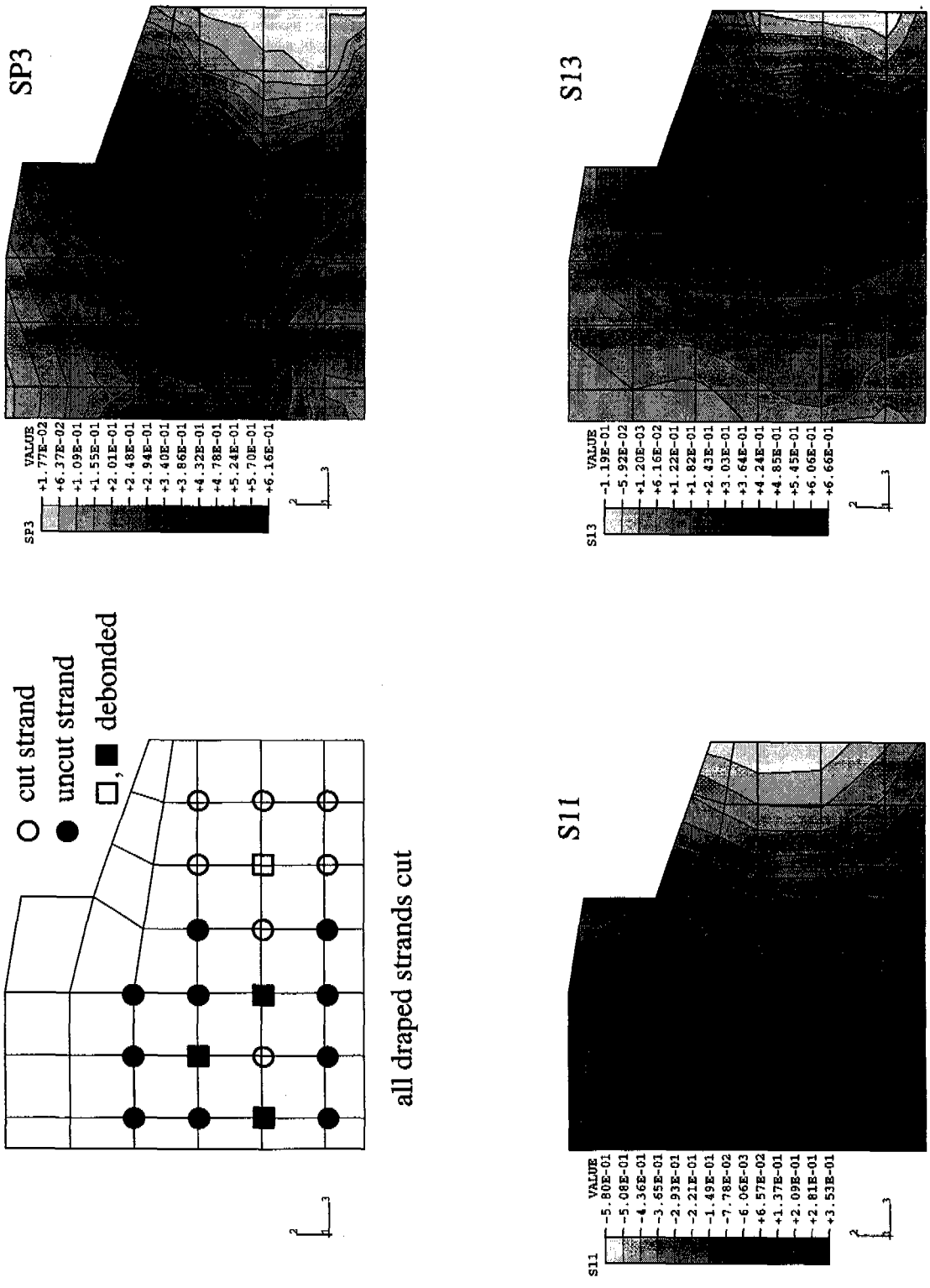

Figure 5.7c Stress Contours for Pattern 72F, Step 6, at 6 in. From End

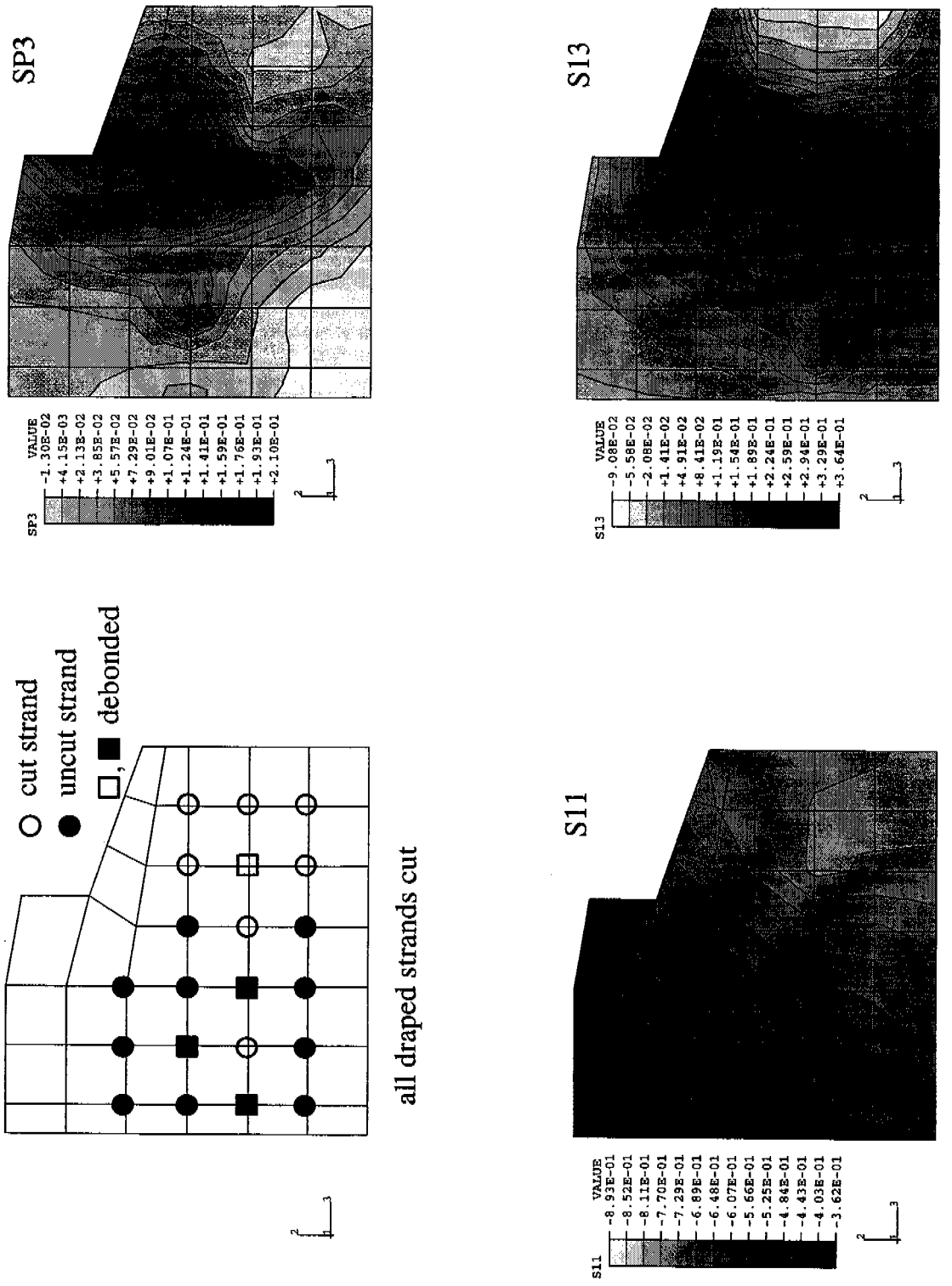

Figure 5.7d Stress Contours for Pattern 72F, Step 6, at 24 in. From End

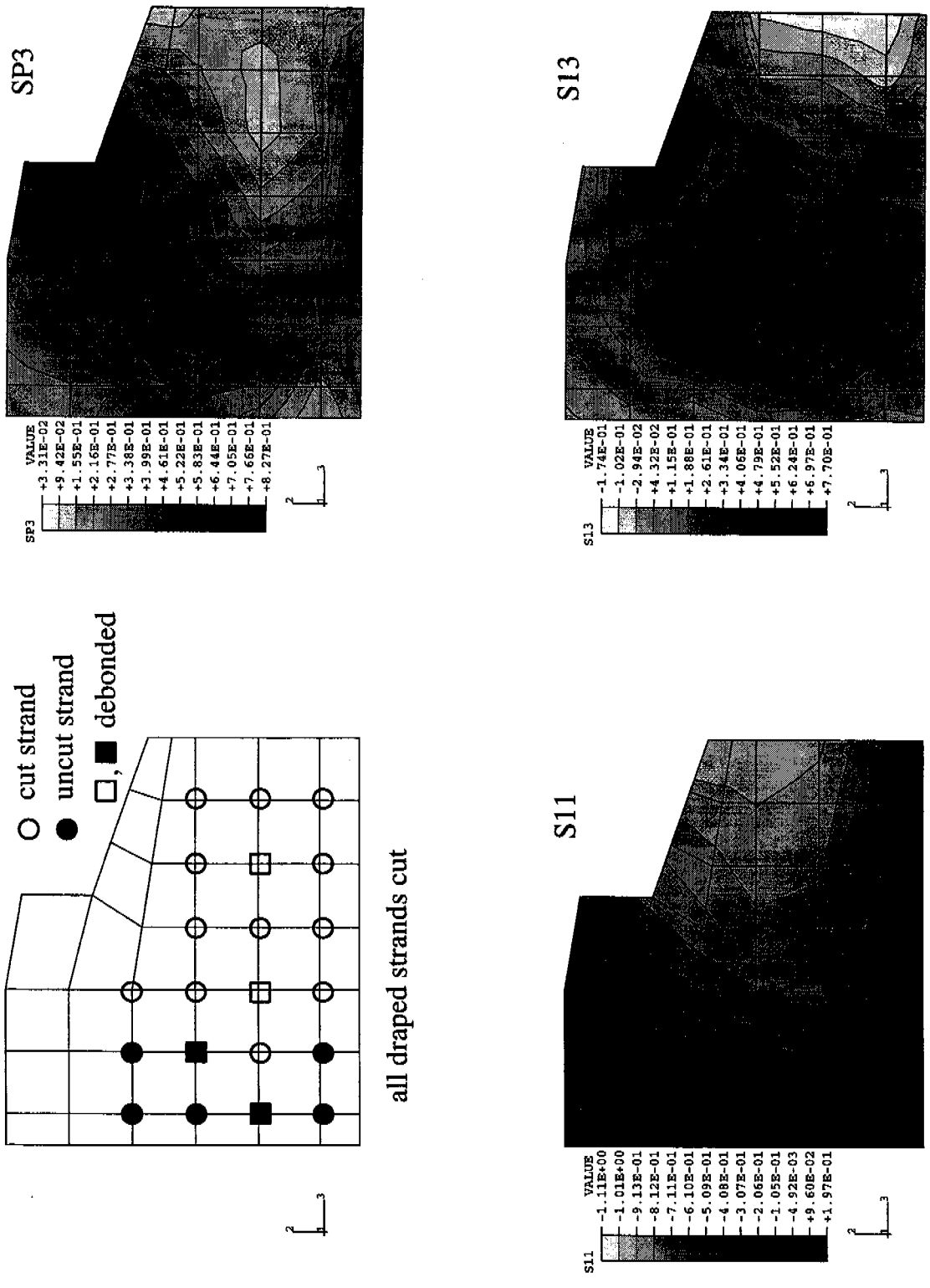

Figure 5.7e Stress Contours for Pattern 72F, Step 8, at 6 in. From End

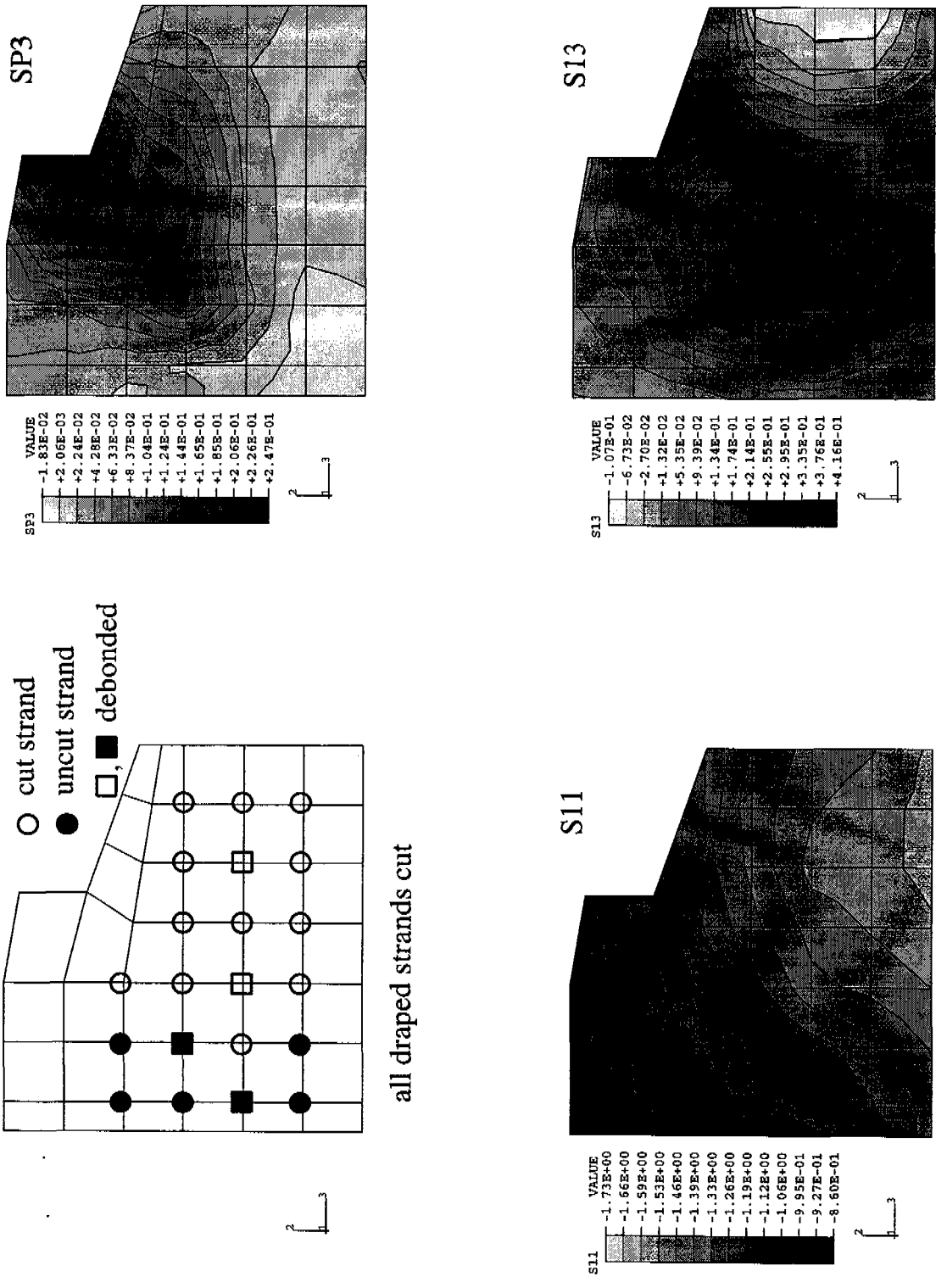

Figure 5.7f Stress Contours for Pattern 72F, Step 8, at 24 in. From End

Figure 5.7g Stress Contours for Pattern 72F, Step 10, at 6 in. From End

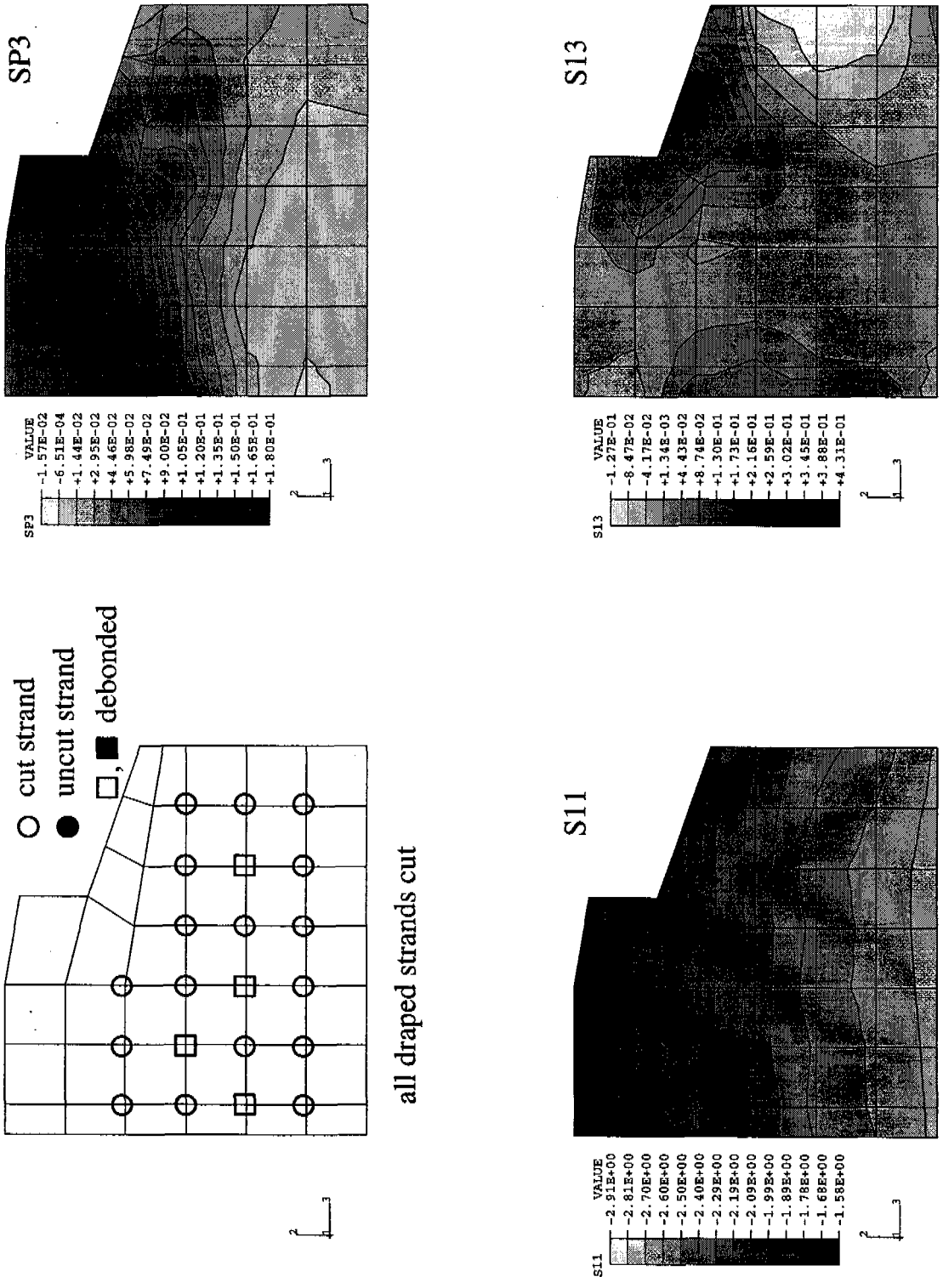

Figure 5.7h Stress Contours for Pattern 72F, Step 10, at 24 in. From End

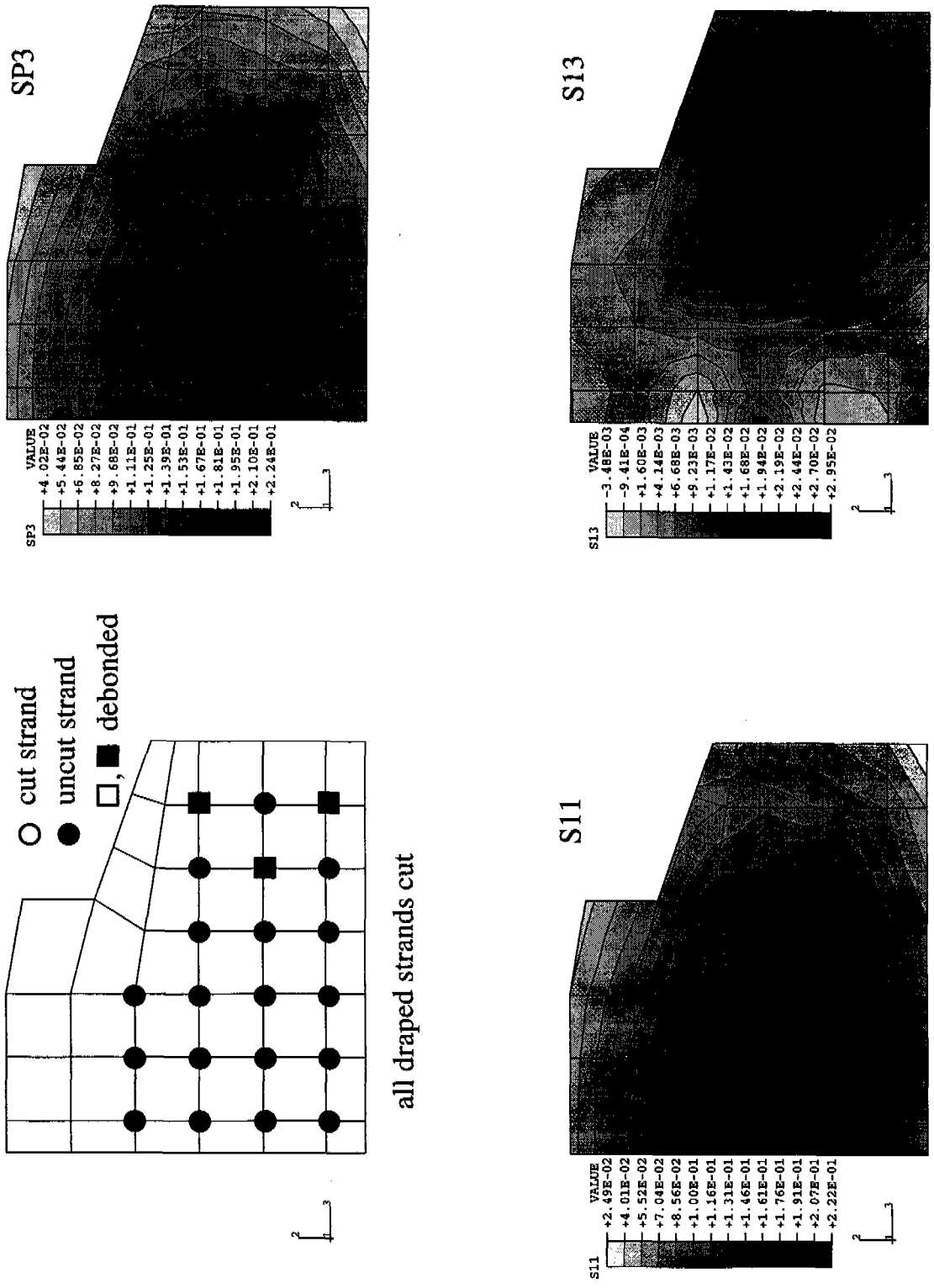

Figure 5.8a Stress Contours for Pattern 72G, Step 3, at 6 in. From End

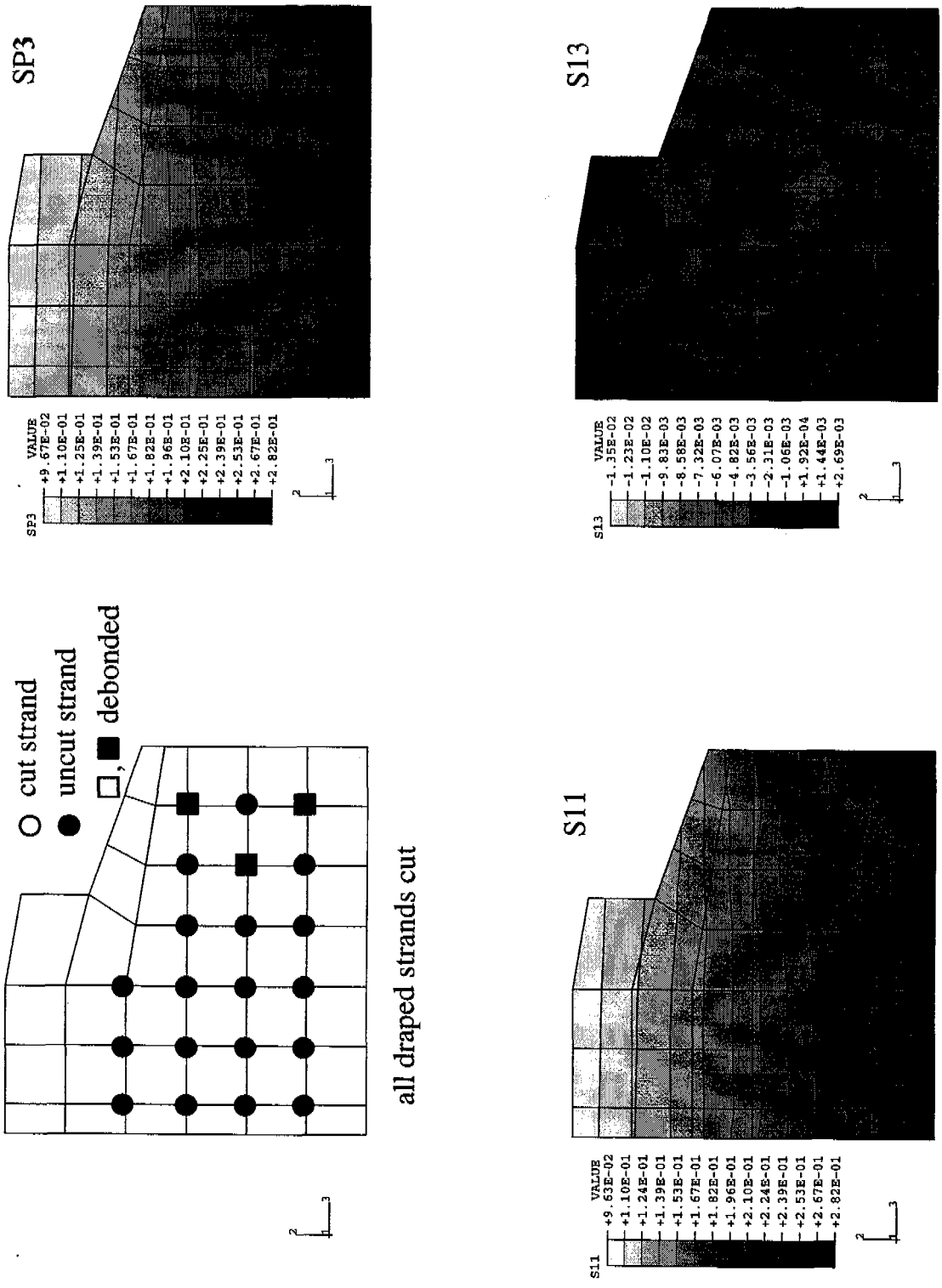

Figure 5.8b Stress Contours for Pattern 72G, Step 3, at 24 in. From End

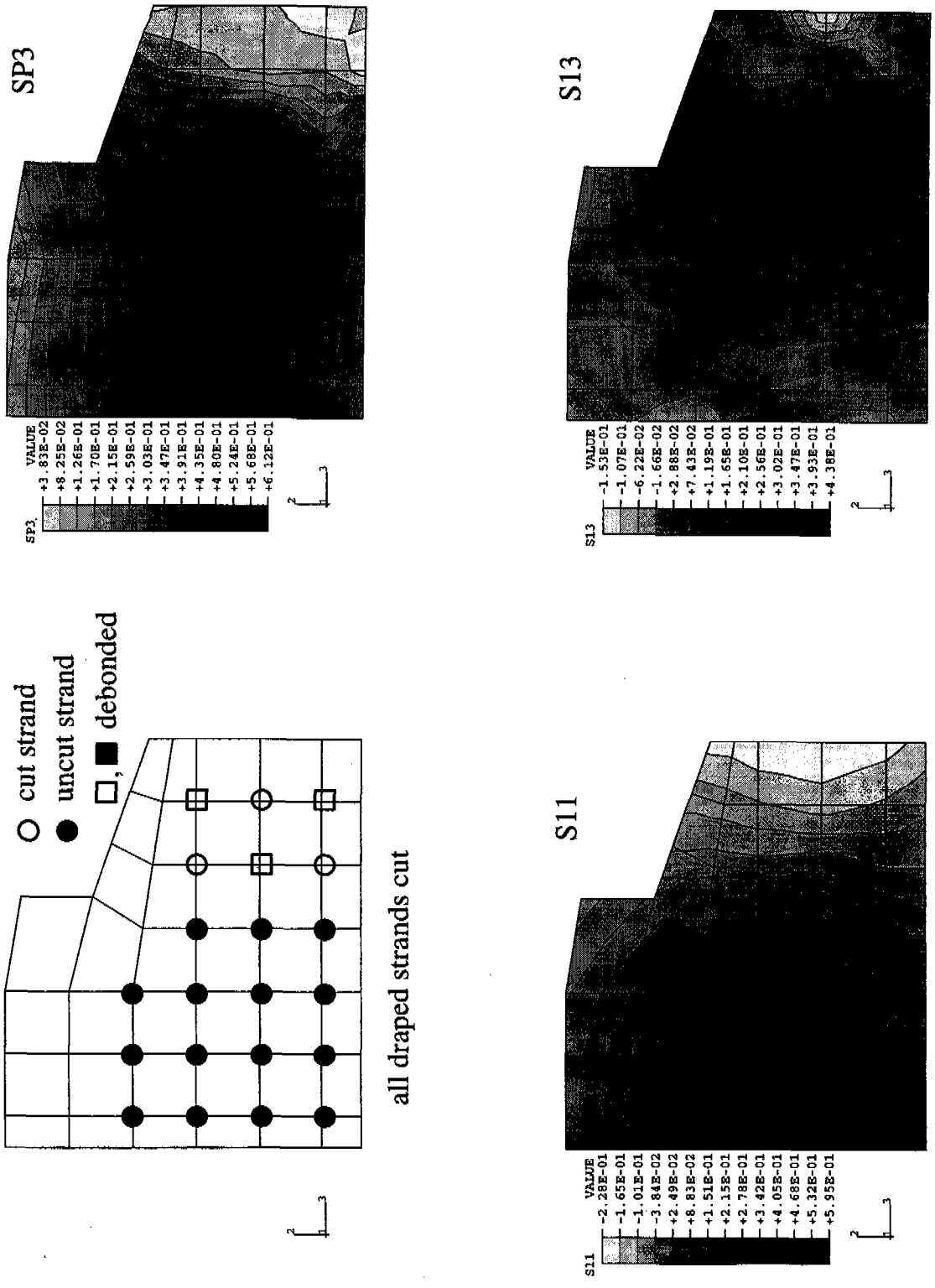

Figure 5.8c Stress Contours for Pattern 72G, Step 5, at 6 in. From End

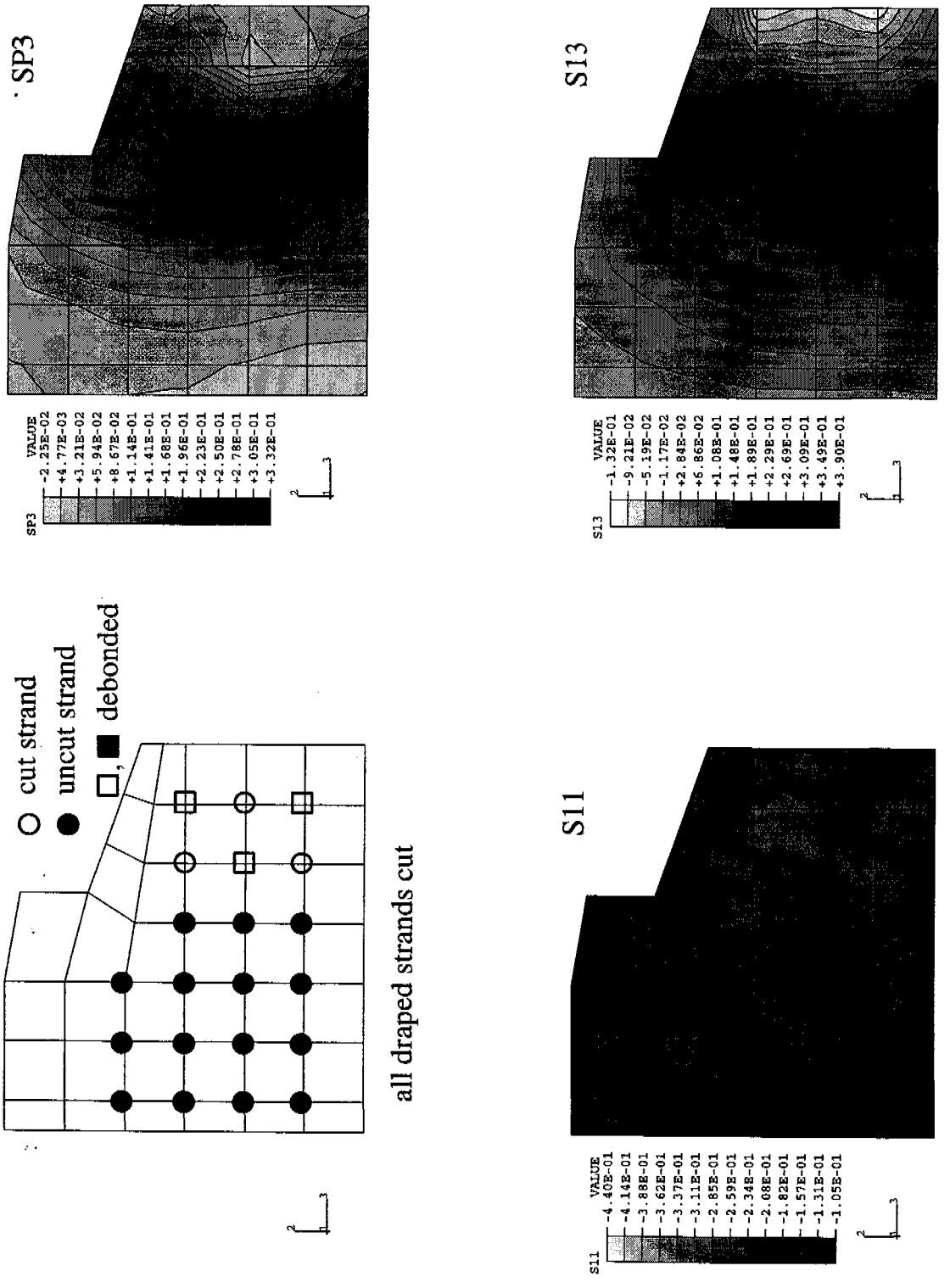

Figure 5.8d Stress Contours for Pattern 72G, Step 5, at 24 in. From End

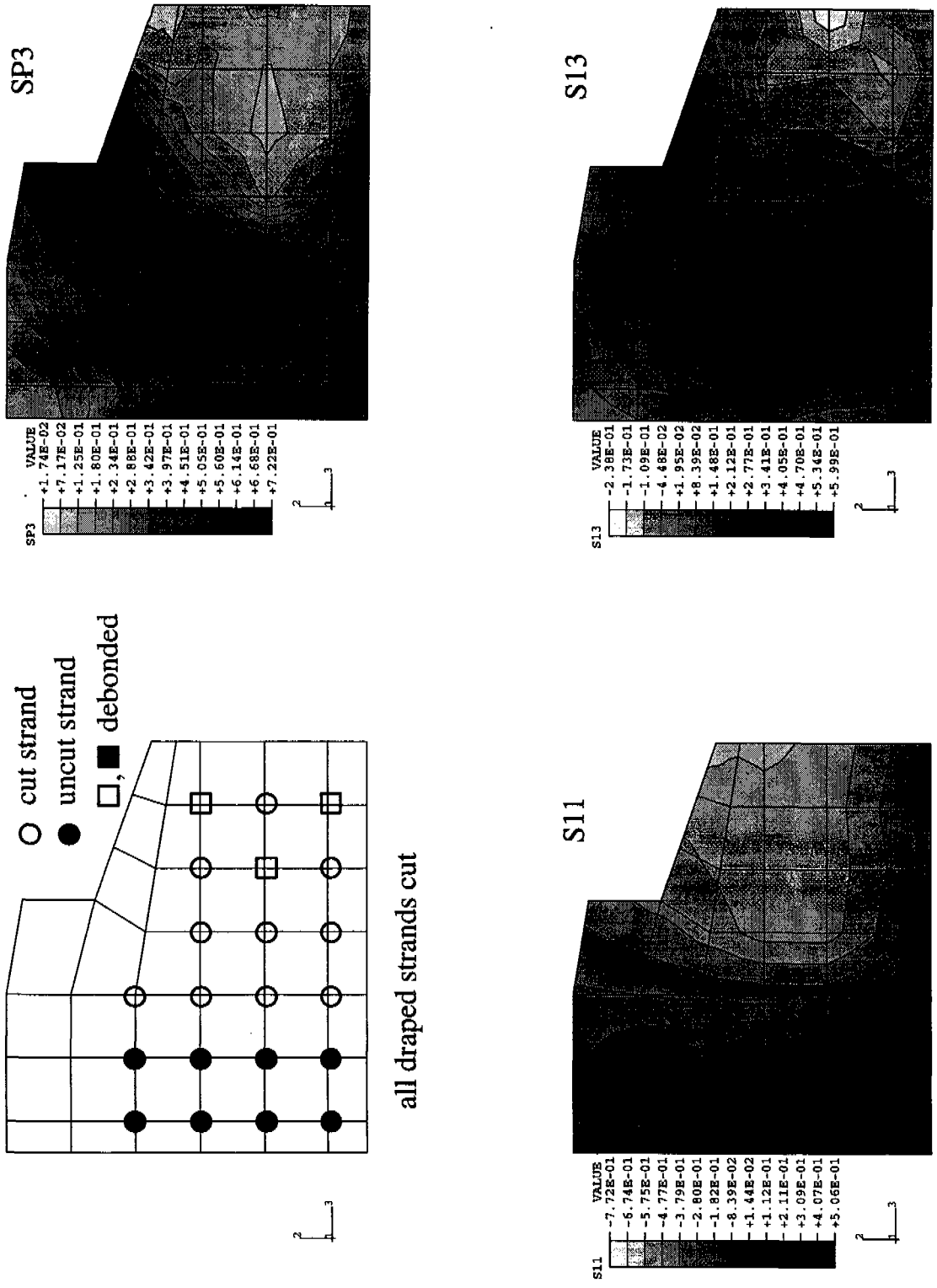

Figure 5.8e Stress Contours for Pattern 72G, Step 7, at 6 in. From End

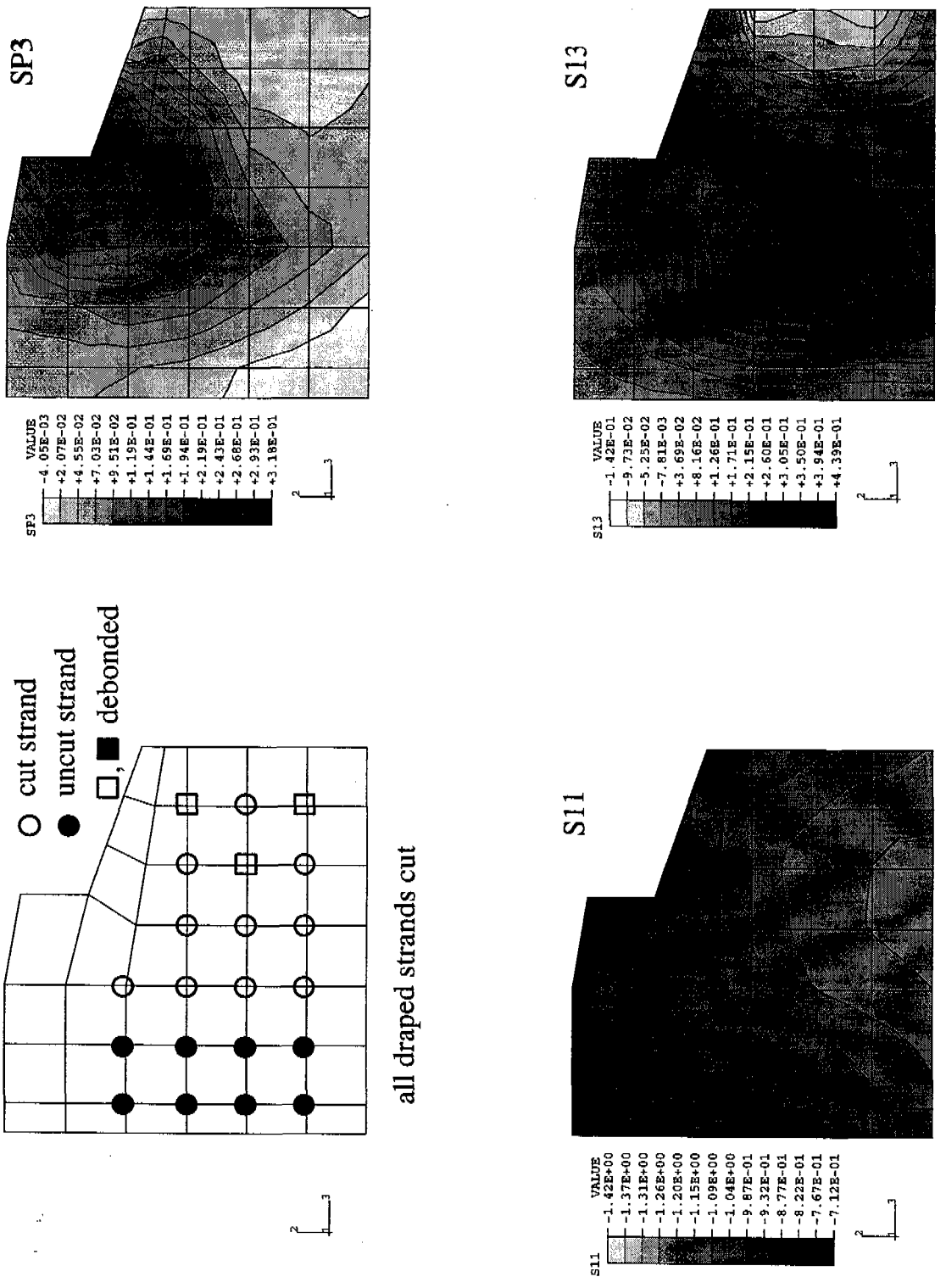

Figure 5.8f Stress Contours for Pattern 72G, Step 7, at 24 in. From End

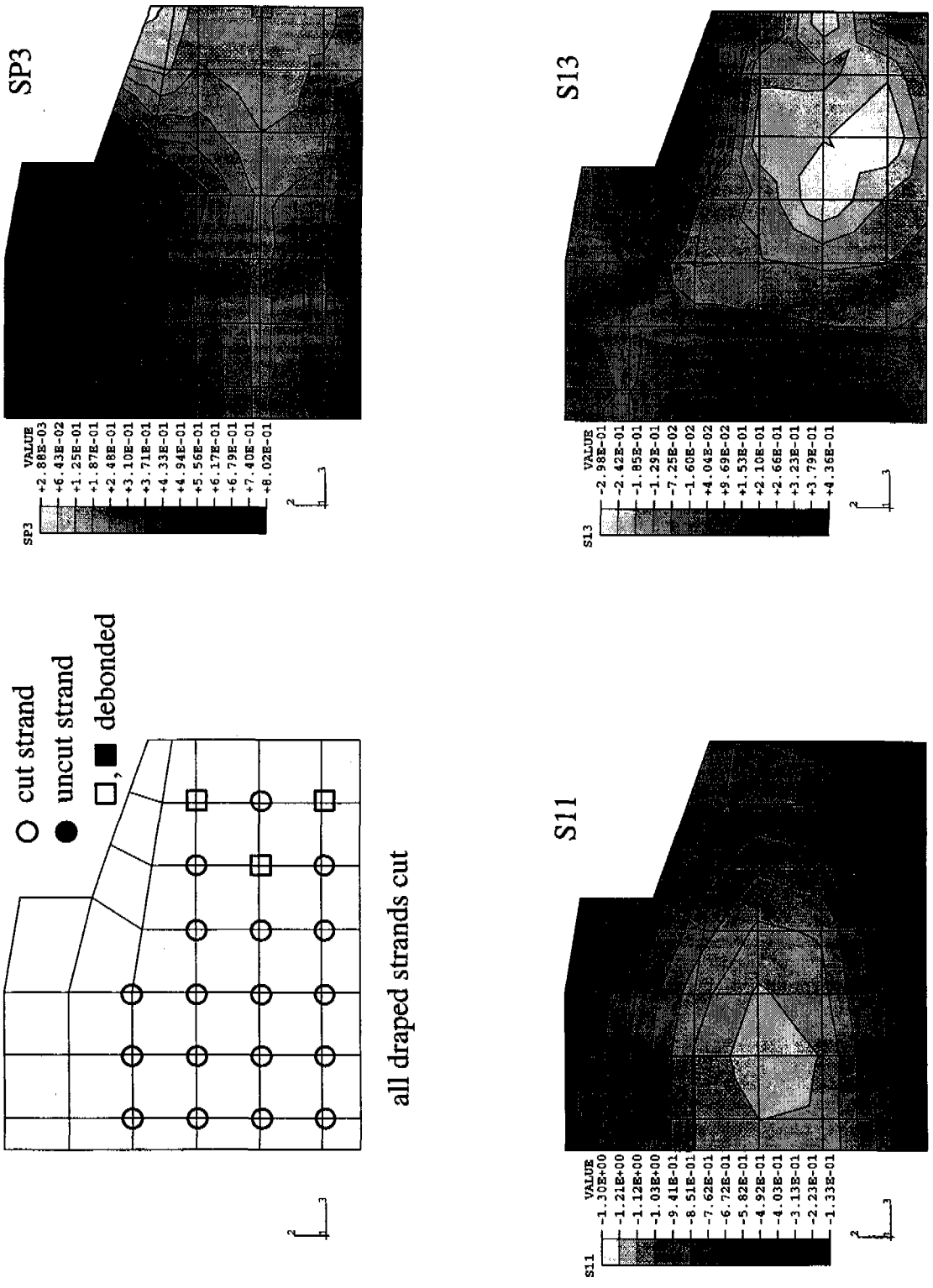

Figure 5.8g Stress Contours for Pattern 72G, Step 9, at 6 in. From End

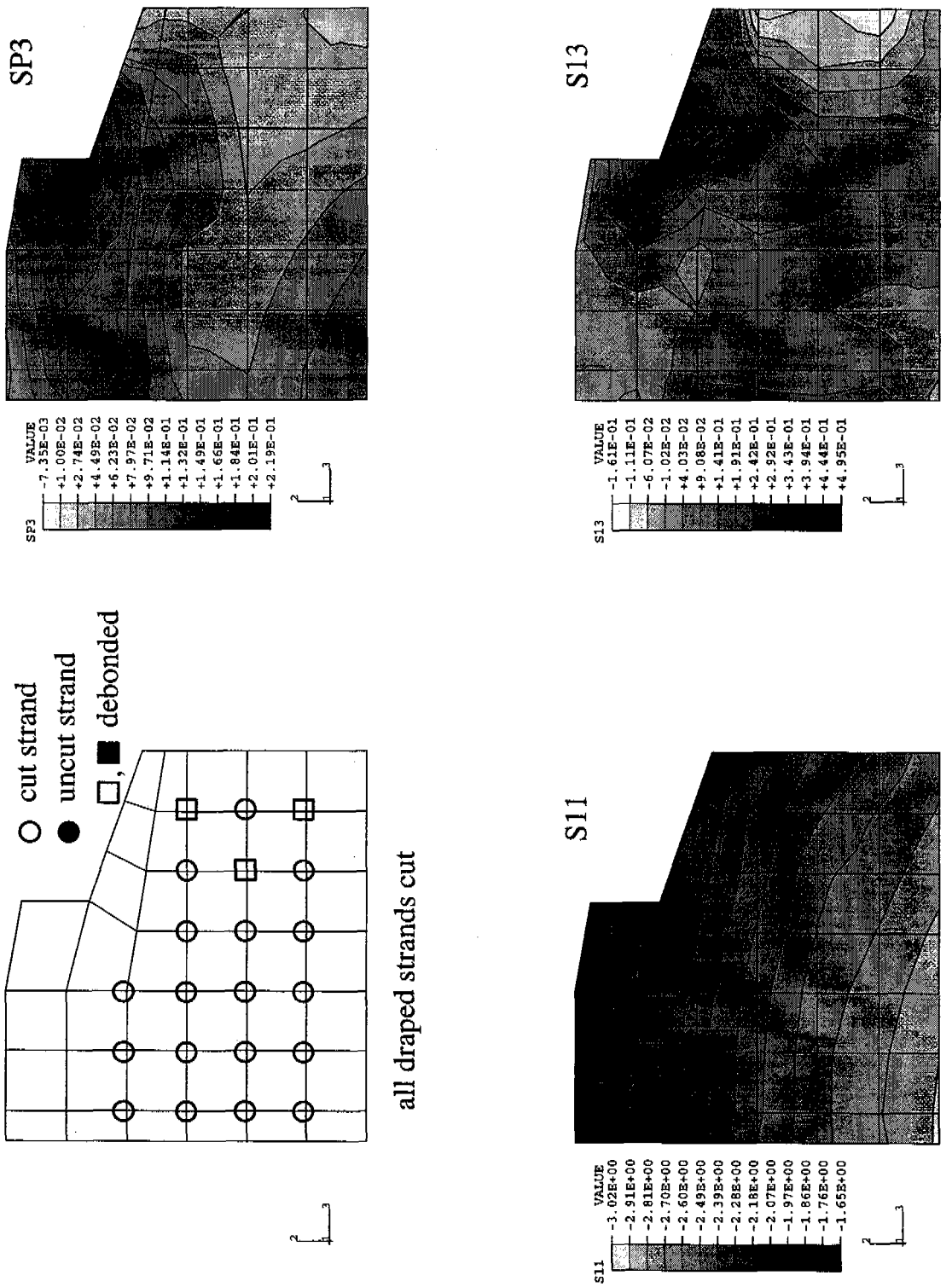

Figure 5.8h Stress Contours for Pattern 72G, Step 9, at 24 in. From End

Figure 5.9 Stress Concentration at Base of Web at Full Release As–Built

Figure 5.10 Stress Concentration at Base of Web at Full Release
Top of Bottom Flange – Slope Doubled

Figure 5.11 Stress Concentration at Base of Web at Full Release
Top of Bottom Flange – Slope Tripled

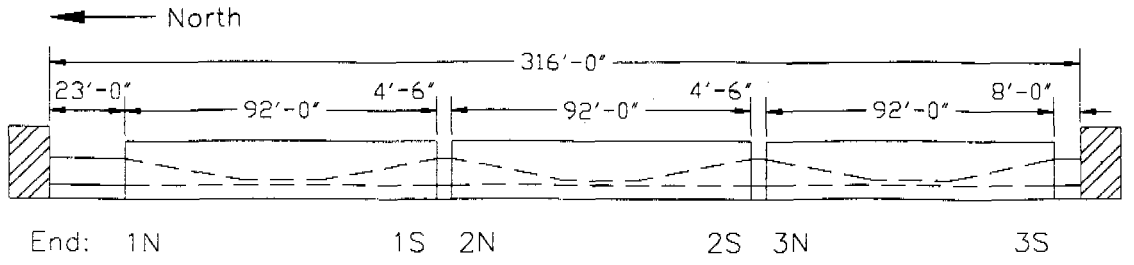

Figure 6.1 Bed Layout for 45 in. Girders

Draped Strands = Pairs 1–6, Steps 2–3
Hold down cut after Pair 6, in Step 4

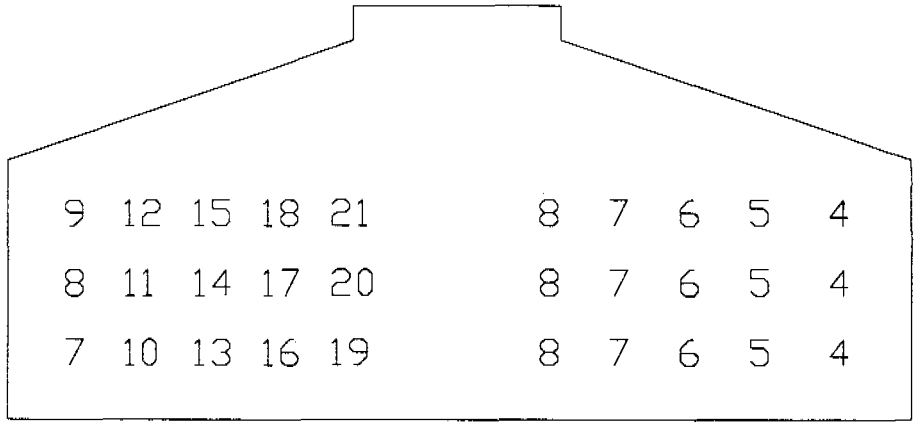

Figure 6.2 Cutting Pattern 45A

Draped Strands = Pairs 2–7, Steps 3–4
Hold down cut after Pair 7, in Step 5

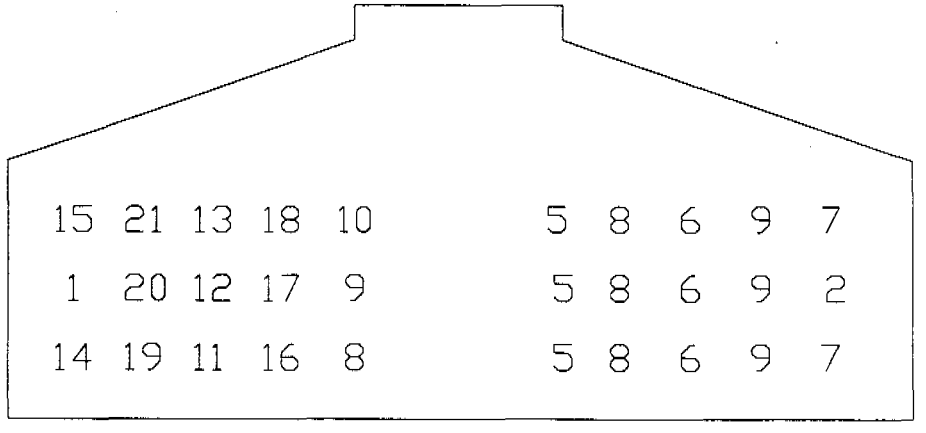

Figure 6.3 Cutting Pattern 45B

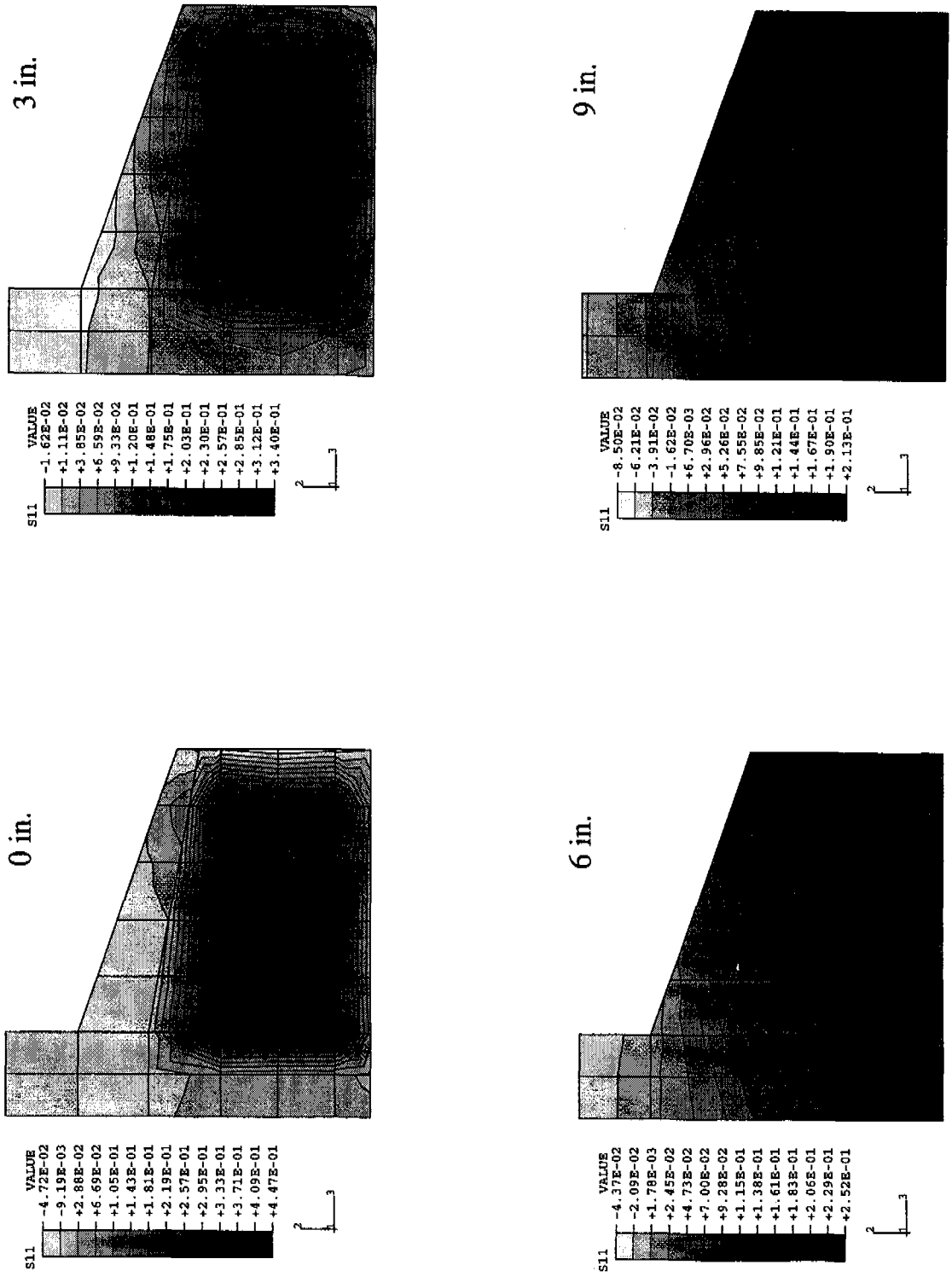

Figure 6.4a S11 Contours for Pattern 45A, Step 3

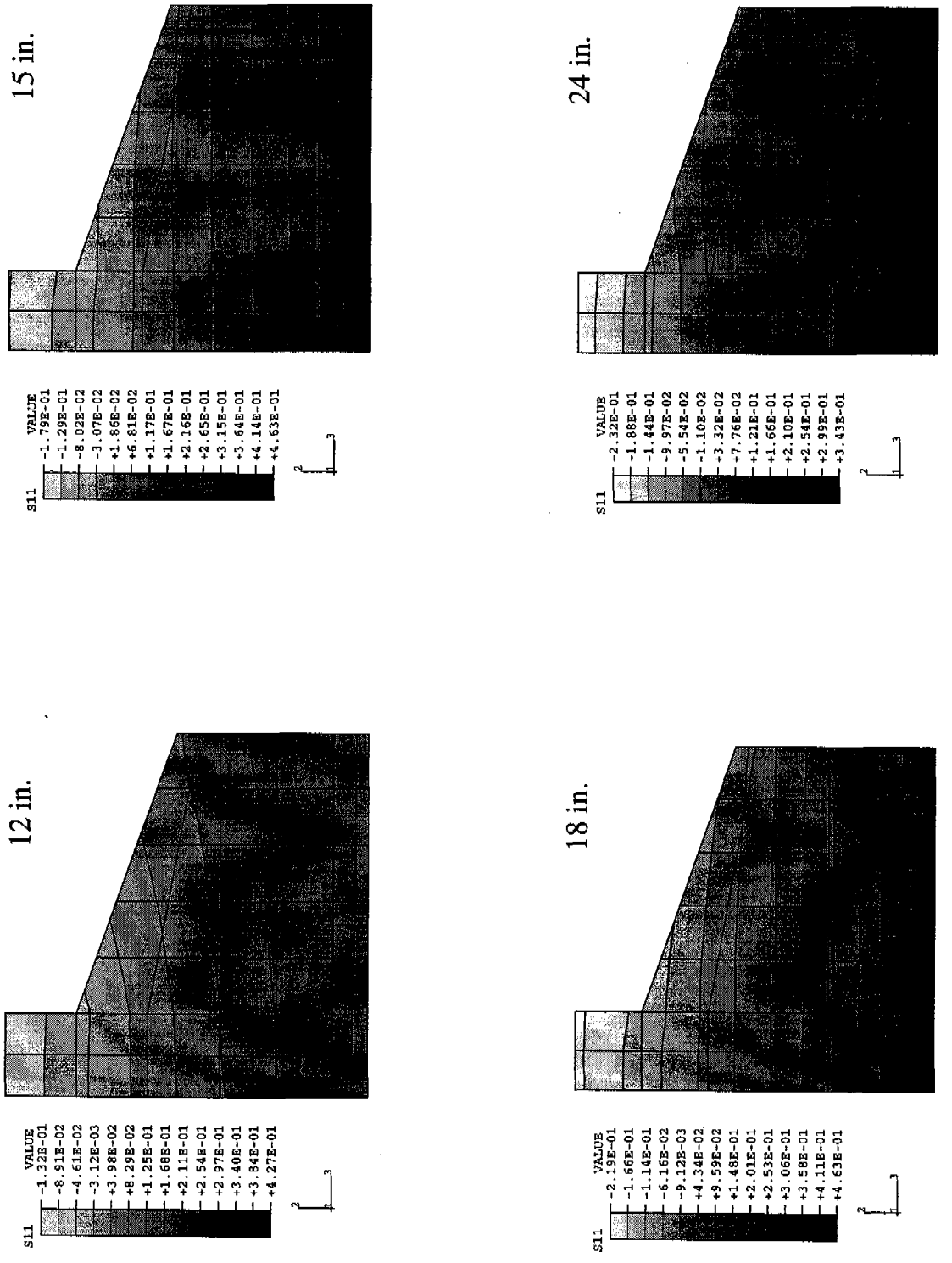

Figure 6.4b S11 Contours for Pattern 45A, Step 3

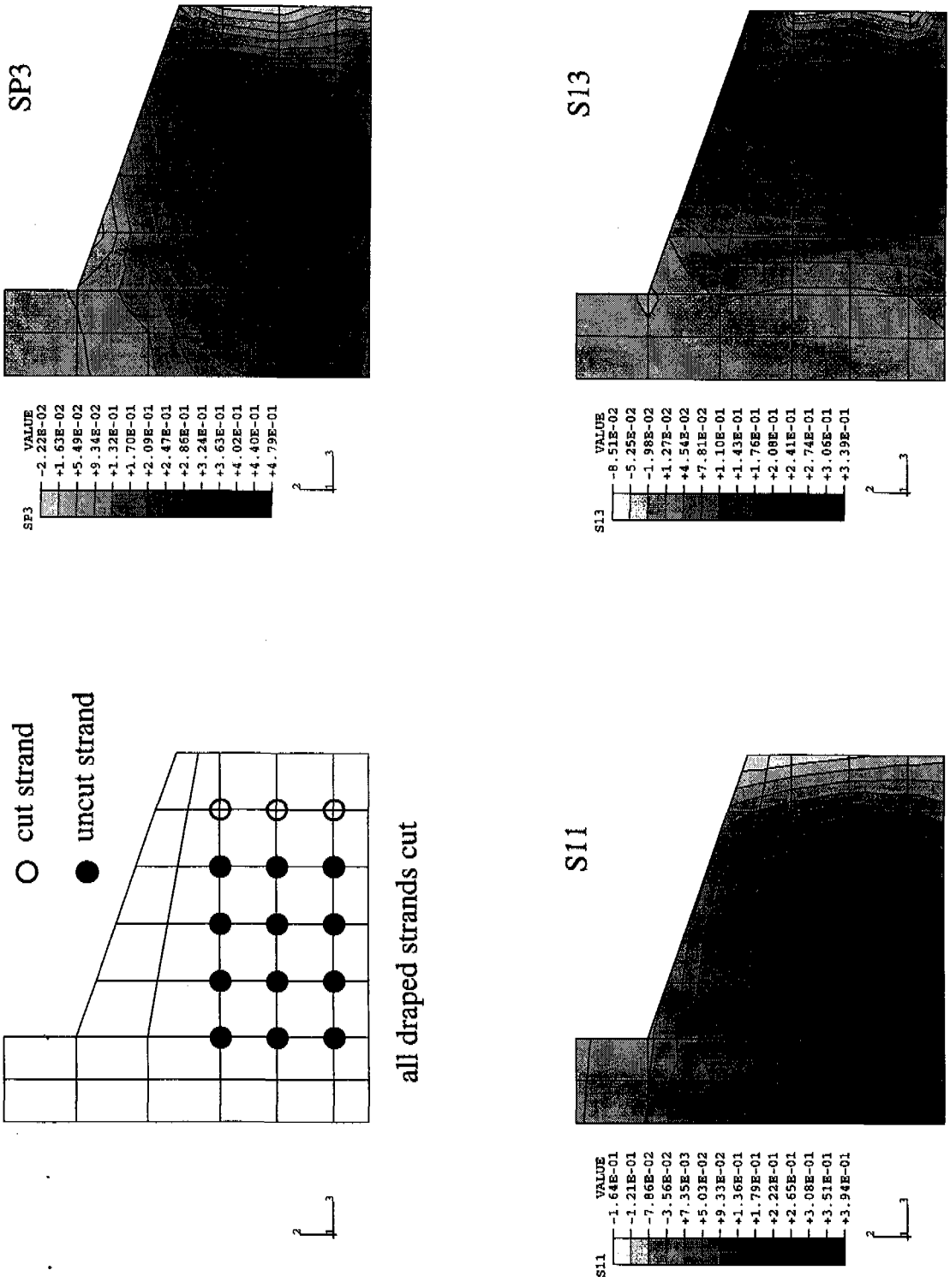

Figure 6.4c Stress Contours for Pattern 45A, Step 4, at 6 in. From End

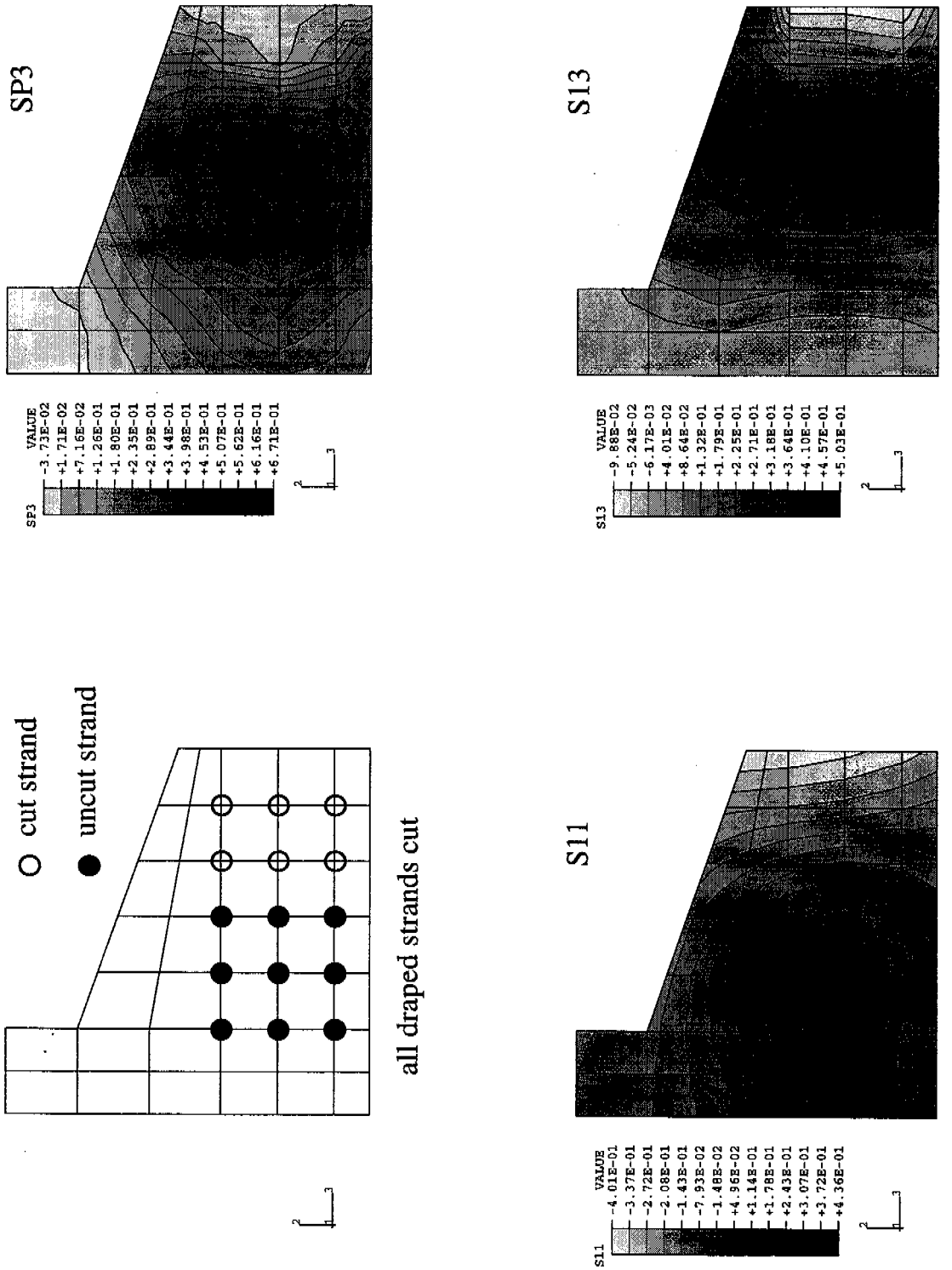

Figure 6.4d Stress Contours for Pattern 45A, Step 5, at 6 in. From End

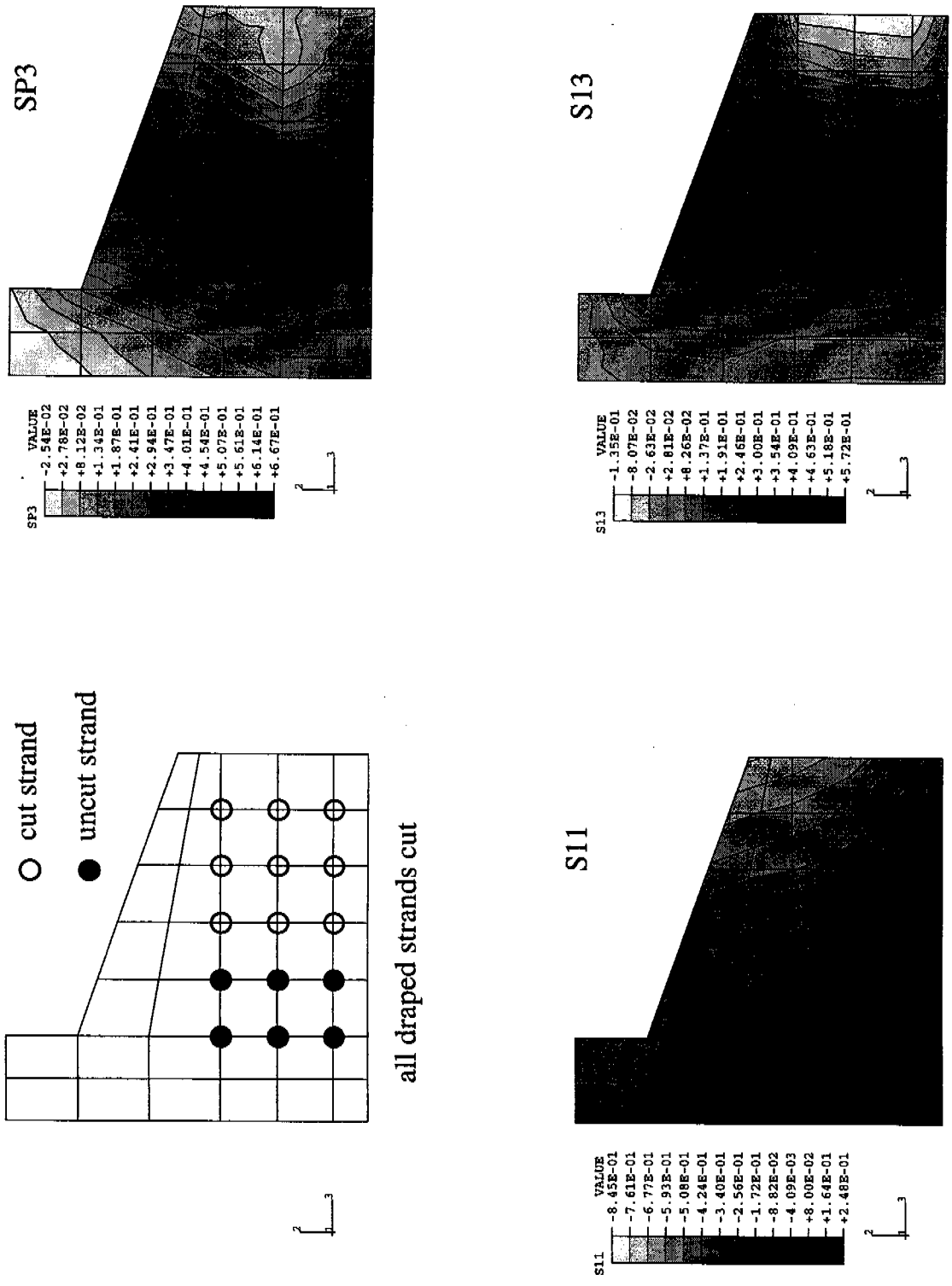

Figure 6.4e Stress Contours for Pattern 45A, Step 6, at 6 in. From End

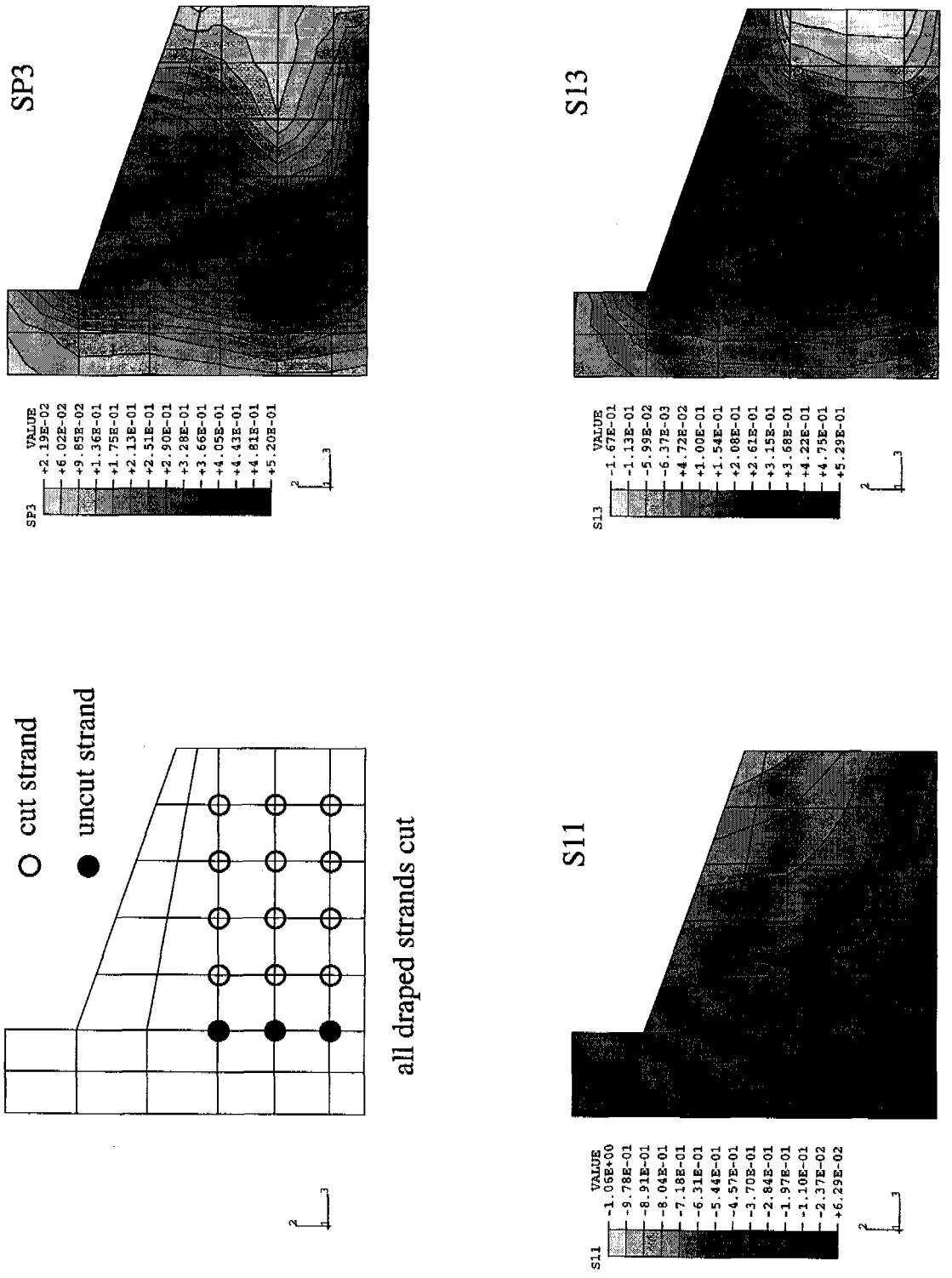

Figure 6.4f Stress Contours for Pattern 45A, Step 7, at 6 in. From End

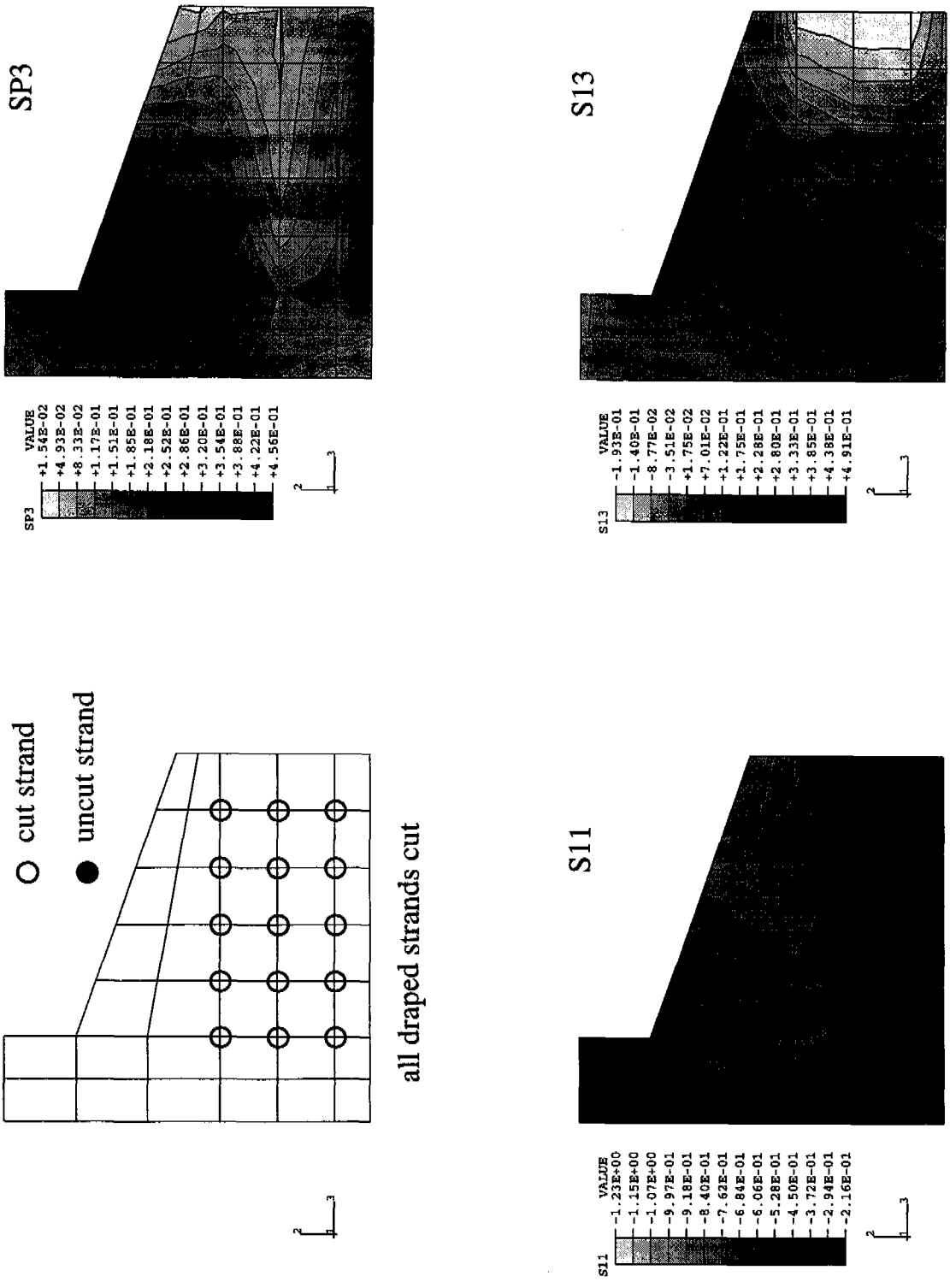

Figure 6.4g Stress Contours for Pattern 45A, Step 8, at 6 in. From End

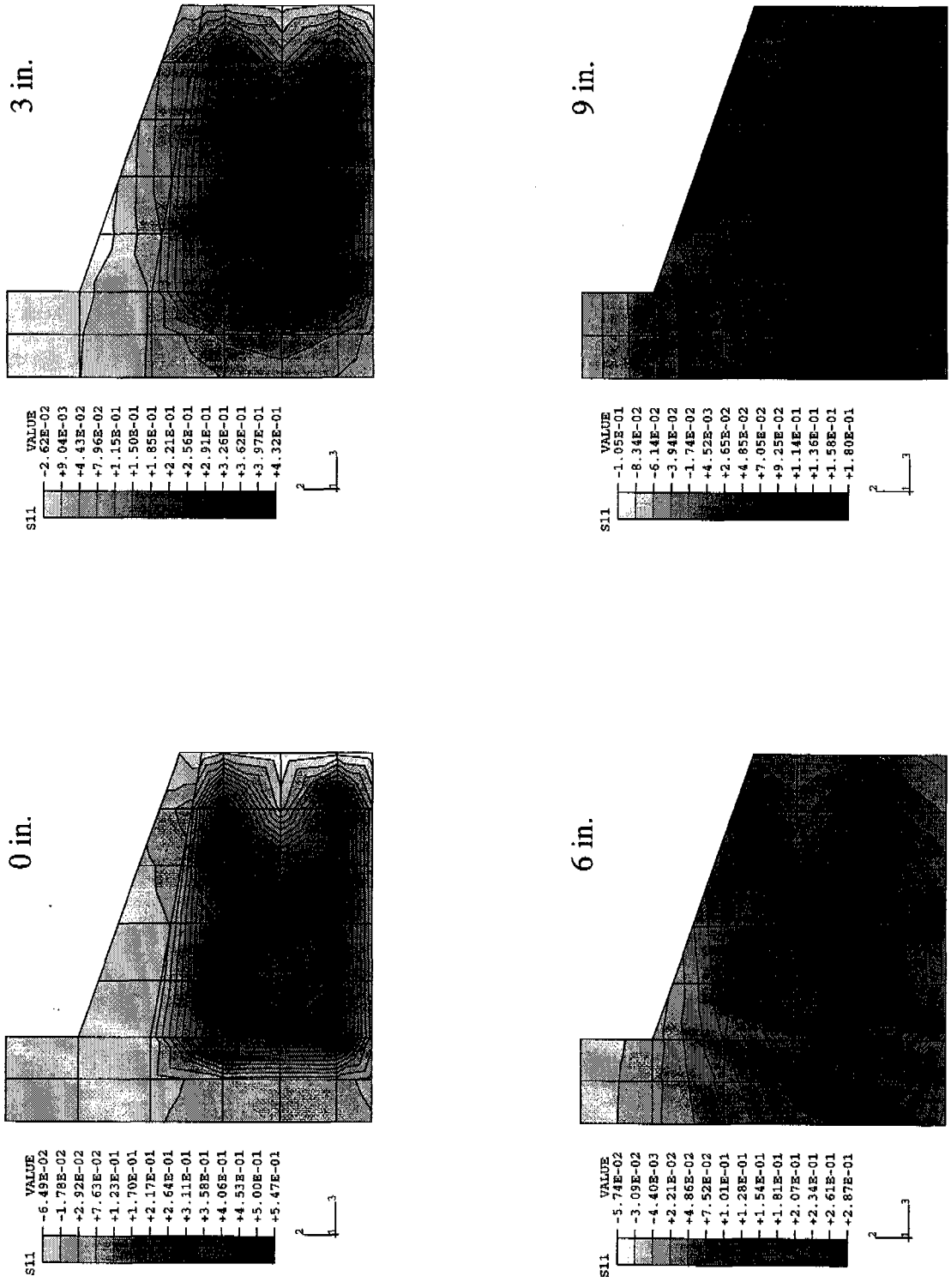

Figure 6.5a S11 Contours for Pattern 45B, Step 4

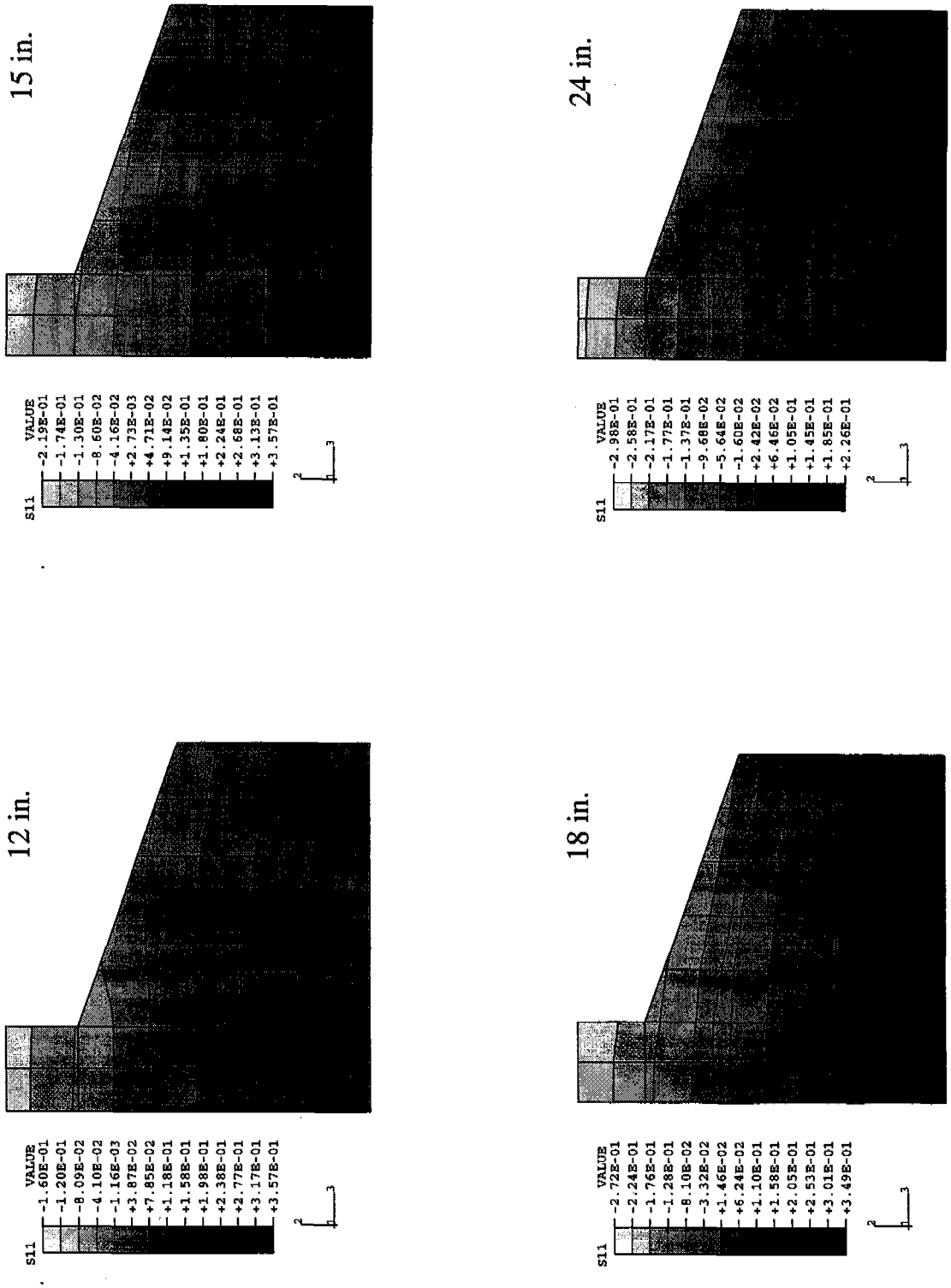

Figure 6.5b S11 Contours for Pattern 45B, Step 4

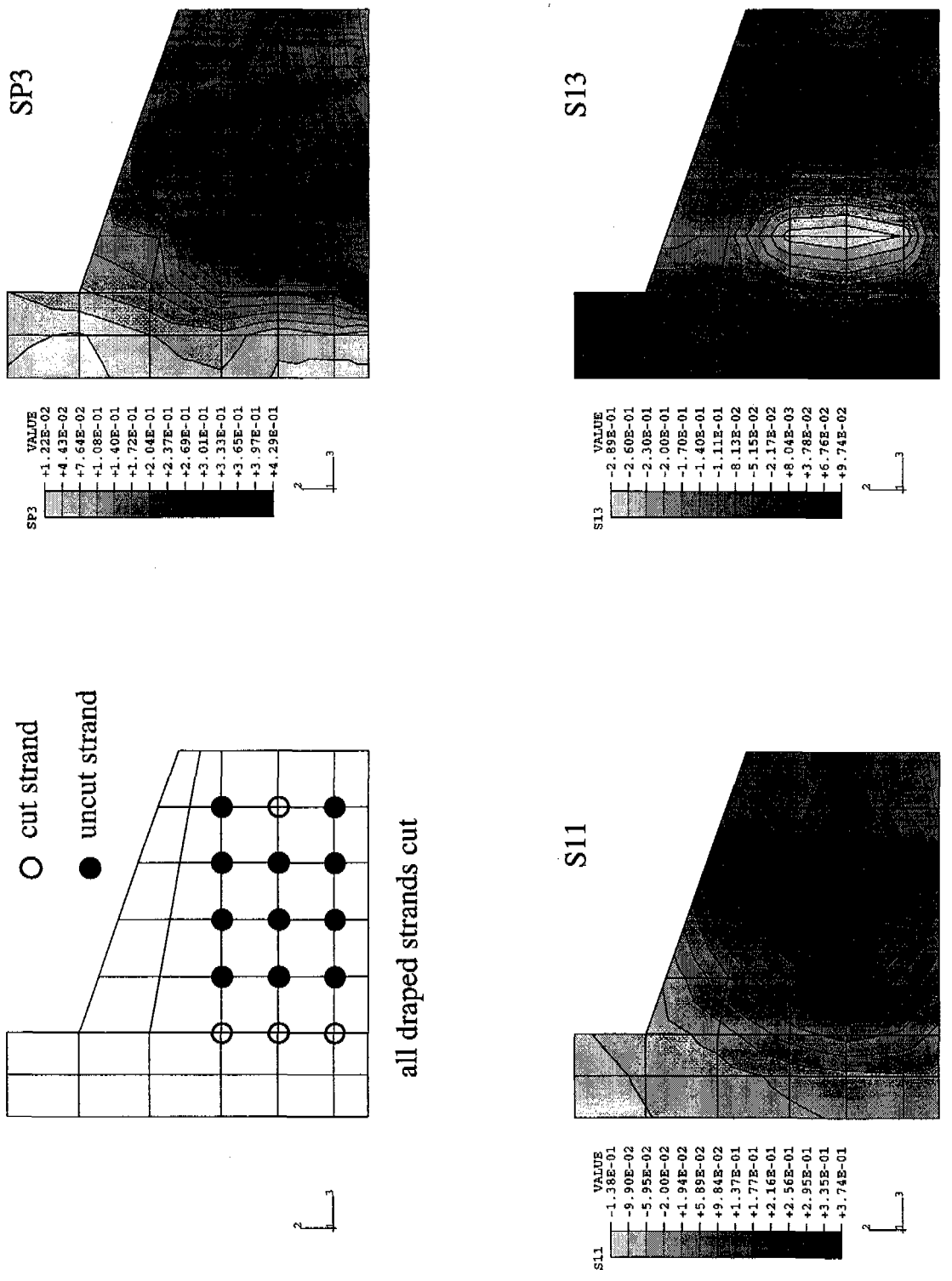

Figure 6.5c Stress Contours for Pattern 45B, Step 5, at 6 in. From End

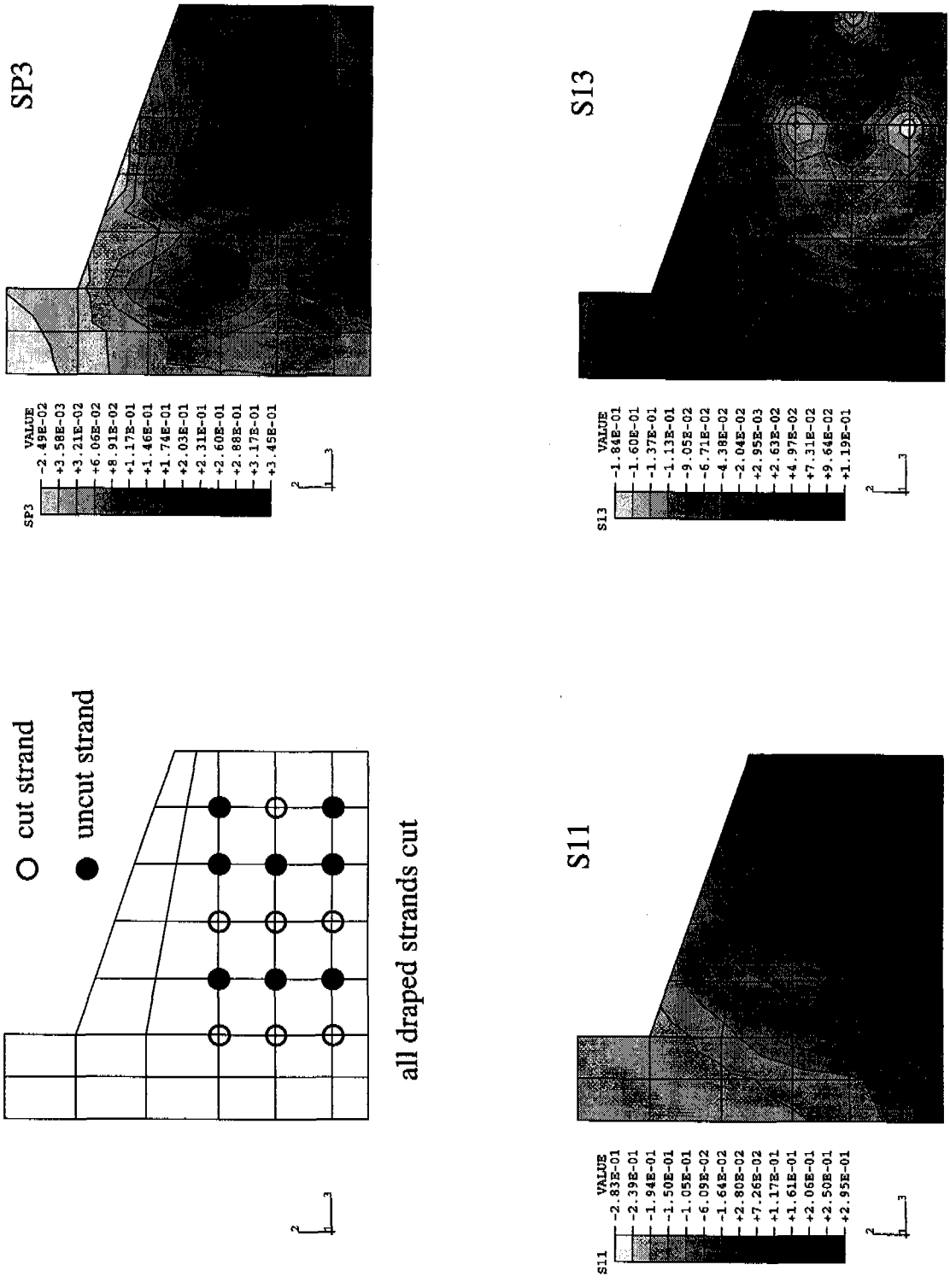

Figure 6.5d Stress Contours for Pattern 45B, Step 6, at 6 in. From End

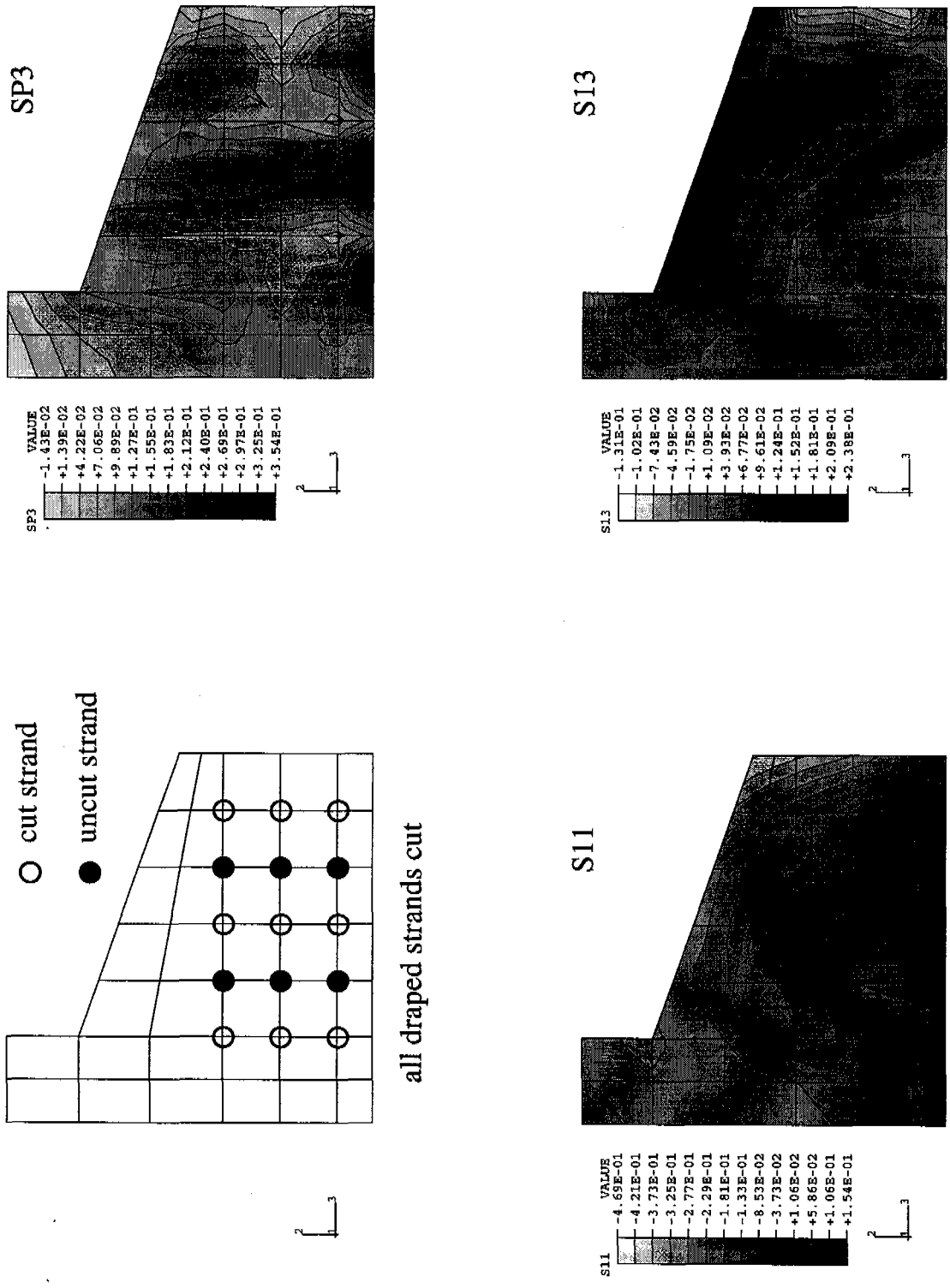

Figure 6.5e Stress Contours for Pattern 45B, Step 7, at 6 in. From End

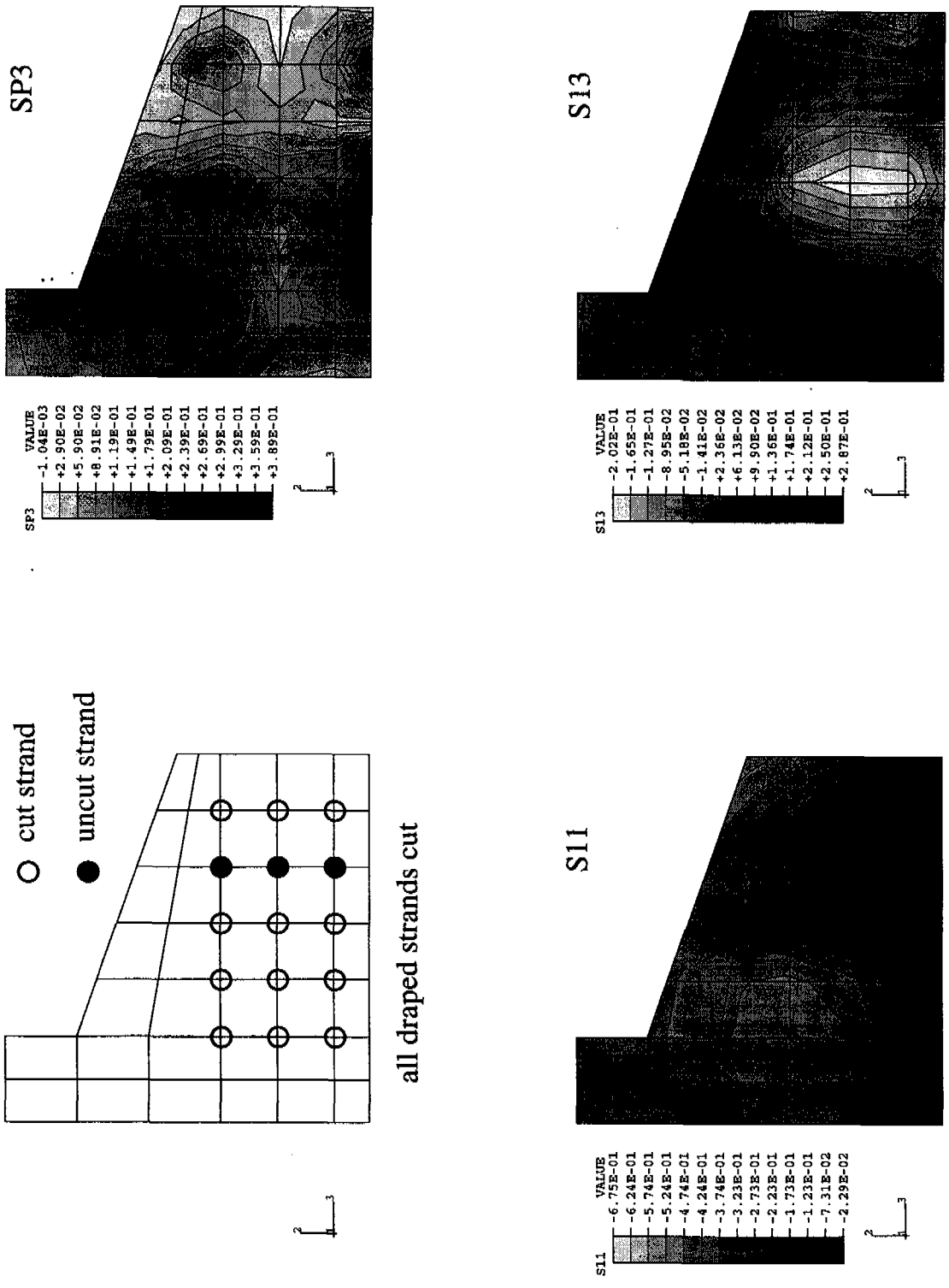

Figure 6.5f Stress Contours for Pattern 45B, Step 8, at 6 in. From End

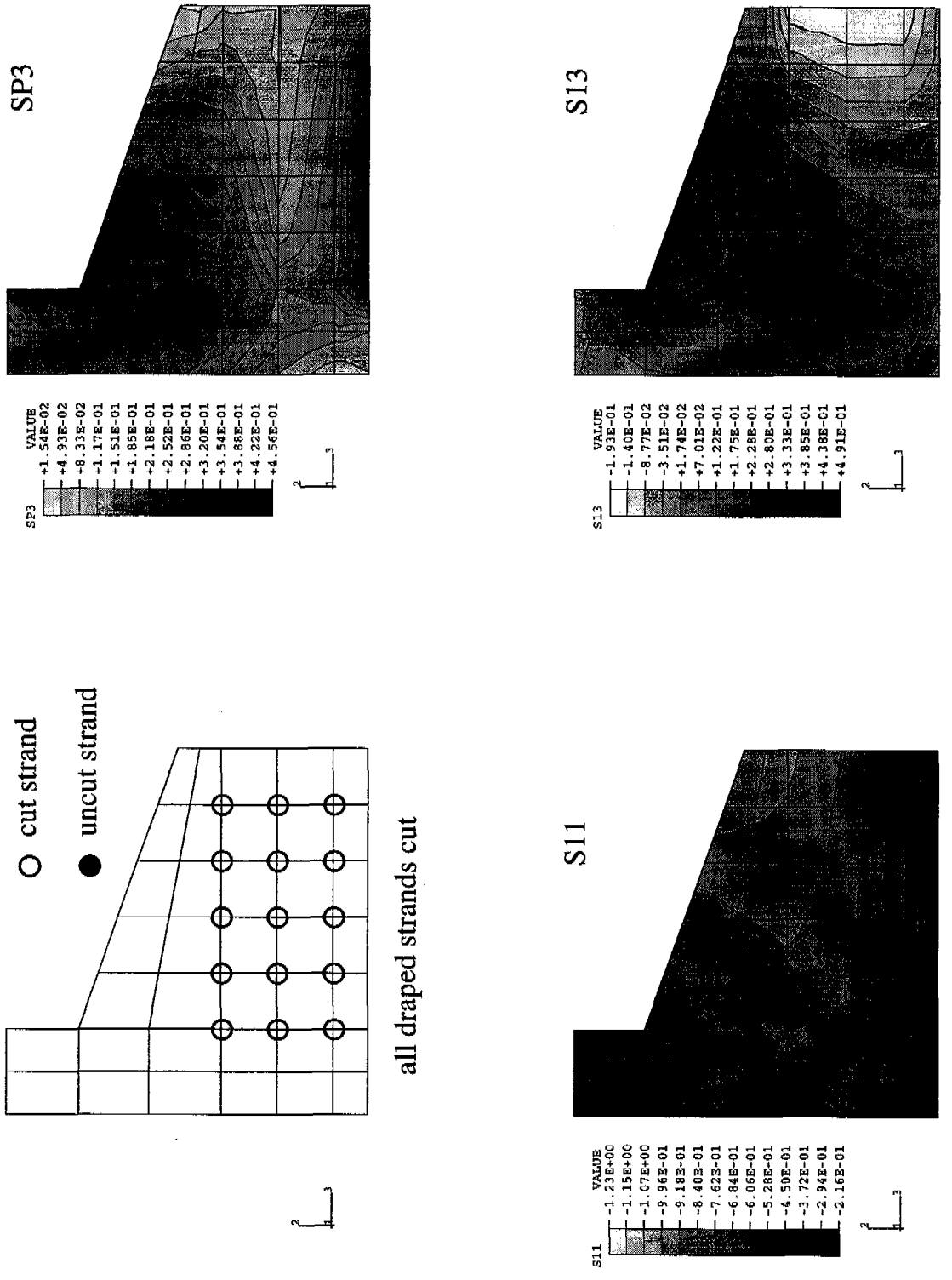

Figure 6.5g Stress Contours for Pattern 45B, Step 9, at 6 in. From End

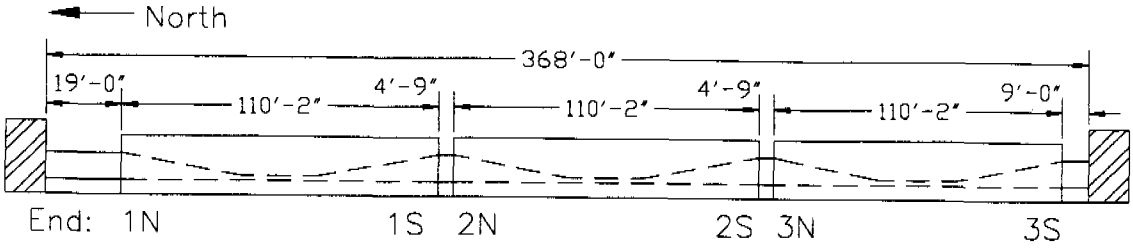

Figure 6.6 Bed Layout for 54 in. Girders

Draped Strands = Pairs 1–6, Steps 2–3
Hold down cut after Pair 6, in Step 4

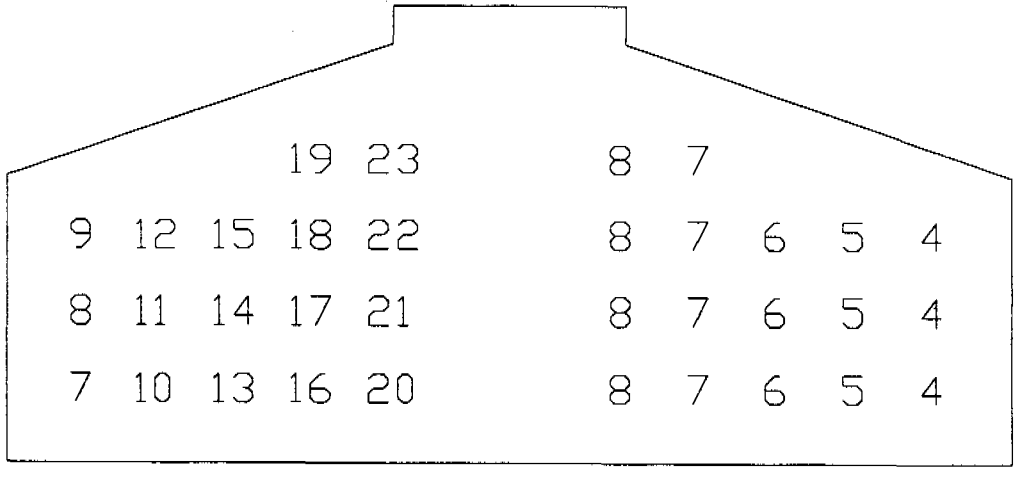

Figure 6.7a Cutting Pattern 54A

Draped Strands = Pairs 4–9, Steps 3–4
Hold down cut after Pair 9, in Step 5

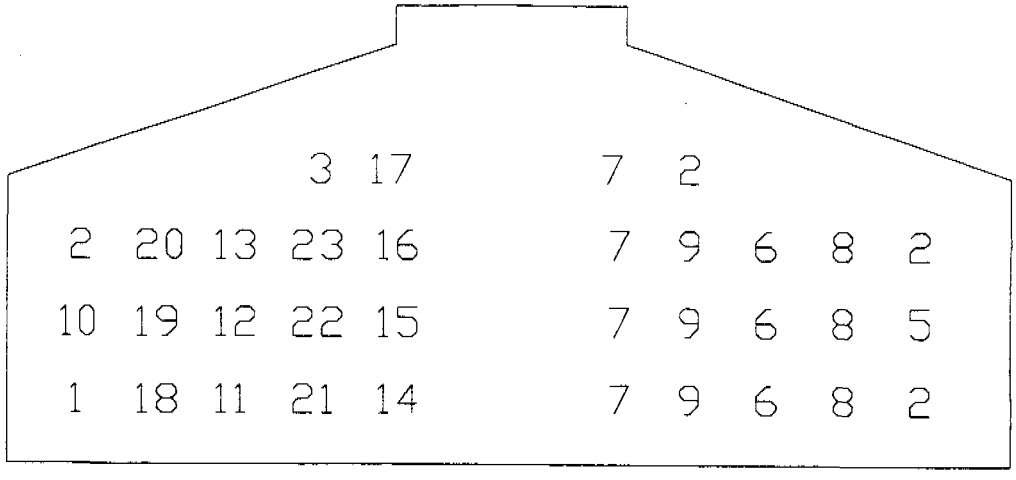

Figure 6.7b Cutting Pattern 54B

Circled strands are debonded 20 inches
Draped Strands = Pairs 4–9, Steps 3–4
Hold down cut after Pair 9, in Step 5

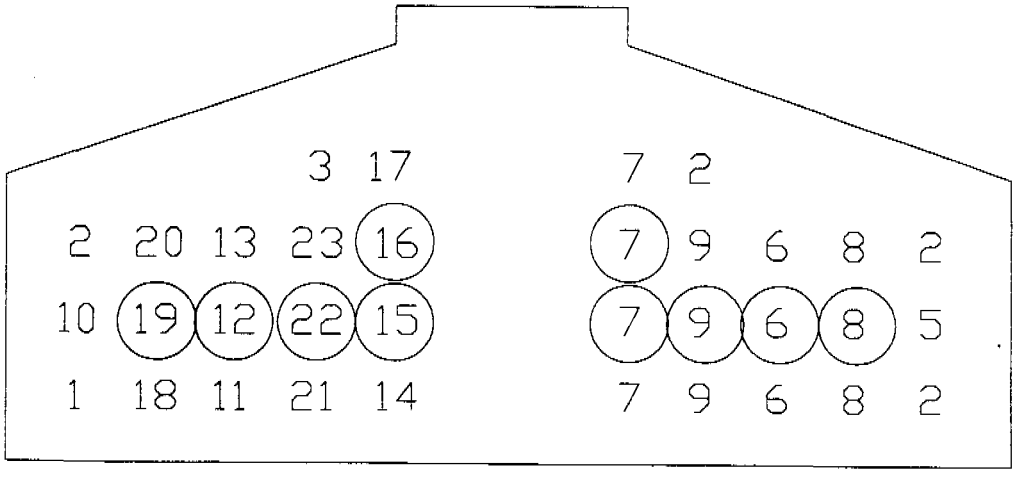

Figure 6.7c Cutting Pattern 54C

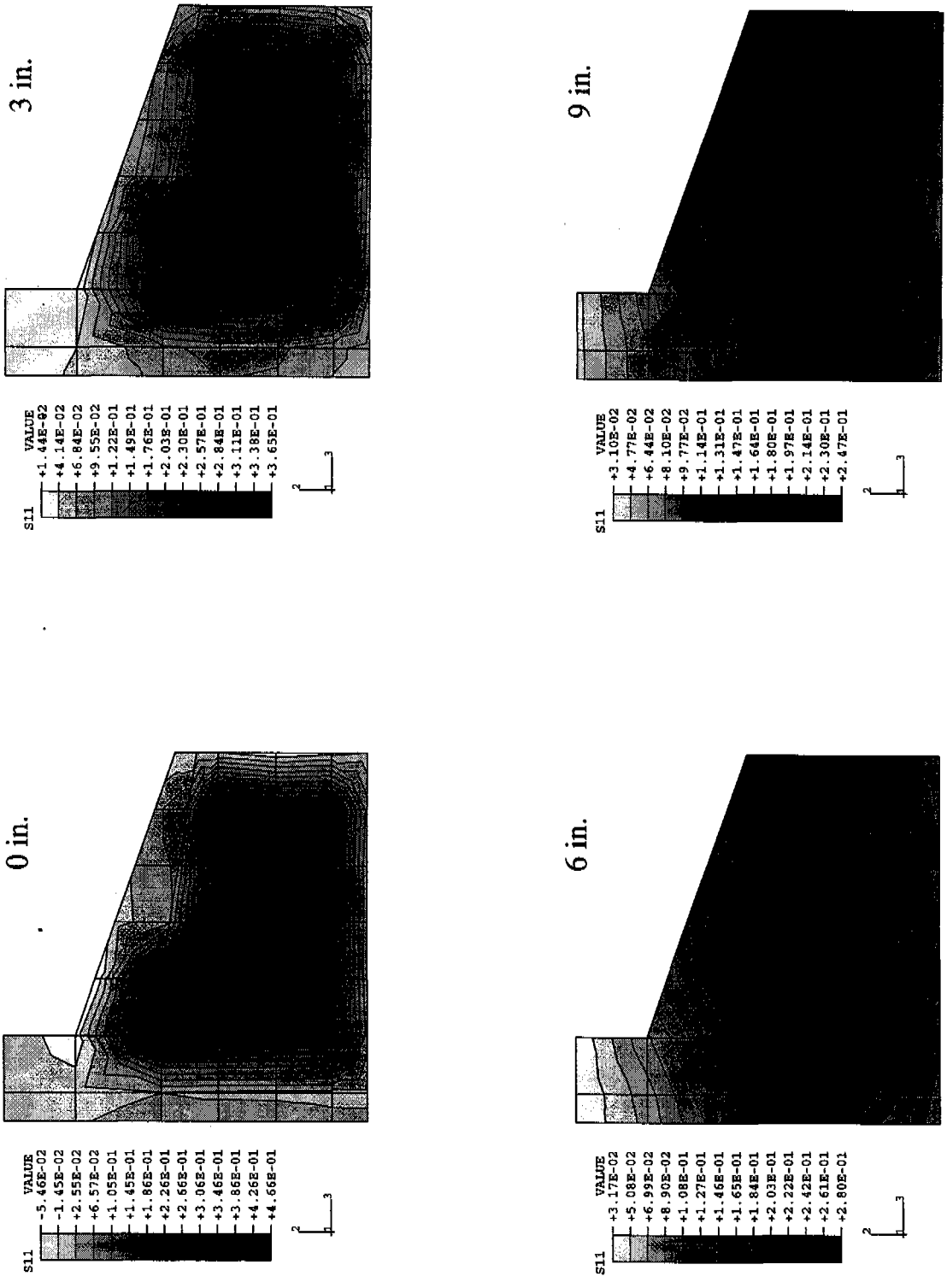

Figure 6.8a S11 Contours for Pattern 54A, Step 3

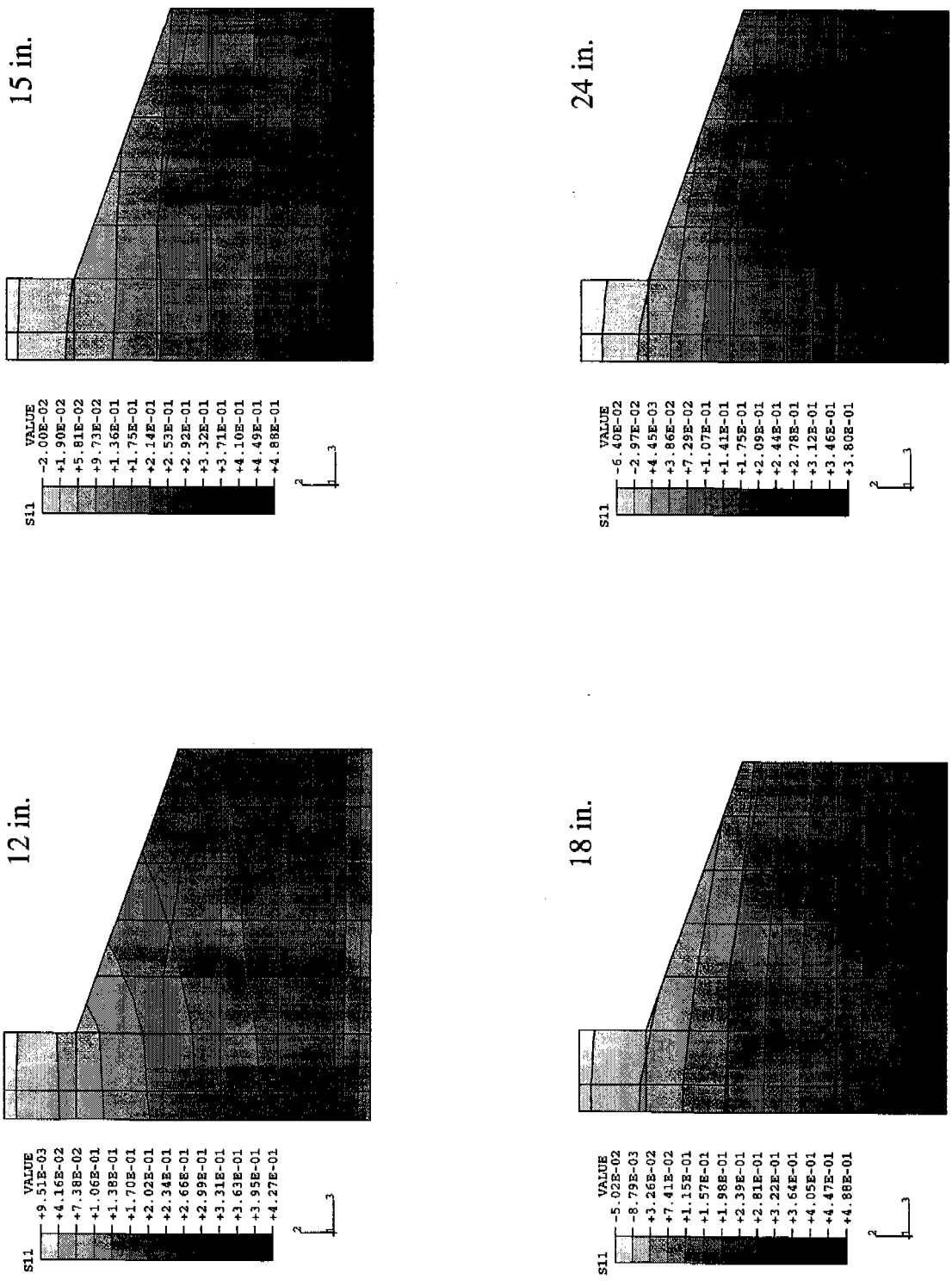

Figure 6.8b S11 Contours for Pattern 54A, Step 3

Figure 6.8c Stress Contours for Pattern 54A, Step 4, at 6 in. From End

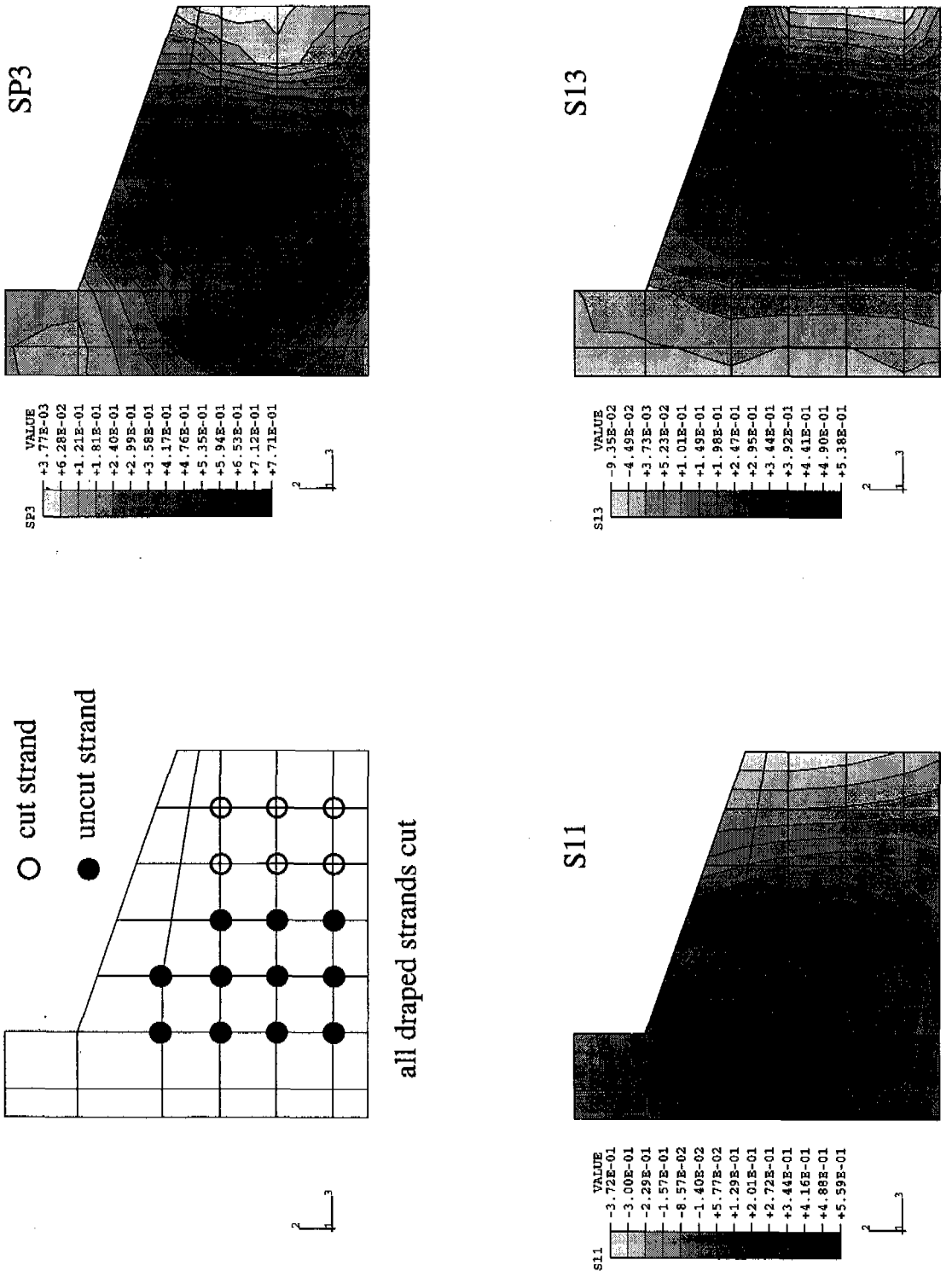

Figure 6.8d Stress Contours for Pattern 54A, Step 5, at 6 in. From End

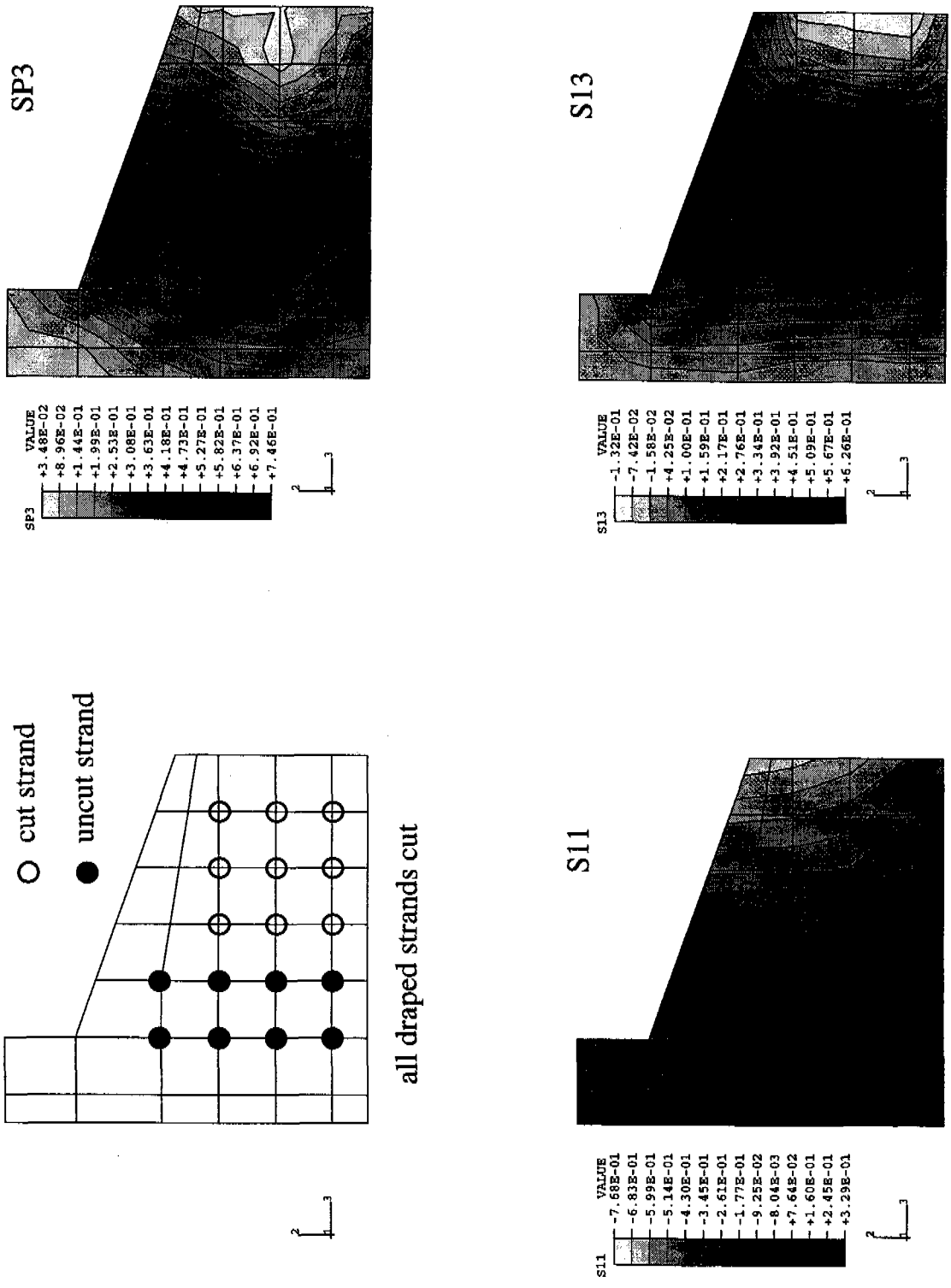

Figure 6.8e Stress Contours for Pattern 54A, Step 6, at 6 in. From End

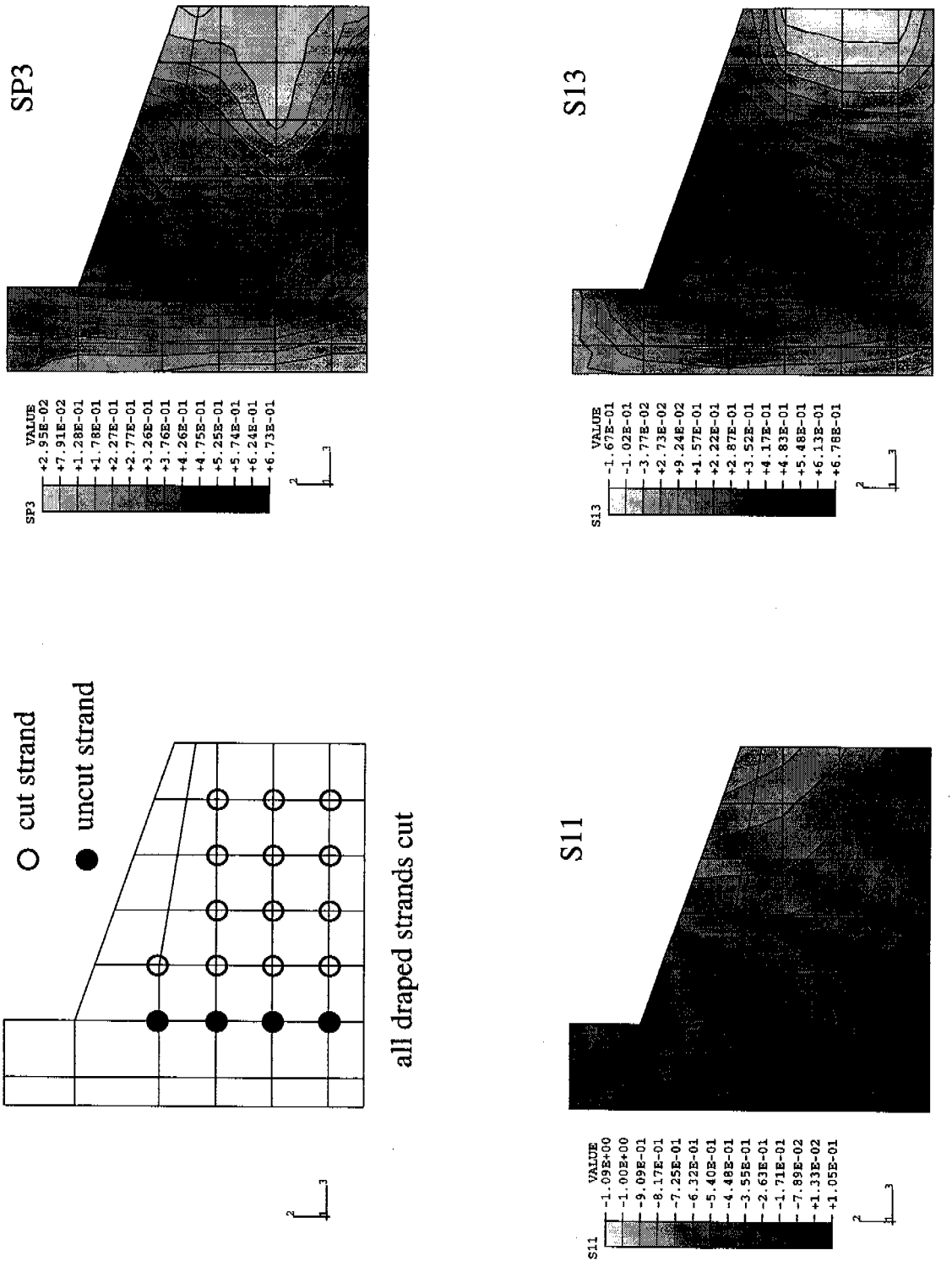

Figure 6.8f Stress Contours for Pattern 54A, Step 7, at 6 in. From End

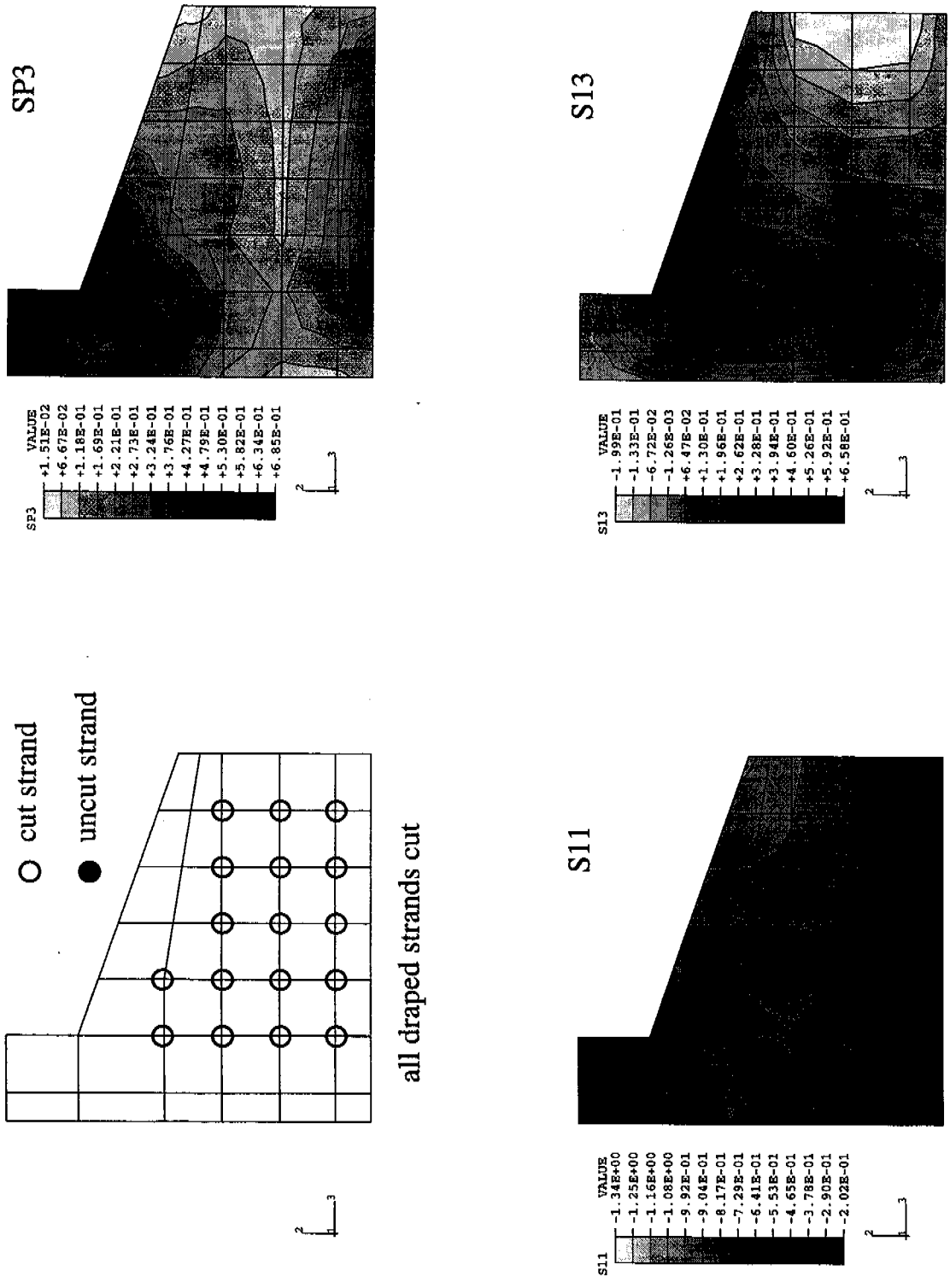

Figure 6.8g Stress Contours for Pattern 54A, Step 8, at 6 in. From End

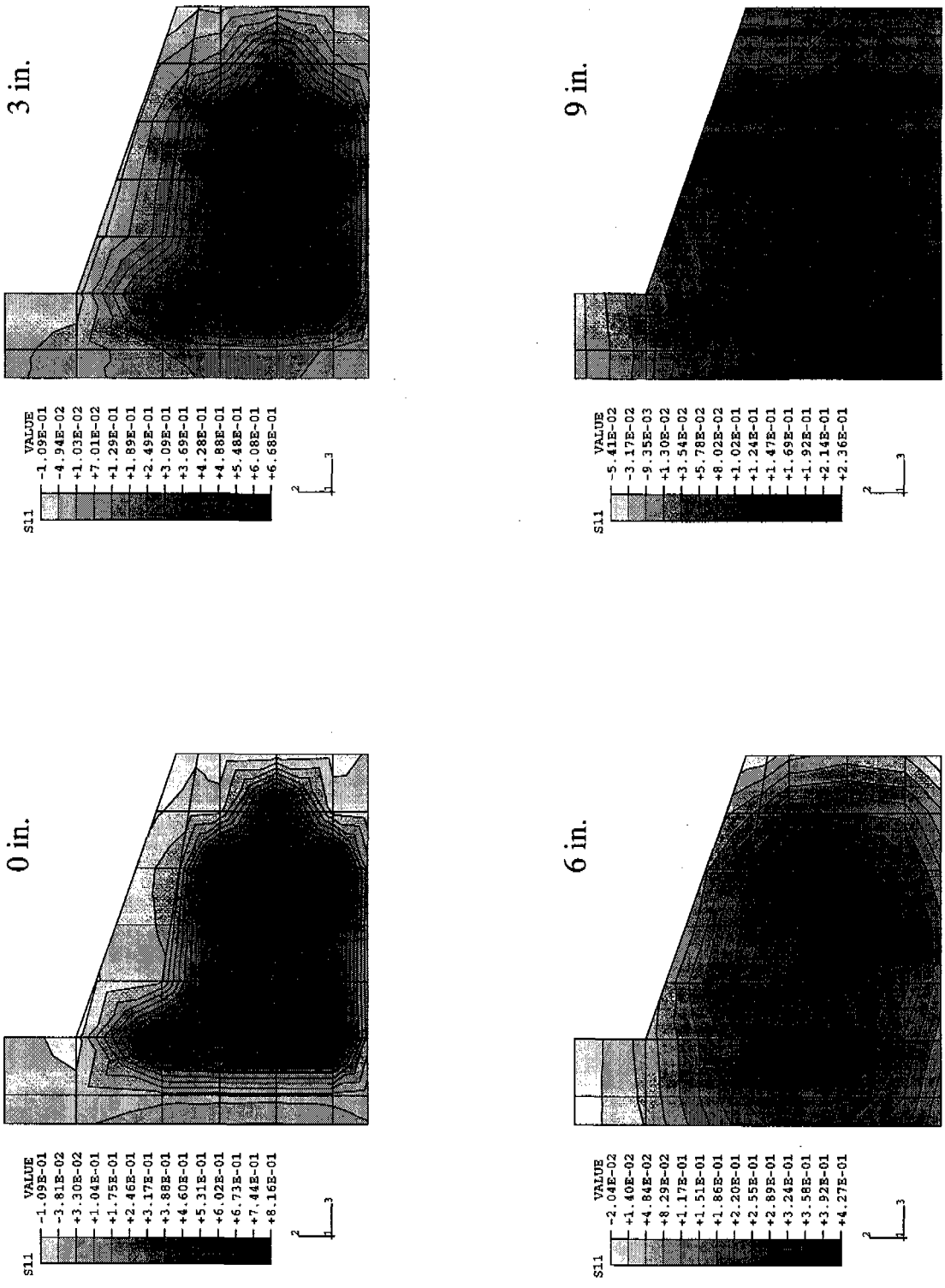

Figure 6.9a S11 Contours for Pattern 54B, Step 4

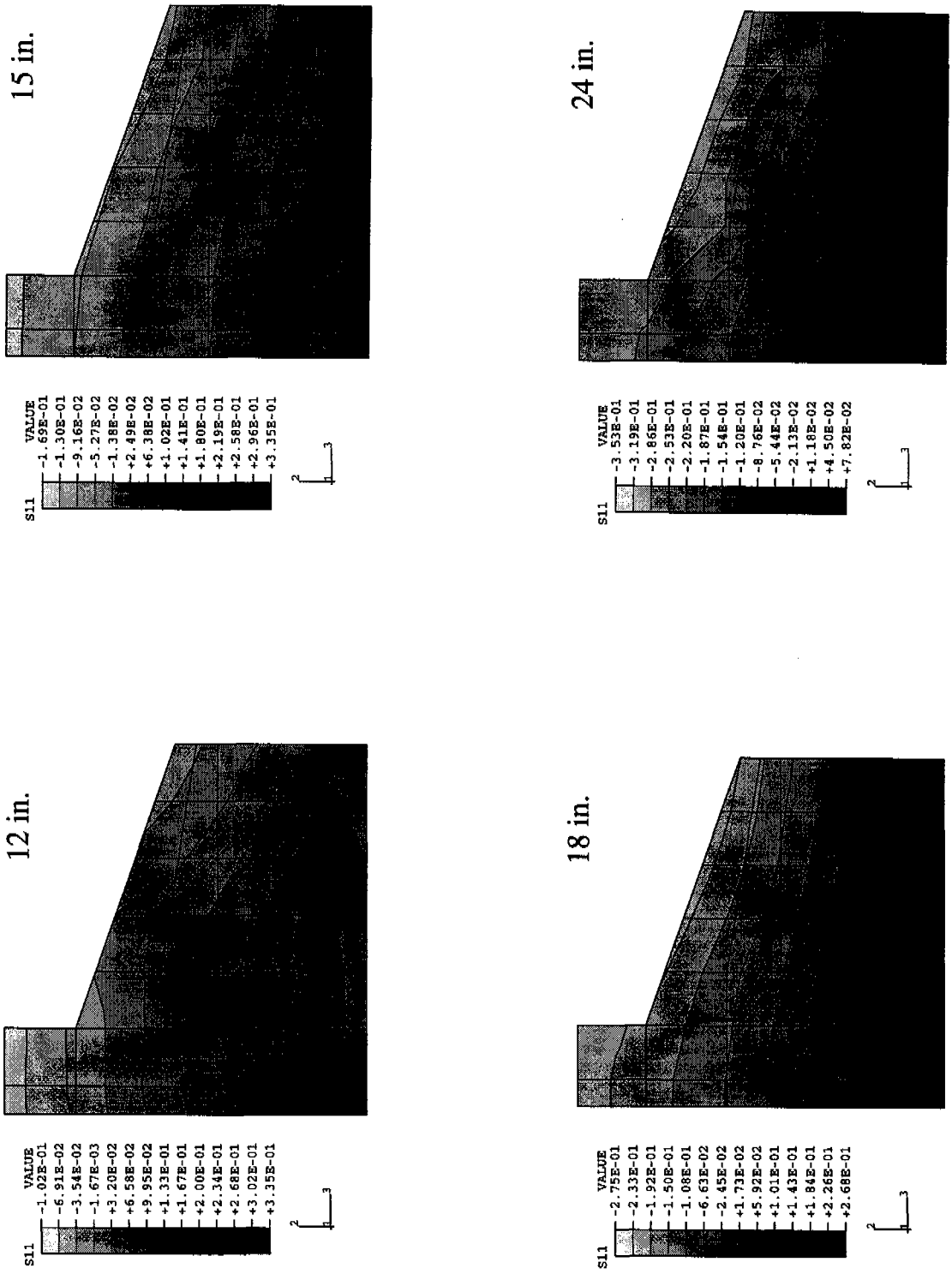

Figure 6.9b S11 Contours for Pattern 54B, Step 4

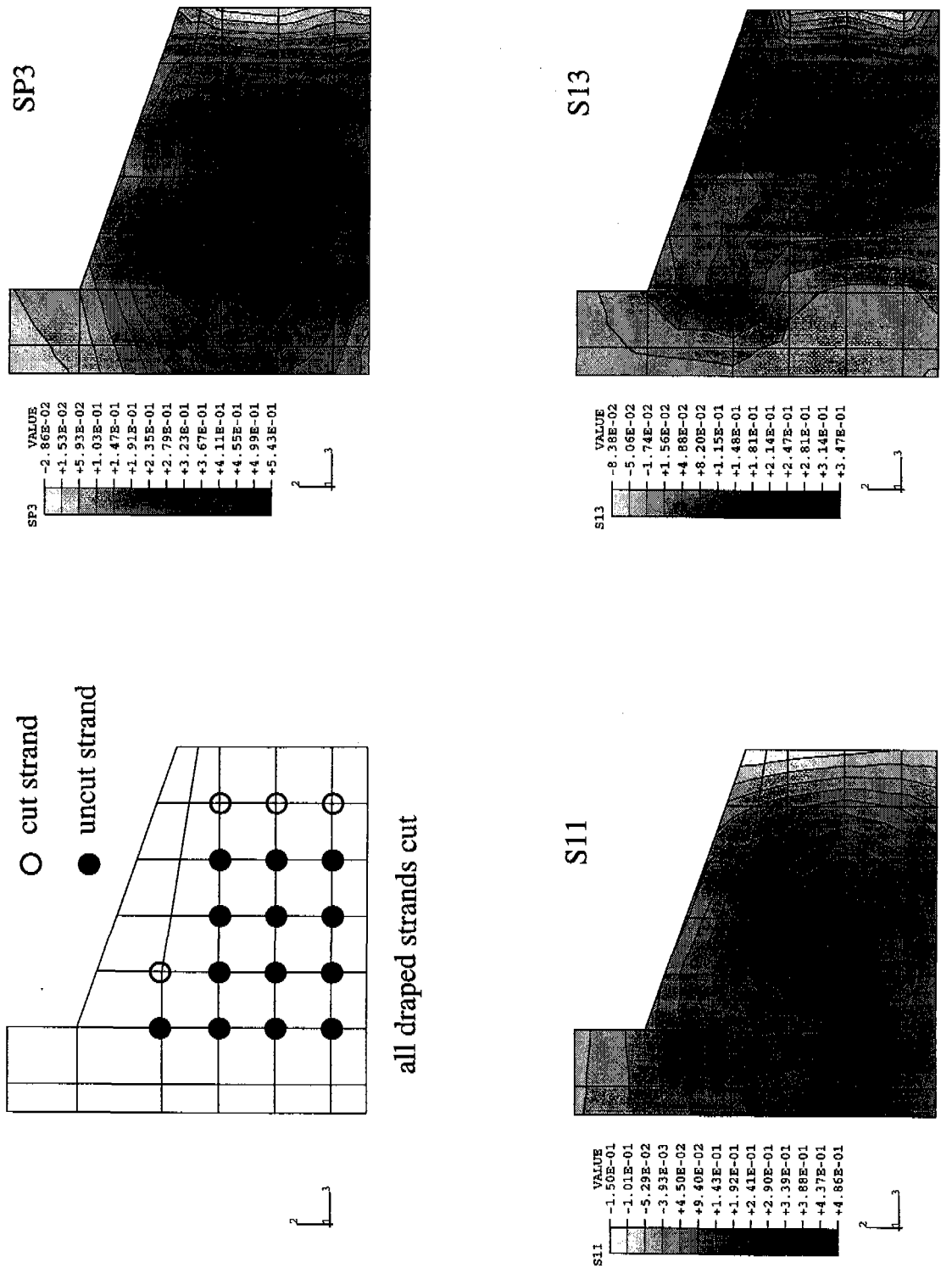

Figure 6.9c Stress Contours for Pattern 54B, Step 5, at 6 in. From End

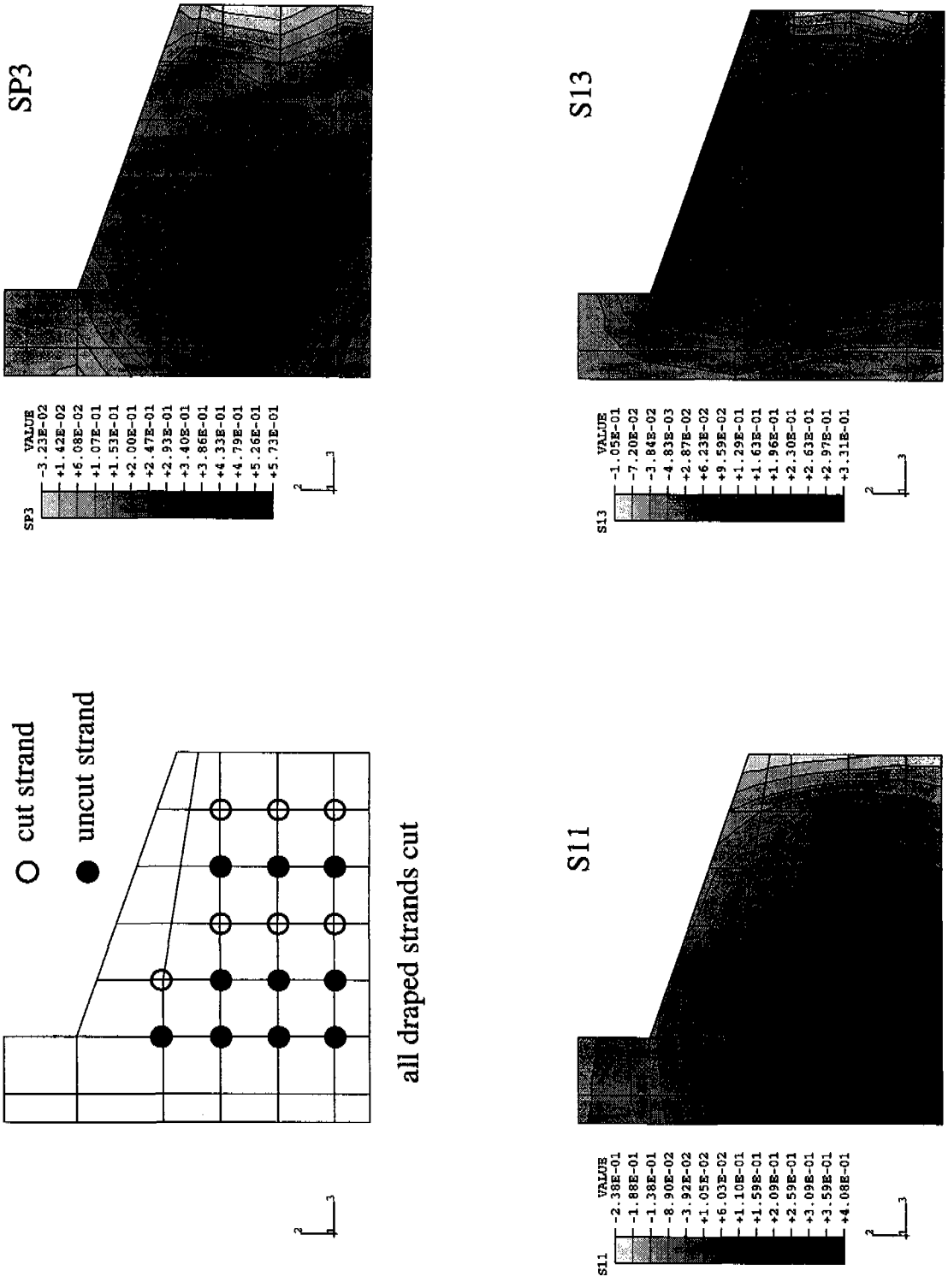

Figure 6.9d Stress Contours for Pattern 54B, Step 6, at 6 in. From End

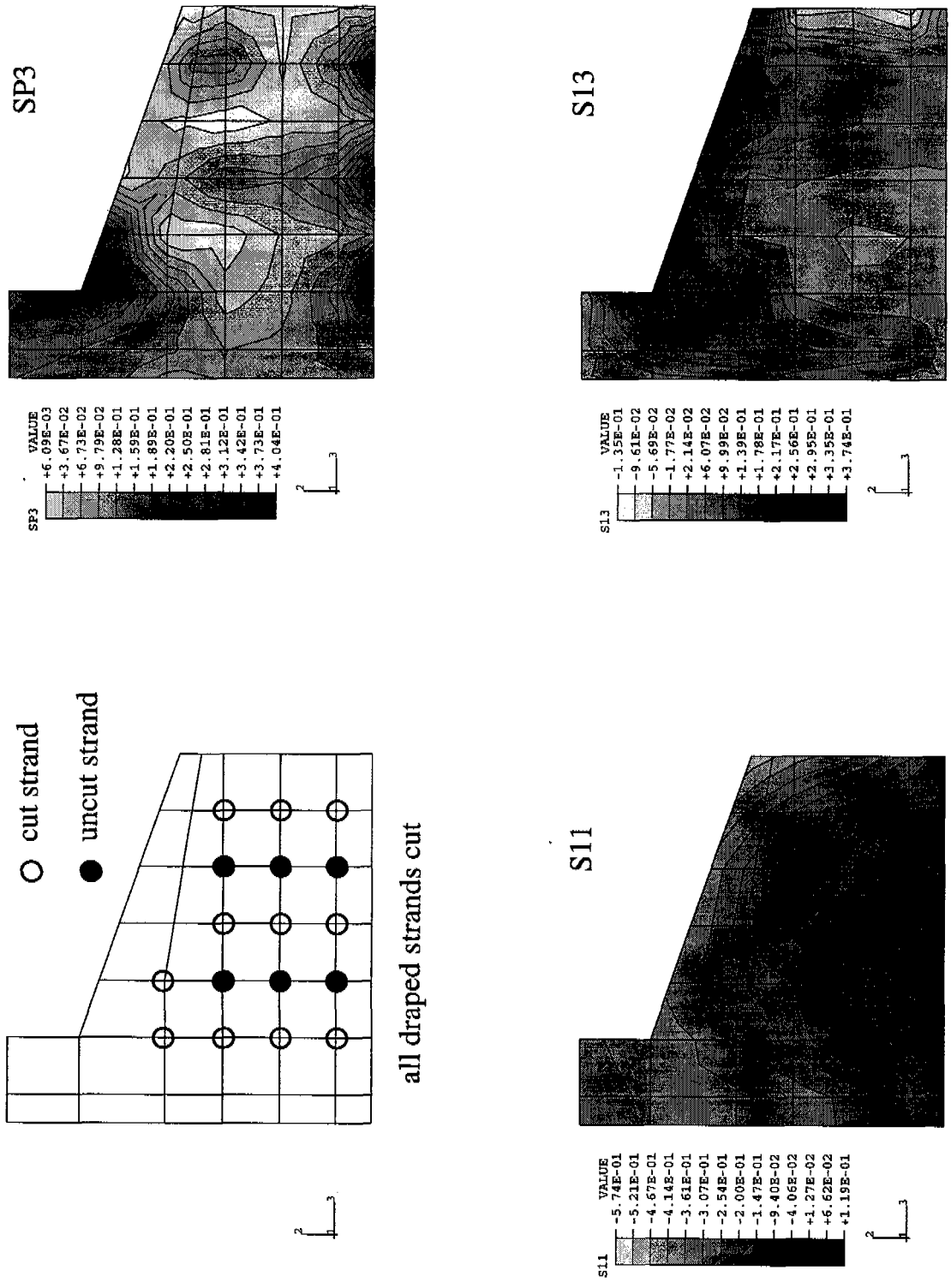

Figure 6.9e Stress Contours for Pattern 54B, Step 7, at 6 in. From End

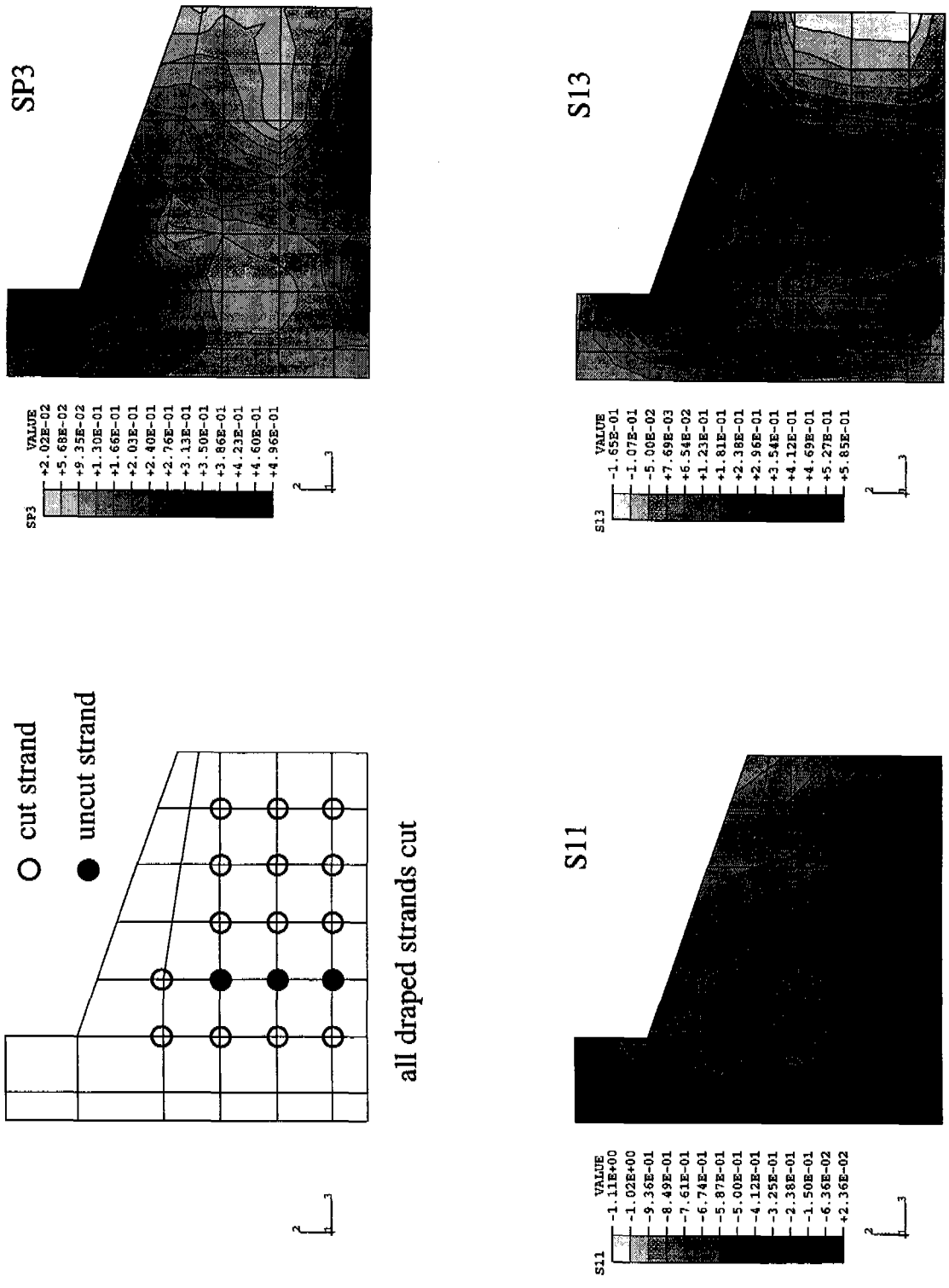

Figure 6.9f Stress Contours for Pattern 54B, Step 8, at 6 in. From End

Figure 6.9g Stress Contours for Pattern 54B, Step 9, at 6 in. From End

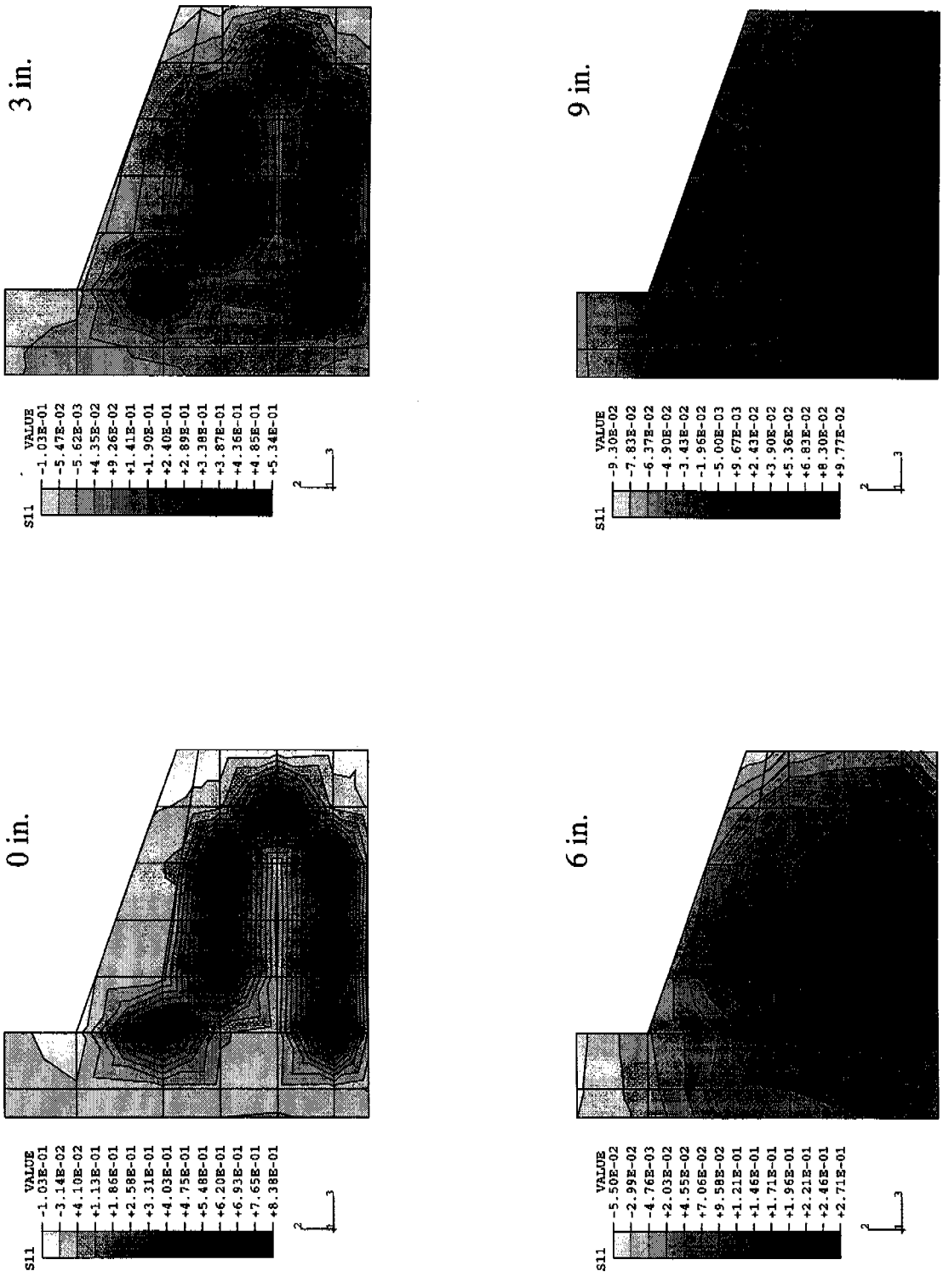

Figure 6.10a S11 Contours for Pattern 54C, Step 4

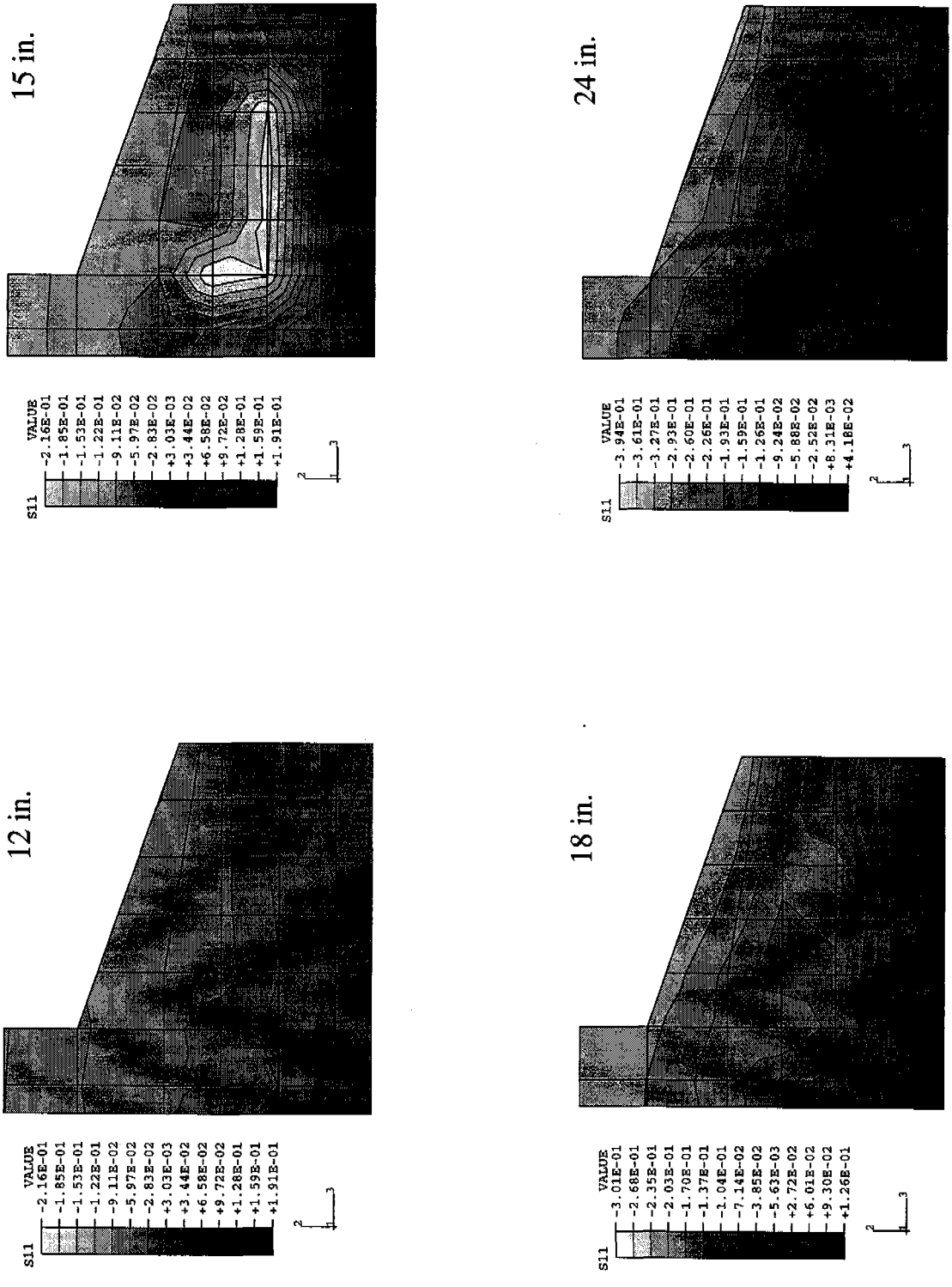

Figure 6.10b S11 Contours for Pattern 54C, Step 4

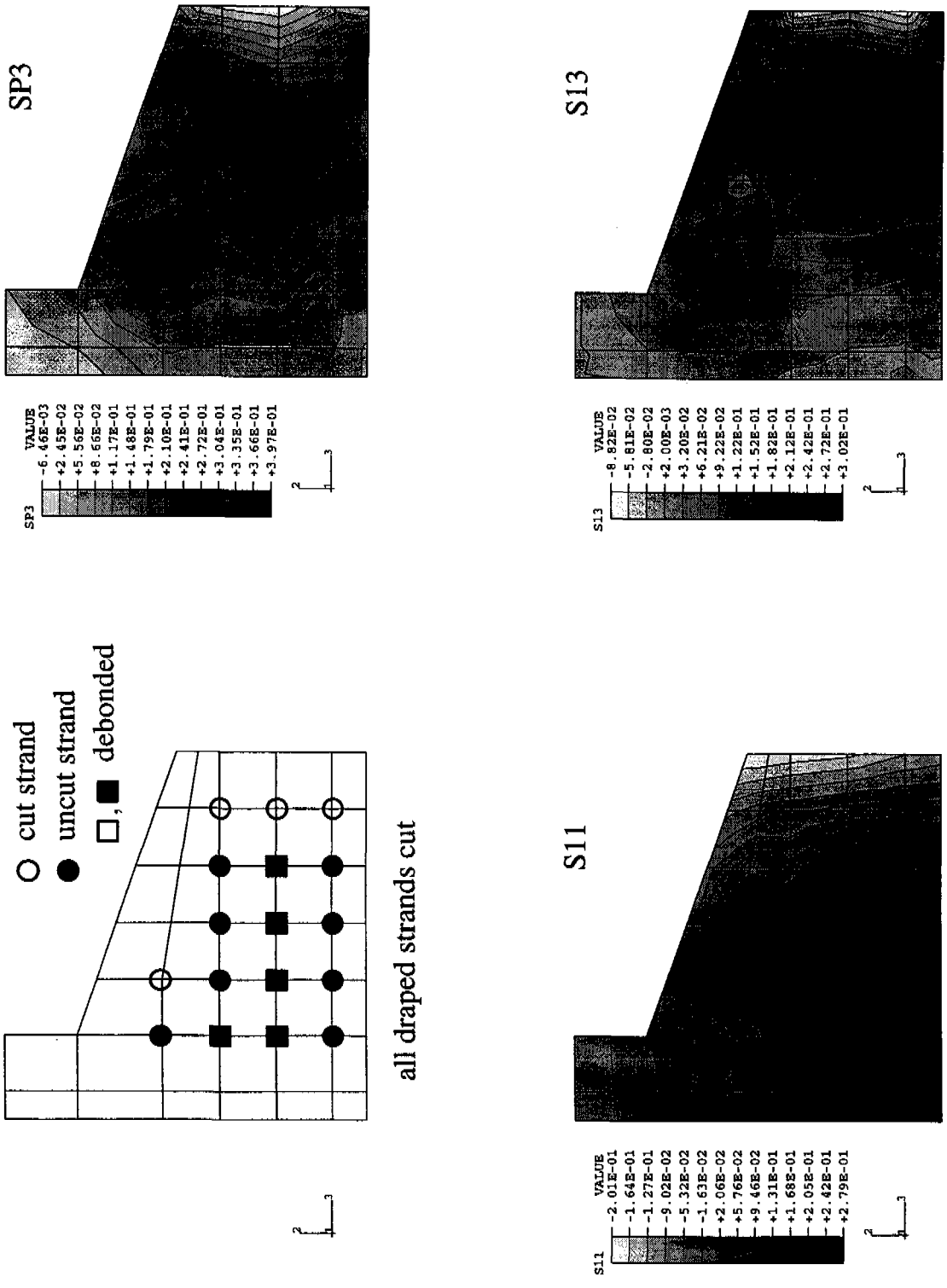

Figure 6.10c Stress Contours for Pattern 54C, Step 5, at 6 in. From End

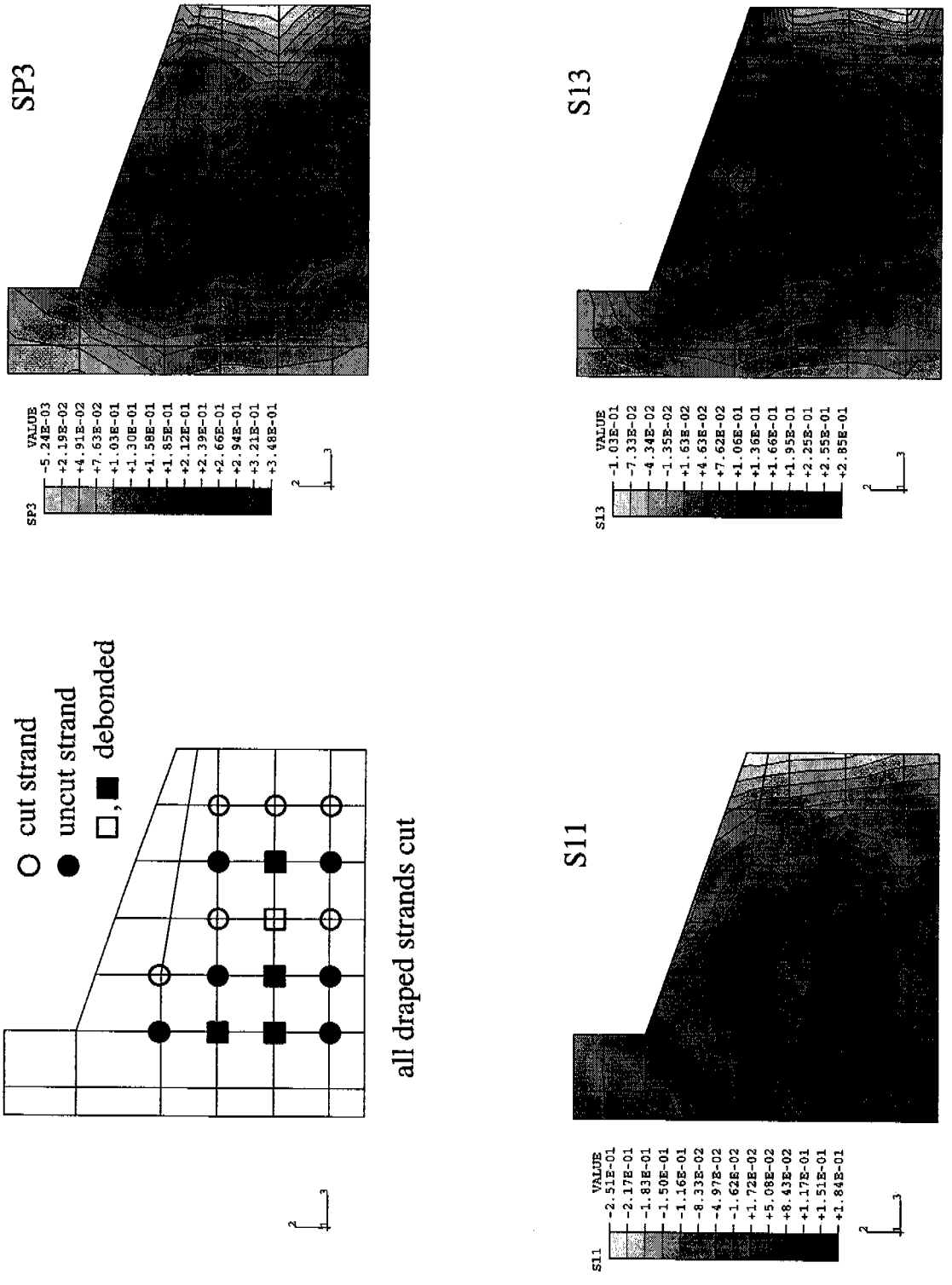

Figure 6.10d Stress Contours for Pattern 54C, Step 6, at 6 in. From End

Figure 6.10e Stress Contours for Pattern 54C, Step 7, at 6 in. From End

Figure 6.10f Stress Contours for Pattern 54C, Step 8, at 6 in. From End

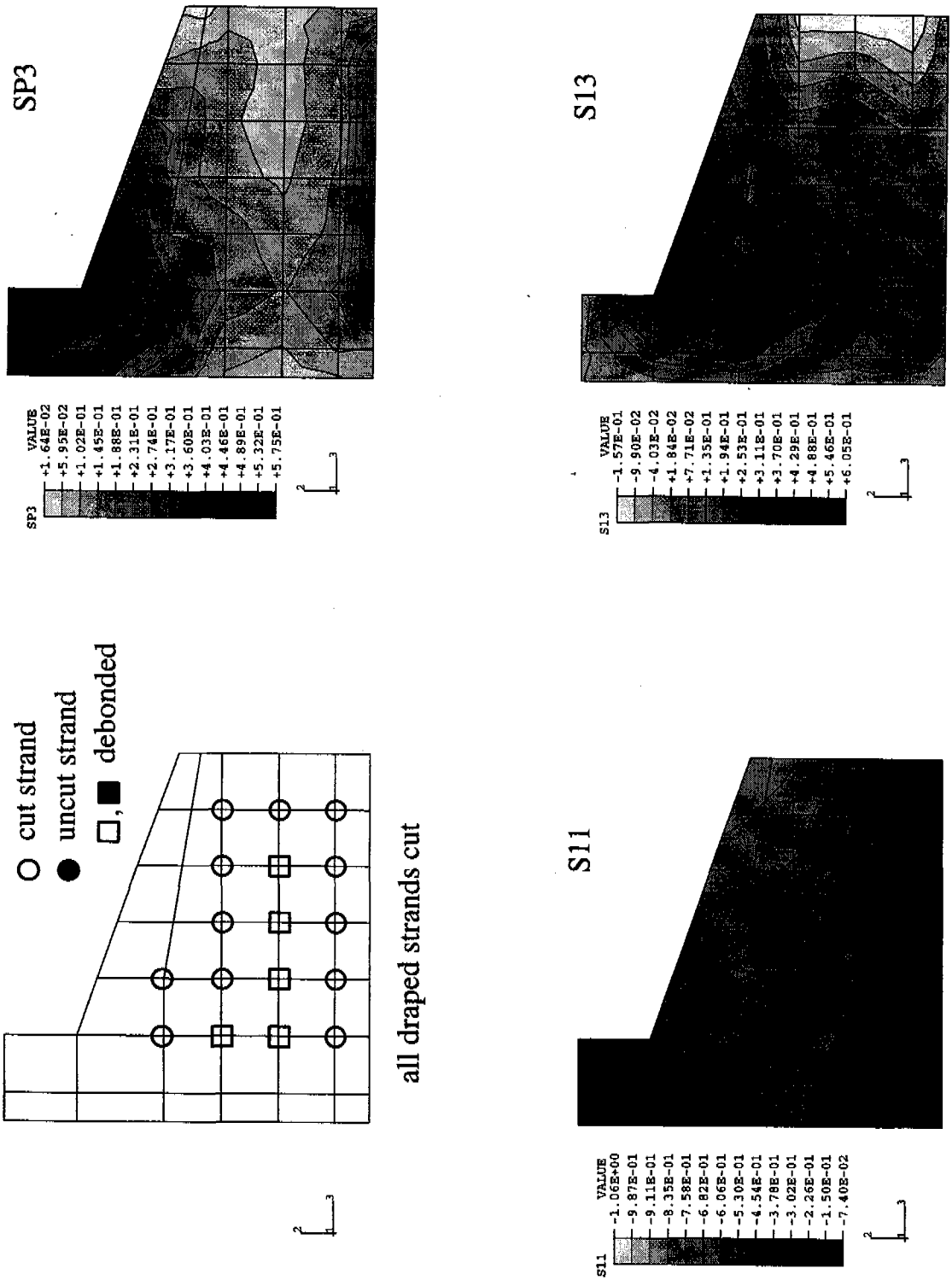

Figure 6.10g Stress Contours for Pattern 54C, Step 9, at 6 in. From End

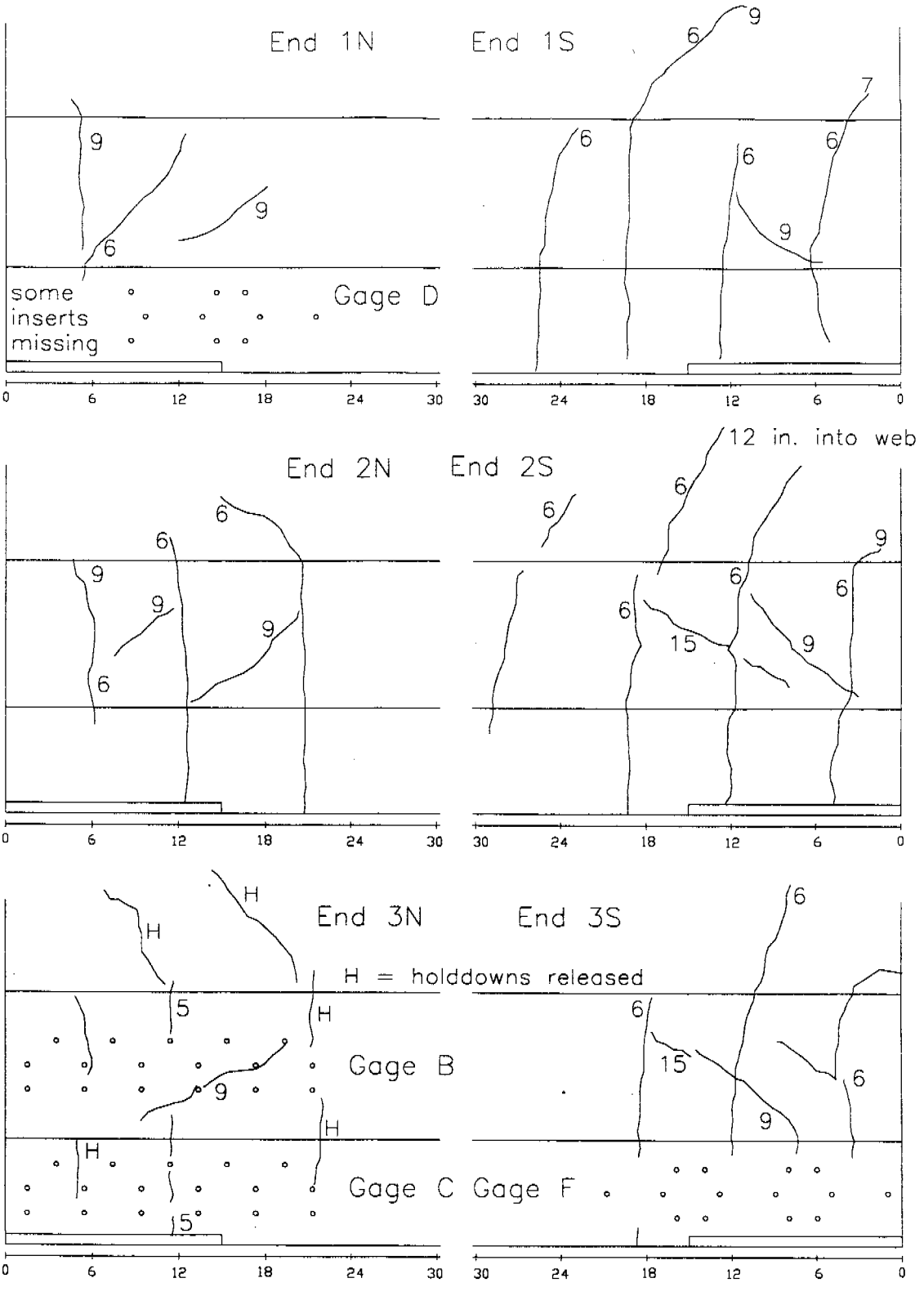

Figure 6.11 Observed Cracks for Bed #1, Pattern 54A

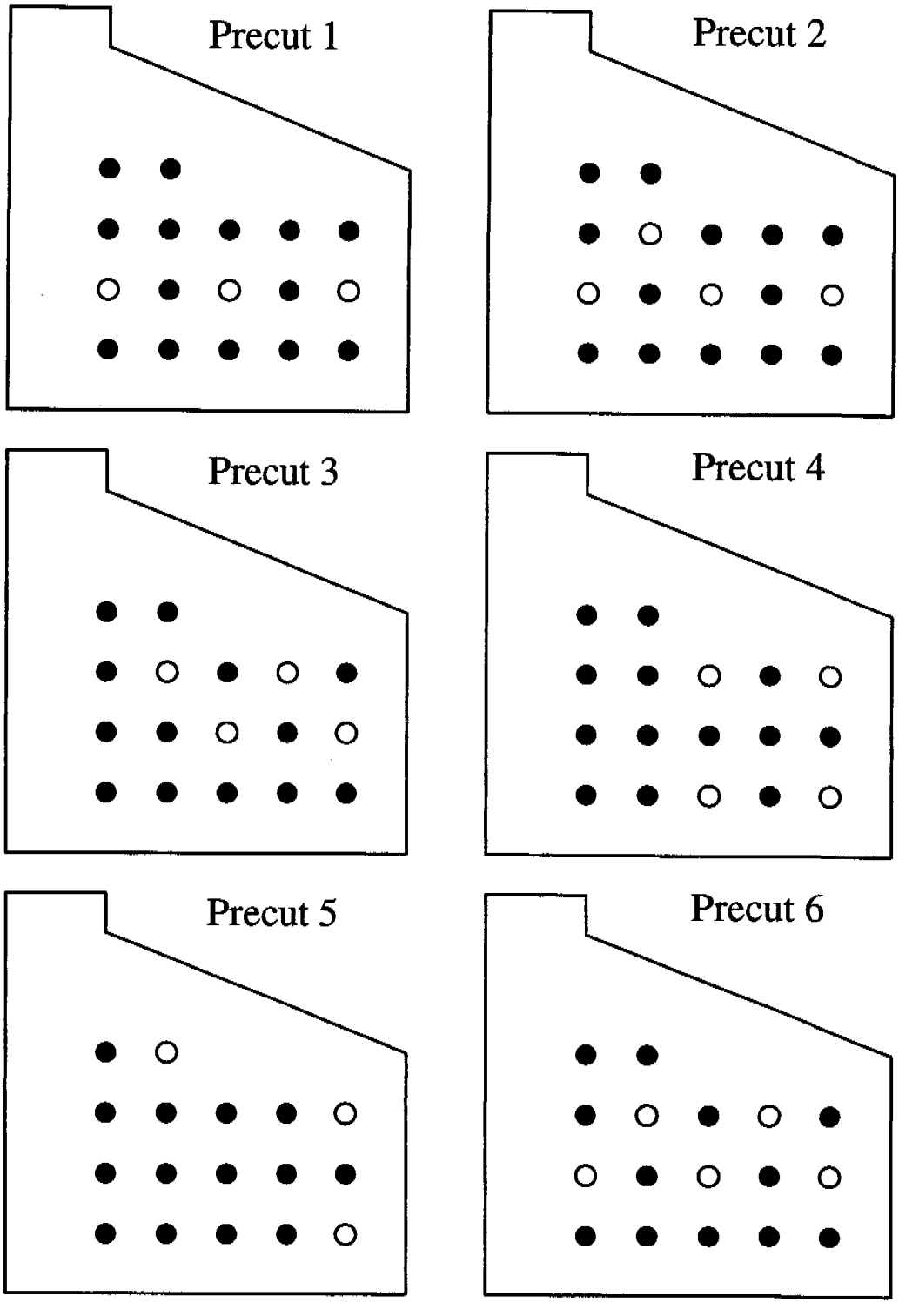

Figure 6.12 Precutting Patterns, ○ = precut strand

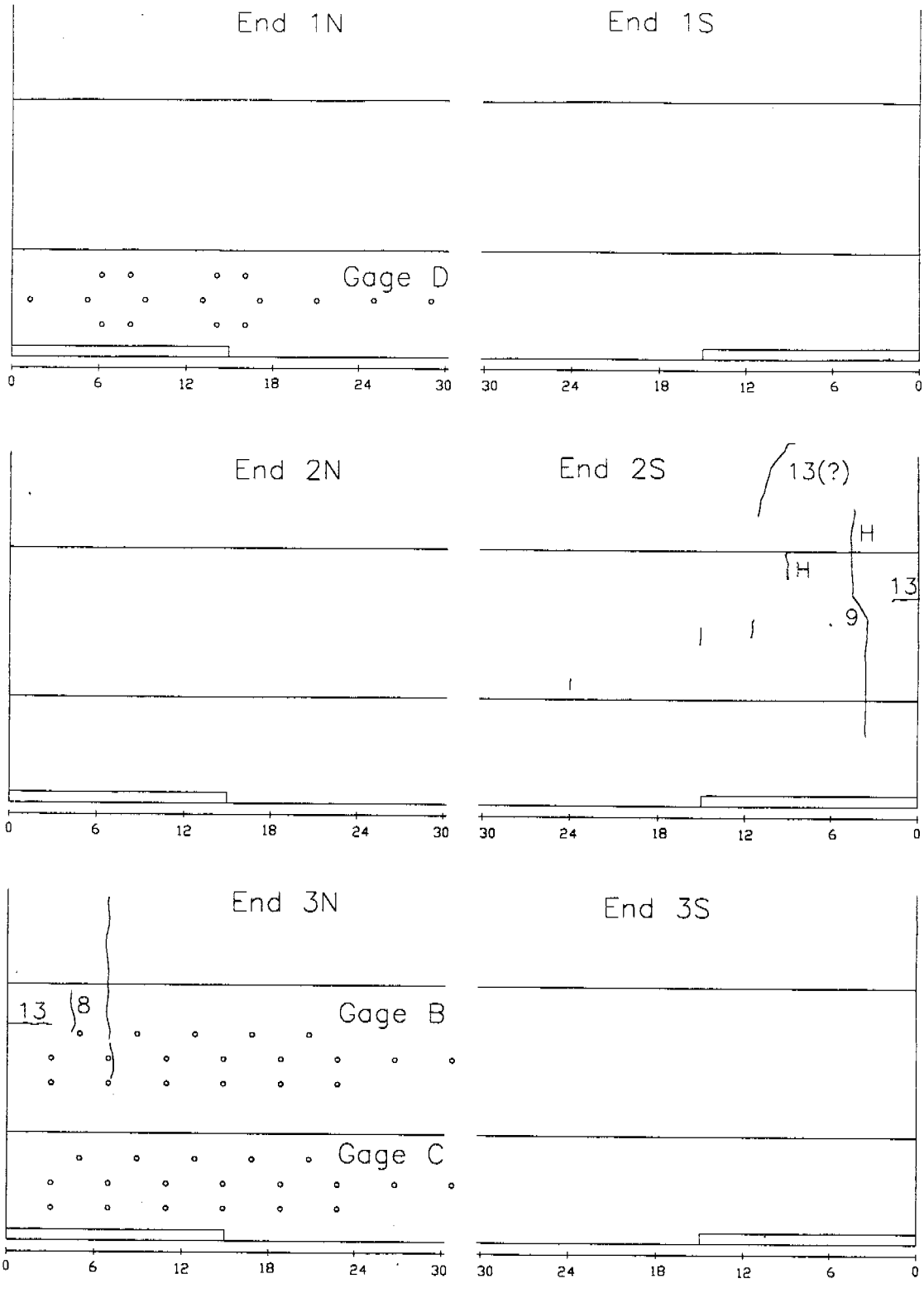

Figure 6.13a Observed Cracks for Bed #2, Pattern 54B

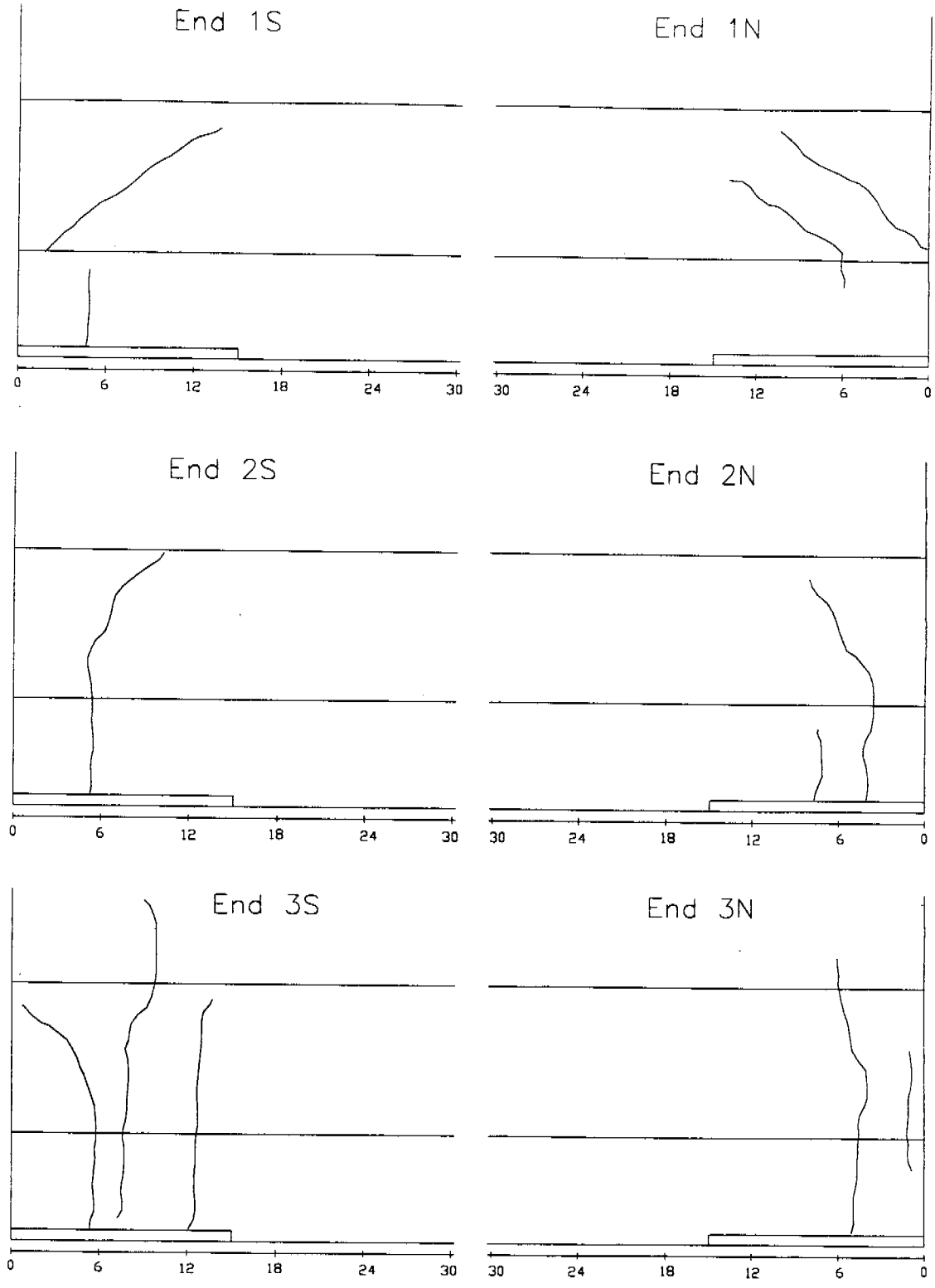

Figure 6.13b Cracks for Bed #2 from Survey Form

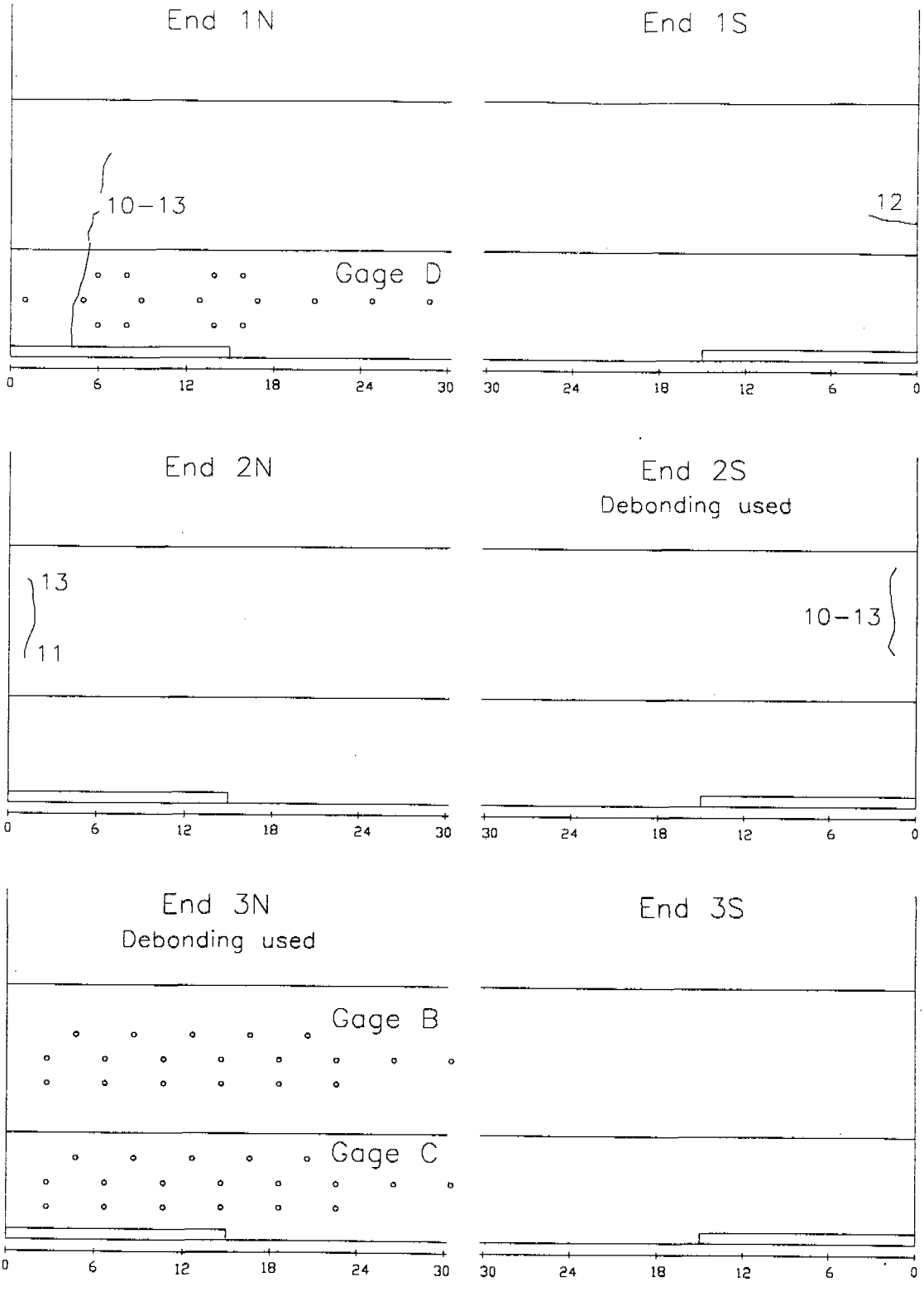

Figure 6.14 Observed Cracks for Bed #3, Pattern 54C

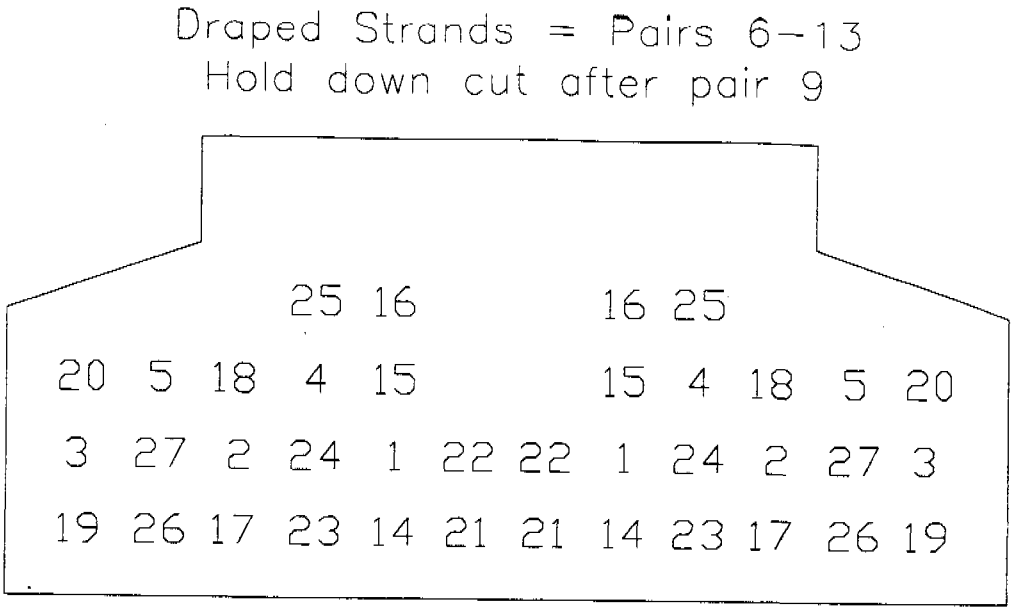

Figure 6.15 Cutting Pattern 72H

A = in web, just above flange
B = top of bottom flange
C,D,E,F = side of bottom flange

Gages A and E were never used, and Gage F was only used for Bed #1, Pattern 54A

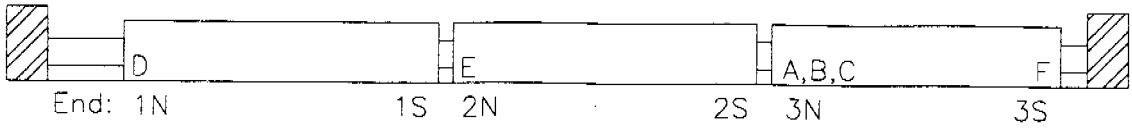

DEMEC pattern used for Gages B and C

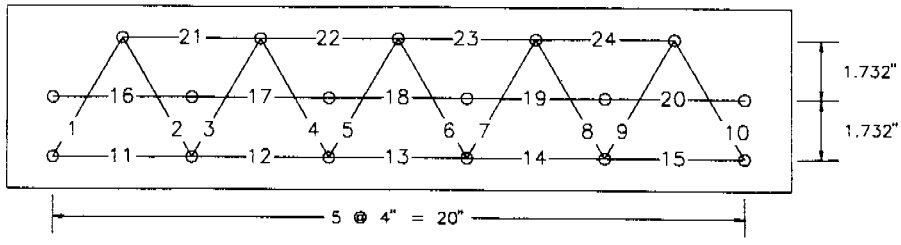

DEMEC pattern used for Gages D and F

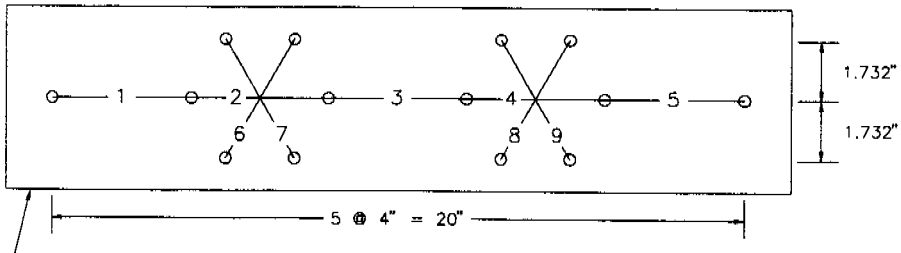

Patterns drilled into aluminum plates. Brass inserts are screwed to plates, which are then screwed onto inside of girder forms. Prior to form removal, plates are unscrewed from form, leaving plate on surface of girder. The brass inserts are then unscrewed from plate, allowing the plate to be pried off, leaving inserts embedded in the girder. Finally, contact points are screwed into the brass inserts.

For beds #2 and #3, two plates were used end to end to cover the entire transfer zone. Only the central line of DEMEC points was used for the second plate.

Figure 7.1 Plan for DEMEC Gages

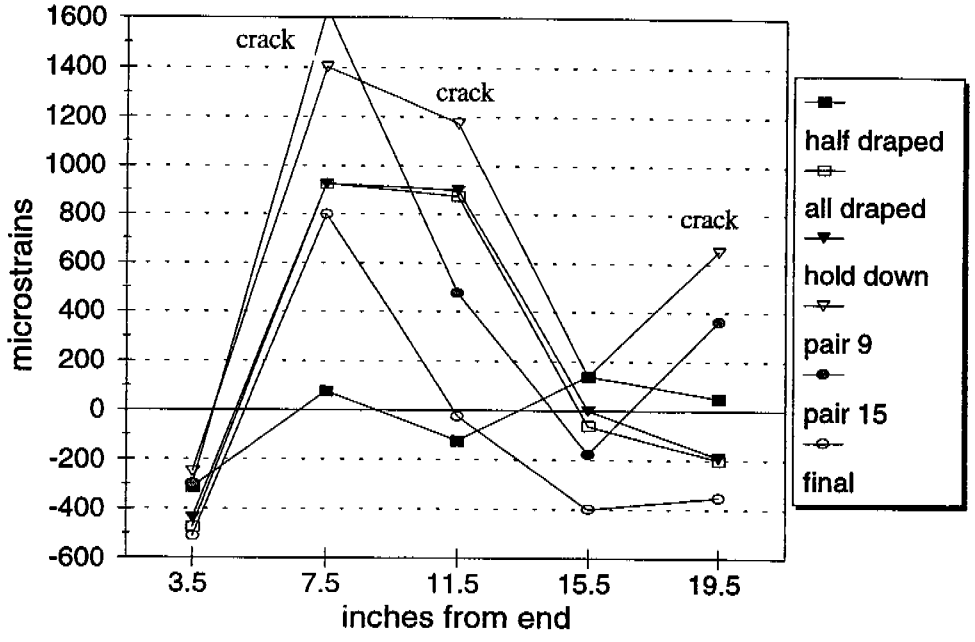

Figure 7.2a Bed #1, Middle Line of Gage B

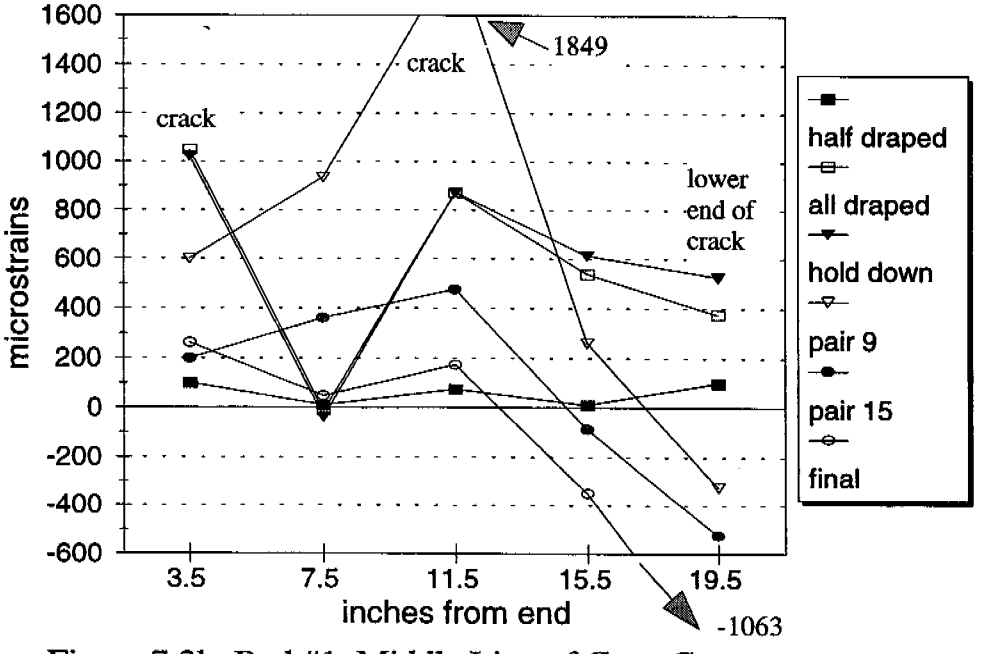

Figure 7.2b Bed #1, Middle Line of Gage C

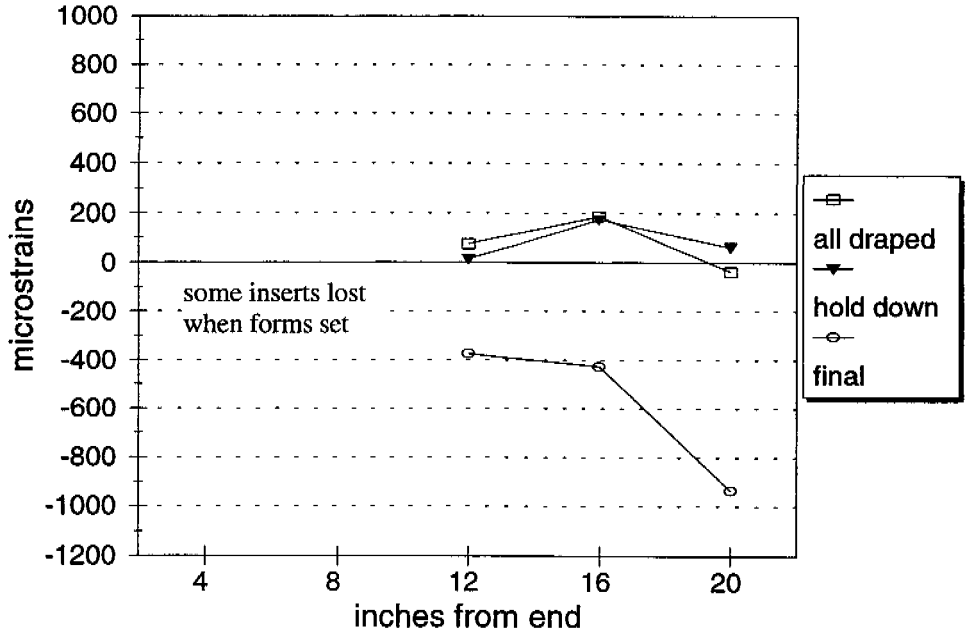

Figure 7.2c Bed #1, Middle Line of Gage D

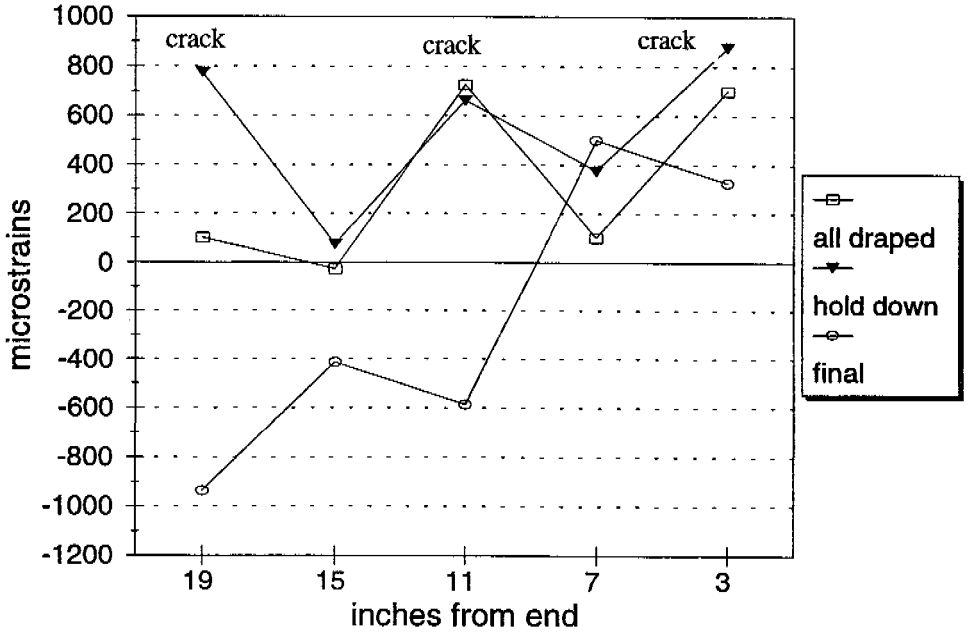

Figure 7.2d Bed #1, Middle Line of Gage F

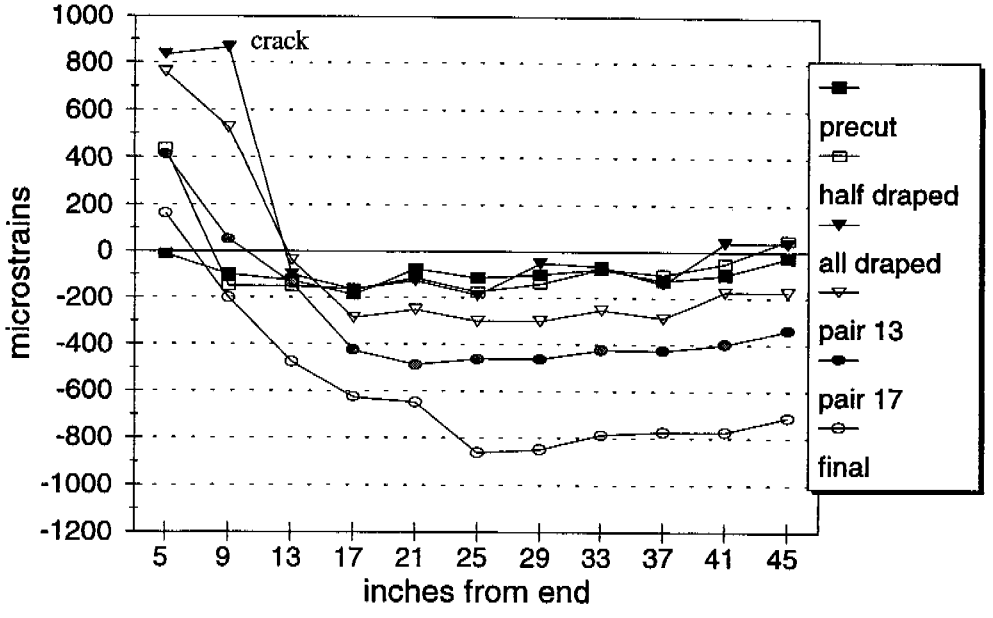

Figure 7.3a Bed #2, Middle Line of Gage B

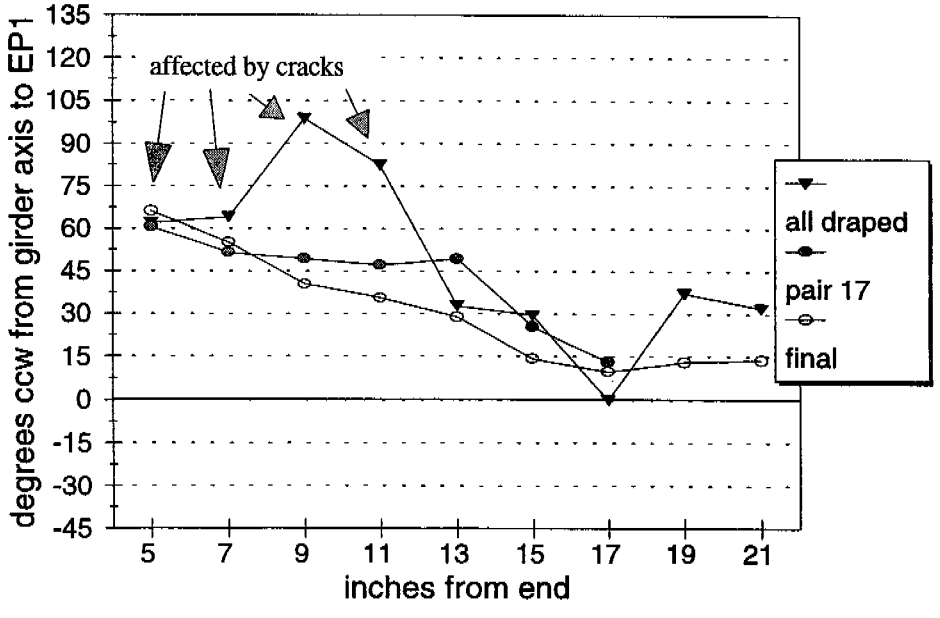

Figure 7.3b Bed #2, Principal Strain Angle, Gage B

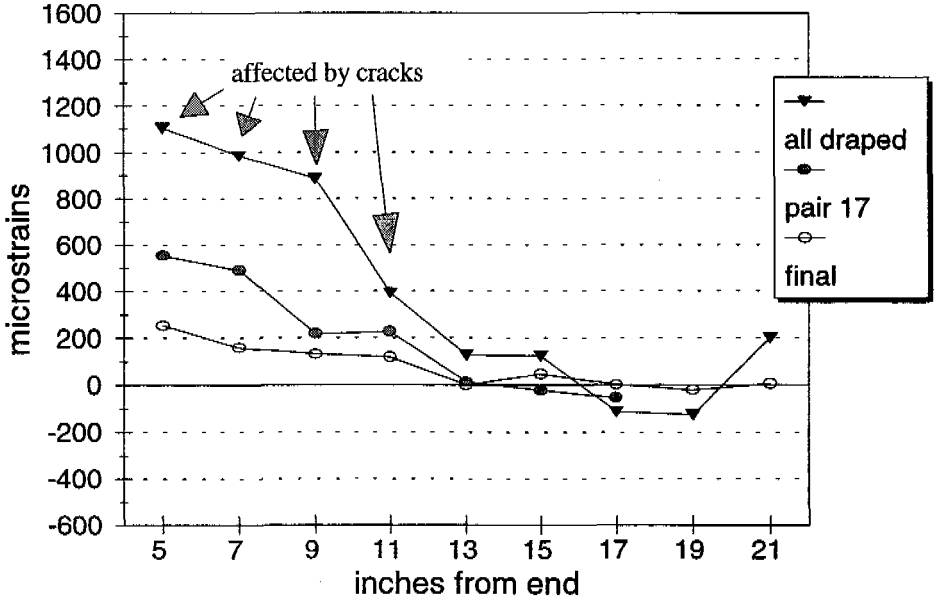

Figure 7.3c Bed #2, Maximum Principal Strain, Gage B

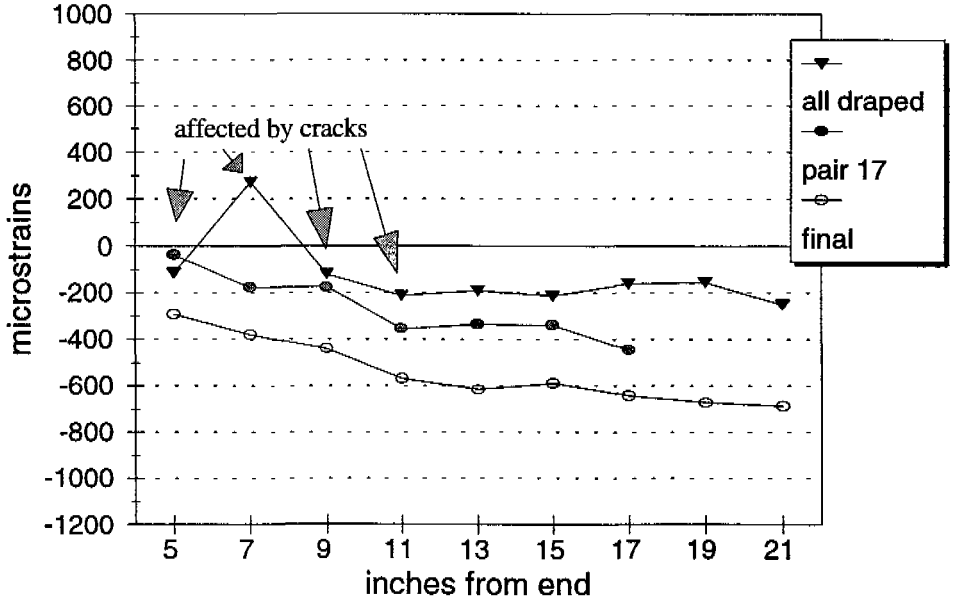

Figure 7.3d Bed #2, Minimum Principal Strain, Gage B

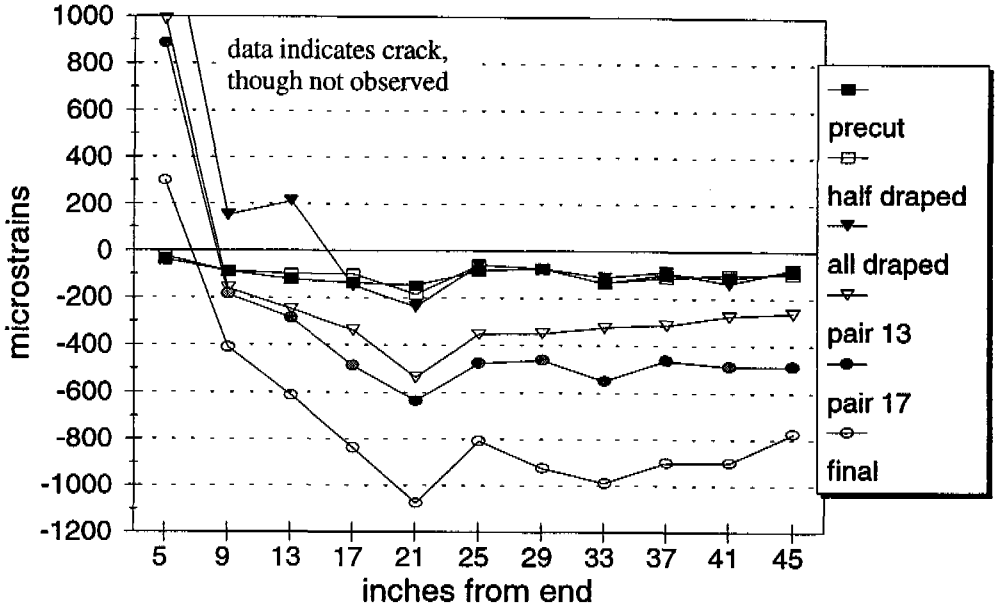

Figure 7.3e Bed #2, Middle Line of Gage C

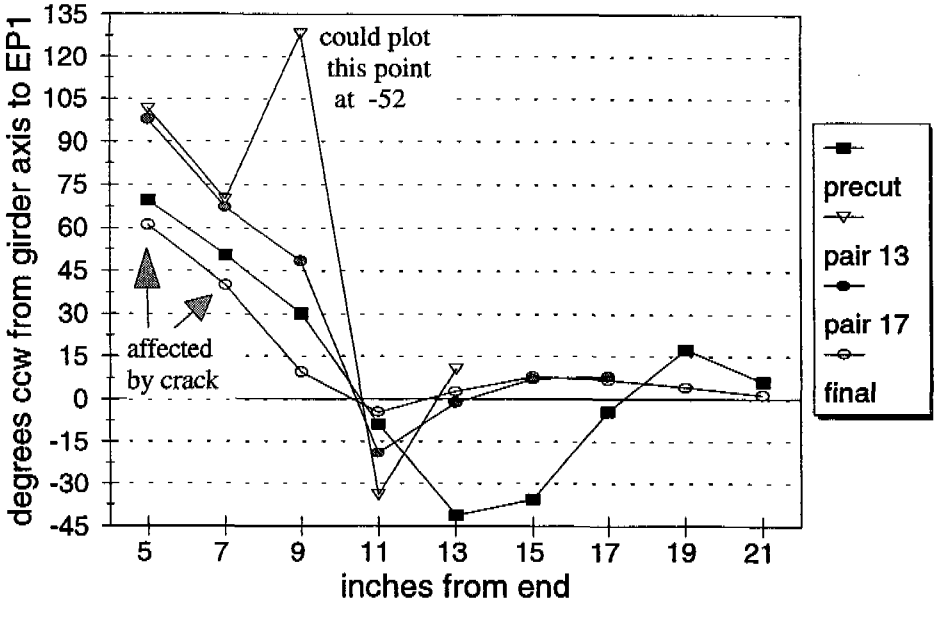

Figure 7.3f Bed #2, Principal Strain Angle, Gage C

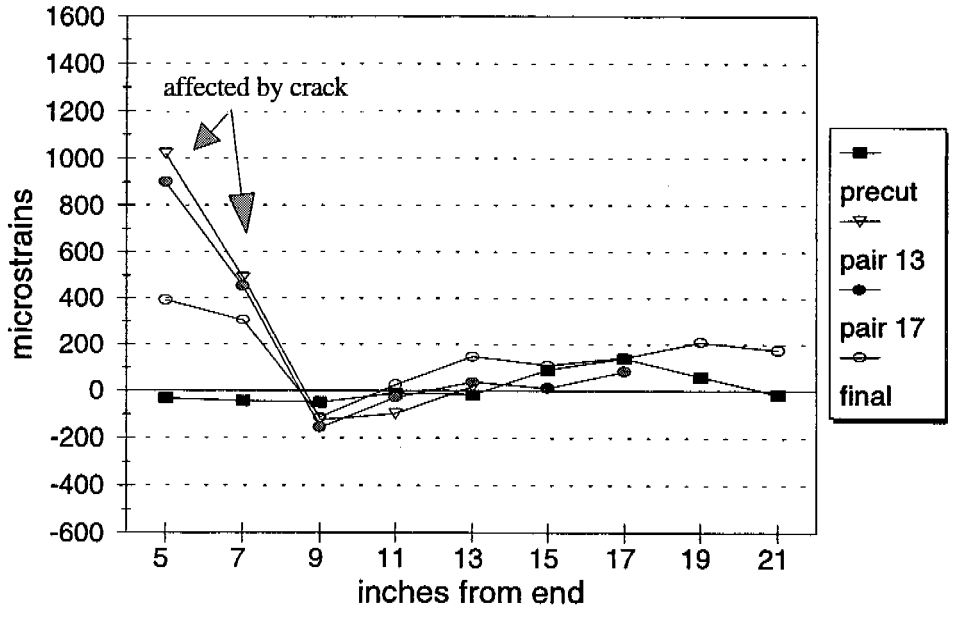

Figure 7.3g Bed #2, Maximum Principal Strain, Gage C

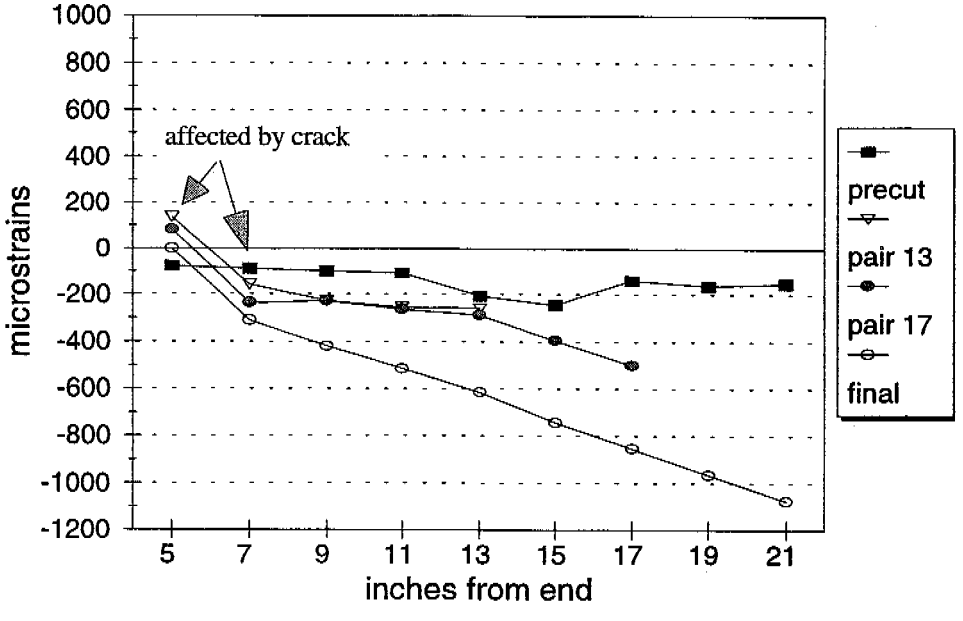

Figure 7.3h Bed #2, Minimum Principal Strain, Gage C

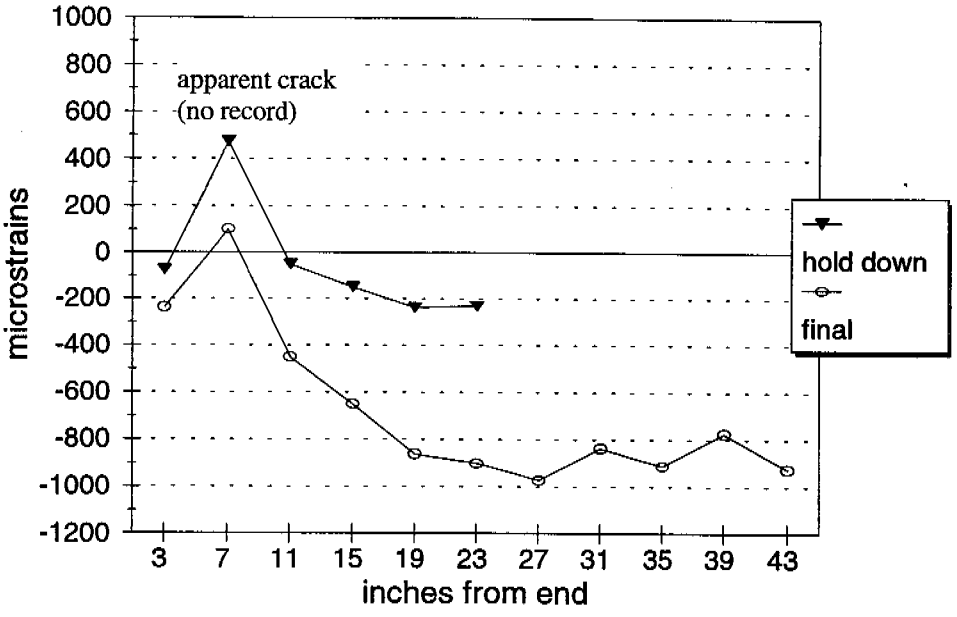

Figure 7.3i Bed #2, Middle Line of Gage D

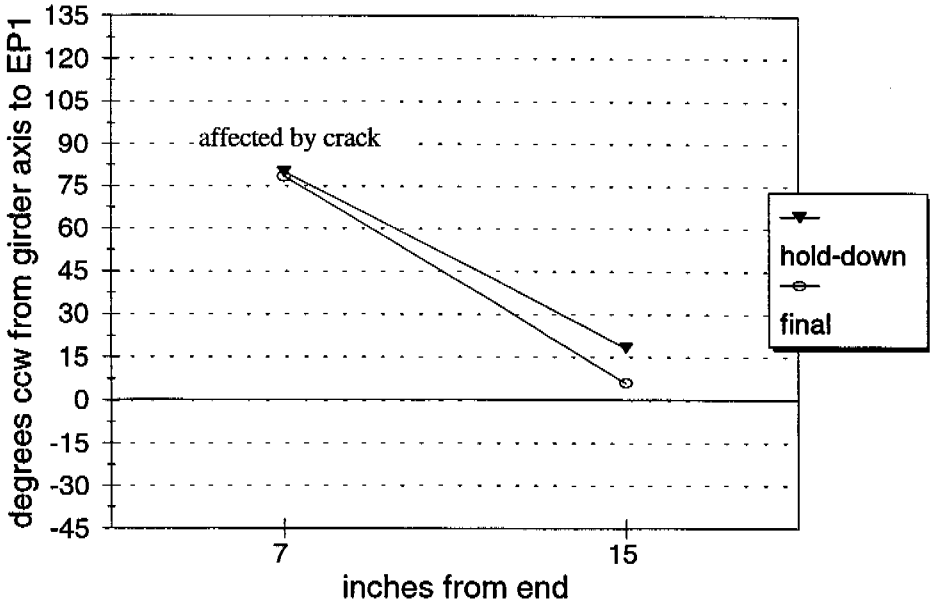

Figure 7.3j Bed #2, Principal Strain Angle, Gage D

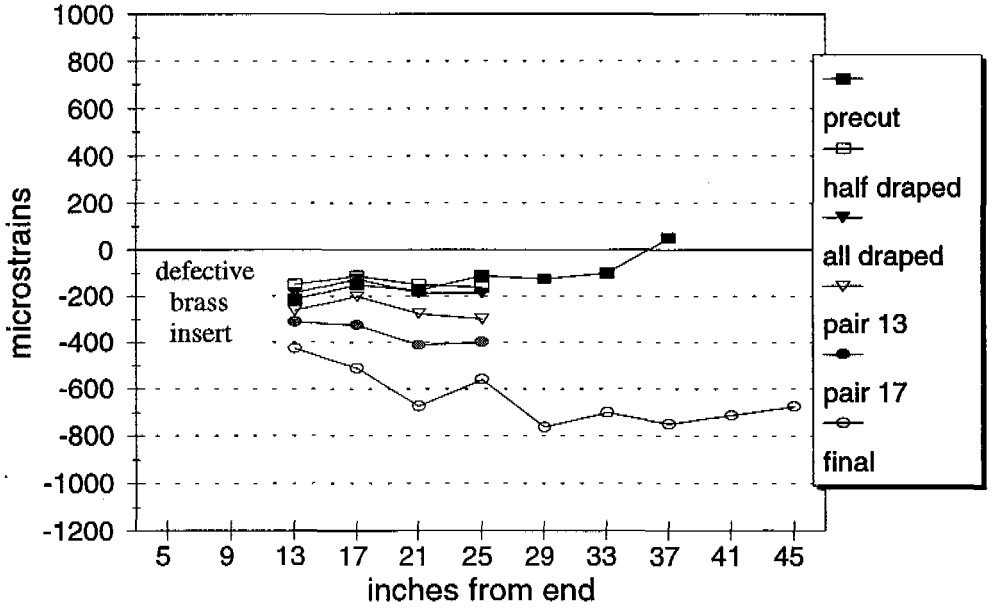

Figure 7.4a Bed #3, Middle Line of Gage B

Figure 7.4b Bed #3, Principal Strain Angle, Gage B

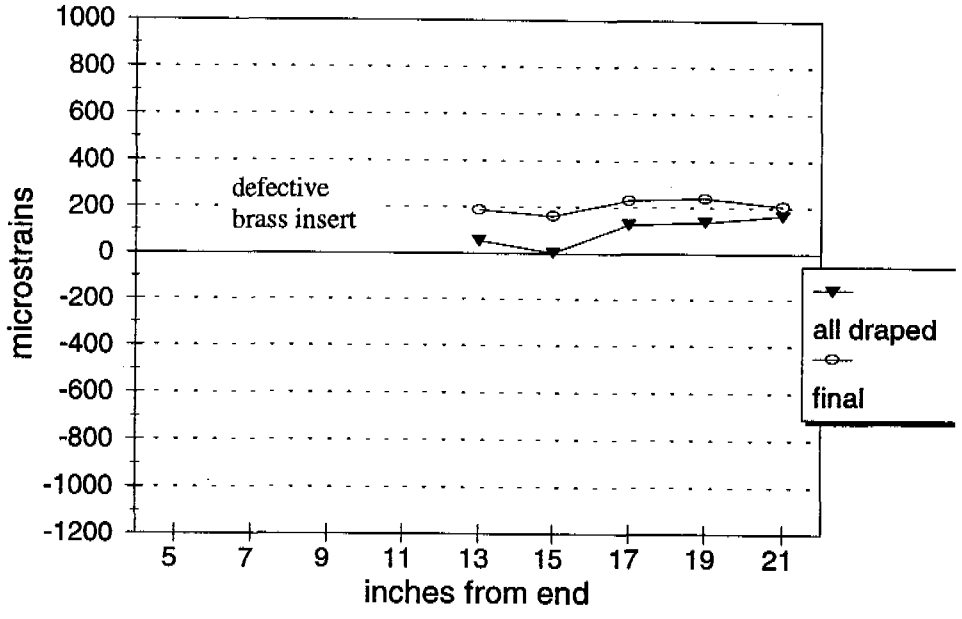

Figure 7.4c Bed #3, Maximum Principal Strain, Gage B

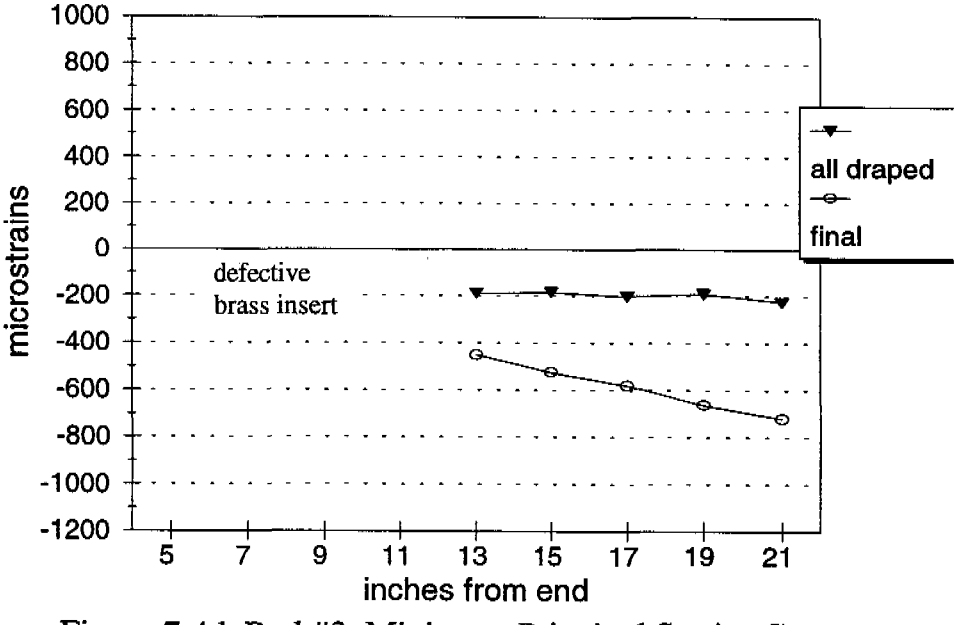

Figure 7.4d Bed #3, Minimum Principal Strain, Gage B

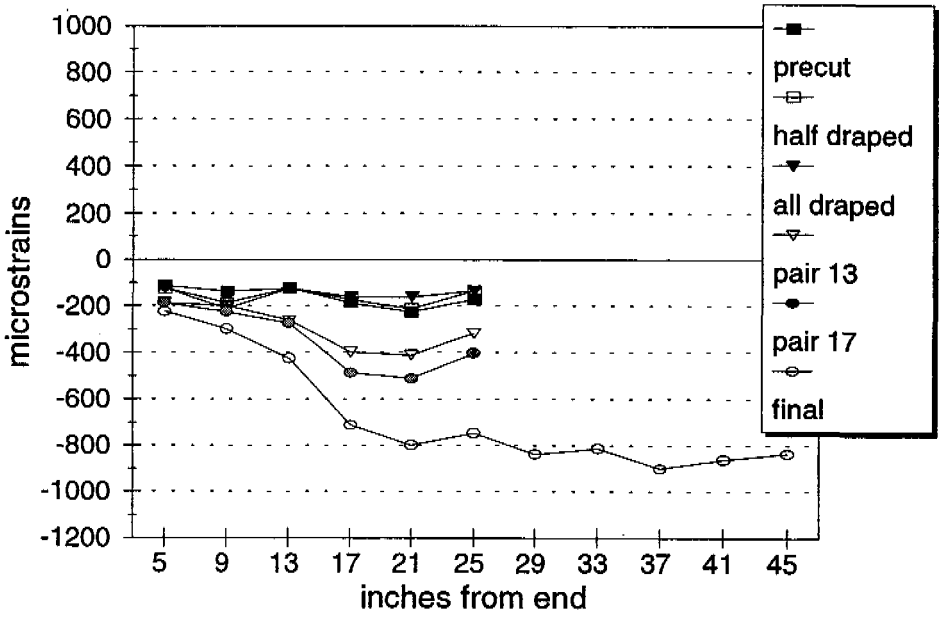

Figure 7.4e Bed #3, Middle Line of Gage C

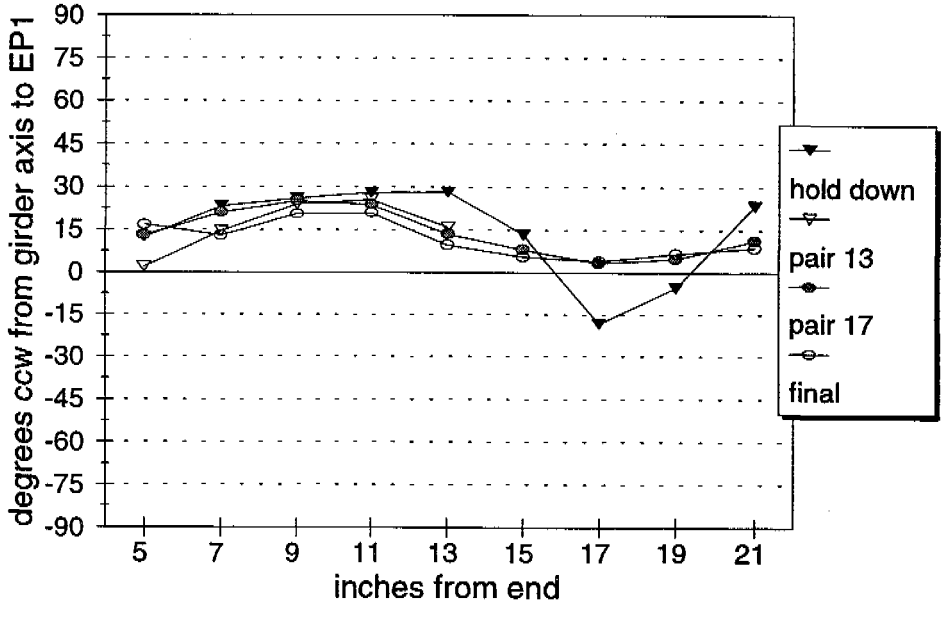

Figure 7.4f Bed #3, Principal Strain Angle, Gage C

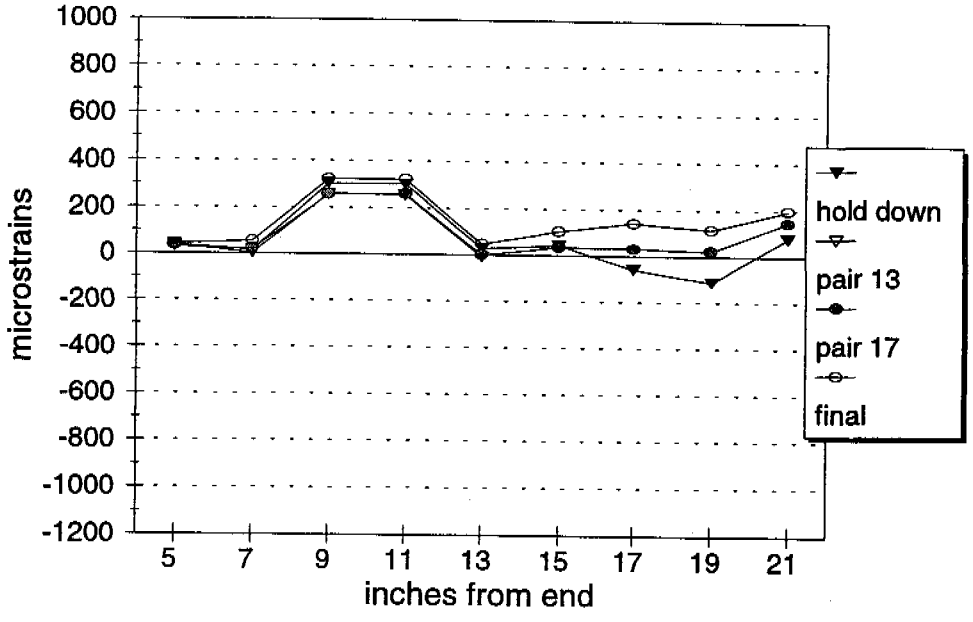

Figure 7.4g Bed #3, Maximum Principal Strain, Gage C

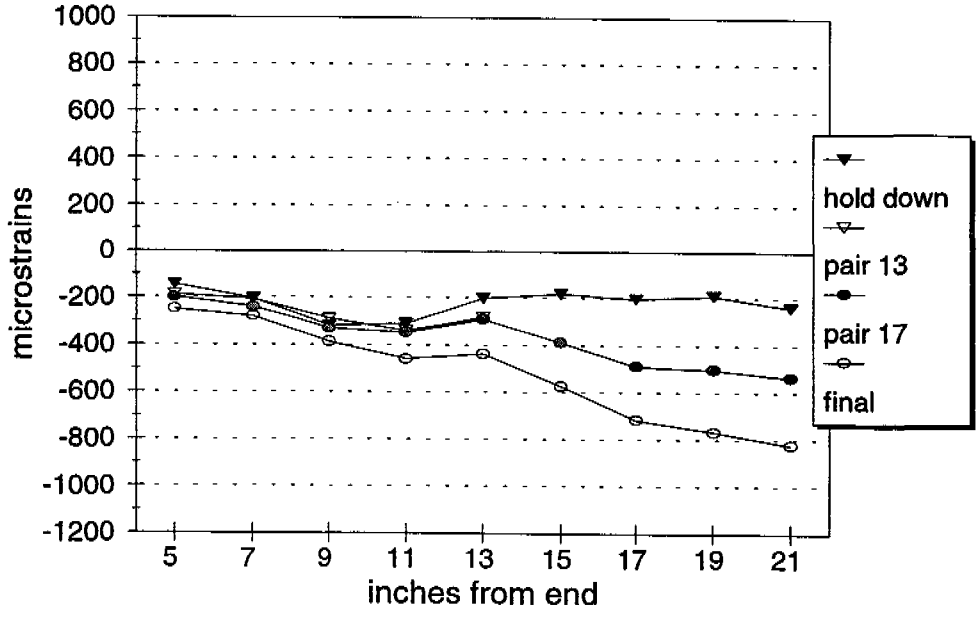

Figure 7.4h Bed #3, Minimum Principal Strain, Gage C

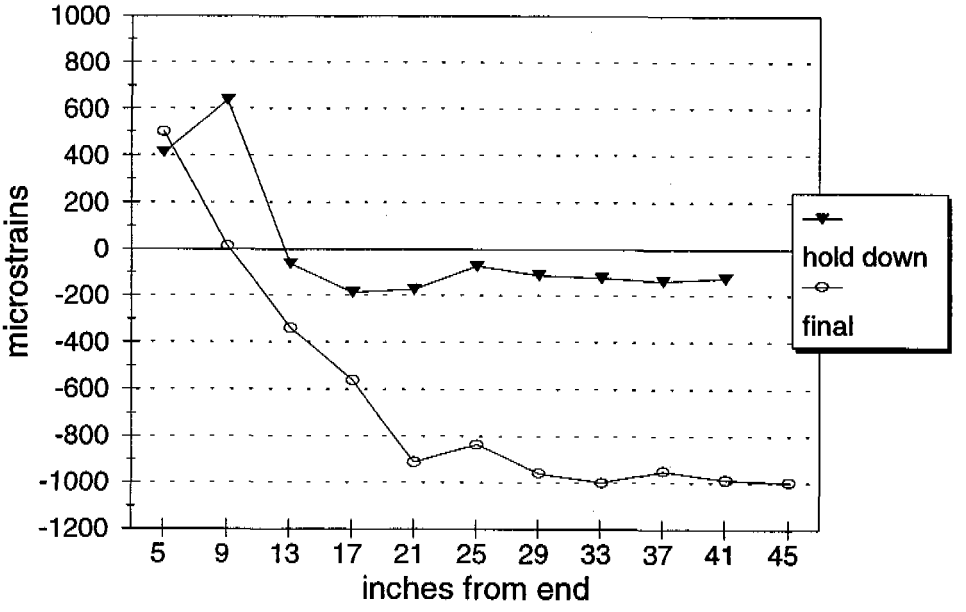

Figure 7.4i Bed #3, Middle Line of Gage D

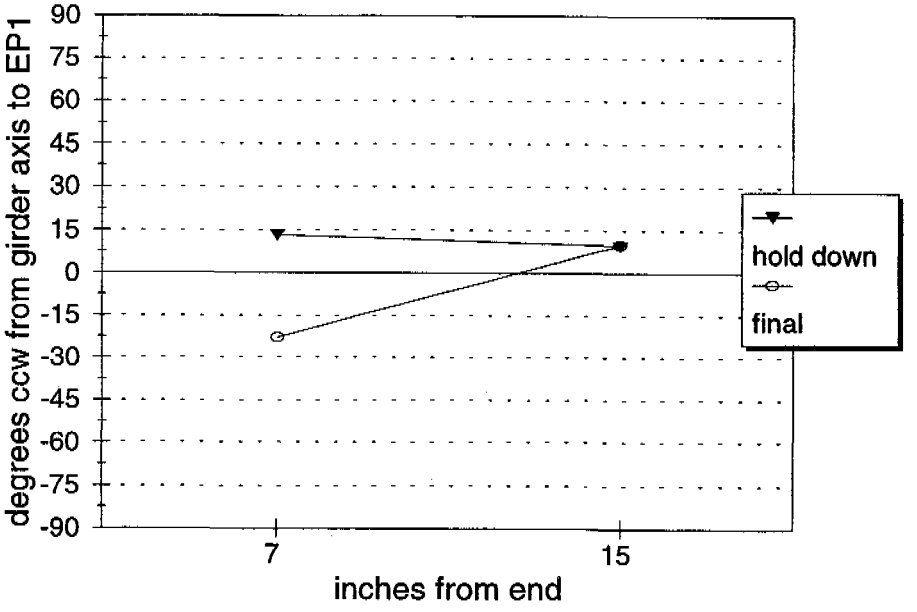

Figure 7.4j Bed #3, Principal Strain Angle, Gage D

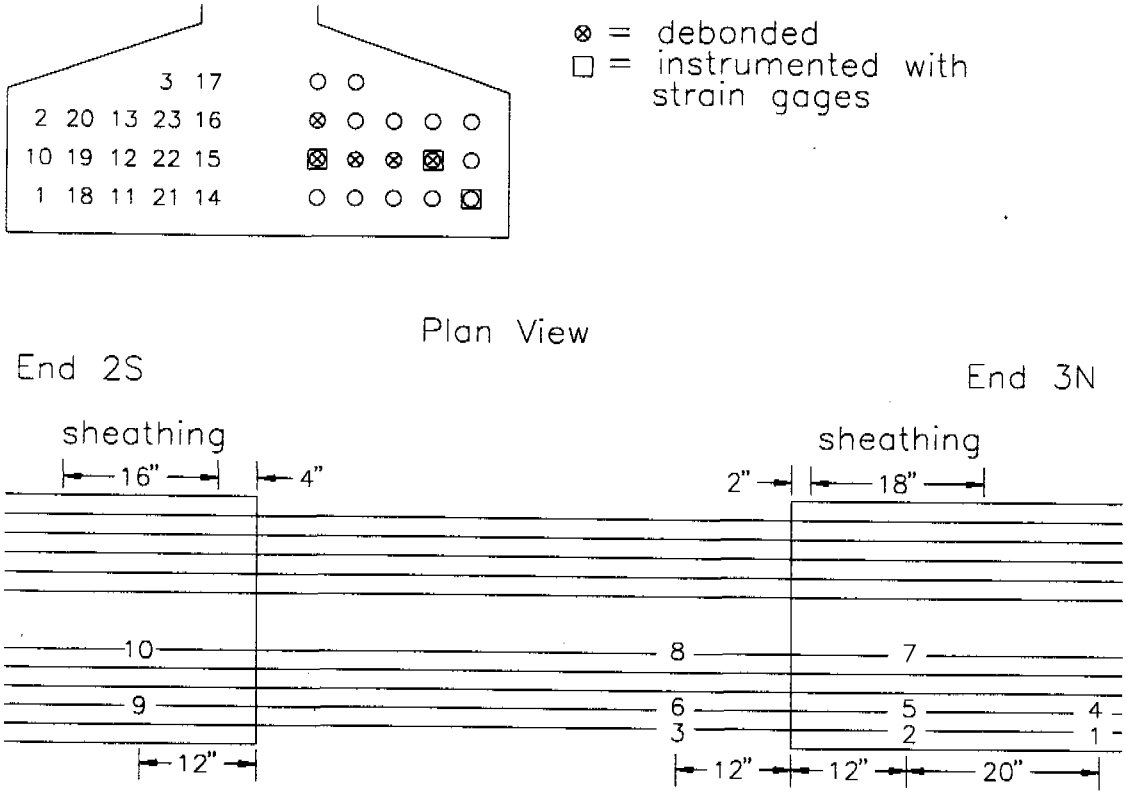

Figure 7.5 Strand Gages for Bed #3

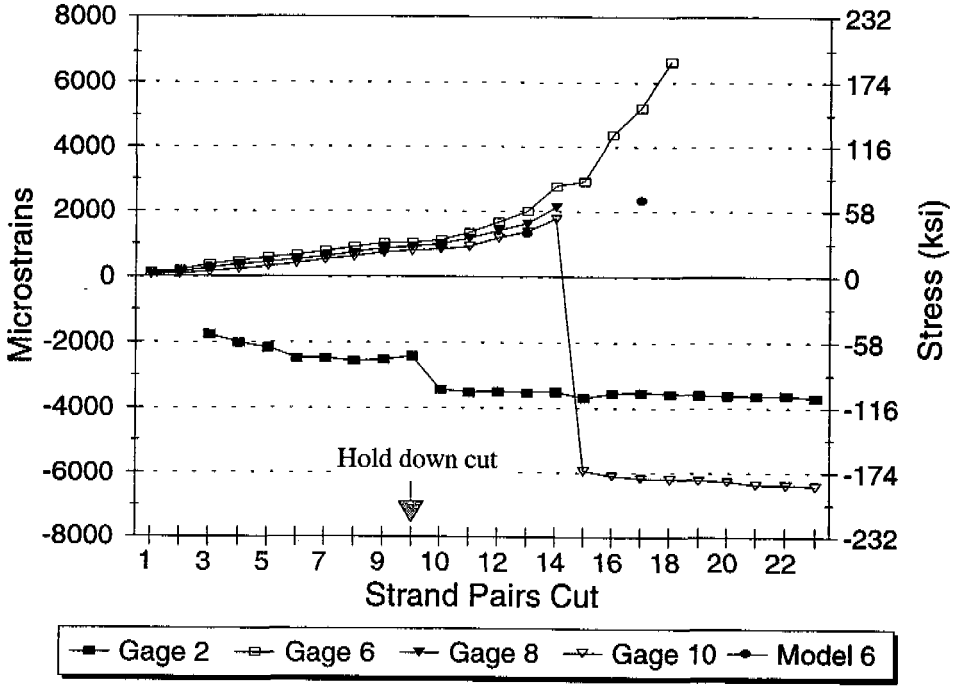

Figure 7.6 Bed #3, Strain Gages on Strands

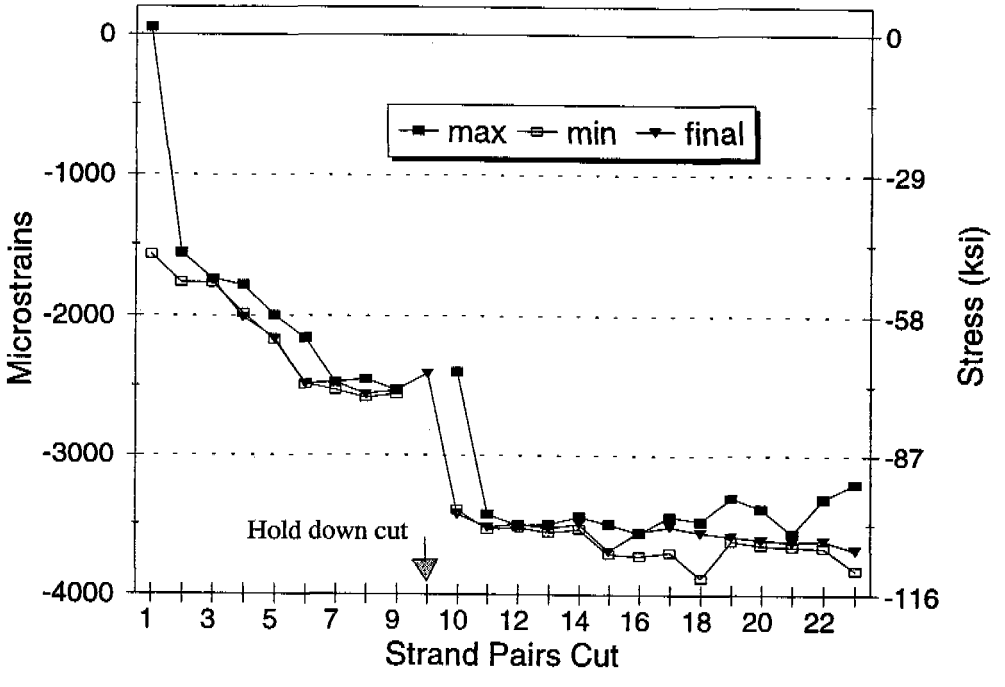

Figure 7.7 Peak Readings on Gage #2

END CRACKING IN PRESTRESSED GIRDERS

Girder ID: Bridge #12345, Beam #9	Name: I. M. Cracked	Initial Pull = 30.98 kips/strand
Cast on 9/1/95 at 11:00 (am)/pm	Release Method= (flame cut) slow release (in groups, all at once), other:	
Released 9/2/95 at 7:00 (am)/pm	Release Order = (all points at once), ends of bed first, other:	

Draw bed layout, including lengths of girders and free strands.
Indicate anything restricting movement of free strands.
Assign a number to the ends of the girders.

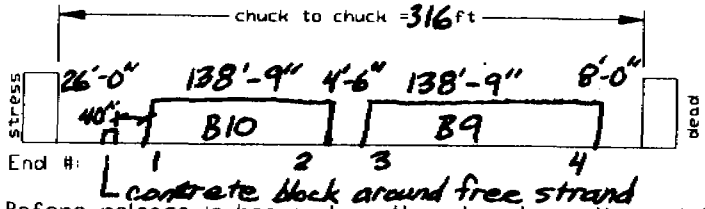

Concrete Strength measured at release = 6940 psi
Ambient air temperature (average while curing) = 60 °F
Curing (method/temperature): covered with insulated tarp
Lubricants-anything reducing friction between bed & girder? Quick Strip XL - pallet, Slippit - sole plate

Before release is begun, draw the strands on the end face and number them by the planned release pattern. Indicate which end and which side of the face will be observed. During release, sketch all cracks and circle the point of crack initiation where appropriate. Number primary cracks and fill in the data table.

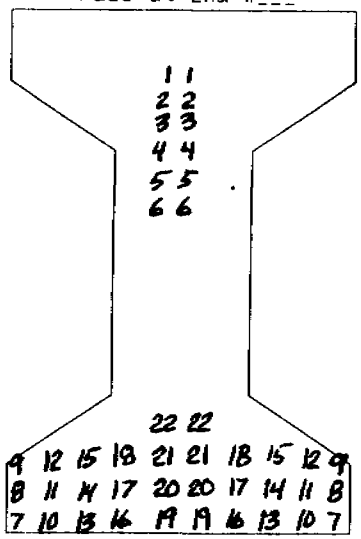

Hold down points released after cut strand #___

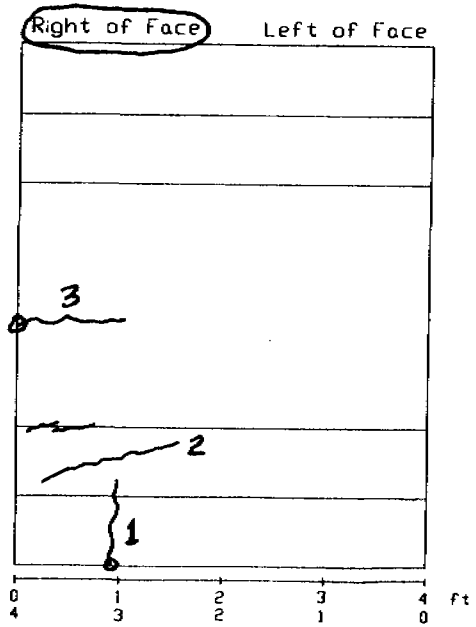

Crack #	Formed when cut strand #	* Closed when cut strand #	Width (mils/mm) Maximum	Final
1	6	18	9	5
2	9	-	13	9
3	21	-	7	7
4				
5				
6				
7				

* If applicable

Did any of these cracks form right at the edge of a sole plate? Y/N, crack #___

Comments:

Figure 8.1a Sample Survey Form, Page 1

END CRACKING IN PRESTRESSED GIRDERS

Girder ID: Bridge #12345, beam9	Location: on bed, (in yard) at site, in place	Date: 9/3/95	Name: I. M. Cracked

Explain observational hindrances (e.g. surface grouted): surface grout obscured small cracks

Fill out applicable data on page 1. Label faces with end numbers from page 1 and indicate corners observed during release. For all other corners and the end faces if possible, draw all cracks and indicate their width.

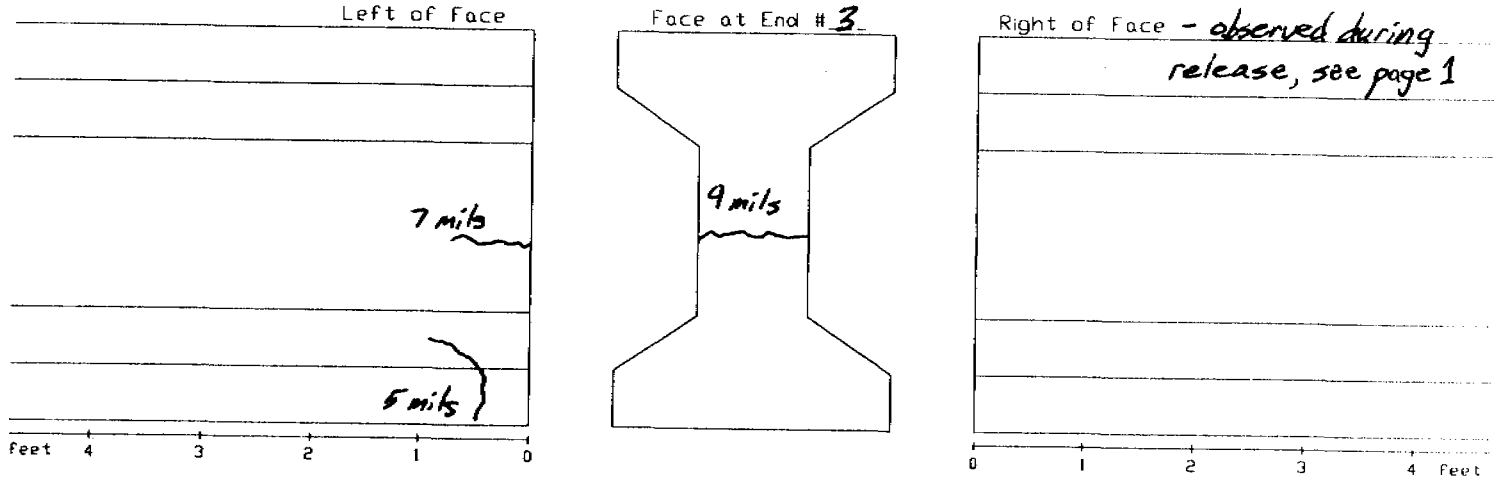

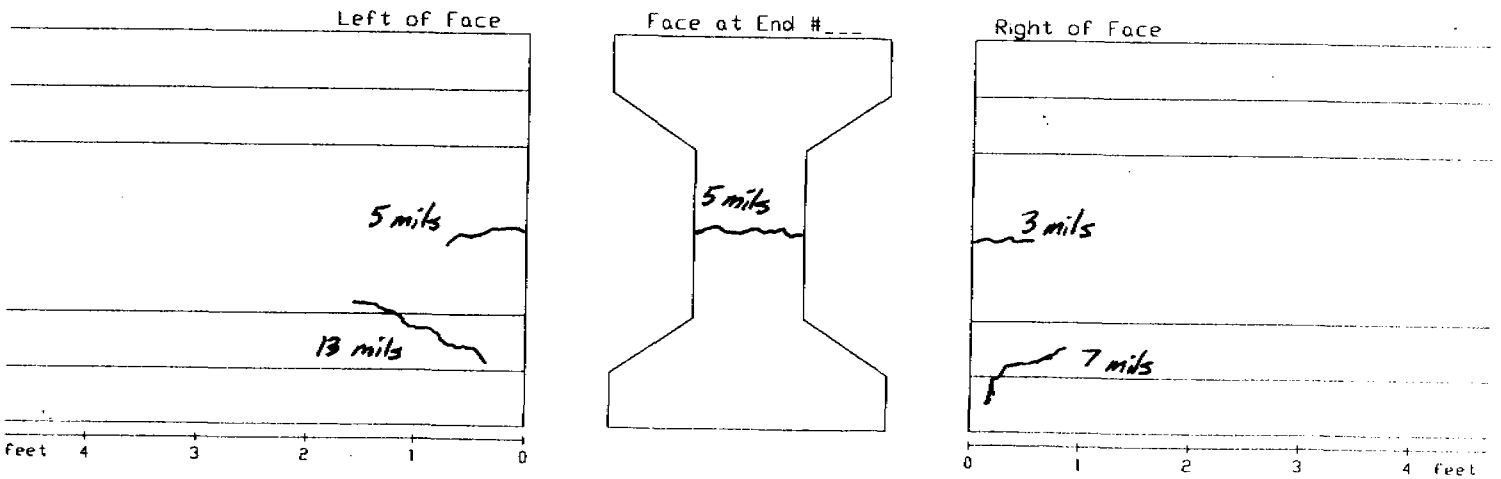

Figure 8.1b Sample Survey Form, Page 2

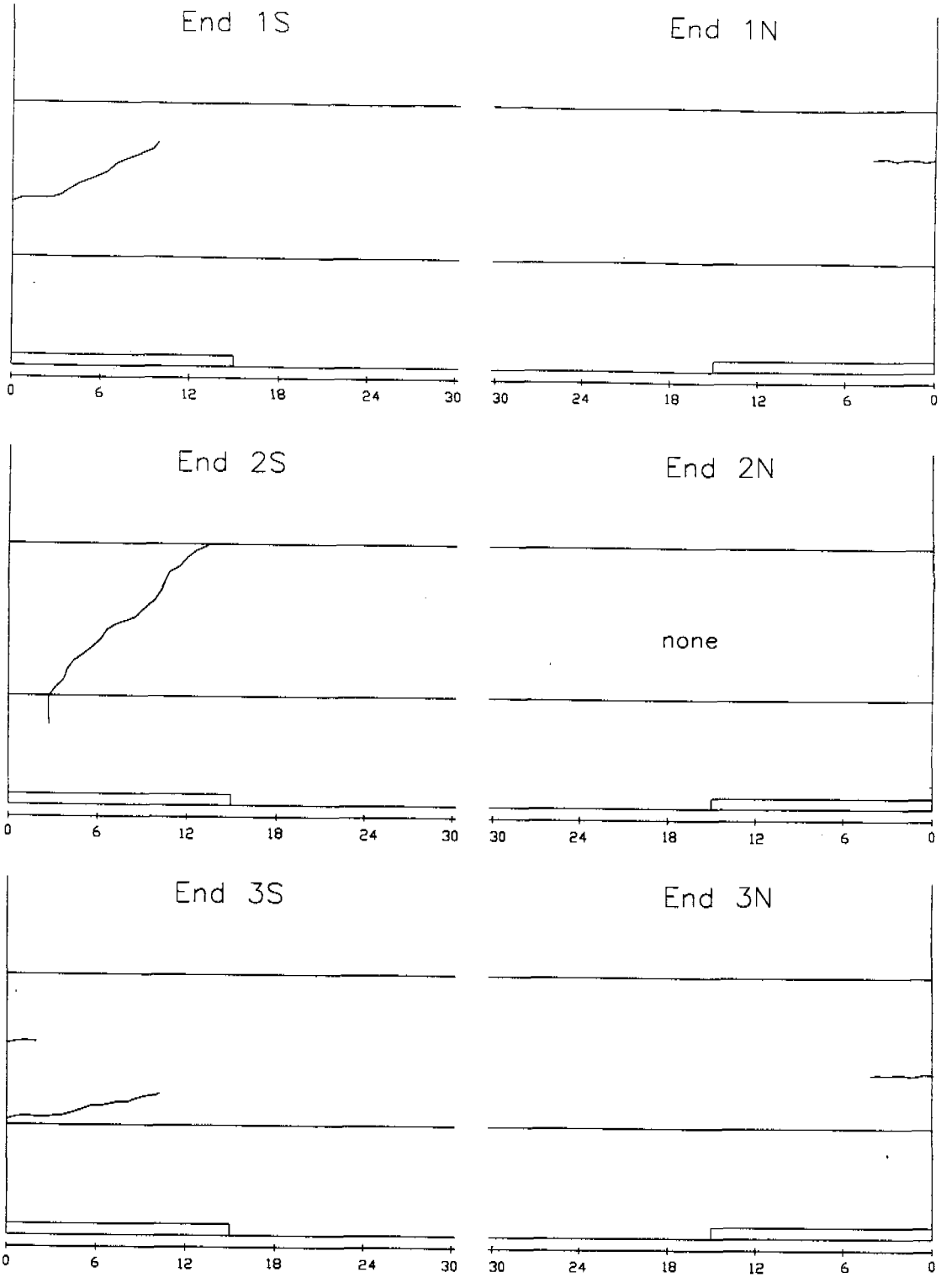

Figure 8.2a Survey Form for 45 in. Girders, 8-4-95
Cut with pattern 45A

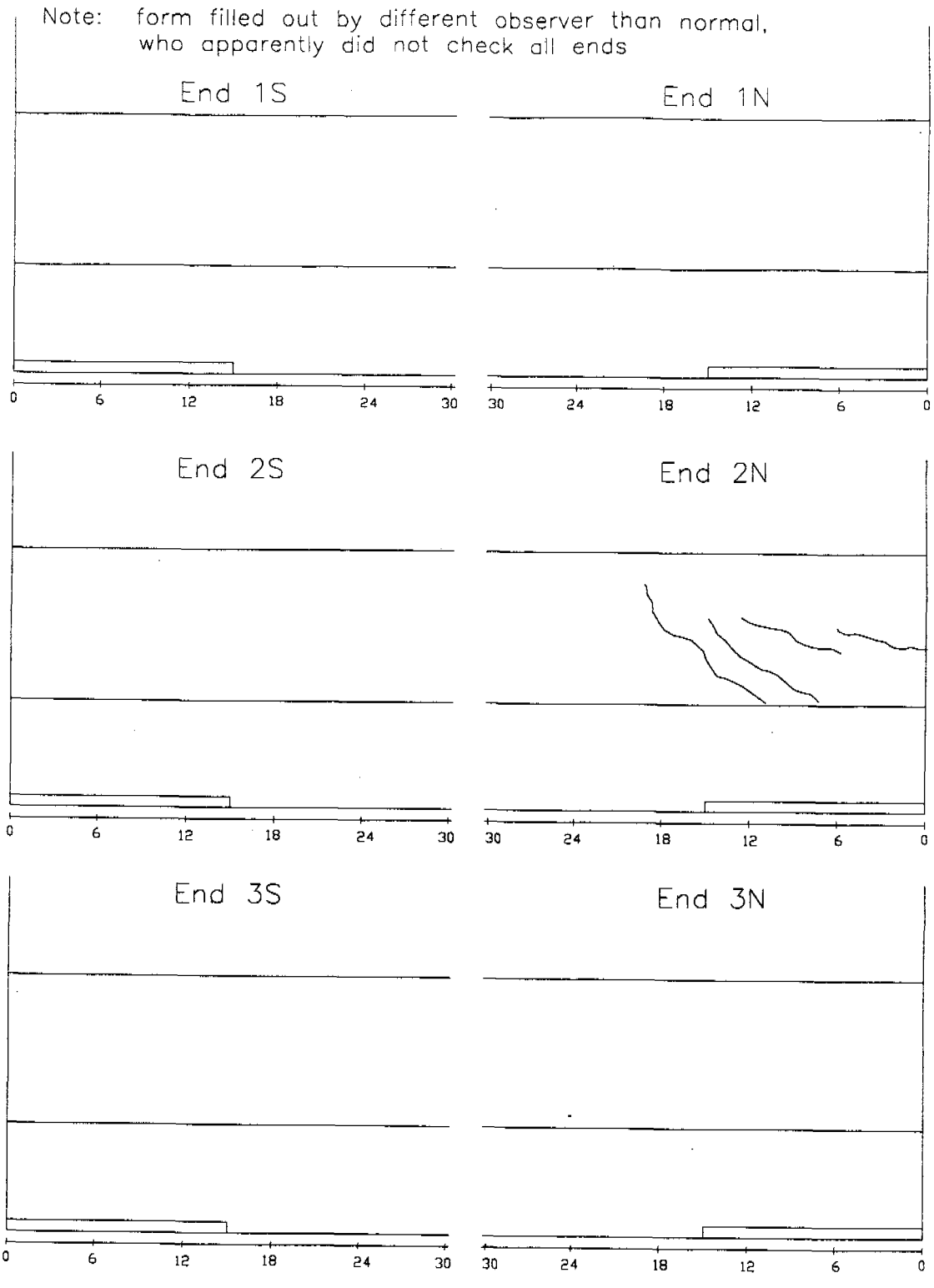

Figure 8.2b Survey Form for 45 in. Girders, 8–9–95
Cut with pattern 45A

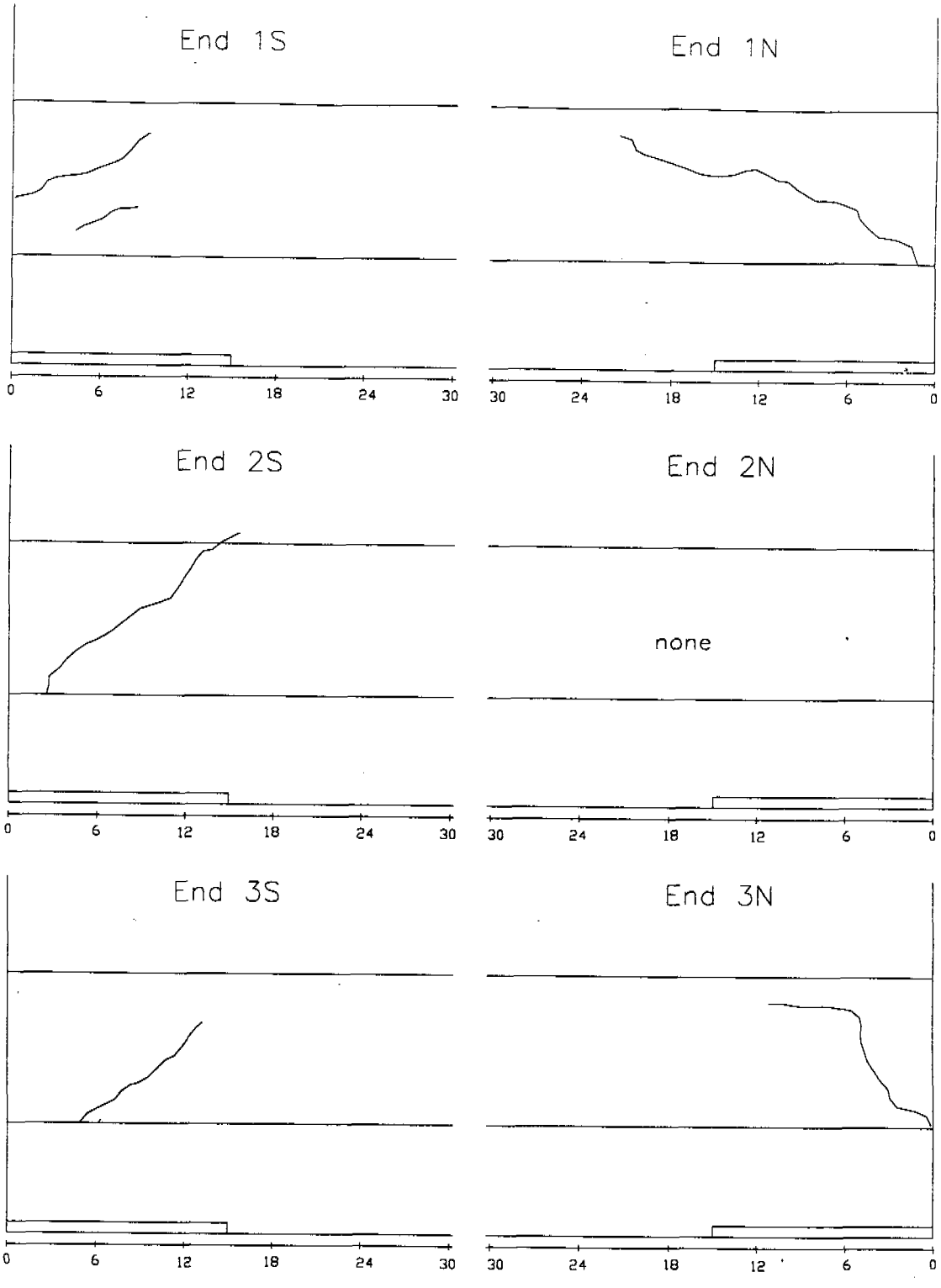

Figure 8.2c Survey Form for 45 in. Girders, 8-15-95
Cut with pattern 45A

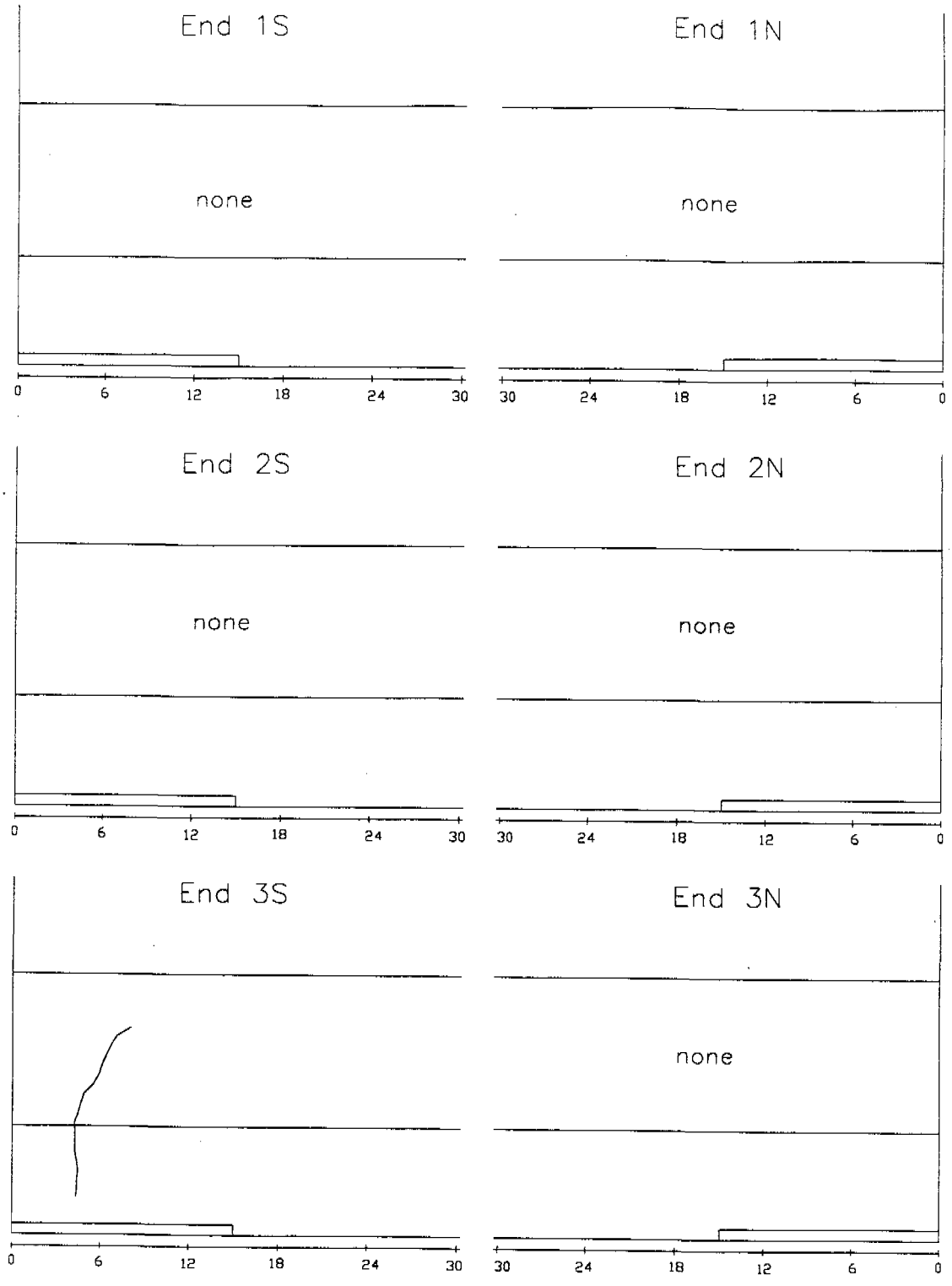

Figure 8.2d Survey Form for 45 in. Girders, 8-16-95
Cut with pattern 45B

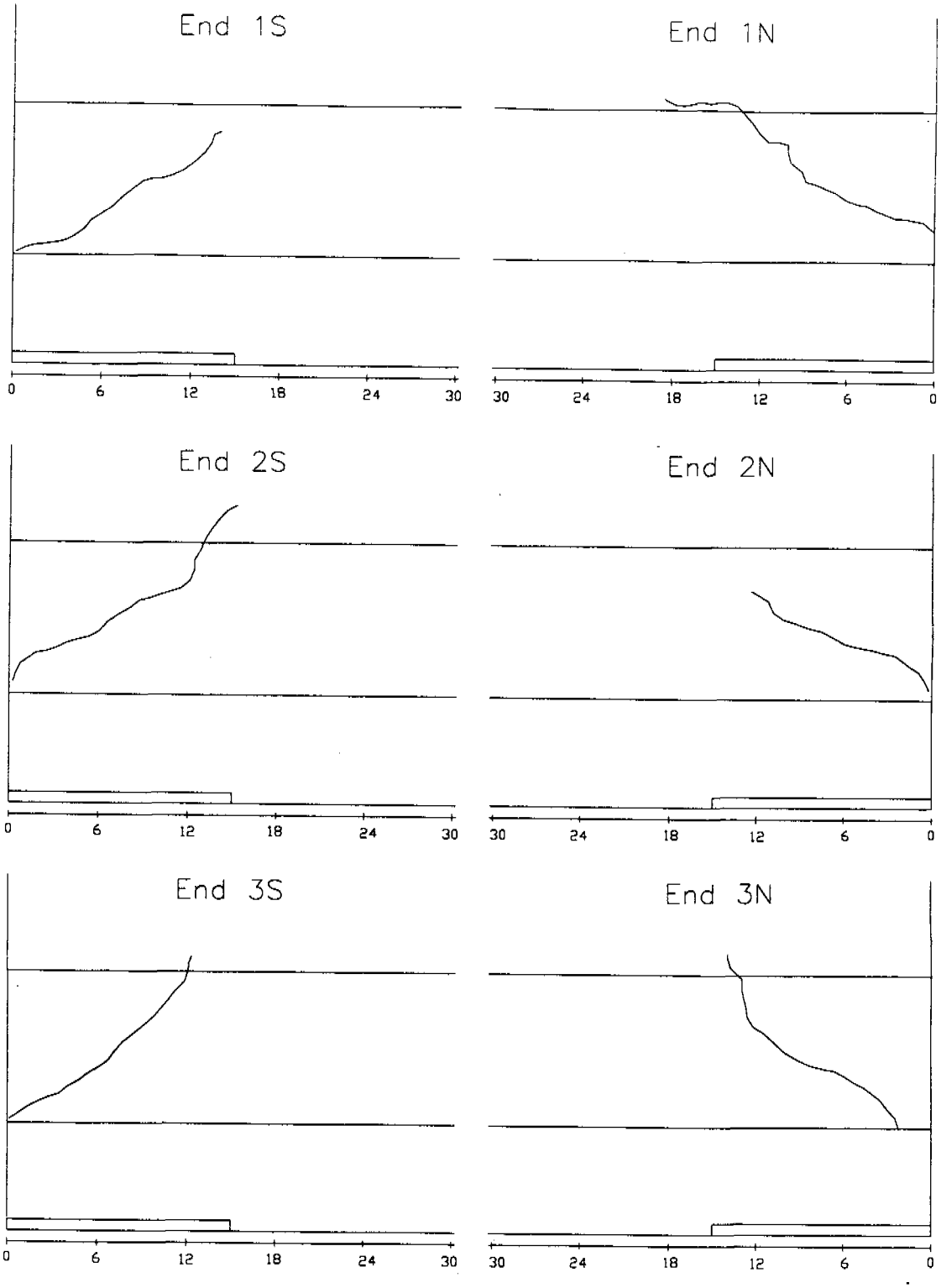

Figure 8.3a Survey Form for 63 in. Girders, 8–3–95
Released with original cutting pattern

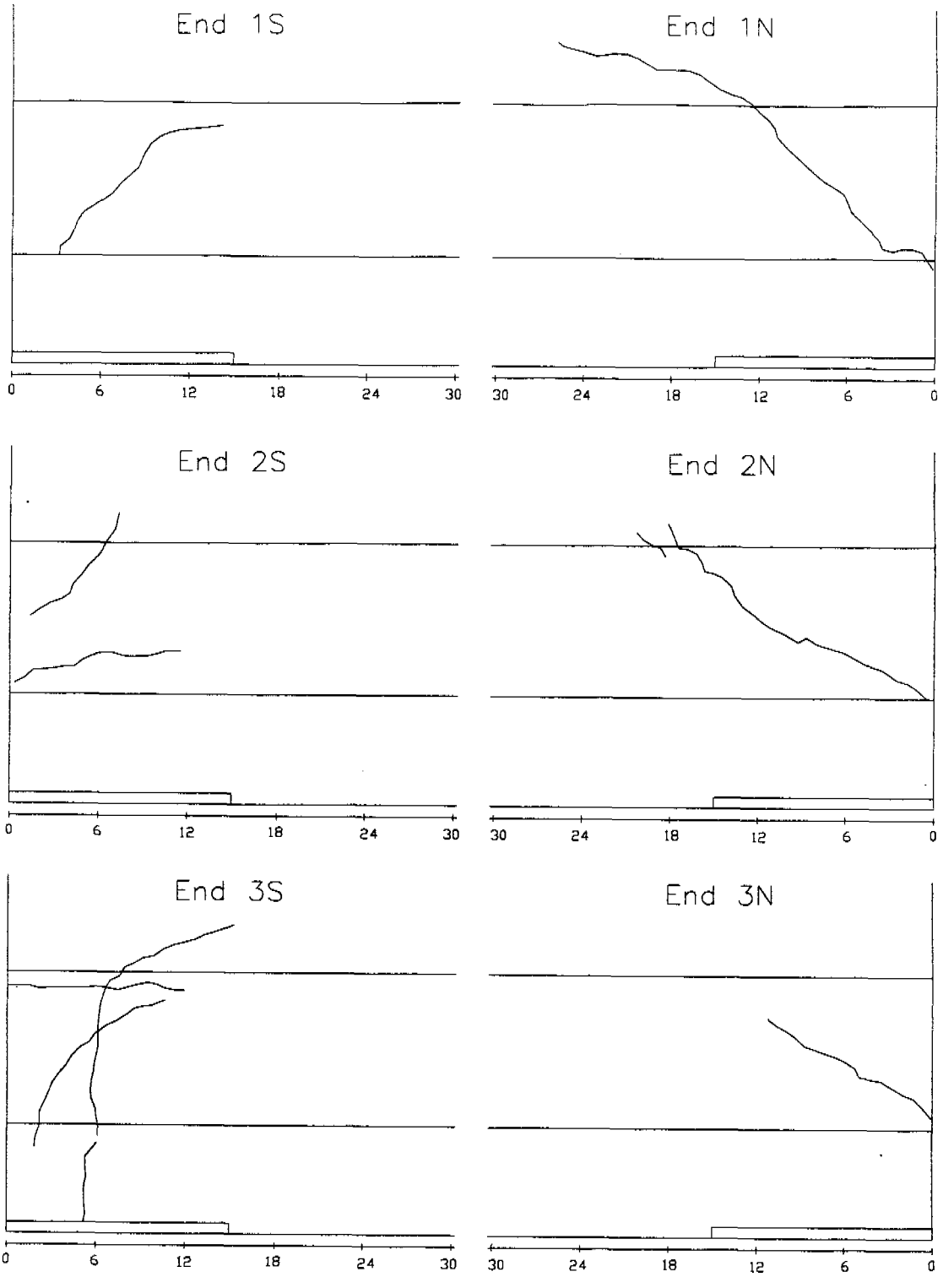

Figure 8.3b Survey Form for 63 in. Girders, 8-11-95
Released with original cutting pattern

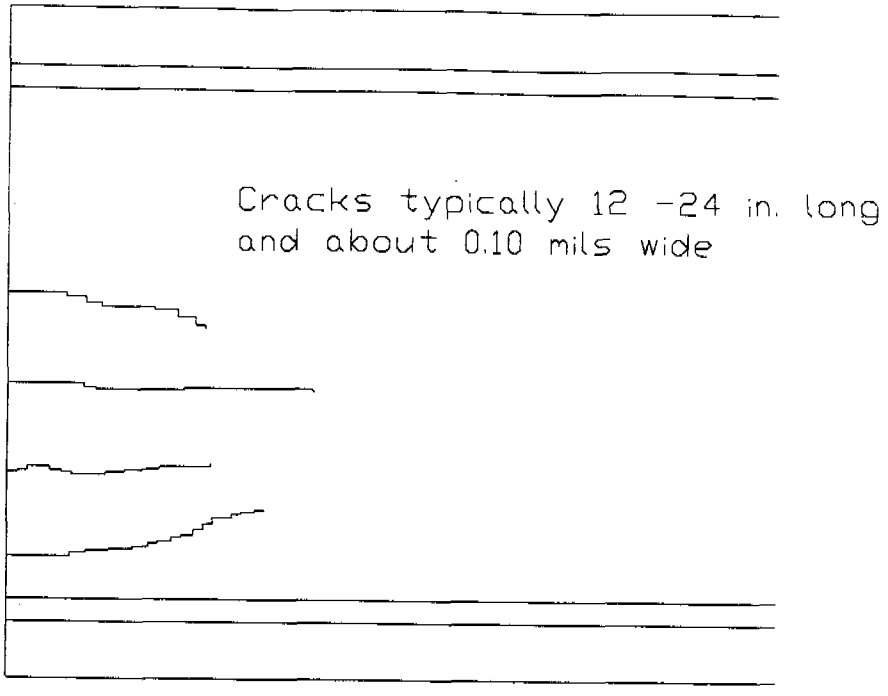

Figure 8.4 Web Cracks in 81 in. Girders

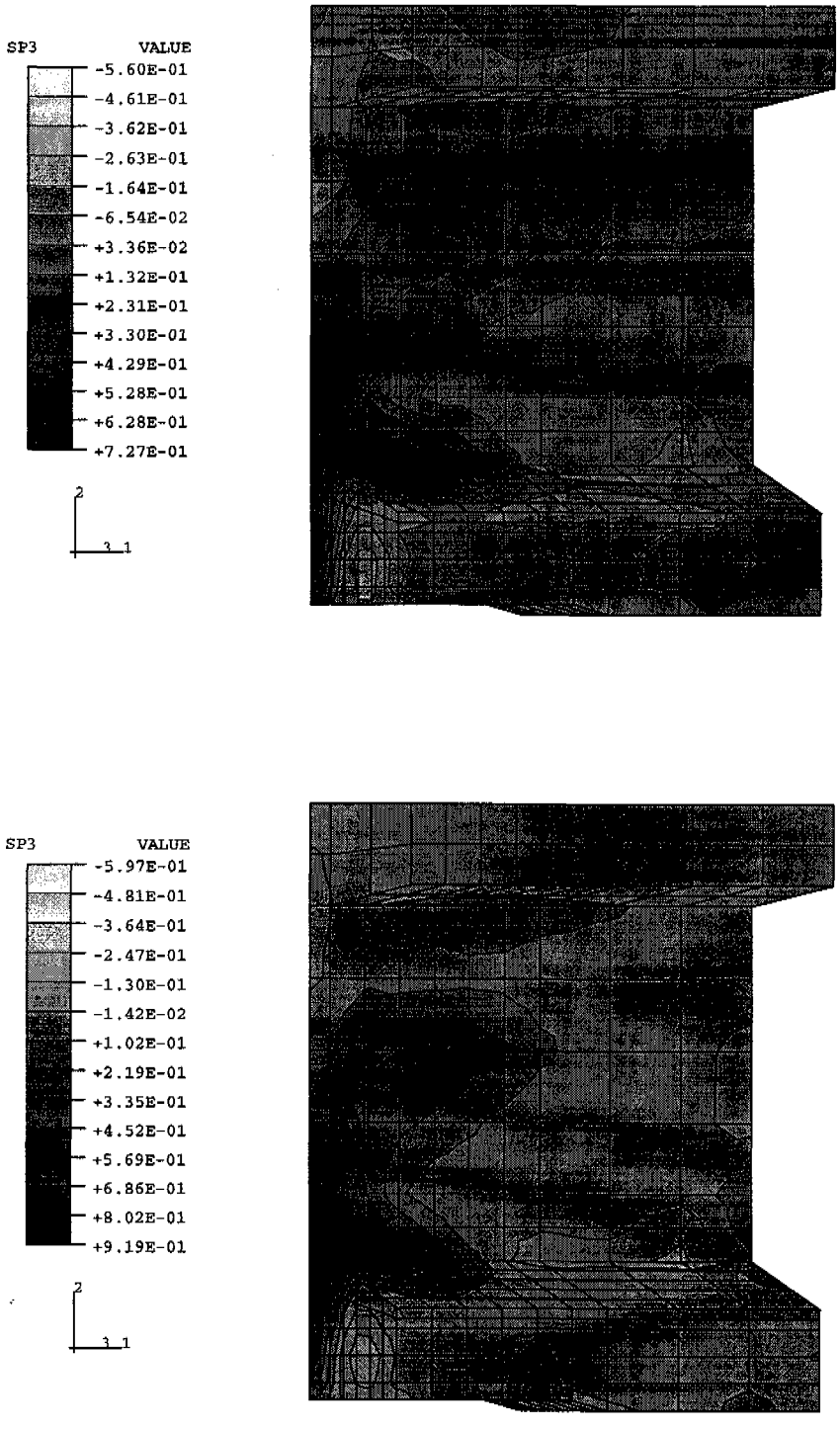

Figure 8.5 SP3 at Full Release for Original Model of 45 in. Girders (top), and Model of Shortened 45 in. Girders (bottom)

APPENDIX A

APPENDIX A
MODELLING EFFECTS

This appendix addresses some issues regarding the FEM model. Section A.1 compares an alternate method of modelling the transfer length to the method described in Section 3.2. Section A.2 examines the effect of refining the continuum element mesh, decreasing the size of the elements. Finally, Section A.3 discusses the stress concentration at the end of the sole plate.

A.1 Transfer Length Modelled with Springs

The transfer length approximation described in Section 3.2 did an adequate job of modelling the compressive transfer length after a strand was cut, but was not able to model the reverse tensile transfer length before a strand was cut. The difficulty lied in using the same nodes for the truss and continuum elements because this did not allow slipping between the strands and the concrete. The alternative was to use separate nodes for the truss and continuum elements, connecting them with springs defined to simulate an assumed bond-slip relationship. This method was eventually tried with a one-half girder model of the 54 in. deep girders. Notice that use of the springs still requires the concrete nodes to line up with the strand nodes. In the draped strand region, the continuum element mesh for the concrete would have to be refined extensively to match the angle of the draped strands (see Figure C.1), so the original transfer length method was maintained for the draped strands.

The springs were given a rigid-plastic behavior. It was assumed that after a strand was cut, all of the springs in the compressive transfer zone would be yielding, with the sum of the forces in the springs equal to the prestress force in the strands. To maintain an appropriate stress transfer rate, the springs were defined to yield at a force level equal to one kip per inch of tributary length attributed to each node, as shown in Figure A.1. In this way the 31 kip prestress force in each strand was transferred to the concrete over approximately the same transfer length, 30 in., as that used in the previous models. A perfectly rigid-plastic behavior was not possible with ABAQUS. The force - displacement history that had to be used to avoid numerical difficulties is shown in Figure A.2. For simplicity, the springs were given the same behavior in

both tension and compression. Notice that for compression, similar results could be obtained by simply applying nodal forces after a strand was cut. However, use of the springs allowed the reverse transfer length to adjust to the level of tension in the uncut strands.

Contours of SP3 for the original 54 in. girder model and the spring model, each using cutting pattern 54A, are shown in Figures A.3 and A.4, respectively. Since the differences were greatest near the end of the girder, the contours are given at 0, 6 and 12 in. First notice that when all the draped strands were cut (step 3 of the analyses), the shapes of the contours were the same, but the peak SP3 stress at 0 in. dropped from 511 psi in the original model to 297 psi in the spring model. In the original model, the entire restraint force was transferred to the girder immediately, while in the spring model only a portion of the restraint force was transferred at the end face. Starting around 12 in. from the end the models gave similar results. In the following steps the shapes of the contours continued to be similar and the stress magnitudes with the spring model continued to be lower near the girder face. The stress magnitudes were approximately the same for both models starting around 12 in. from the girder face. At full release the two models give nearly identical results, suggesting neither model was superior to the other for approximating the compressive transfer length.

The spring model was also used to investigate patterns 54B and 54C through the draped strand release, when the distribution of axial stress within the end of the girder is of primary importance. Table A.1 duplicates the information from Table 6.3 and adds the data from the spring models. The table shows that the stress was greatly reduced for the spring model in the first foot of the girder, but the stress was similar to the original model beyond that point. While precutting caused the stress in the original model to increase dramatically at the face of the girder, the stress in the spring model barely changed. This was because the force being transferred from each truss element to the concrete at the end face was limited to 1.5 kips in the spring model.

Table A.1 Peak S11 for 54 in. Girders at Full Draped Strand Release, Original and Spring Models (psi)

in. from end	0	3	6	9	12	15	18	24
original models								
54A, step 3	466	365	280	247	226	430	488	362
54B, step 4	816	668	427	236	185	335	268	78
54C, step 4	838	534	271	98	67	191	126	42
spring models								
54A, step 3	260	240	236	212	219	415	479	377
54B, step 4	280	336	316	220	172	298	244	72
54C, step 4	245	210	140	88	46	147	76	16

A.2 Mesh Effects

While the mesh of continuum elements was finer in the region of cracking than elsewhere, it was still relatively coarse. The smallest basic element was 2 x 2 x 3 in., which matched the 2 in. grid of the strands. Therefore a test of the 54 in. one-half girder model was made using refined 1 x 1 x 2 in. basic elements. The resulting contours of SP3 using pattern 54A are shown in Figure A.5. Contours for the original mesh were shown in Figure A.3. At the end of the girder, the peak stresses for the fine mesh were significantly greater than those obtained with the original mesh. The reason can be seen in the contours at the end face when all the draped strands have been cut. The stress was high around the nodes where the truss elements were attached, but the stress was low at the other nodes since no force was applied directly to them. The larger elements of the original mesh caused the restraint force to be applied to every node within the strand group, eliminating the stress peaks and valleys. From the other perspective, the smaller the elements get, the smaller the area over which the tensile force is

distributed, the greater the peak stresses. Second order elements tried early in the model development gave very high peak stresses for much the same reason.

A.3 Stress Concentration at End of Sole Plate

The models consistently showed a stress concentration at the end of the sole plate during release of the draped strands. To test how much the modelling affected this stress concentration, two alterations were made to the 54 in. girder model. Model "sole1" eliminated the notch in the concrete at the end of the sole plate. Model "sole2" eliminated the notch and changed the properties of the sole plate elements to concrete, effectively removing the sole plate entirely. Side views of the girder for the original model, sole1, and sole2 are shown in Figures A.6 through A.8. The figures show the SP3 stress at the end of the draped strand release, with no precuts.

First of all, the contours for the original model show a steadily increasing stress on the surface of the flange in the first few inches of the model as the tension from the uncut strands spreads out. The stress concentration at the end of the sole plate is readily visible and appears to influence a large area. The contours also show the effect of forcing the nodes to stay in a plane at the junction with the beam elements. The contours for sole1 are very similar to the original model and indicate the notch had little effect on the results. The contours for sole2, without any sole plate, have the same general shape as before and appear to be the result of bending of the flange. The magnitude of the stress at the end of the sole plate is, however, much lower. In reality, there probably is a stress concentration, and in a large enough database a greater percentage of cracks may be found to form at the end of the sole plate.

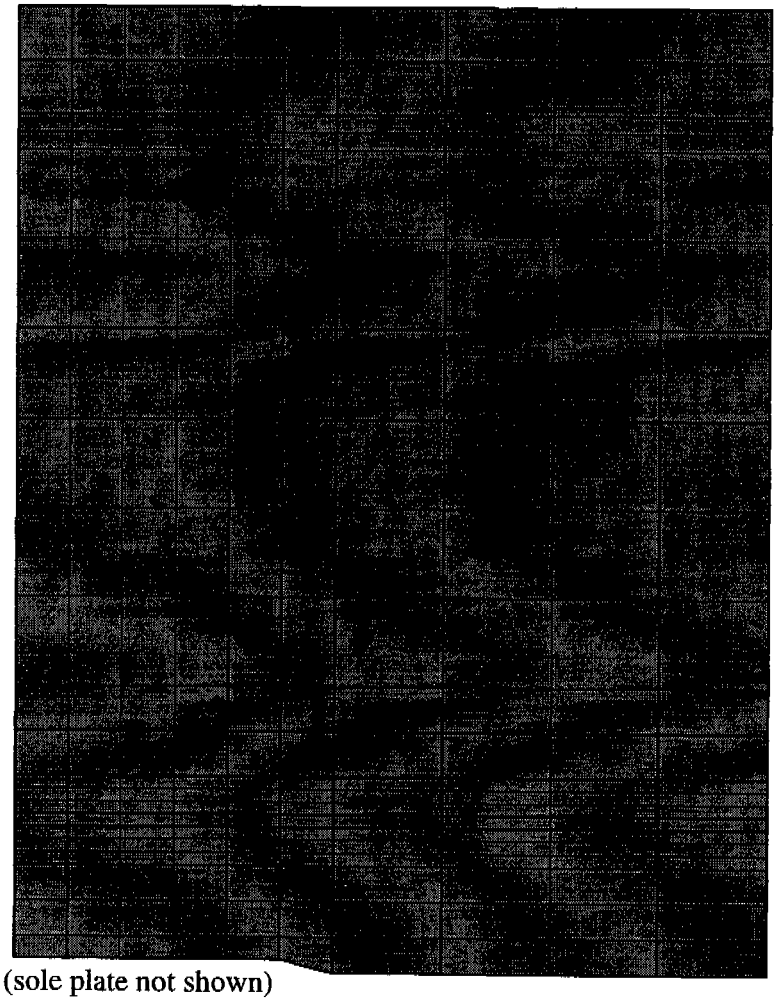

in. from end	0	3	6	9	12	15	18	24	30	36	42
yield level of springs (kips)	1.5	3	3	3	3	3	4.5	6	6	6	no spring

Figure A.1 Yield Level of Springs in Transfer Zone

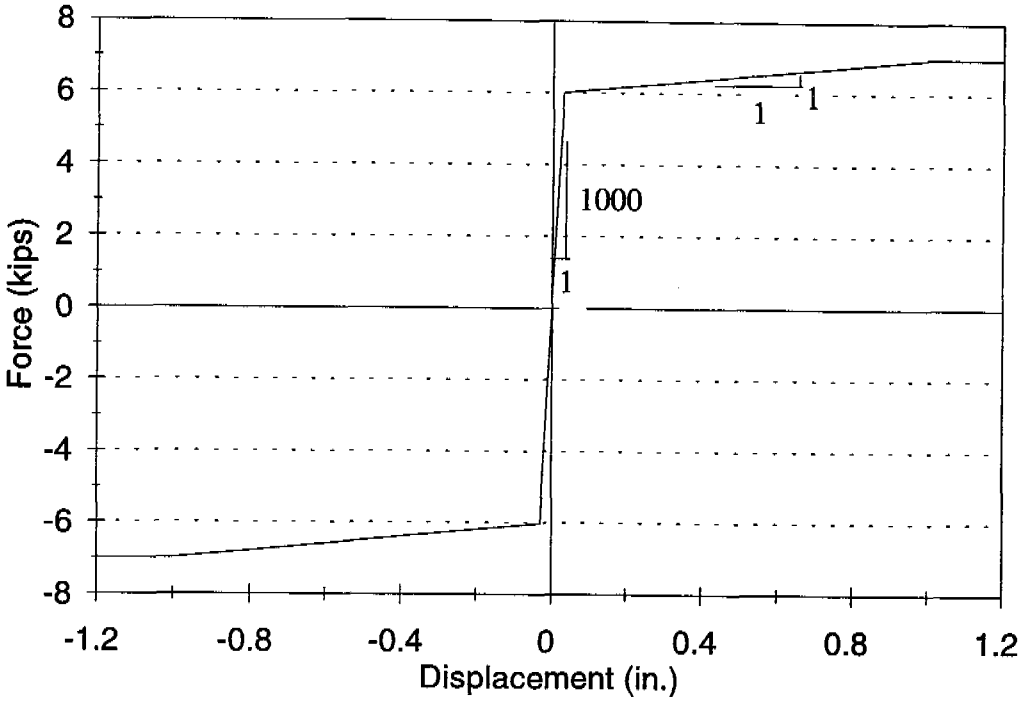

Figure A.2 Defined Behavior of 6-kip Spring

Figure A.3a SP3 Contours for Original Model, Pattern 54A, Step 2

Figure A.3b SP3 Contours for Original Model, Pattern 54A, Step 3

Figure A.3c SP3 Contours for Original Model, Pattern 54A, Step 4

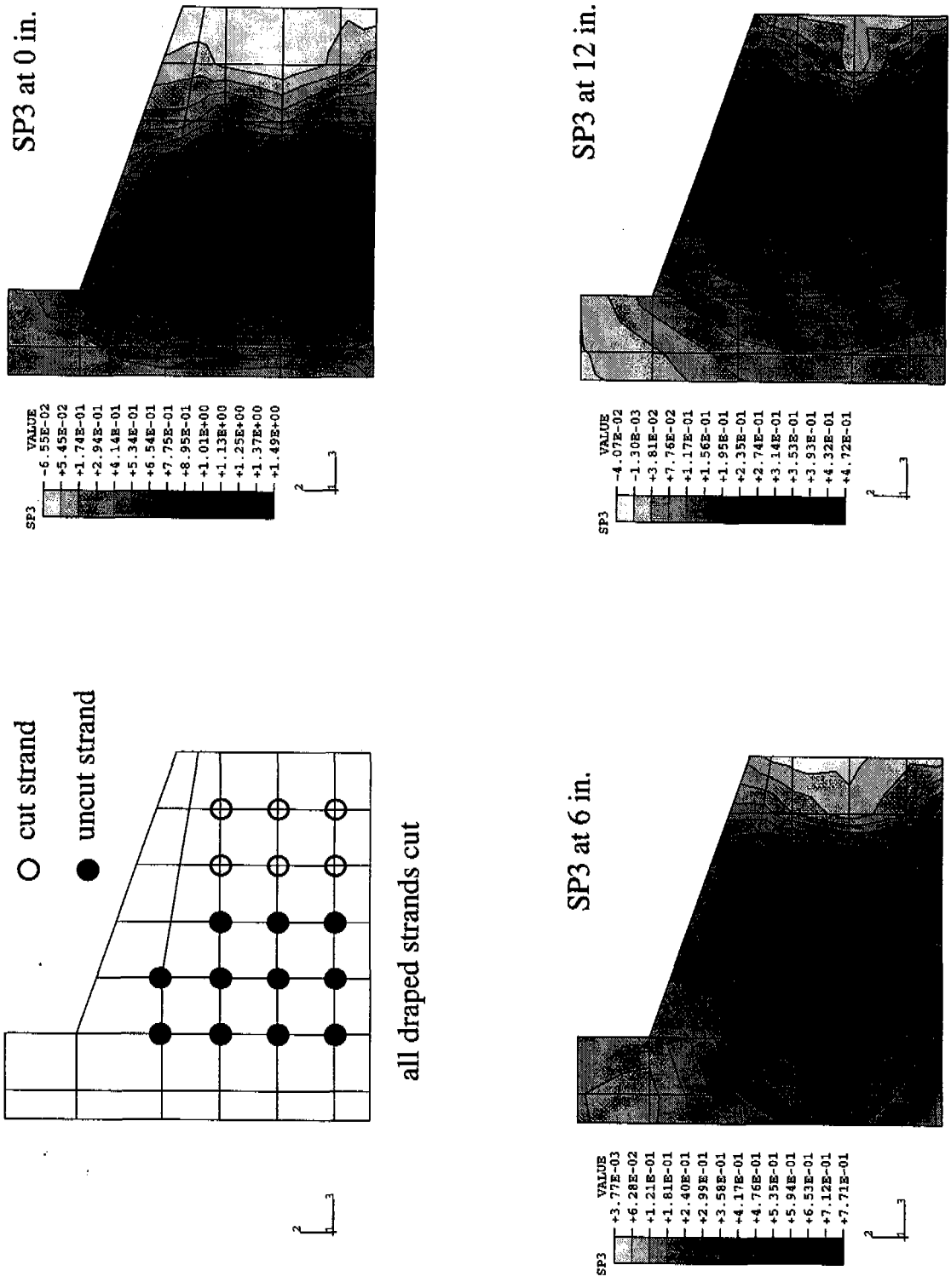

Figure A.3d SP3 Contours for Original Model, Pattern 54A, Step 5

Figure A.3e SP3 Contours for Original Model, Pattern 54A, Step 6

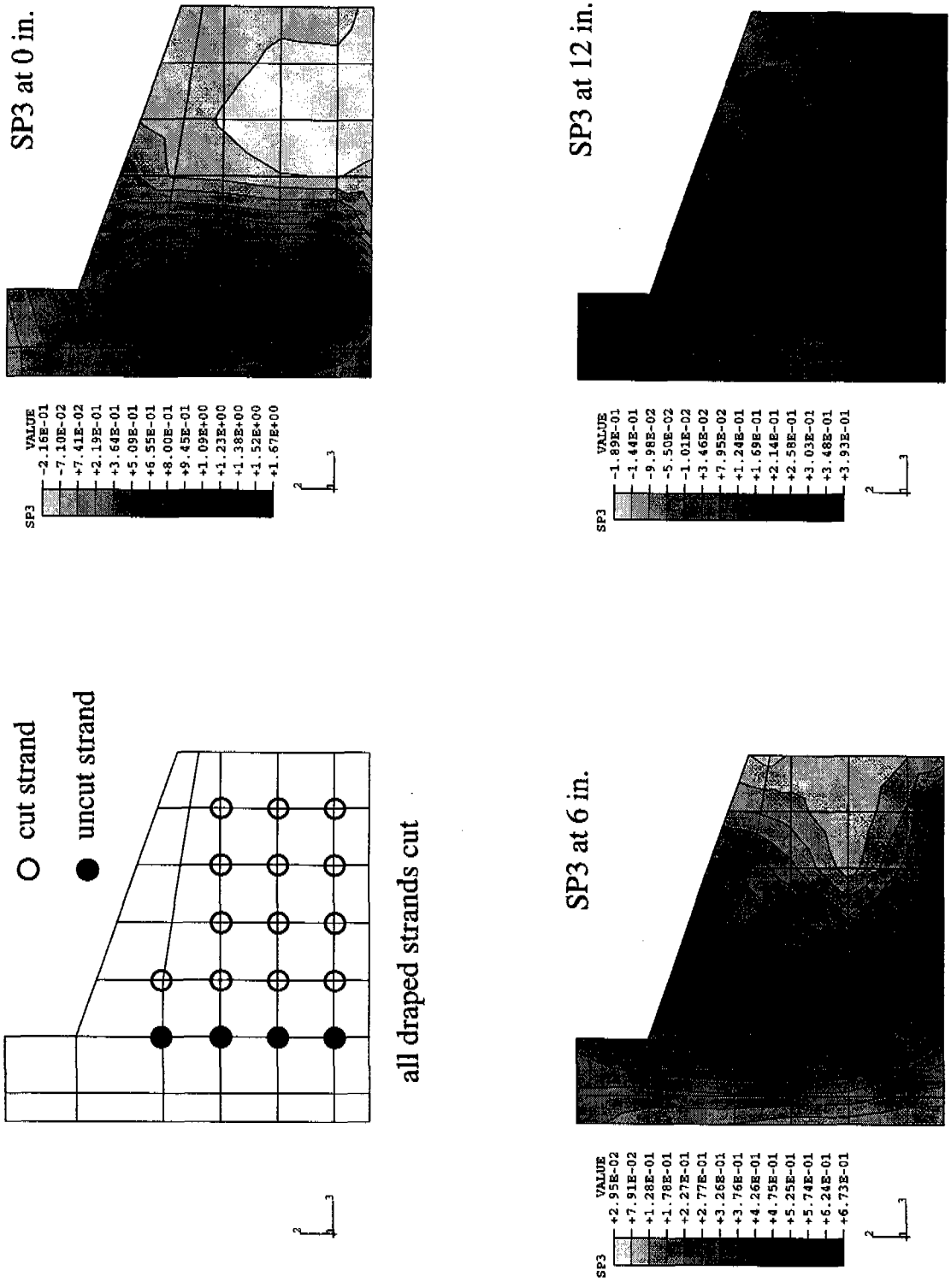

Figure A.3f SP3 Contours for Original Model, Pattern 54A, Step 7

Figure A.3g SP3 Contours for Original Model, Pattern 54A, Step 8

Figure A.4a SP3 Contours for Spring Model, Pattern 54A, Step 2

Figure A.4b SP3 Contours for Spring Model, Pattern 54A, Step 3

Figure A.4c SP3 Contours for Spring Model, Pattern 54A, Step 4

Figure A.4d SP3 Contours for Spring Model, Pattern 54A, Step 5

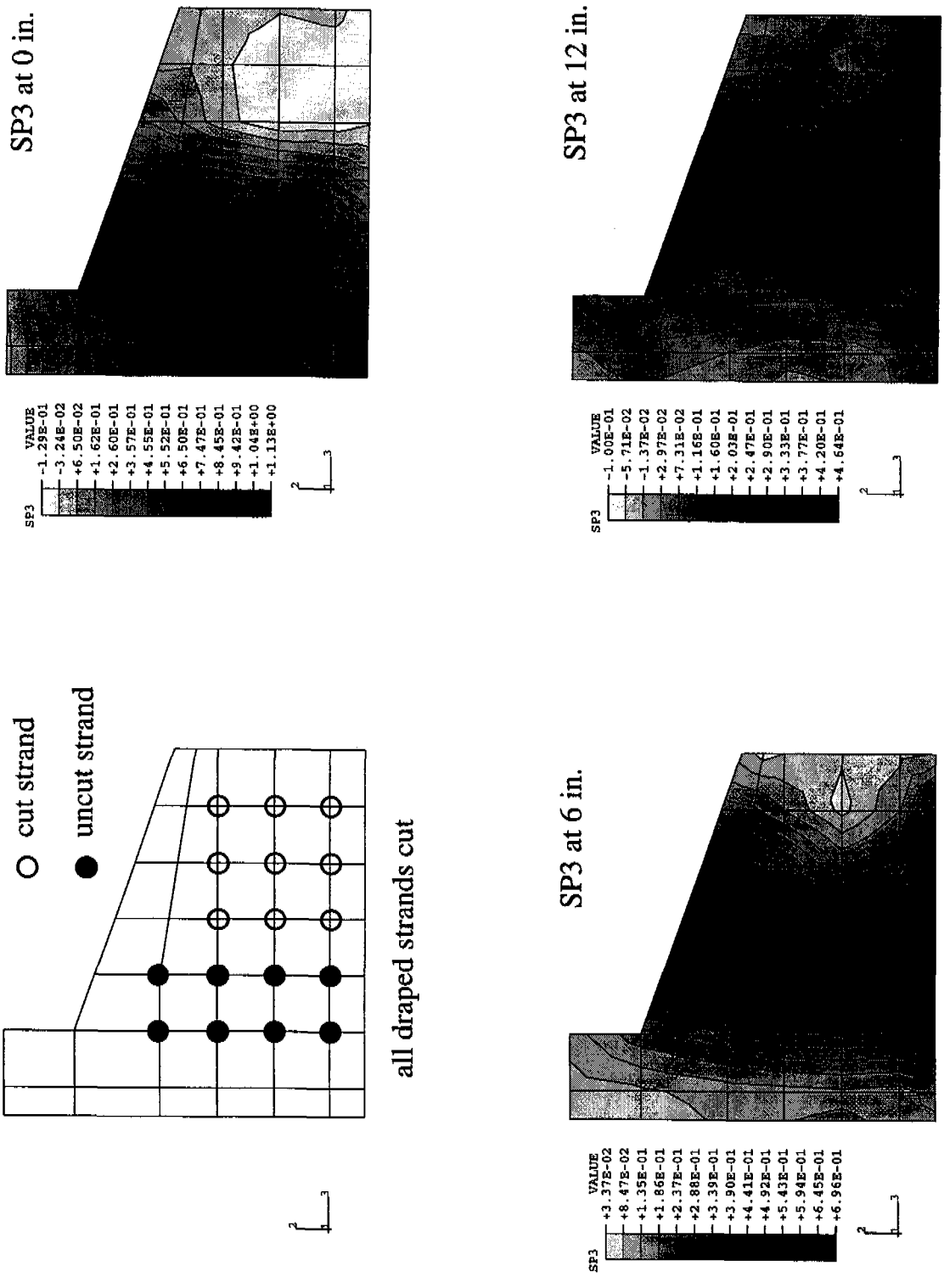

Figure A.4e SP3 Contours for Spring Model, Pattern 54A, Step 6

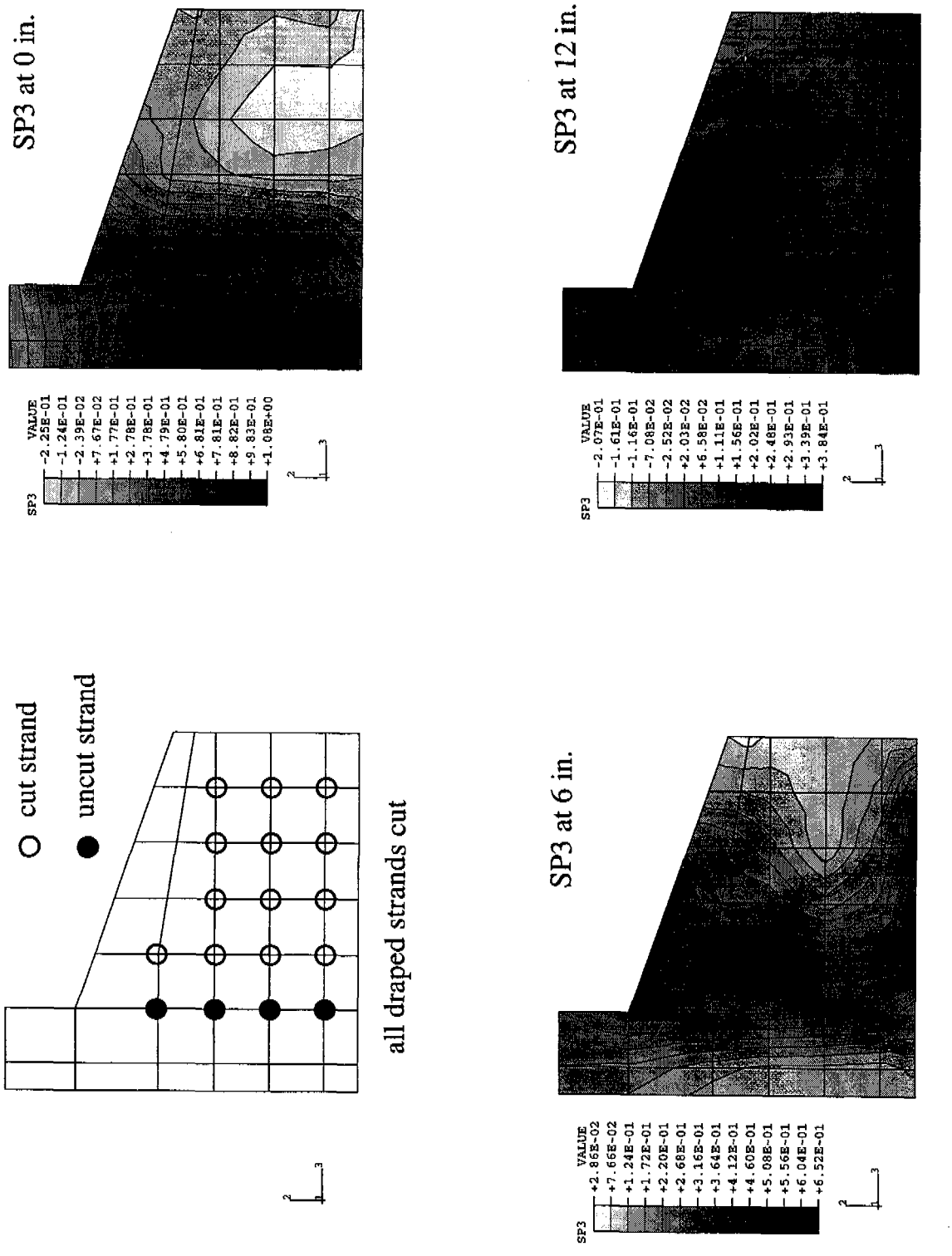

Figure A.4f SP3 Contours for Spring Model, Pattern 54A, Step 7

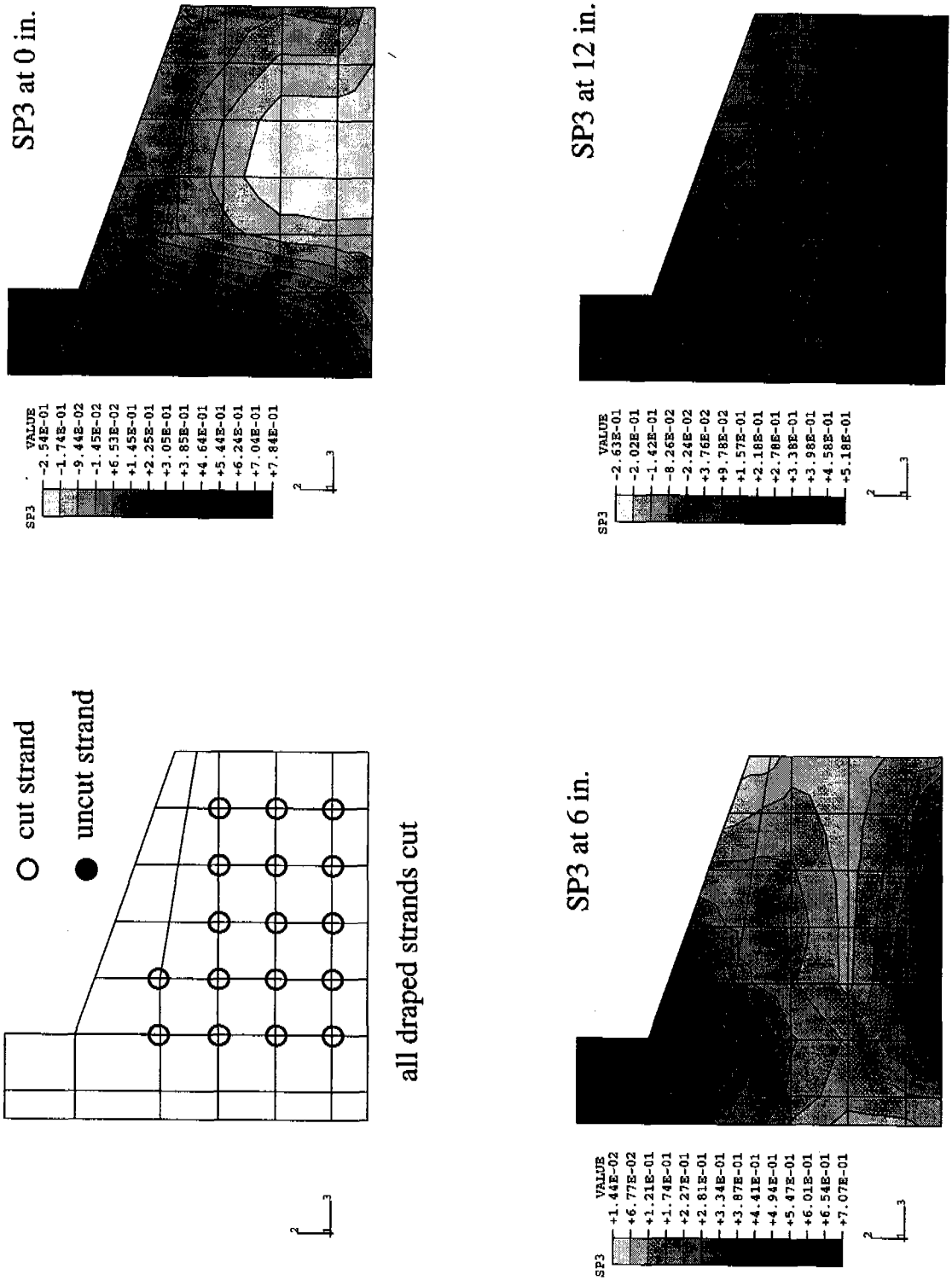

Figure A.4g SP3 Contours for Spring Model, Pattern 54A, Step 8

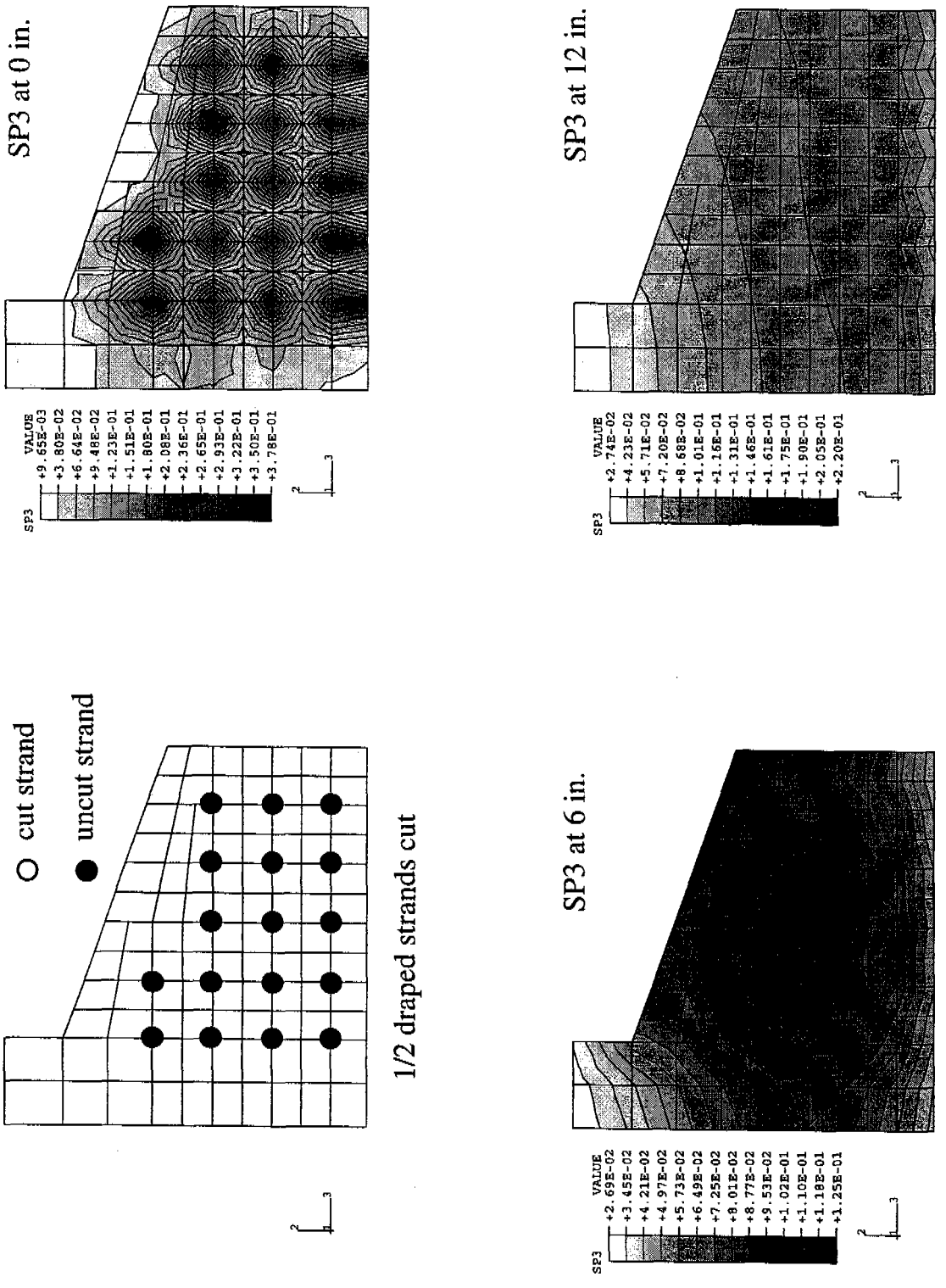

Figure A.5a SP3 Contours for Refined Mesh, Pattern 54A, Step 2

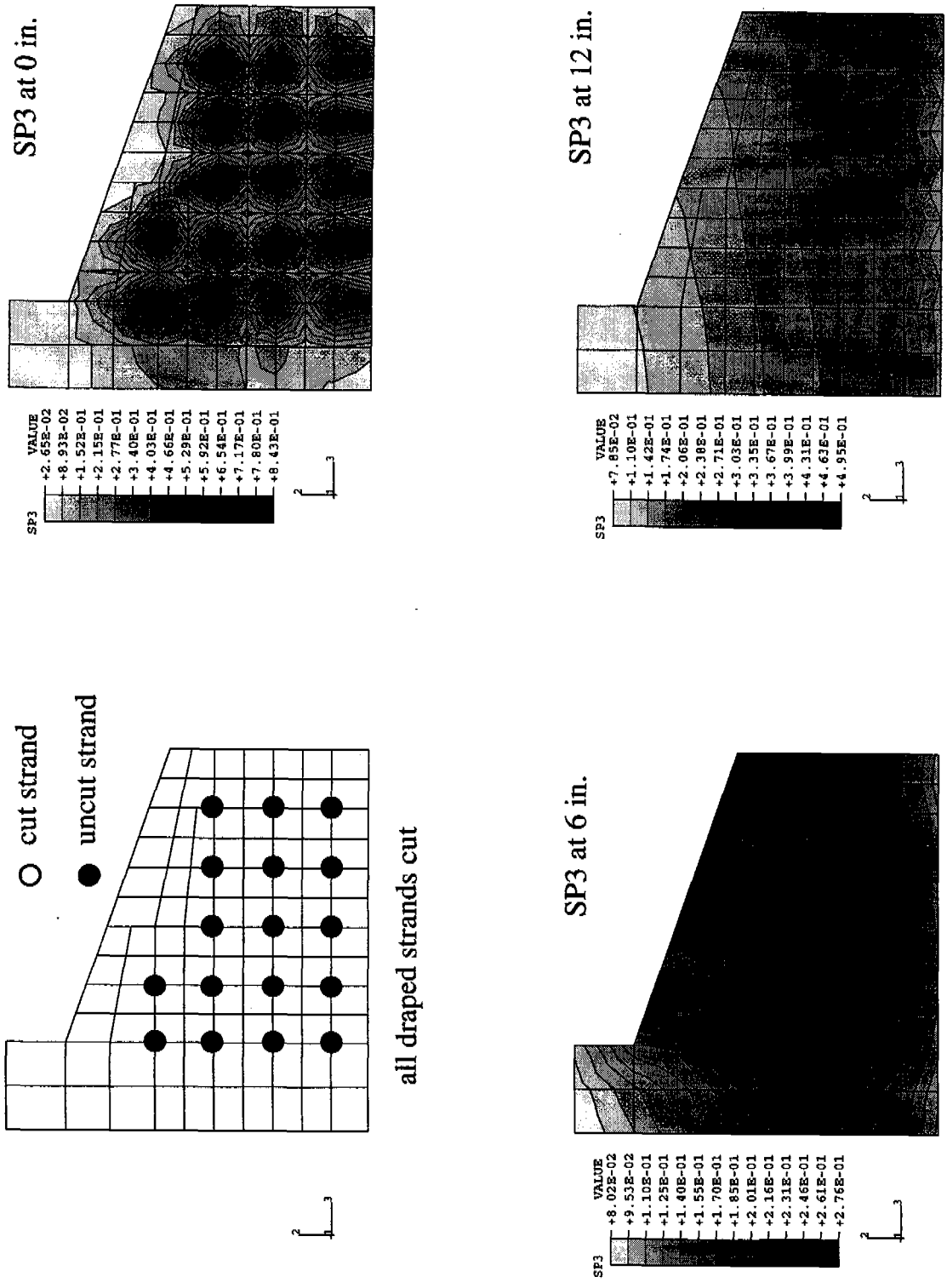

Figure A.5b SP3 Contours for Refined Mesh, Pattern 54A, Step 3

Figure A.5c SP3 Contours for Refined Mesh, Pattern 54A, Step 4

Figure A.5d SP3 Contours for Refined Mesh, Pattern 54A, Step 5

Figure A.5e SP3 Contours for Refined Mesh, Pattern 54A, Step 6

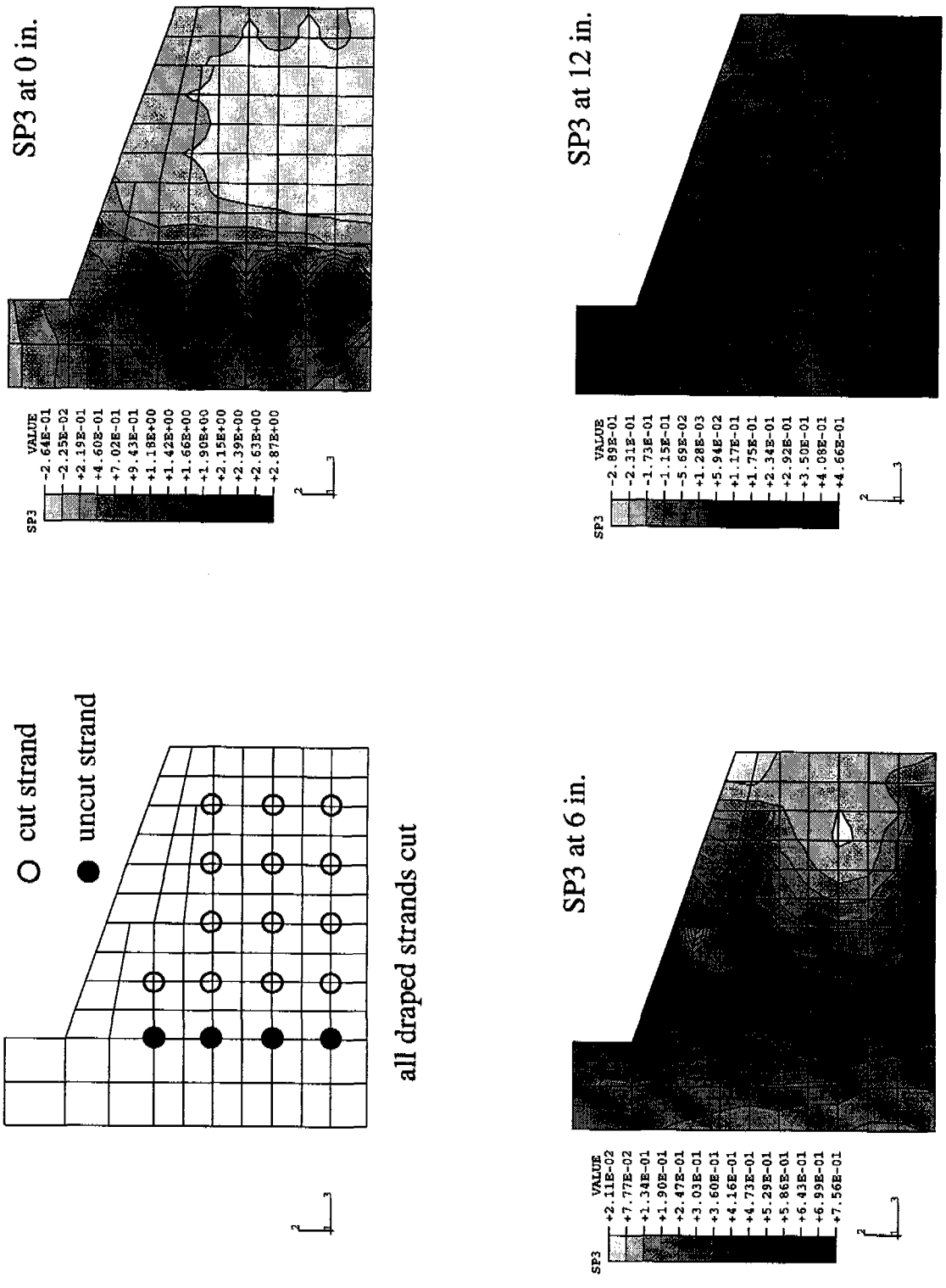

Figure A.5f SP3 Contours for Refined Mesh, Pattern 54A, Step 7

Figure A.5g SP3 Contours for Refined Mesh, Pattern 54A, Step 8

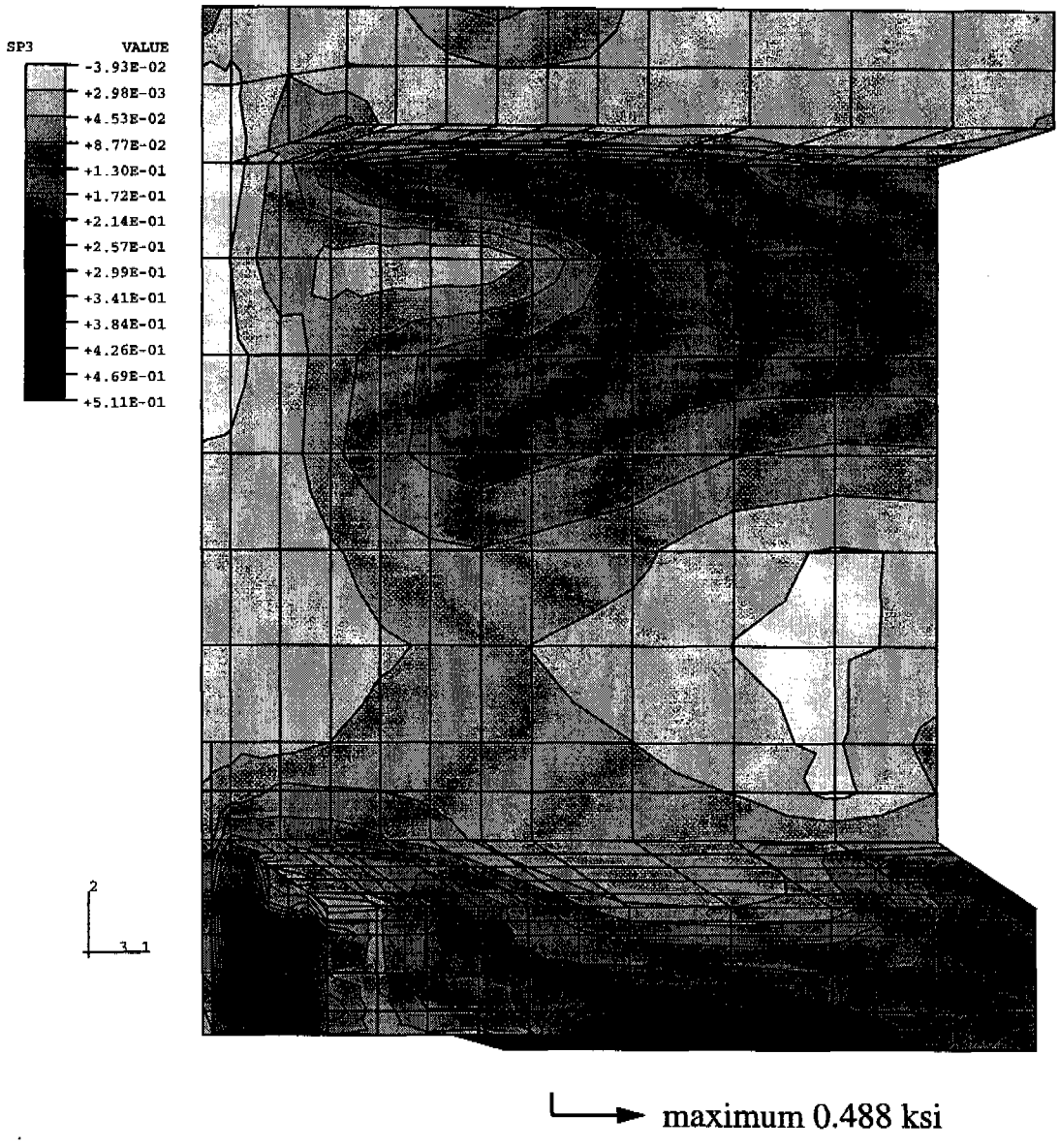

Figure A.6 SP3 at Full Draped Strand Release (no precuts)
Original Model

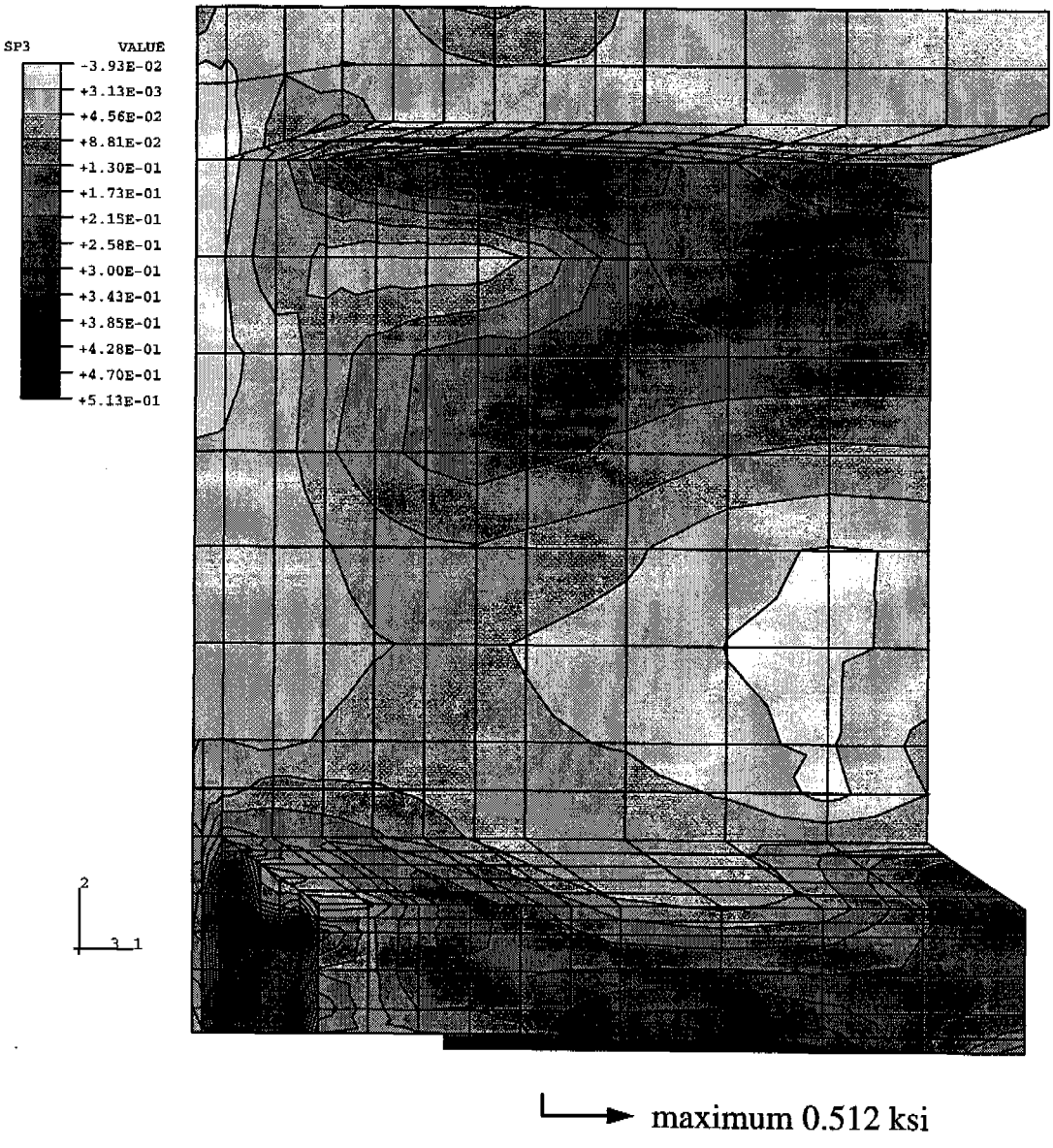

Figure A.7 SP3 at Full Draped Strand Release (no precuts) Model Sole1

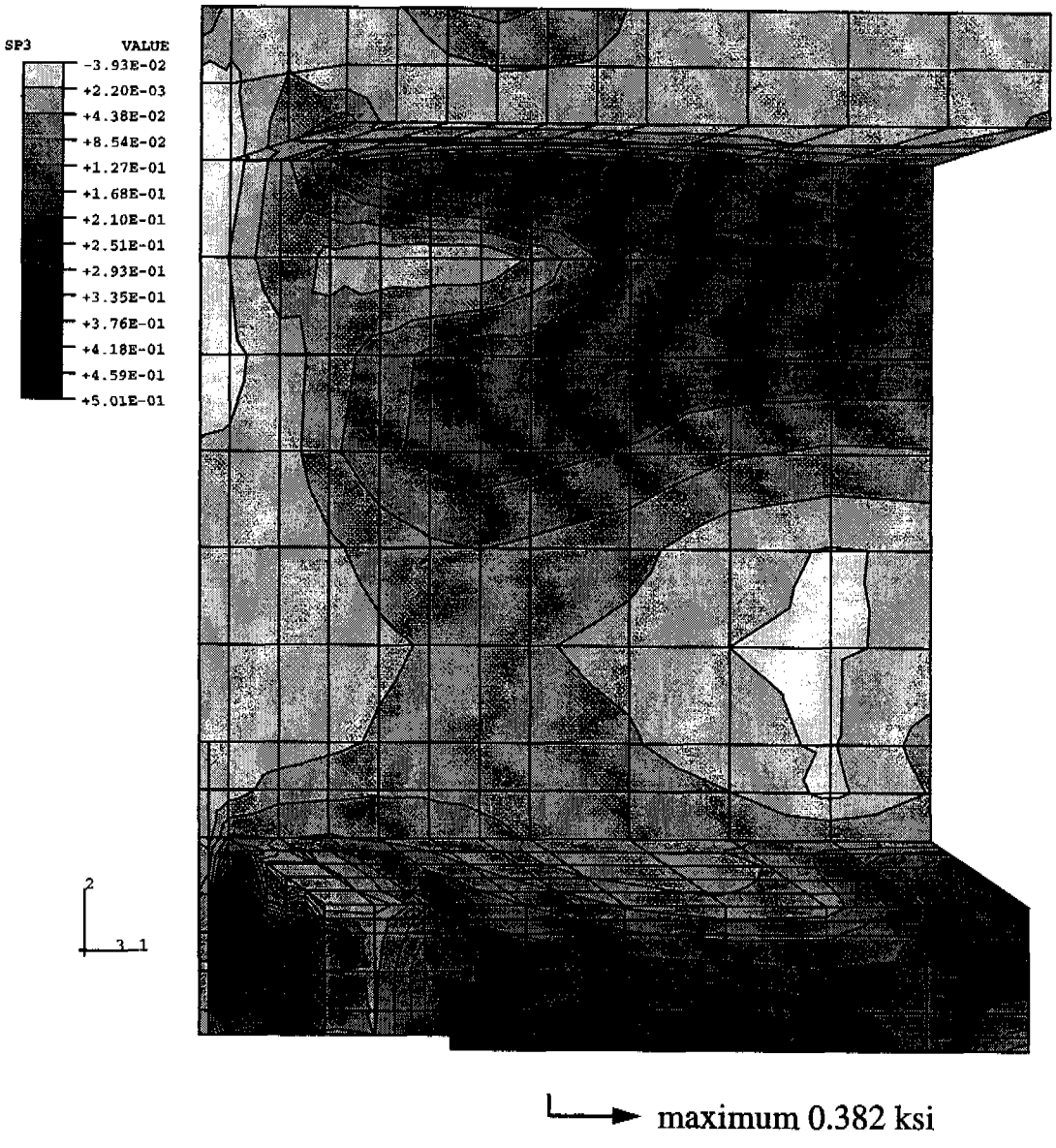

Figure A.8 SP3 at Full Draped Strand Release (no precuts)
Model Sole2

APPENDIX B

APPENDIX B
HORIZONTAL WEB CRACKING

The survey forms showed that horizontal cracking in the middle of the web was common among larger girders with end blocks (see Chapter 8). Although not part of the original scope of this project, these cracks were studied with a one-half girder model of the 72 in. deep, 139 ft. long girders and are discussed briefly below.

The mechanism that causes the web cracks was recognized by Gergely and Sozen [3]. They used a free body diagram to estimate the force in a vertical stirrup which crosses a web crack. The free body diagram, shown in Figure B.1, was defined by a horizontal cut at the position of an assumed crack, and a vertical cut at the end of the anchorage zone, where the longitudinal stress has reached a linear distribution over the height of the girder. As a rule, the location of the resultant force in the strands will be lower than the location of the resultant force in the concrete at the vertical cut defining the free body. This generates a moment which must be resisted by the vertical forces in the web. Once a girder cracks, the tension force is provided by the stirrups in the web. Gergely and Sozen used this fact to estimate the forces in the stirrups and to design them appropriately.

Although end blocks help to resist the web cracks, it can be shown that the end blocks are partly responsible for the high vertical stress in the web. This is because the location of the compressive resultant in the concrete at the vertical face will be higher in a girder with an endblock, increasing the moment arm between the compressive force in the concrete and the tension in the strands. Gergely and Sozen compared rectangular and I-beams and found that, for the sections being used in the their study, the moments would be 1.8 times greater in the rectangular sections. This difference was confirmed experimentally by the force measured in the stirrups.

The effect of the endblock on the 72 in. girders was studied using four different one-half girder models. The first model, "FullBlock", was unchanged except for using a slightly refined mesh in the web. The second model, "NoBlock", eliminated the endblock. In the third model, "PartBlock", the web tapered from 16 in. wide at the end face to 6 in. wide at 4 ft. from the end of the girder. In the fourth model, "PartBlock2",

the web tapered from 16 in. to 6 in. over just 2 ft. For an even comparison, none of the models included any rebar. The models were compared by considering a free body diagram cut at 23 in. above the base (the approximate location of the peak stress) and 30 in. from the end face, as shown in Figure B.2. For each model, the stress contours at full release were used to calculate the resultant forces and moments listed in Table B.1.

A convenient parameter for comparing the models is the moment of each force about corner B. First notice that the shear forces produce no moment about B, and the moment from the bearing at the sole plate was virtually identical for each model. The moment due to the strands was also relatively constant. The primary differences were in the moments due to C1 and T2. Notice that the moment about B due to C1 was lowest for model FullBlock because the endblock kept the resultant force C1 higher than in the other models. This causes the unbalanced moment with the strand force to be high, creating the need for a large moment from T2 to maintain equilibrium. At the other extreme, the resultant force C1 was lowest for model NoBlock, so that T2 did not need to be as great. However, due to the smaller area of the web, the tensile stress in the web is slightly greater than that in model FullBlock.

The ideal situation would be a narrow web at the end of the transfer zone to lower the resultant force C1, and a wide web at the end of the girder. This is what the other two models tried to accomplish. Table B.1 shows that these models did indeed decrease the stress in the web. Although it was not modelled, the optimal design for minimizing the tension in the web would be to make the web the full width of the flange at the end face, and to taper it over the first 2 or 3 feet of the girder. This also allows for an efficient distribution of vertical stirrups.

Because there were no loads applied directly to the web in the vicinity of the peak stress, and there were no other stress concentrators in the web, the magnitudes of the stresses should be relatively accurate compared to the stresses in the flanges. However, it must be remembered that these results were obtained assuming simple elastic behavior of the concrete, and ignoring the effects of rebar and pre-existing shrinkage cracks. Immediately tapering the end block will also affect the shear capacity of the girder. Therefore, it is left to the reader to determine whether/how to apply the results discussed here.

Table B.1 Effect of Endblock on Horizontal Web Cracking

(all units inches and kips)		FullBlock	NoBlock	PartBlock	PartBlock2
Max S22 in Web (psi)		1350	1420	1240	1130
% of FullBlock		100	105	92	84
S11 in strands	T1	562	551	556	553
	a	4.59	4.58	4.59	4.58
	moment -A	-2578	-2524	-2551	-2533
	moment -B	10351	10140	10243	10180
S11 vert. face	C1	-524	-521	-514	-513
	b	7.85	6.29	7.00	6.51
	moment -A	4119	3275	3592	3339
	moment -B	-7944	-8706	-8218	-8453
+S22 in web	T2	59	20	45	34
	c	4.11	3.58	3.45	2.87
	moment -A	243	70	156	97
	moment -B	-1533	-519	-1199	-918
-S22 in web	C2	-31	-15	-30	-26
	d	5.92	6.67	7.32	8.92
	moment -A	-757	-348	-685	-548
	moment -B	186	100	221	232
S12 vert. face	S1	-57	-33	-44	-37
	moment -A	-1700	-985	-1320	-1106
	moment -B	0	0	0	0
S12 in web	S2	-31	-23	-36	-32
	moment -A	711	524	823	739
	moment -B	0	0	0	0
Bearing	C3	30	28	29	29
	S3	-7	-7	-7	-7
	moment -A	0	0	0	0
	moment -B	-1072	-1016	-1036	-1026
Sums	horiz. force	1.06	0.32	-0.03	-0.34
	vert. force	-0.77	-0.24	-0.28	0.71
	moment -A	38	13	16	-12
	moment -B	-11	-2	11	15

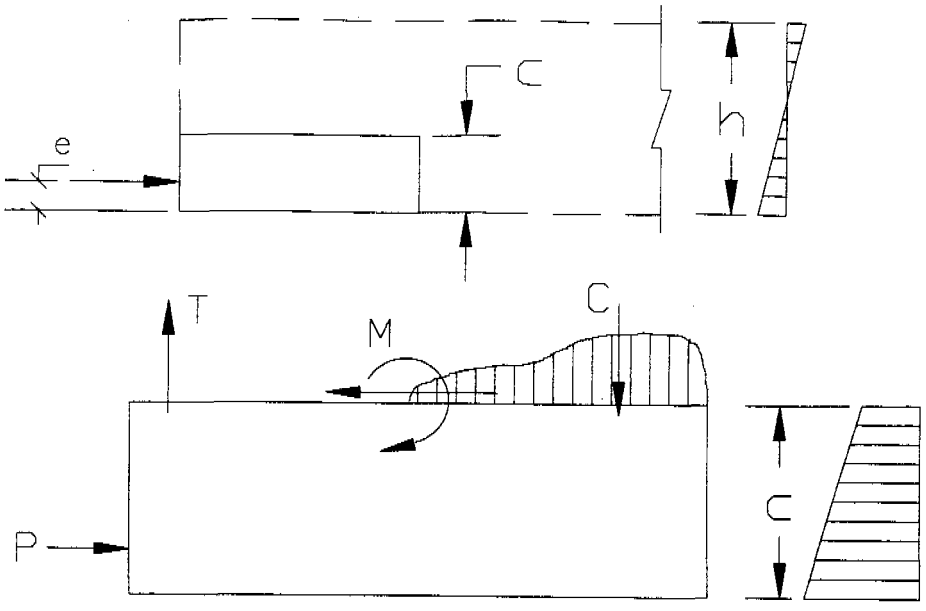

Figure B.1 Free Body Diagram used by Gergely and Sozen

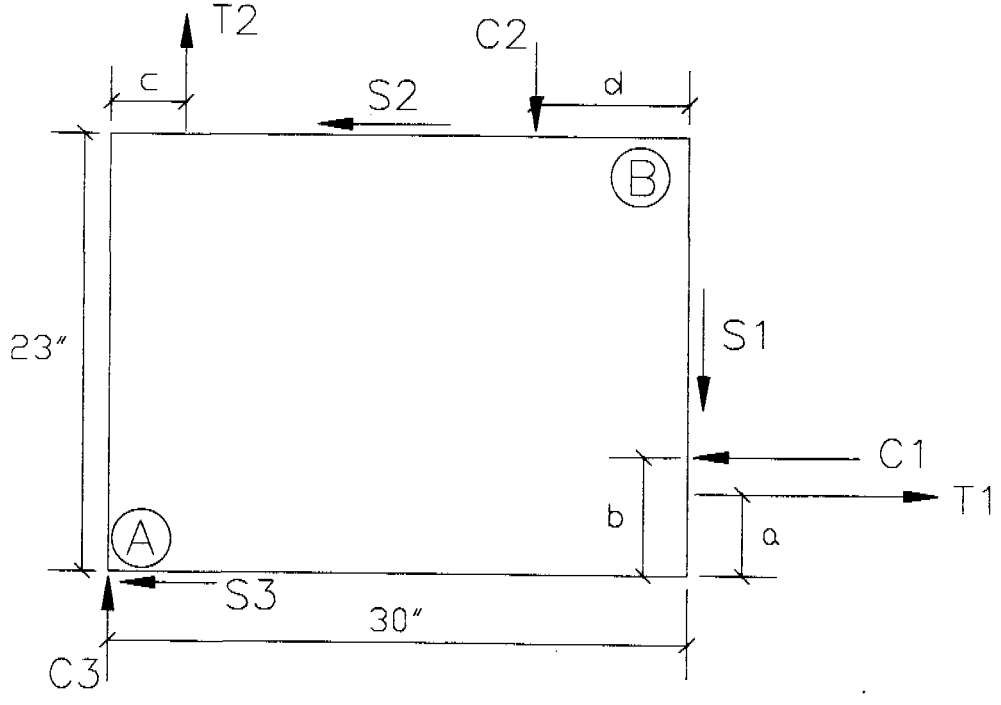

Figure B.2 Free Body Diagram used to compare FEM models

APPENDIX C

APPENDIX C

SAMPLE INPUT FILE FOR ONE-HALF GIRDER MODEL

The following is the input file for the 54 in. girder model, using release pattern 54a. The node numbering scheme is shown in Figure C.1.

```
*HEADING
 BRIDGE 25011, GIRDER SIZE 54M-111, PATTERN 54A
**
** end block nodes
**
*NODE,NSET=SECT1                {nodes at end face}
 1001,75.,0.,13.                {node #, 1-axis, 2-axis, 3-axis}
 1007,75.,0.,1.
 1008,75.,0.,0.
 1011,75.,0.75,13.
 1017,75.,0.75,1.
 1018,75.,0.75,0.
 1021,75.,2.,13.
 1027,75.,2.,1.
 1028,75.,2.,0.
 1041,75.,4.,13.
 1047,75.,4.,1.
 1048,75.,4.,0.
 1061,75.,6.,13.
 1067,75.,6.,1.
 1068,75.,6.,0.
 1081,75.,6.75,13.
 1085,75.,8.,5.
 1086,75.,8.,3.
 1087,75.,8.,1.
 1088,75.,8.,0.
 1101,75.,7.5,13.
 1106,75.,11.,3.
 1107,75.,11.,1.
 1108,75.,11.,0.
 1136,75.,13.5,3.
 1137,75.,13.5,1.
 1138,75.,13.5,0.
 1166,75.,16.,3.
 1167,75.,16.,1.
 1168,75.,16.,0.
 1460,75.,48.,15.
 1463,75.,47.,9.
 1466,75.,46.,3.
 1468,75.,46.,0.
 1500,75.,51.,15.
 1503,75.,50.5,9.
 1506,75.,50.,3.
 1508,75.,50.,0.
```

```
 1540,75.,54.,15.
 1543,75.,54.,9.
 1546,75.,54.,3.
 1548,75.,54.,0.
*NGEN,NSET=SECT1              {generate nodes on straight line}
 1001,1007
 1011,1017
 1021,1027
 1041,1047
 1061,1067
 1081,1085
 1101,1106
 1166,1466,50                 {below: copy nodes from 0" to 18"}
 1168,1468,50                 {          and from 18" to 42"}
*NCOPY,OLD SET=SECT1,NEW SET=SECT7,CHANGE NUMBER=6000,SHIFT
 18.,0.,0.
 0.,0.,0.,0.,0.,0.,0.
*NCOPY,OLD SET=SECT7,NEW SET=SECT11,CHANGE NUMBER=4000,SHIFT
 24.,0.,0.
 0.,0.,0.,0.,0.,0.,0.
*NFILL                        {fill in rest of end block nodes}
 SECT1,SECT7,6,1000
 SECT7,SECT11,4,1000
**
** end block elements
**
*ELEMENT,TYPE=C3D8I           {3D 8-node incompatible elements}
 1001,1001,2001,2002,1002,1011,2011,2012,1012   {elem #, 8 nodes}
 1011,1011,2011,2012,1012,1021,2021,2022,1022
 6011,6011,7001,7002,6012,6021,7021,7022,6022
 7001,7001,8001,8002,7002,7021,8021,8022,7022
 1021,1021,2021,2022,1022,1041,2041,2042,1042
 1106,1106,2106,2107,1107,1136,2136,2137,1137
 1166,1166,2166,2168,1168,1216,2216,2218,1218
 1460,1460,2460,2463,1463,1500,2500,2503,1503
 1466,1466,2466,2468,1468,1506,2506,2508,1508
*ELGEN,ELSET=BLOCK            {generate elems from master elems}
 1011,7,1,1,5,1000,1000
 6011,7,1,1
 7001,7,1,1,4,1000,1000
 1021,7,1,1,4,20,20,10,1000,1000
 1106,2,1,1,2,30,30,10,1000,1000
 1166,6,50,50,10,1000,1000
 1460,2,3,3,2,40,40,10,1000,1000
 1466,2,40,40,10,1000,1000
*ELGEN,ELSET=SOLE             {generate sole plate elems}
 1001,7,1,1,5,1000,1000
**
** beam elements
**
*NODE,NSET=BMNODE
 11000,117.,0.,0.             {at solid-beam element interface}
 17000,664.,0.,0.             {at holddown point}
 18000,736.,0.,0.             {at centerline of girder}
*NGEN,NSET=BMNODE
 11000,17000,1000
```

```
*ELEMENT,TYPE=B31H
 11000,11000,12000
*ELGEN,ELSET=BEAMS
 11000,7,1000,1000
**
** straight strands outside of end block
**
*NODE,NSET=STR0                 {at abutment}
 22,0.,2.,11.
 26,0.,2.,3.
 42,0.,4.,11.
 46,0.,4.,3.
 62,0.,6.,11.
 66,0.,6.,3.
 85,0.,8.,5.
 86,0.,8.,3.
*NGEN,NSET=STR0
 22,26
 42,46
 62,66
*NCOPY,OLD SET=STR0,NEW SET=STR11,CHANGE NUMBER=11000,SHIFT
 117.,0.,0.
 0.,0.,0.,0.,0.,0.,0.
*NCOPY,OLD SET=STR11,NEW SET=STR17,CHANGE NUMBER=6000,SHIFT
 547.,0.,0.
 0.,0.,0.,0.,0.,0.,0.
*NCOPY,OLD SET=STR17,NEW SET=STR18,CHANGE NUMBER=1000,SHIFT
 72.,0.,0.
 0.,0.,0.,0.,0.,0.,0.
*NFILL
 STR11,STR17,6,1000
*ELEMENT,TYPE=T3D2,ELSET=STRAIGHT  {3D 2-node truss elements}
 22,22,1022                     {first 3 are free strands}
 85,85,1085
 86,86,1086
 11022,11022,12022              {next 3 are in first beam segment}
 11085,11085,12085
 11086,11086,12086
*ELGEN,ELSET=STRAIGHT
 22,5,1,1,3,20,20               {generate rest of free strands}
 11022,5,1,1,3,20,20,7,1000,1000  {gen rest of strands in beams}
 11085,7,1000,1000
 11086,7,1000,1000
**
** draped strands outside of end block
**
*NODE
 801,0.,40.680814941,1.         {at abutment}
 806,0.,50.680814941,1.
 901,47.5,40.680814941,1.       {at "horse" or holdup point}
 906,47.5,50.680814941,1.
 1801,75.,39.,1.                {at girder face}
 1806,75.,49.,1.
*NGEN,NSET=DRP0
 801,806
*NGEN,NSET=HORSE
```

```
 901,906
*NGEN,NSET=DRP1
 1801,1806
*NCOPY,OLD SET=DRP1,NEW SET=DRP7,CHANGE NUMBER=6000,SHIFT
 18.,-1.100169779,0.
 0.,0.,0.,0.,0.,0.,0.
*NCOPY,OLD SET=DRP7,NEW SET=DRP11,CHANGE NUMBER=4000,SHIFT
 24.,-1.466893039,0.
 0.,0.,0.,0.,0.,0.,0.
*NCOPY,OLD SET=DRP11,NEW SET=DRP17,CHANGE NUMBER=6000,SHIFT
 547.,-33.432937182,0.
 0.,0.,0.,0.,0.,0.,0.
*NCOPY,OLD SET=DRP17,NEW SET=DRP18,CHANGE NUMBER=1000,SHIFT
 72.,0.,0.
 0.,0.,0.,0.,0.,0.,0.
*NFILL
 DRP1,DRP7,6,1000
 DRP7,DRP11,4,1000
 DRP11,DRP17,6,1000
*ELEMENT,TYPE=T3D2
 801,801,901
 901,901,1801
 11801,11801,12801
 17801,17801,18801
*ELGEN,ELSET=STRAIGHT      {draped strand, but designate as}
 801,6,1,1                 {straight to def. prestress later}
 17801,6,1,1
*ELGEN,ELSET=DRAPED
 901,6,1,1
 11801,6,1,1,6,1000,1000
**
** strands in end block
**
*ELEMENT,TYPE=T3D2
 61022,1022,2022           {define 2 truss elements for each}
 61085,1085,2085           {strand in the end block for    }
 61801,1801,2801           {transfer length approximation  }
 81022,1022,2022
 81085,1085,2085
 81801,1801,2801
*ELGEN
 61022,8,1000,1000
 61085,8,1000,1000
 61801,8,1000,1000
 81022,10,1000,1000
 81085,10,1000,1000
 81801,10,1000,1000
*ELGEN,ELSET=THROW1        {6XXXX elements removed(cut)}
 61022,5,1,1,3,20,20       {along with the free strands}
 61085,2,1,1
*ELGEN,ELSET=THROW2
 62022,5,1,1,3,20,20
 62085,2,1,1
*ELGEN,ELSET=THROW3
 63022,5,1,1,3,20,20
 63085,2,1,1
```

```
*ELGEN,ELSET=THROW4
 64022,5,1,1,3,20,20
 64085,2,1,1
*ELGEN,ELSET=THROW5
 65022,5,1,1,3,20,20
 65085,2,1,1
*ELGEN,ELSET=THROW6
 66022,5,1,1,3,20,20
 66085,2,1,1
*ELGEN,ELSET=THROW7
 67022,5,1,1,3,20,20
 67085,2,1,1
*ELGEN,ELSET=THROW8
 68022,5,1,1,3,20,20
 68085,2,1,1
*ELGEN,ELSET=THROW1D
 61801,6,1,1
*ELGEN,ELSET=THROW2D
 62801,6,1,1
*ELGEN,ELSET=THROW3D
 63801,6,1,1
*ELGEN,ELSET=THROW4D
 64801,6,1,1
*ELGEN,ELSET=THROW5D
 65801,6,1,1
*ELGEN,ELSET=THROW6D
 66801,6,1,1
*ELGEN,ELSET=THROW7D
 67801,6,1,1
*ELGEN,ELSET=THROW8D
 68801,6,1,1
*ELGEN,ELSET=KEEP1          {8XXXX elements are kept after}
 81022,5,1,1,3,20,20        {free strand is cut, with area}
 81085,2,1,1                {increasing along transfer length}
*ELGEN,ELSET=KEEP2
 82022,5,1,1,3,20,20
 82085,2,1,1
*ELGEN,ELSET=KEEP3
 83022,5,1,1,3,20,20
 83085,2,1,1
*ELGEN,ELSET=KEEP4
 84022,5,1,1,3,20,20
 84085,2,1,1
*ELGEN,ELSET=KEEP5
 85022,5,1,1,3,20,20
 85085,2,1,1
*ELGEN,ELSET=KEEP6
 86022,5,1,1,3,20,20
 86085,2,1,1
*ELGEN,ELSET=KEEP7
 87022,5,1,1,3,20,20
 87085,2,1,1
*ELGEN,ELSET=KEEP8
 88022,5,1,1,3,20,20
 88085,2,1,1
*ELGEN,ELSET=KEEP9
```

```
 89022,5,1,1,3,20,20
 89085,2,1,1
*ELGEN,ELSET=KEEP10
 90022,5,1,1,3,20,20
 90085,2,1,1
*ELGEN,ELSET=KEEP1D
 81801,6,1,1
*ELGEN,ELSET=KEEP2D
 82801,6,1,1
*ELGEN,ELSET=KEEP3D
 83801,6,1,1
*ELGEN,ELSET=KEEP4D
 84801,6,1,1
*ELGEN,ELSET=KEEP5D
 85801,6,1,1
*ELGEN,ELSET=KEEP6D
 86801,6,1,1
*ELGEN,ELSET=KEEP7D
 87801,6,1,1
*ELGEN,ELSET=KEEP8D
 88801,6,1,1
*ELGEN,ELSET=KEEP9D
 89801,6,1,1
*ELGEN,ELSET=KEEP10D
 90801,6,1,1
*ELSET,ELSET=THROW
 THROW1,THROW2,THROW3,THROW4,THROW5,THROW6,THROW7,THROW8
*ELSET,ELSET=THROWD
 THROW1D,THROW2D,THROW3D,THROW4D,THROW5D,THROW6D,THROW7D,THROW8D
*ELSET,ELSET=KEEP
 KEEP1,KEEP2,KEEP3,KEEP4,KEEP5,KEEP6,KEEP7,KEEP8,KEEP9,KEEP10
*ELSET,ELSET=KEEPD
 KEEP1D,KEEP2D,KEEP3D,KEEP4D,KEEP5D
 KEEP6D,KEEP7D,KEEP8D,KEEP9D,KEEP10D
**
** group elements of a given strand to be tossed
**
*ELSET,ELSET=TOSS22,GENERATE
 61022,68022,1000
*ELSET,ELSET=TOSS23,GENERATE
 61023,68023,1000
.
.
.
*ELSET,ELSET=TOSS805,GENERATE
 61805,68805,1000
*ELSET,ELSET=TOSS806,GENERATE
 61806,68806,1000
**
** materials
**
*MATERIAL,NAME=CRETE      {define concrete properties}
*ELASTIC
 4750.,0.15               {elastic modulus, Poisson's ratio}
*DENSITY                  {based on 150 lbs per cubic foot}
 2.25E-7
```

```
*MATERIAL,NAME=STEEL        {define steel properties}
*ELASTIC
 29000.,0.30
*PLASTIC
 245.,0.
 270.,0.005
*DENSITY
 7.36E-7
**
** property assignments              {assign materials to elems, etc.}
**
*SOLID SECTION,ELSET=BLOCK,MATERIAL=CRETE
*SOLID SECTION,ELSET=SOLE,MATERIAL=STEEL
*BEAM SECTION,ELSET=BEAMS,MATERIAL=CRETE,SECTION=I
 0.,54.,13.,15.,9.25,7.,3.          {beam dimensions - adjusted to }
 0.,0.,-1.                          {give correct section properies}
*SOLID SECTION,ELSET=STRAIGHT,MATERIAL=STEEL
 0.153                               {strand area=0.153 in^2}
*SOLID SECTION,ELSET=DRAPED,MATERIAL=STEEL
 0.153
*SOLID SECTION,ELSET=THROW1,MATERIAL=STEEL  {sum of throw & keep}
 0.14535                            {areas = 0.153 in^2}
*SOLID SECTION,ELSET=THROW2,MATERIAL=STEEL
 0.13005
*SOLID SECTION,ELSET=THROW3,MATERIAL=STEEL
 0.11475
*SOLID SECTION,ELSET=THROW4,MATERIAL=STEEL
 0.09945
*SOLID SECTION,ELSET=THROW5,MATERIAL=STEEL
 0.08415
*SOLID SECTION,ELSET=THROW6,MATERIAL=STEEL
 0.06885
*SOLID SECTION,ELSET=THROW7,MATERIAL=STEEL
 0.04590
*SOLID SECTION,ELSET=THROW8,MATERIAL=STEEL
 0.01530
*SOLID SECTION,ELSET=THROW1D,MATERIAL=STEEL
 0.14535
*SOLID SECTION,ELSET=THROW2D,MATERIAL=STEEL
 0.13005
*SOLID SECTION,ELSET=THROW3D,MATERIAL=STEEL
 0.11475
*SOLID SECTION,ELSET=THROW4D,MATERIAL=STEEL
 0.09945
*SOLID SECTION,ELSET=THROW5D,MATERIAL=STEEL
 0.08415
*SOLID SECTION,ELSET=THROW6D,MATERIAL=STEEL
 0.06885
*SOLID SECTION,ELSET=THROW7D,MATERIAL=STEEL
 0.04590
*SOLID SECTION,ELSET=THROW8D,MATERIAL=STEEL
 0.01530
*SOLID SECTION,ELSET=KEEP1,MATERIAL=STEEL
 0.00765
*SOLID SECTION,ELSET=KEEP2,MATERIAL=STEEL
 0.02295
```

```
*SOLID SECTION,ELSET=KEEP3,MATERIAL=STEEL
0.03825
*SOLID SECTION,ELSET=KEEP4,MATERIAL=STEEL
0.05355
*SOLID SECTION,ELSET=KEEP5,MATERIAL=STEEL
0.06885
*SOLID SECTION,ELSET=KEEP6,MATERIAL=STEEL
0.08415
*SOLID SECTION,ELSET=KEEP7,MATERIAL=STEEL
0.10710
*SOLID SECTION,ELSET=KEEP8,MATERIAL=STEEL
0.13770
*SOLID SECTION,ELSET=KEEP9,MATERIAL=STEEL
0.153
*SOLID SECTION,ELSET=KEEP10,MATERIAL=STEEL
0.153
*SOLID SECTION,ELSET=KEEP1D,MATERIAL=STEEL
0.00765
*SOLID SECTION,ELSET=KEEP2D,MATERIAL=STEEL
0.02295
*SOLID SECTION,ELSET=KEEP3D,MATERIAL=STEEL
0.03825
*SOLID SECTION,ELSET=KEEP4D,MATERIAL=STEEL
0.05355
*SOLID SECTION,ELSET=KEEP5D,MATERIAL=STEEL
0.06885
*SOLID SECTION,ELSET=KEEP6D,MATERIAL=STEEL
0.08415
*SOLID SECTION,ELSET=KEEP7D,MATERIAL=STEEL
0.10710
*SOLID SECTION,ELSET=KEEP8D,MATERIAL=STEEL
0.13770
*SOLID SECTION,ELSET=KEEP9D,MATERIAL=STEEL
0.153
*SOLID SECTION,ELSET=KEEP10D,MATERIAL=STEEL
0.153
**
** girder-bed surface interaction
**
*NODE
1,500.,0.,0.
*ELSET,ELSET=BOTBLOCK,GENERATE
7001,7007
8001,8007
9001,9007
*SURFACE DEFINITION,NAME=SOLESURF,TRIM=YES {define surfaces}
SOLE,S1
*SURFACE DEFINITION,NAME=BLCKSURF,TRIM=YES
BOTBLOCK,S1
*SURFACE DEFINITION,NAME=BEAMSURF
BEAMS,S2
*RIGID SURFACE,NAME=BED,REF NODE=1,TYPE=CYLINDER
400.,0.,0.,400.,0.,100.
500.,0.,0.
START,-100.,0.
LINE,100.,0.
```

```
*CONTACT PAIR,INTERACTION=ST-ST {specify contact interaction}
 SOLESURF,BED
*CONTACT PAIR,INTERACTION=CONC-ST
 BLCKSURF,BED
*CONTACT PAIR,INTERACTION=CONC-ST
 BEAMSURF,BED
*SURFACE INTERACTION,NAME=ST-ST          {define contact interactions}
*FRICTION,ELASTIC SLIP=0.01
 0.25                                    {friction coefficient}
*SURFACE INTERACTION,NAME=CONC-ST
*FRICTION,ELASTIC SLIP=0.01
 0.4
**
** mesh refinement constraints      {reduce # of elements in web}
**
*MPC
 LINEAR,1167,1166,1168                 {first node interpolated}
 LINEAR,2167,2166,2168                 {between other two nodes}
 LINEAR,3167,3166,3168
 LINEAR,4167,4166,4168
 LINEAR,5167,5166,5168
 LINEAR,6167,6166,6168
 LINEAR,7167,7166,7168
 LINEAR,8167,8166,8168
 LINEAR,9167,9166,9168
 LINEAR,10167,10166,10168
**
** constrain strand nodes in end block {draped strands don't line}
**                                    {up with concrete nodes}
*MPC
 BILINEAR,1801,1366,1368,1418,1416     {strand node interpolated}
 LINEAR,1802,1416,1418                 {between 4 closest nodes}
 BILINEAR,1803,1416,1418,1468,1466
 BILINEAR,1804,1416,1418,1468,1466
 BILINEAR,1805,1466,1468,1508,1506
 BILINEAR,1806,1466,1468,1508,1506
.
. {similar for sections 2 - 10}
.
 BILINEAR,11801,11366,11368,11418,11416
 BILINEAR,11802,11366,11368,11418,11416
 BILINEAR,11803,11366,11368,11418,11416
 BILINEAR,11804,11416,11418,11468,11466
 BILINEAR,11805,11416,11418,11468,11466
 BILINEAR,11806,11466,11468,11508,11506
**
** constrain solid-beam interface   {keep continuum element}
**                                  {nodes in a plane}
*NODE
 11900,117.,0.,15.
 11920,117.,2.,15.
*MPC
 SLIDER,11460,11920,11900          {first node must stay on same}
 SLIDER,11500,11920,11900          {line as the other two nodes }
 SLIDER,11540,11920,11900
 SLIDER,11041,11021,11001
```

SLIDER,11061,11021,11001
SLIDER,11081,11021,11001
SLIDER,11101,11021,11001
SLIDER,11042,11022,11002
SLIDER,11062,11022,11002
SLIDER,11082,11022,11002
SLIDER,11102,11022,11002
SLIDER,11043,11023,11003
SLIDER,11063,11023,11003
SLIDER,11083,11023,11003
SLIDER,11103,11023,11003
SLIDER,11463,11023,11003
SLIDER,11503,11023,11003
SLIDER,11543,11023,11003
SLIDER,11044,11024,11004
SLIDER,11064,11024,11004
SLIDER,11084,11024,11004
SLIDER,11104,11024,11004
SLIDER,11045,11025,11005
SLIDER,11065,11025,11005
SLIDER,11085,11025,11005
SLIDER,11105,11025,11005
SLIDER,11046,11026,11006
SLIDER,11066,11026,11006
SLIDER,11086,11026,11006
SLIDER,11106,11026,11006
SLIDER,11136,11026,11006
SLIDER,11166,11026,11006
SLIDER,11216,11026,11006
SLIDER,11266,11026,11006
SLIDER,11316,11026,11006
SLIDER,11366,11026,11006
SLIDER,11416,11026,11006
SLIDER,11466,11026,11006
SLIDER,11506,11026,11006
SLIDER,11546,11026,11006
SLIDER,11047,11027,11007
SLIDER,11067,11027,11007
SLIDER,11087,11027,11007
SLIDER,11107,11027,11007
SLIDER,11137,11027,11007
SLIDER,11167,11027,11007
SLIDER,11048,11028,11008
SLIDER,11068,11028,11008
SLIDER,11088,11028,11008
SLIDER,11108,11028,11008
SLIDER,11138,11028,11008
SLIDER,11168,11028,11008
SLIDER,11218,11028,11008
SLIDER,11268,11028,11008
SLIDER,11318,11028,11008
SLIDER,11368,11028,11008
SLIDER,11418,11028,11008
SLIDER,11468,11028,11008
SLIDER,11508,11028,11008
SLIDER,11548,11028,11008

```
SLIDER,11900,11007,11008
SLIDER,11001,11007,11008
SLIDER,11002,11007,11008
SLIDER,11003,11007,11008
SLIDER,11004,11007,11008
SLIDER,11005,11007,11008
SLIDER,11006,11007,11008
SLIDER,11920,11027,11028
SLIDER,11021,11027,11028
SLIDER,11022,11027,11028
SLIDER,11023,11027,11028
SLIDER,11024,11027,11028
SLIDER,11025,11027,11028
SLIDER,11026,11027,11028
BEAM,11007,11000              {connect solid node to beam node}
BEAM,11027,11000              {with equivalent of a rigid beam}
BEAM,11028,11000
TIE,11008,11000               {nodes have equal displacements}
**
** constrain strands to beam nodes
**
*MPC
BEAM,12022,12000              {connect truss node to beam node}
BEAM,12023,12000              {with equivalent of a rigid beam}
BEAM,12024,12000
.
.
.
BEAM,18804,18000
BEAM,18805,18000
BEAM,18806,18000
**
** set boundary conditions and prestress
**
*NSET,NSET=SLICE,GENERATE     {set of all nodes on the}
11000,18000,1000              {longitudinal symmetry cut}
1008,10008,1000
1018,6018,1000
1028,10028,1000
1048,10048,1000
1068,10068,1000
1088,10088,1000
1108,10108,1000
1138,10138,1000
1168,10168,1000
1218,10218,1000
1268,10268,1000
1318,10318,1000
1368,10368,1000
1418,10418,1000
1468,10468,1000
1508,10508,1000
1548,10548,1000
*BOUNDARY
1,ENCASTRE                    {fix master node of rigid surface}
STR0,PINNED                   {pin truss nodes at abutment}
```

```
DRP0,PINNED                    {pin truss nodes at abutment}
HORSE,2,3                      {hold horse nodes in 2 & 3 directions}
17000,2                        {hold beam node vertically at holddown}
18000,XSYMM                    {centerline beam node held x-symmetric}
SLICE,ZSYMM                    {nodes on longitudinal cut z-symmetric}
*INITIAL CONDITIONS,TYPE=STRESS
STRAIGHT,200.36                {equilibrium requires greater stress}
DRAPED,200.7338956             {in the draped strands}
THROW,200.36
THROWD,200.7338956
KEEP,200.36
KEEPD,200.7338956
**
** define layers for plotting
**
*ELSET,ELSET=LAY1,GENERATE
1011,1107
*ELSET,ELSET=LAY2,GENERATE
2011,2107
*ELSET,ELSET=LAY3,GENERATE
3011,3107
*ELSET,ELSET=LAY4,GENERATE
4011,4107
*ELSET,ELSET=LAY5,GENERATE
5011,5107
*ELSET,ELSET=LAY6,GENERATE
6011,6107
*ELSET,ELSET=LAY7,GENERATE
7001,7107
**
** begin release
**
*STEP,INC=3                     {step 1 solve initial equilibrium}
*STATIC
1.,1.,0.334,1.
*DLOAD                         {define gravity}
BLOCK,GRAV,386.4,0.,-1.,0.
BEAMS,GRAV,386.4,0.,-1.,0.
*RESTART,WRITE,FREQUENCY=5
*PRINT,CONTACT=YES             {set ouput parameters}
*CONTACT PRINT,TOTALS=YES,FREQUENCY=5
*NODE PRINT,TOTALS=YES,FREQUENCY=5
RF
*NODE PRINT,NSET=BMNODE,FREQUENCY=5
U
*EL PRINT,ELSET=BEAMS,FREQUENCY=5
S
*ENDSTEP
*STEP,INC=4                     {release 1/2 draped strands}
*STATIC
1.,1.,0.334,1.
*MODEL CHANGE,REMOVE
806,805,804,906,905,904,TOSS806,TOSS805,TOSS804
*BOUNDARY                      {pin horse nodes to avoid}
906,PINNED                     {solver problems}
905,PINNED
```

```
 904,PINNED
*ENDSTEP
*STEP,INC=4                          {release rest of draped strands}
*STATIC
 1.,1.,0.334,1.
*MODEL CHANGE,REMOVE
 803,802,801,903,902,901,TOSS803,TOSS802,TOSS801
*BOUNDARY
 903,PINNED
 902,PINNED
 901,PINNED
*ENDSTEP
*STEP,INC=4
*STATIC
 1.,1.,0.334,1.
*BOUNDARY,OP=NEW,FIXED               {release beam node 17000 to}
 1,ENCASTRE                          {release holddown}
 STR0,PINNED
 DRP0,PINNED
 HORSE,PINNED
 18000,XSYMM
 SLICE,ZSYMM
*MODEL CHANGE,REMOVE
 22,42,62,TOSS22,TOSS42,TOSS62
*ENDSTEP
*STEP,INC=4
*STATIC
 1.,1.,0.334,1.
*MODEL CHANGE,REMOVE
 23,43,63,TOSS23,TOSS43,TOSS63
*ENDSTEP
*STEP,INC=4
*STATIC
 1.,1.,0.334,1.
*MODEL CHANGE,REMOVE
 24,44,64,TOSS24,TOSS44,TOSS64
*ENDSTEP
*STEP,INC=4
*STATIC
 1.,1.,0.334,1.
*MODEL CHANGE,REMOVE
 25,45,65,85,TOSS25,TOSS45,TOSS65,TOSS85
*ENDSTEP
*STEP,INC=4
*STATIC
 1.,1.,0.334,1.
*MODEL CHANGE,REMOVE
 26,46,66,86,TOSS26,TOSS46,TOSS66,TOSS86
*ENDSTEP
```

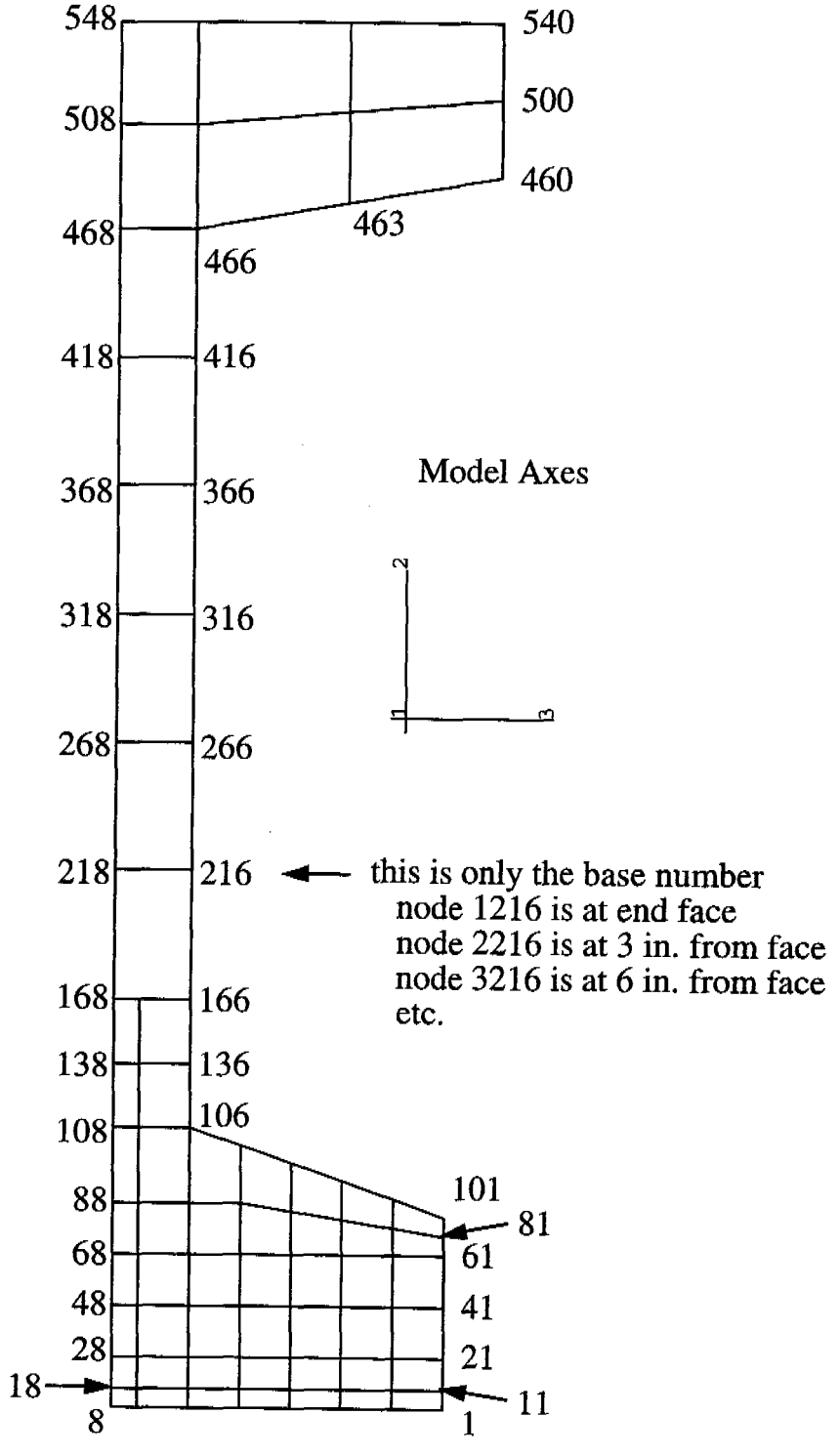

Figure C.1 Node Numbering for 54 in. Girder Model

APPENDIX D

APPENDIX D

PASCAL CODE FOR MIRZA AND TAWFIK ANALYSIS

The following is the Pascal code for a program developed at the University of Minnesota to perform the matrix analysis proposed by Mirza and Tawfik.

```
(*********************************************************************)
(** Created By: JEFF KANNEL                                          **)
(** Date:     4-24-96                                                **)
(** Title:    Elastic Spring Model developed by Mirza and Tawfik     **)
(** Limitations: maximum of 6 girders in a bed (easily changed below)**)
(**          need #cables / #cuts per release = 0                   **)
(*********************************************************************)

PROGRAM SapBed (input, output);

CONST maxgirders = 6;
    maxdof = 2 * maxgirders;
    maxcuts = 60;
    tol = 0.0000001;

TYPE  tymember = array [1..(2*maxgirders+1)] of real;
    tycuts  = array [1..maxcuts,1..(2*maxgirders+1)] of integer;
    tyiter        = array [1..maxcuts] of integer;
    tydof   = array [1..maxdof] of real;
    tystiff  = array [1..maxdof,1..maxdof] of real;
    tyeccen  = array [1..80] of real;

VAR   length, addstrain, oldstrain, addFPS, stress, newEs : tymember;
    force, displace : tydof;
    stiff       : tystiff;
    eccen        : tyeccen;
    cuts      : tycuts;
    iter      : tyiter;
    NG, NCM, NS, NC, release : integer;
    Es, Ec, As, Ac1, Ac2, Sb, FPS, prestrain : real;
    ystress1, ystrain1, ystress2, ystrain2  : real;
    infile  : string;
    problem, pass : boolean;

(*********************************************************************)
(** This procedure reads in data from an input file with a specific format **)
(*********************************************************************)

PROCEDURE GETDATA (VAR length:tymember;  VAR NG, NS, NC:integer;
                   VAR Ec, Ac1, Ac2, Sb, As, FPS, Es :real;
                   VAR ystress1, ystress2, ystrain2 :real;
                   VAR eccen:tyeccen;  VAR cuts:tycuts);

VAR  count, num, dum : integer;
```

```
BEGIN
 for count:=1 to 4 do
  readln;
 readln (Ec, Ac1, Ac2, Sb, NG);
 readln;
 readln;
 readln (NS, As, FPS, Es, ystress1, ystress2, ystrain2);
 readln;
 readln;
 for num:=1 to (2*NG+1) do
  read (length[num]);
 readln;
 readln;
 readln;
 for count:=1 to (NS+1) do
  readln (eccen[count]);
 readln;
 readln;
 readln (NC);
 for count:=1 to NC do begin
  read (dum);
  for num:=1 to (2*NG+1) do
   if (num mod 2)=1 then read (cuts[count,num]);
  readln;
  end;
END;

(*********************************************************)
(** This procedure forms the vector of nodal forces based on the    **)
(** release stage and the initial force in each cable.              **)
(*********************************************************)

PROCEDURE FORMFORCE (release, NG:integer;  FPS:real;  cuts:tycuts;
                     VAR force:tydof);

VAR node : integer;

BEGIN
 for node:=1 to (2*NG) do
  if (node mod 2) = 1
   then force[node]:=  cuts[release,node] * FPS
   else force[node]:= -cuts[release,node+1] * FPS;
 for node:= (2*NG+1) to maxdof do
  force[node]:=0;
END;

(*********************************************************)
(** This procedure checks whether the strands are elastic.  If not,  **)
(** the elastic modulus is decreased for the next pass through the   **)
(** solver.  The strains from the previous run are also saved.       **)
(*********************************************************)

PROCEDURE ELASTIC (NG:integer;  Es, ystress1, ystrain1, ystress2,
```

```
            ystrain2, prestrain:real;  addstrain:tymember;
            VAR newEs, oldstrain:tymember);

VAR  NCM : integer;
    totstrain : real;

BEGIN
  for NCM:=1 to (2*NG+1) do
    if (NCM mod 2) = 1 then begin
      totstrain:= prestrain + addstrain[NCM];
      if totstrain>ystrain2
           then newEs[NCM]:=ystress2/totstrain
           else if totstrain>ystrain1
             then newEs[NCM]:=((ystress2-ystress1)*(totstrain-ystrain1)/
          (ystrain2-ystrain1)+ystress1)/totstrain
             else newEs[NCM]:=Es;
      oldstrain[NCM]:= addstrain[NCM];
      end;
END;

(*******************************************************)
(** This procedure uses the given data to calculate the stiffness    **)
(** matrix. Since the abutments are fixed, rows and columns          **)
(** corresponding to their movement are not included.                **)
(*******************************************************)

PROCEDURE FORMSTIFF (NG, NS, release:integer;  Ec, As, Ac1:real;
              cuts:tycuts; length, newEs:tymember;
              VAR stiff:tystiff);

VAR  row, col, NCM, shift : integer;
    K : real;

BEGIN
  for row:=1 to maxdof do
    for col:=1 to maxdof do
      stiff[row,col]:= 0;
  for NCM:=1 to (2*NG+1) do begin
    if (NCM mod 2)=0
      then K:= Ec * Ac1 / length[NCM]
      else K:= newEs[NCM] * As * (NS-cuts[release,NCM]) / length[NCM];
    if (NCM=1) or (NCM=2*NG+1)
      then if NCM=1 then stiff[1,1]:= stiff[1,1] + K
                    else stiff[2*NG,2*NG]:= stiff[2*NG,2*NG] + K
      else begin
        shift:= NCM-1;
        stiff[shift,shift]:=  stiff[shift,shift] + K;
        stiff[shift,NCM]:= stiff[shift,NCM] - K;
        stiff[NCM,shift]:= stiff[shift,NCM];
        stiff[NCM,NCM]:=  stiff[NCM,NCM] + K;
        end;
  end;
  for row:=(2*NG+1) to maxdof do
    stiff[row,row]:=1;
```

```
END;

(*******************************************************)
(** This procedure factors the stiffness matrix into an upper      **)
(** triangular matrix, a diagonal matrix, and a lower triagular    **)
(** matrix using the modified Cholesky decomposition approach.**)
(*******************************************************)

PROCEDURE FACTOR (VAR stiff:tystiff;  VAR problem:boolean);

VAR  row, col, rowless1, colless1, num : integer;
     sum, temp : real;

BEGIN
  problem:= stiff[1,1] <= 0;
  if not problem then for col:=2 to maxdof do begin
    colless1:= col - 1;
    if colless1<>1 then for row:=2 to colless1 do begin
      sum:= stiff[row,col];
      rowless1:= row - 1;
      for num:=1 to rowless1 do
        sum:= sum - stiff[num,row] * stiff[num,col];
      stiff[row,col]:= sum
      end;
    sum:= stiff[col,col];
    for num:=1 to colless1 do begin
      temp:= stiff[num,col] / stiff[num,num];
      sum:= sum - temp * stiff[num,col];
      stiff[num,col]:= temp
      end;
    problem:= sum <= 0;
    if not problem then stiff[col,col]:= sum
    end
END;

(*********************************************************)
(** This procedure uses the factored matrix from the FACTOR      **)
(** procedure and uses it to solve the original system of equations    **)
(** for the unknown displacements.                                     **)
(*********************************************************)

PROCEDURE SOLVER (stiff:tystiff;  force:tydof;  VAR displace:tydof);

VAR  row, num : integer;
     sum : real;

BEGIN
  for row:= 1 to maxdof do begin
    sum:= force[row];
    if row<>1 then for num:=1 to (row-1) do
      sum:= sum - stiff[num,row] * displace[num];
    displace[row]:= sum
    end;
  for row:=1 to maxdof do
```

```
    displace[row]:= displace[row] / stiff[row,row];
  for row:= maxdof downto 1 do begin
    sum:= displace[row];
    if row<>(maxdof) then for num:=(row+1) to maxdof do
      sum:= sum - stiff[row,num] * displace[num];
    displace[row]:= sum
    end
END;

(*********************************************************)
(** This procedure calculates the primary results of the program.     **)
(** Additional strains and forces in unreleased cables are found      **)
(** from the nodal displacements. From these forces and the section **)
(** properties of the girders, the stress at the bottom end of the      **)
(** girders is calculated                                                    **)
(*********************************************************)

PROCEDURE CALCDATA (displace:tydof;  length:tymember;  NG, NS, release:
                integer;  Es, As, Ac2, Sb, prestrain, ystress1,
                ystrain1, ystress2, ystrain2:real;  eccen:tyeccen;
                cuts:tycuts;  VAR addstrain, addFPS, stress:
                tymember);

VAR  NCM : integer;
    totstrain : real;

BEGIN
  for NCM:=1 to (2*NG+1) do
    if (NCM mod 2) = 1 then begin
      if (NCM=1) or (NCM=2*NG+1)
          then if NCM=1 then addstrain[1]:= displace[1] / length[1]
                        else addstrain[NCM]:= -displace[2*NG] / length[NCM]
          else addstrain[NCM]:= (displace[NCM] - displace[NCM-1]) / length[NCM];
      totstrain:= prestrain + addstrain[NCM];
      if totstrain>ystrain2
          then addFPS[NCM]:= ystress2*As - FPS
          else if totstrain>ystrain1
            then addFPS[NCM]:=((ystress2-ystress1)*(totstrain-ystrain1)/(ystrain2-ystrain1)+ystress1)*As - FPS
            else addFPS[NCM]:= addstrain[NCM] * Es * As;
      stress[NCM]:= ((NS-cuts[release,NCM])*addFPS[NCM]/Ac2) +
(addFPS[NCM]*eccen[cuts[release,NCM]+1]/Sb);
      end;
END;

(*********************************************************)
(** This procedure writes the calculated data to a text file.      **)
(*********************************************************)

PROCEDURE PRINTOUT (release, NG:integer;  force, displace:tydof;
                    addstrain, addFPS, stress:tymember;  iter:tyiter);

VAR  line : integer;
    ch   : char;
```

```
BEGIN
 if release=1 then begin
  reset (input);
  for line:=1 to 3 do begin
   while not eoln do begin
    read (ch);
    write (ch);
    end;
   readln;
   writeln;
   end;
  end;
 writeln;
 writeln ('Release #', release:2, '  Girder End  Force  Displacement');
 for line:=1 to (2*NG) do
  if line=1 then writeln (iter[release]:2, ' iterations', (line div 2)+1:5, 'left':8, force[line]:9:1, displace[line]:13:4)
            else if (line mod 2) = 1 then writeln ((line div 2)+1:18, 'left':8, force[line]:9:1, displace[line]:13:4)
                                     else writeln ('right':26, force[line]:9:1, displace[line]:13:4);
 writeln;
 writeln (' ':15, 'Free Strand Restraint  Concrete');
 writeln (' ':15, 'Span Strain per strand  Stress');
 for line:=1 to (2*NG+1) do
  if (line mod 2) = 1 then writeln (' ':15, (line div 2)+1:3,
          addstrain[line]*1000000:8:0, addFPS[line]:10:3, stress[line]:12:4);
END;



(*************************************************************)
(** The MAIN PROGRAM queries the user for an input file and reads   **)
(** the data it contains. Then it cycles through each release stage,  **)
(** solving a new matrix problem and writing the results to 'BEDOUT'  **)
(** for each stage.                                                   **)
(*************************************************************)

BEGIN
 write ('Enter name of input file: ');
 readln (infile);
 assign (input, infile);
 reset (input);
 assign (output, 'BEDOUT');
 rewrite (output);
 GETDATA (length, NG, NS, NC, Ec, Ac1, Ac2, Sb, As, FPS, Es, ystress1, ystress2, ystrain2, eccen, cuts);
 prestrain:= FPS/(As*Es);
 ystrain1:= ystress1/Es;
 for release:=1 to NC do begin
  FORMFORCE (release, NG, FPS, cuts, force);
  for NCM:=1 to (2*NG+1) do
   addstrain[NCM]:=0;
  iter[release]:=0;
  repeat
  iter[release]:= iter[release] + 1;
  ELASTIC (NG, Es, ystress1, ystrain1, ystress2, ystrain2, prestrain, addstrain, newEs, oldstrain);
```

```
   FORMSTIFF (NG, NS, release, Ec, As, Ac1, cuts, length, newEs, stiff);
   FACTOR (stiff, problem);
   if not problem then begin
    SOLVER (stiff, force, displace);
    CALCDATA (displace, length, NG, NS, release, Es, As, Ac2, Sb, prestrain,
                  ystress1, ystrain1, ystress2, ystrain2, eccen, cuts, addstrain, addFPS, stress);
    pass:=true;
    for NCM:=1 to (2*NG+1) do
        if (NCM mod 2=1) and ((prestrain+addstrain[NCM])>ystrain1) and ((addstrain[NCM] -
oldstrain[NCM])>tol) then pass:=false;
    end;
   until pass;
   if problem=true then writeln ('Stiffness matrix is not positive definite')
    else PRINTOUT (release, NG, force, displace, addstrain, addFPS, stress, iter);
   end;
 close (output);
END.
```

Office of Research & Strategic Services
395 John Ireland Blvd., Mail Stop 330
Saint Paul, Minnesota 55155

(651) 282-2274